Acta morphologica et anthropologica 26 (3–4)

Prof. Marin Drinov Publishing House
of Bulgarian Academy of Sciences

ISSN 1311-8773 (print)
ISSN 2535-0811 (online)

Acta morphologica et anthropologica

26
(3-4)

26 (3-4) ● Sofia ● 2019
Institute of Experimental Morphology, Pathology and Anthropology with Museum
Bulgarian Anatomical Society

Contents

Morphology

Anthropology and Anatomy

Review Articles

Institute of Experimental Morphology, Pathology and Anthropology with Museum
Bulgarian Anatomical Society

Acta morphologica et anthropologica, 26 (3-4)
Sofia ● 2019

Histochemical Localization of NADPH-Diaphorase Reactive Neurons in the Colorectal Region of the Rat

Todor Kirov[1], Dimitrinka Atanasova[2,3], Lina Malinova[1], Lazar Jelev[1], Nikolai Lazarov[1,3]

[1] *Department of Anatomy and Histology, Medical University of Sofia, Sofia, Bulgaria*
[2] *Department of Anatomy, Faculty of Medicine, Trakia University, Stara Zagora, Bulgaria*
[3] *Institute of Neurobiology, Bulgarian Academy of Sciences, Sofia, Bulgaria*

* Corresponding author e-mail: tvkirov@gmail.com

The presence and distribution of nitrergic structures have been examined by means of NADPH-d histochemistry in the myenteric plexus, applied to the four main divisions of the rat large intestine. We first identified the exact location of the myenteric ganglia, the distribution of their internodal strands and fiber bundles in the adjacent muscle layers. Many NADPH-d–positive neurons were registered in the myenteric ganglia of all the examined segments and their morphology was categorized as Dogiel-type-1. Only single reactive fibers were found penetrating the longitudinal muscle, whereas in the circular muscle layer the varicose nerve fibers formed prominent bundles, running between the myocytes. We also observed an obvious predominance in the reaction intensity of NADPH-d-positive nerve structures in the recto-anal region, compared to the more proximal gut segments. In conclusion, our results provide histochemical evidence for the presence of nitrergic neurons in the rat colorectal region.

Key words: enteric neurons, myenteric plexus, nitrergic structures, NANC transmission, NADPH-diaphorase

Introduction

The inhibitory motor neurons of the enteric nervous system are an essential executor of a series of colonic reflexes and, therefore, have been a subject of interest for many years. There is now an abundance of evidence for the role this neuronal population plays not only during normal conditions, but also in a variety of disorders, like oesophageal or internal anal sphincter achalasia, hypertrophic pyloric stenosis and Hirschprung's disease [2, 8].

These neurons are the sole substrate of the so-called non-adrenergic, non-cholinergic (NANC) transmission. For many years, endogenous nitric oxide has been appointed as their main neurotransmitter, although a significant amount of evidence has shown extensive coexistence with vasoactive intestinal polypeptide (VIP) and adenosine

triphosphate (ATP) [1, 4, 6, 7, 10]. There is a distinct difference in the proportional distribution of these nitrergic neurons in the two enteric plexuses [2]. While they represent only a few percent of the total neuronal count in the submucous plexus, in the myenteric plexus their proportion can exceed 50%. This is hardly a surprise, since most of them are either inhibitory motor neurons, or inhibitory interneurons, both of which are involved exclusively in the innervation of the intestinal smooth muscle.

In different tissues, nitric oxide (NO) can be produced by all three isoforms, i.e. neuronal, endothelial and inducible, of the enzyme nitric oxide synthase (NOS). Naturally, in the enteric neurons the predominant isoform is neuronal NOS (nNOS). Nevertheless, the other two isoforms are also shown to be present there in small quantities, and, even more, their relative functions may alter during pathological conditions [2, 9].

The nNOS is proven to colocalize with NADPH-diaphorase [11]. Therefore, in this study we aimed to define the presence, distribution and staining intensity of nitrergic structures in the rat myenteric plexus that have been examined by means of NADPH-d histochemistry.

Material and Methods

In our study we used 20 mature (3-month-old) Wistar rats of both sexes with average weight (200-300 g). The entire array of experiments was carried out at the Institute of Neurobiology, Bulgarian Academy of Sciences in accordance with ethical principles of the Medical University of Sofia for the care and use of laboratory animals. Following a routine transcardial perfusion with 4% paraformaldehyde, we collected four colonic segments, each measuring approximately 10 mm, from the four major parts of the rat large intestine – proximal and distal colon, rectum and anal canal. Thereafter, the specimen was cut via a freezing microtome into 30 μm sections and mounted on glass slides, precoated with chrome gelatin. For the detection of NADPH-d activity, we applied the histochemical technique of Scherer-Singler et al. (1983). Briefly, the sections were incubated for 30–60 min at 37◦C in a staining solution consisting of 1mg/ml NADPH, 0.25mg/ml nitroblue tetrazolium (both from Sigma), and 0.3% Triton X-100 dissolved in Tris-buffered saline (TBS), pH 7.4. This mixture was freshly prepared and filtered just prior to use. After incubation, the sections were first rinsed in TBS, followed by washing in distilled water (3×15 min) and coverslipped in an aqueous-based mounting medium, glycerol jelly. For control purposes, sections were treated in the same way with omission of the substrate from the incubation medium. The slides were examined and photographed with Nicon Eclipse 80i (Japan), equipped with image analysis software NIS-Elements Advanced Research (ver. 2.30), and the images processed with Adobe Photoshop CC software.

Results

We first identified the exact location of the myenteric ganglia and the internodal strands connecting them. We observed many NADPH-d–positive neurons and their internodal fibers, located in the myenteric ganglia of all of the examined segments (**Fig. 1**). Those appeared to be monoaxonal, multipolar neurons – the stellate somata had numerous dendrites, oriented in a plane, parallel to the muscle layer. We also registered a definite predominance in the reaction intensity of NADPH-d–positive nerve structures of the recto-anal region (**Fig. 1 c, d**), relative to the colonic one (**Fig. 1 a, b**). Moreover, image analysis revealed that in the rectum the reaction intensity was slightly lower than that in the anal canal.

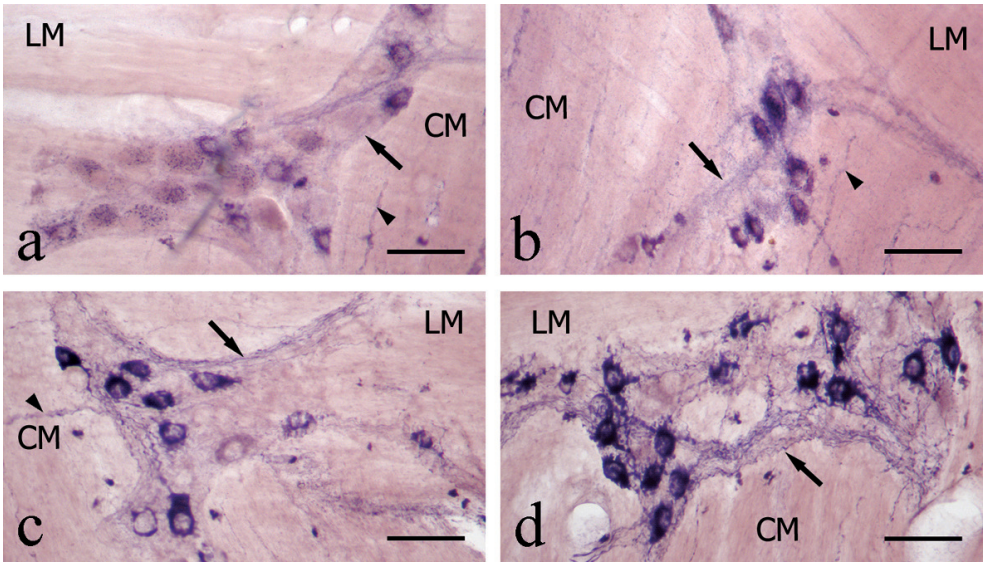

Fig. 1. Histochemical demonstration of NADPH-d activity in neuronal somata and fibers in the myenteric plexus of the colo-rectal region. Note the typical shape of the classical motor Dogiel-type-1 neurons. LM – longitudinal muscle; CM – circular muscle; arrows – internodal strands; arrowheads – fiber bundles in the circular muscle layer. Scale bar: 50 µm. (a) Proximal colon; (b) Distal colon; (c) Rectum; (d) Anal canal.

Analysis of the fiber system revealed only single positive fibers in close contact with the longitudinal muscle, but rarely penetrating it (**Fig. 2**). On the other hand, large fiber bundles, with extensive varicosities, were found traversing the circular muscle. Their orientation was perfectly aligned with the longitudinal axis of the myocytes.

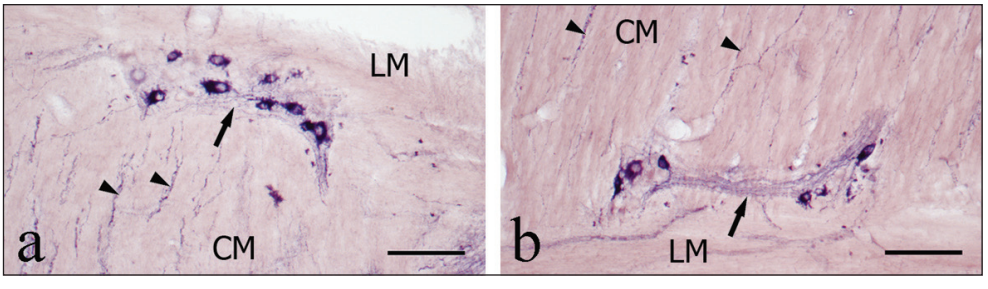

Fig. 2. Distribution of NADPH-d-positive neuronal perikarya and fibers in the myenteric plexus and the surrounding muscle layers. LM – longitudinal muscle; CM – circular muscle; arrows – internodal strands; arrowheads – fiber bundles in the circular muscle layer. Scale bar: 100 µm. (a) Rectum; (b) Anal canal.

Discussion

The aim of this study was to evaluate the morphology of inhibitory nitrergic neurons in the rat colonic myenteric plexus and to compare the results to previous findings. Virtually all of the registered NADPH-d-positive neurons appeared to possess the characteristic Dogiel-type-1 morphology. According to classical descriptions those neurons are

monoaxonal and have flattened stellate somata and numerous lamellar dendrites placed in the plane of the myenteric plexus itself [3]. Such studies have also indicated that those neurons serve as motor neurons and, to a lesser extent, as interneurons. Thorough research in the area has shown that the reported cases of nitrergic positive neurons expressing the features of Dogiel type 2 morphology (multiaxonal neurons with oval and seemingly smooth perikarya) is only due to insufficient magnification [5]. Therefore, the present study fully supports previous findings regarding the morphology of the nitrergic neurons.

Our results are also consistent with another aspect of past research – the perception that colonic myenteric nitrergic neurons exclusively send anal projections, which are responsible mainly for the inhibition of the circular muscle [2, 4]. Moreover, in animal species that possess only a thin layer of longitudinal muscle (such as the rat), the latter receives its innervation solely from the so-called tertiary myenteric plexus (a fine network of thin fiber bundles). In accordance with those postulates, we registered only a scant amount of poorly stained fibers in the longitudinal muscle, whereas in the circular layer fibers showed intense staining reaction and formed distinctive bundles with abundance of varicosities.

Conclusions

We provide histochemical evidence for the presence of abundant NADPH-d-positive neuronal structures in the rat colo-rectal region. Moreover, our results fully support the typical morphology and distribution of nitrergic neurons in the rat large intestine as previously described.

References

1. **Barbiers, M., J.-P. Timmermans, D. Scheuermann, D. Adriaensen, B. Mayer, M. Groodt-Lasseel.** Distribution and morphological features of nitrergic neurons in the porcine large intestine. – *Histochemistry*, **100**, 1993, 27-34.
2. **Bodi, N., Z. Szalai, M. Bagyanszki.** Nitrergic enteric neurons in health and disease – focus on animal models. – *Int. J. Mol. Sci.,* **20**(8), 2019, 2003.
3. **Brehmer, A., F. Schrödl, W. Neuhuber.** Morphological classification of enteric neurons – 100 years after Dogiel. – Anat. Embryol. (Berl), **200**(2), 1999, 125-135.
4. **Furness, J.** Types of neurons in the enteric nervous system. – *J. Auton. Nerv. Syst*., **81**(1-3), 2000, 87-96.
5. **Furness, J., J. Bornstein, S. Pompolo, H. Young, W. Kunze, H. Kelly**. The circuitry of the enteric nervous system. - *Neurogastroenterol. Mot*., **6**, 1994, 241-253.
6. **Lomax, A., J. Furness.** Neurochemical classification of enteric neurons in the guinea-pig distal colon. – *Cell Tissue Res.,* **302**(1), 2000, 59-72.
7. **Nichols, K., A. Krantis, W. Staines.** Histochemical localization of nitric oxide-synthesizing neurons and vascular sites in the guinea-pig intestine. – *Neuroscience,* **51**(4), 1992, 791-799.
8. **Rivera, L., D. Poole, M. Thacker, J. Furness.** The involvement of nitric oxide synthase neurons in enteric neuropathies. – *Neurogastroenterol. Motil.,* **23**(11), 2011, 980-988.
9. **Vannucchi, M.-G., L. Corsani, D. Bani, M.-S. Faussone-Pellegrini.** Myenteric neurons and interstitial cells of Cajal of mouse colon express several nitric oxide synthase isoforms. – *Neurosci. Lett.,* **326**(3), 2002, 191-195.
10. **Wang, Y., Y. Mao, J. Fox-Threlkeld, T. McDonald, E. Daniel.** Colocalization of inhibitory mediators, NO, VIP and galanin, in canine enteric nerves. – Peptides, **19**(1), 1998, 99-112.
11. **Ward, S., C. Xue, C. Shuttleworth, D. Bredt, S. Snyder, K. Sanders.** NADPH diaphorase and nitric oxide synthase colocalization in enteric neurons of canine proximal colon. – *Am. J. Physiol.,* **263**(2 Pt 1), 1992, 277-284.

Institute of Experimental Morphology, Pathology and Anthropology with Museum
Bulgarian Anatomical Society

Acta morphologica et anthropologica, 26 (3-4)
Sofia ● 2019

Effects of Leptin on NADPH-d Reactivity in the Dentate Gyrus of Rats

Teodor Angelov[1], Milen Hristov[2], Boycho Landzhov[1]*

[1] Department of Anatomy, Histology and Embryology, Faculty of Medicine, Medical University of Sofia, Bulgaria
[2] Department of Pharmacology and Toxicology, Faculty of Medicine, Medical University of Sofia, Bulgaria

*Corresponding author e-mail: teodor_angelovv@abv.bg

Leptin is a peptide hormone regulating food intake and body weight. The effects of leptin are mediated via leptin receptors present in the central nervous system (including hippocampal regions and gyrus dentatus). It is known that leptin induces phosphorylation of the neuronal isoform of nitric oxide synthase (nNOS) in defined hypothalamic regions. Identification of specific extrahypothalamic sites of leptin-induced activation of nNOS has been largely ignored. The present study was therefore undertaken to investigate the effects of leptin on NO expression in gyrus dentatus of rats. Six male Wistar rats were injected i.p. with either leptin (0,5 mg/kg) or saline (control group) and anesthetized 45 min later. Serial coronal sections were stained with the histochemical nicotinamide adenine dinucleotide phosphate diaphorase (NADPH-d) technique and examined with a light microscope. Our results demonstrated that leptin-treated animals had a significant increase in NADPH-d positive neurons in the dentate gyrus compared to that seen in the control group. These data suggest that leptin results in increased expression of NO in dentate gyrus of rats. We speculate that leptin may exert an effect on the hippocampal neurogenesis or neuroprotective properties by activating the endogenous nitric oxide synthase system.

Key words: leptin, nitric oxide, NADPH-d, dentate gyrus, rats

Introduction

Leptin is an adipokine, expressed and synthesized by the adipocytes [28]. It has a role in regulating energy homeostasis and neuroendocrine function [20, 25]. Different isoforms of the leptin receptor were found, but only the long form of the receptor, LepRb, appears to be the critical receptor for leptin action [3]. LepRb is expressed in different areas of the central nervous system (CNS) such as hypothalamus, cerebellum, cerebral cortex and hippocampus, including dentate gyrus (DG) [11].

The dentate gyrus (DG) is located mainly in the antero-medial temporal lobe, referred to allocortex [9]. It is main part of hippocampal formation and is specialized in associative memory (consolidating events and what is happening) [22]. The dentate gyrus (DG) is composed by three layers: molecular layer (primarily interneurons – the axo-axonic cells and the MOPP cells (molecular layer perforant path-associated cells),

the dendrites of the granule cells, pyramidal basket cells and mossy cells and the terminal axonal arbors from the entorhinal cortex), granular layer with the subgranular zone (the granule cells and the pyramidal basket cells), and the polymorphic zone (hilum, containing the mossy cells, a number of fusiform cells and also multipolar or triangular cells) [24]. The granule and the mossy cells project axons to make excitatory synapses on the dendrites of CA3 pyramidal neurons. The only cortical structure from which DG gets direct inputs is the entorhinal cortex.

It has been found that the effects of leptin in the CNS are mediated by nitric oxide (NO) [2]. NO is a freely diffusible gaseous neurotransmitter. It is biosynthesized endogenously from the amino acid L-arginine and oxygen, by nitric oxide synthase (NOS) [12]. Nicotinamide adenine dinucleotide phosphate diaphorase (NADPH-d) is routinely used as a histochemical marker for NOS [15, 26]. Since DG neurons are known to express LepRb, we investigated the effects of leptin on NADPH-d reactivity in the DG of male Wistar rats.

Material and Methods

Animals: Male Wistar rats, with average body weight 250-300 g, were housed in a temperature-controlled room (20–22°C) on a 12:12-h light-dark cycle (07:00 to 19:00 h). They were divided in 2 groups (3 rats per group): the first one treated with leptin and the second one (control group) – with saline. Rats had ad libitum access to standard pelleted chow and water. All experiments were conducted in accordance with the Directive 2010/63/EU of the European Parliament and of the Council of 22 September 2010 on the protection of animals used for scientific purposes and approved by the Ethical Council of the Bulgarian Food Safety Agency.

Leptin stimulation and NADPH-d histochemistry: On the day of the experiment, rats were injected i.p. with leptin (0.5 mg/kg) or vehicle (saline) and anesthetized 45 min later with thiopental (40 mg/kg i.p.). Transcardial perfusion was performed using 4% paraformaldehyde in 0.1M phosphate buffer, pH 7.4. The brains were removed and postfixed overnight in the same fixative solution at 4ºC. Serial coronal sections from septal part of dentate gyrus (from bregma -2.12 mm to -3.30 mm) on a freezing microtome (Reichert-Jung) at a thickness of 40 μm were done. Every fifth section was processed for NADPH-d histochemical examination.

The DG levels were identified according to their stereotaxic coordinated in the rat brain atlas (Paxinos and Watson, 2007). Sections were then stained with the NADPH-d-technique using 0.1–0.2 mg/ml of nitroblue tetrazolium, 1 mg/ml β-NADPH and 0.3–0.5 % Triton X-100 in 0.1 M TRIS – HCl buffer (pH 7.4) at 37 °C for 30–60 min. Afterwards, the sections were given three consecutive 5-min rinses in the same phosphate buffer and mounted on gelatin-coated glass slides. The slides were air dried overnight at room temperature, rinsed three times with distilled water, dried again and cover-slipped with Entellan (Merck, Germany).

Data analysis: NADPH-d-labeled neurons were visualized using a 20 X objective on a light microscope (Nikon Eclipse 80i microscope). The analysis started with digitally capturing (a digital camera Nikon DMX 1200) and storing the areas of interest. The density of nerve cell bodies and the amount of the cells in the DG areas were estimated using the same Nikon's NIS Elements Digital Imaging software. DG sections were used for cell counts and the average of the cells was calculated. The neuronal densities of the selected brain areas were quantified by determining the percentage of the measurement grid occupied by stained cells. Data were statistically assessed by one-way analysis of variance (ANOVA) and Holm–Sidak post hoc test. All values are presented as mean ± standard error of the mean (SEM). A p-value equal to or less than 0.05 was considered to be statistically significant.

Results

Our results have shown NADPH-d reactivity in the DG of both saline treated and leptin – treated rats (**Fig. 1**).

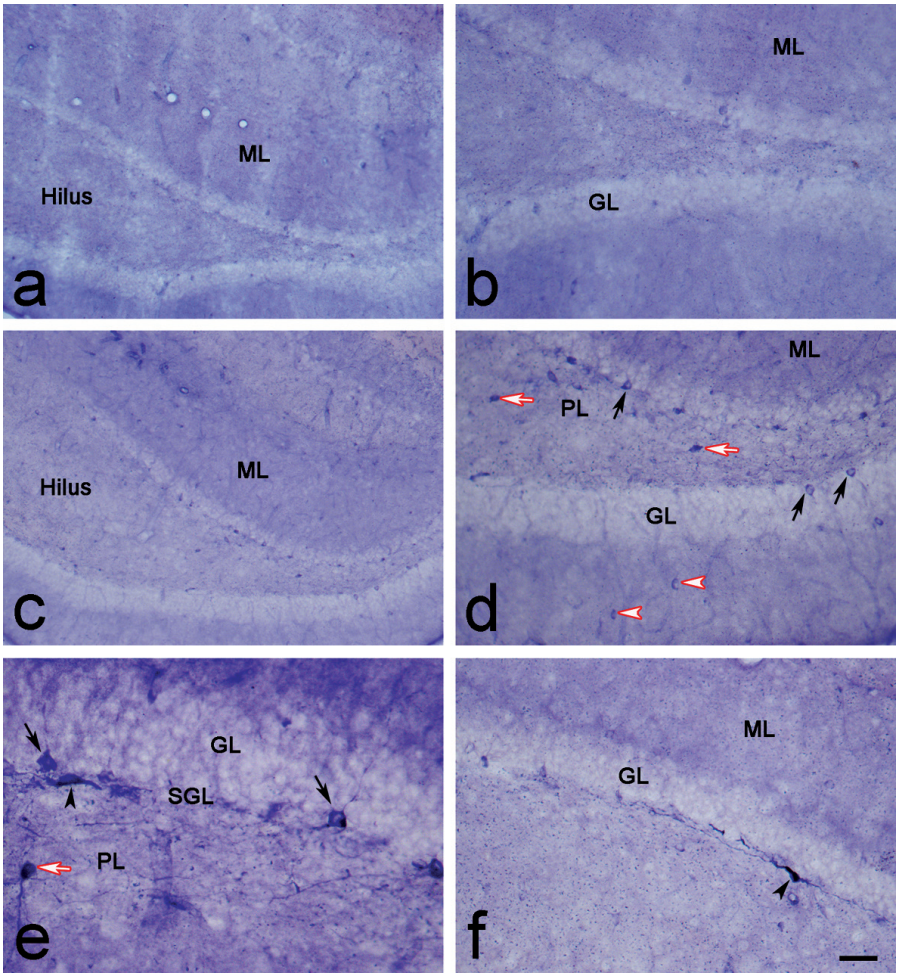

Fig. 1. NADPH-diaphorase reactivity of DG neurons in the control (a, b) and leptin treated groups (c-f). ML – molecular layer, GL – granular layer, SGL – subgranular layer, PL – polymorphic layer. The pyramidal basket cells – black arrows, the mossy cells – white arrows, the elongated cells on the border of subgranular zone – black arrowheads, the neurons in molecular layer – white arrowheads. Scale Bar: 100 μm (a, c), 50 μm (b, d, f), 25 μm (e).

There was statistically significant increase in the number of NADPH-d positive neurons in leptin-treated rats compared to that observed in the control group ($p<0.01$, **Fig.2**). NADPH-d reactivity was seen as cytoplasmic staining into cell bodies and their branches. The cytoplasm was diffusely filled with NADPH-d reaction products unlike the nucleus that was stain-free. Based on the cell body shape, the neurons were multipolar, pyramidal, bipolar, oval, and pear-shaped. Representation by zones included

round or fusiform NADPH-d reactive neurons in molecular layer, single cone-shaped or oval cells in granular layer, larger pyramidal-basket cells in the subgranular zone and some mossy cells in the hilus.

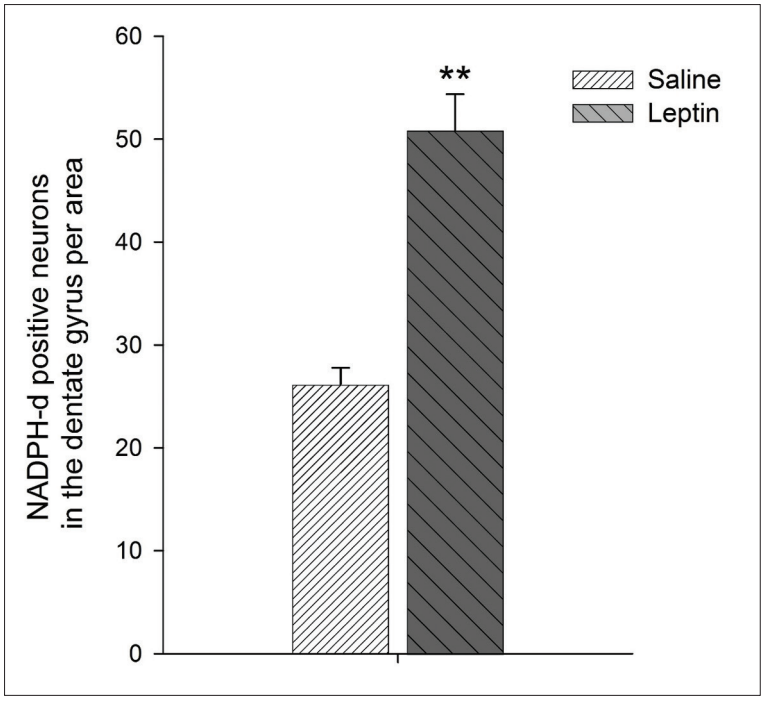

Fig. 2. The number of NADPH-d positive cells in the dentate gyrus of saline- and leptin-treated rats. Animals were fasted overnight and injected with leptin or saline and euthanized 45 min later. One of five series from each animal was analyzed. Statistical significance compared with saline group: **P<0.01 (n=3 per group). Values represent the mean ± SEM

There was a number of branched pyramidal-basket cells from subgranular zone which single aspiny apical dendrites traverse the granular layer, between the cell bodies of granule neurons stretch to the molecular layer. These cells had also several basal dendrites that extend into the polymorphic cell layer. The pyramidal-shaped neurons were larger than the granule cells. The granule cell layer had single NADPH-d reactive oval or elliptical-shaped neurons. The NADPH-d reactive cells were located mainly on the border between granular, subgranular and polymorphic layers.

The cells from polymorphic layer were different in shape and size. The main type of cells we seen in this layer were the mossy cells, who had got triangular or multipolar-shaped large cell bodies. Some of cell with elongated shape were situated along to the axis of subgranular layer. Two or more thick long dendrites originated from their cell body and run parallel to layer's border. They could be divided into primary and secondary spiny dendrites.

Discussion

Our results have shown that systemic administration of leptin resulted in increased NADPH-d positive cell number in the DG. In hippocampal neurons (areas CA1, CA3 and the dentate gyrus), leptin receptors are located at both presynaptic and postsynaptic sites [23]. As a neurotrophic growth factor, leptin promotes synaptogenesis, synaptic plasticity, axon growth and neuronal migration in the hippocampal formation [14]. It has a key role in improving memory formation and retention [13]. Studies have demonstrated deficiencies in brain myelin, reduced neuronal soma size, altered dendritic orientation in ob/ob and db/db mice [4].

The neural stem cells (NSCs) are pluripotent cells, located in CNS [10]. They may differentiate into neurons, astrocytes, and oligodendrocytes depending on the received signals for differentiation and maturation [6]. In adult CNS, NSCs are found in the subventricular zone (SVZ) of the lateral ventricles and in the subgranular zone (SGZ) of the hippocampal formation. In SGZ, the NSCs maturate into the granule cells [21]. Increasing studies indicate that NO has a substantial role for the proliferation of NSCs. Recently, Carreira et al. have demonstrated that extracellular NO participates in the regulation of NSC proliferation [5]. They found that treatment with 10 μM of NO donor NOC-18 for 24 h increases NSC growth, whereas higher concentrations (100 μM) decrease cell growth. Moreover, Luo et al. have shown that NO, produced from nNOS, plays an important role in NSC proliferation [17]. Collectively, we suggest that leptin-induced NO production in the DG may affect the neurogenesis occurs in the hippocampal formation.

It has been found that leptin has neuroprotective effects under a variety of neurotoxic conditions [7, 27, 29]. Using primary cultured hippocampal neurons, Martins et al. have demonstrated that leptin reduces amyloid-β (Aβ) oligomers-induced production of superoxide and mitochondrial membrane depolarization, improving cell survival, and inhibit cell death through a receptor-dependent mechanism, thus highlighting its potential therapeutic role in Alzheimer‘s disease [18]. Additionally, in organotypic slices from rabbit hippocampus, exogenous leptin increases the basal expression levels of insulin-like growth factor-1 (IGF-1), a neuroprotective and neurotrophic factor, and reverses the Aβ-mediated decrease in IGF-1 levels [19]. Few studies have been published on neuroprotective properties of NO, caused through induction of the cGMP pathway [1, 8, 16]. Thus, we hypothesize that leptin, inducing NO synthesis in DG neurons, may have neuroprotective effects.

Conclusions

Our results have shown that leptin increases NADPH-d reactivity in the DG of male Wistar rats. We speculate that leptin may exert an effect on the hippocampal neurogenesis or possess neuroprotective properties by activating the endogenous nitric oxide synthase system. Additional studies are needed to examine this hypothesis.

References:

1. **Arancio, O., V. Lev-Ram, R.Y. Tsien, E. R. Kandel, R. D. Hawkins.** Nitric oxide acts as a retrograde messenger during long-termpotentiation in cultured hippocampal neurons – *J. Physiol. Paris*, **90**, 1996, 321-322.

2. **Bellefontaine, N., K. Chachlaki, J. Parkash, C. Vanacker, W. Colledge, X. d'Anglemont de Tassigny, J. Garthwaite, S. G. Bouret, V. Prevot.** Leptin-dependent neuronal NO signaling in the preoptic hypothalamus facilitates reproduction – *J. Clin. Invest.,* **124**, 2014, 2550-2559.
3. **Bjørbaek, C., B. B. Kahn.** Leptin signaling in the central nervous system and the periphery – *Recent Prog. Horm. Res.,* **59**, 2004, 305-331.
4. **Bouret, S. G., S. J. Draper, R. B. Simerly**. Trophic action of leptin on hypothalamic neurons that regulate feeding – *Science*, **304**, 2004, 108-110.
5. **Carreira, B. P., M. I. Morte, A. Inácio, G. Costa, J. Rosmaninho-Salgado, F. Agasse, A. Carmo, P. Couceiro, P. Brundin, A. F. Ambrósio, C. M. Carvalho, I. M. Araújo.** Nitric oxide stimulates the proliferation of neural stem cells bypassing the epidermal growth factor receptor – *Stem Cells*, **28**, 2010, 1219-1230.
6. **Costa, M. R., F. Ortega, M. S. Brill, R. Beckervordersandforth, C. Petron, T. Schroeder, M. Götz, B. Berninger.** Continuous live imaging of adult neural stem cell division and lineage progression in vitro – *Development*, **138**, 2011, 1057-1068.
7. **Dicou, E., S. Attoub , P. Gressens.** Neuroprotective effects of leptin in vivo and in vitro – *Neuroreport*, **12**, 2001, 3947-3951.
8. **Ditlevsen, D. K., L. B. Kohler, V. Berezin, E. Bock.** Cyclic guanosine monophosphate signalling pathway plays a role in neural cell adhesion molecule-mediated neurite outgrowth and survival – *J. Neurosci. Res.*, **85**, 2007, 703-711.
9. **El-Falougy, H., J. Benuska.** History, anatomical nomenclature, comparative anatomy and functions of the hippocampal formation – *Bratisl. Lek. Listy,* **107**, 2006, 103-106.
10. **Eriksson, P. S., E. Perfilieva, T. Björk-Eriksson, A. M. Alborn, C. Nordborg, D. A. Peterson, F. H. Gage.** Neurogenesis in the adult human hippocampus – *Nat. Med.,* **11**, 1998, 1313-1317.
11. **Fei, H., H. J. Okano, C. Li, G. H. Lee, C. Zhao, R. Darnell, J. M. Friedman.** Anatomic localization of alternatively spliced leptin receptors (Ob-R) in mouse brain and other tissues – *Proc. Natl. Acad. Sci. USA*, **13**, 1997, 7001-7005.
12. **Garthwaite, J.** Concepts of neural nitric oxidemediated transmission – *Eur. J. Neurosci.,* **27**, 2008, 2783-2802.
13. **Harvey, J.** Leptin regulation of neuronal excitability and cognitive function – *Curr. Opin. Pharmacol.,* **7**, 2007, 643-647.
14. **Harvey, J., N. Solovyova, A. Irving.** Leptin and its role in hippocampal synaptic plasticity – *Prog. Lipid Res.,* **45**, 2006, 369-378.
15. **Hope, B. T., G. J. Michael, K. M. Knigge, S. R. Vincent.** Neuronal NADPH diaphorase is a nitric oxide synthase – *Proc. Natl. Acad. Sci., USA*, **88**, 1991, 2811-2814.
16. **Kohgami, S., T. Ogata, T. Morino, H. Yamamoto, P. Schubert.** Pharmacological shift of the ambiguous nitric oxide action from neurotoxicity to cyclic GMP-mediated protection – *Neurol. Res.,* **32**, 2010, 938-944.
17. **Luo, C. X., X. Jin, C. C. Cao, M. M. Zhu, B. Wang, L. Chang, Q. C. Zhou, H. Y. Wu, D. Y. Zhu.** Bidirectional regulation of neurogenesis by neuronal nitric oxide synthase derived from neurons and neural stem cells – *Stem Cells*, **28**, 2010, 2041-2052.
18. **Martins, I., S. Gomes, R. O. Costa, L. Otvos, C. R. Oliveira, R. Resende, C. M. Pereira.** Leptin and ghrelin prevent hippocampal dysfunction induced by Aβ oligomers – *Neuroscience*, **241**, 2013, 41-51.
19. **Marwarha, G., R. P. Jaya, J. Schommer, B. Dasari, O. Ghribi.** Molecular interplay between leptin, insulin-like growth factor-1, and β-amyloid in organotypic slices from rabbit hippocampus – *Mol. Neurodegener.*, **41**, 2011.
20. **Münzberg, H., C. D. Morrison.** Structure, production and signaling of leptin – *Metabolism*, **64**, 2015, 13-23.
21. **Seri, B., J. M. Garcia-Verdugo, L. Collado-Morente, B. S. McEwen, A. Alvarez-Buylla.** Cell types, lineage, and architecture of the germinal zone in the adult dentate gyrus – *J. Comp. Neurol.*, **478**, 2004, 359-378.
22. **Sik, A., M. Penttonen, G. Buzsaki.** Interneurons in the hippocampal dentate gyrus – an in vivo intracellular study – *Eur. J. Neurosci.,* **9**, 1997, 573-588.
23. **Shanley, L. J., A. J. Irving, J. Harvey.** Leptin enhances NMDA receptor function and modulates hippocampal synaptic plasticity – *J. Neurosci.,* **21**, 2001, RC186.

24. **Struble, R., N. L. Desmond, W. B. Levy**. Anatomical evidence for interlamellar inhibition in the fascia dentata – *Brain Res.,* **152**, 1978, 580-585.
25. **Tartaglia, L. A.** The leptin receptor – *J. Biol. Chem.,* **272**, 1997, 6093-6096.
26. **Vincent, S. R., H. Kimura.** Histochemical mapping of nitric oxide synthase in the rat brain – *Neuroscience,* **46**, 1992, 755-784.
27. **Weng, Z., A.P. Signore, Y. Gao, S. Wang, F. Zhang, T. Hastings, X. M. Yin, J. Chen.** Leptin protects against 6-hydroxydopamine-induced dopaminergic cell death via mitogen-activated protein kinase signaling – *J. Biol. Chem.* **282**, 2007, 34479-34491.
28. **Zhang, F., M. B. Basinski, J. M. Beals, S. L. Briggs, L. M. Churgay, D. K. Clawson, R. D. DiMarchi, T. C. Furman, J. E. Hale, H. M. Hsiung, B. E. Schoner, D. P. Smith, X. Y. Zhang, J. P. Wery, R. W. Schevitz.** Crystal structure of the obese protein leptin-E100 – *Nature*, **387**, 1997, 206-209.
29. **Zhang, F., S. Wang, A. P. Signore, J. Chen.** Neuroprotective effects of leptin against ischemic injury induced by oxygen-glucose deprivation and transient cerebral ischemia – *Stroke*, **38**, 2007, 2329-2336.

Institute of Experimental Morphology, Pathology and Anthropology with Museum
Bulgarian Anatomical Society

Acta morphologica et anthropologica, 26 (3-4)
Sofia ● 2019

Histoepidemiological Study of Prostatic Epithelial Metaplasia's Association in Transurethral Resection of the Prostate

Maria Koleva[2], Dorian Dikov[1,2]*

[1] *Service d'Anatomie et Cytologie Pathologiques, Groupement Hospitalier de l'Est Francilien, Hôpital de Jossigny, France*
[2] *Department of General and Clinical Pathology, Medical University – Plovdiv, Bulgaria*

*Corresponding author e-mail: mariya.kolevaivanova@gmail.com

The study examined the relationships and associations of selected pathological features (prostatic epithelial metaplasia – PEM) in a single transurethral resection of the prostate (TURP) material. An additional immunohistochemical investigation with p63 was made. PEM was found in 60.6% : squamous metaplasia in 11.5%; urothelial metaplasia in 27.9%; mucinous metaplasia in 4.9%; eosinophilic metaplasia in 55.7% and basal cell hyperplasia (BCH) in 39.3%. All the cases with PEM (100%) are associated with benign prostate hyperplasia (BPH) and variable degree of histologic prostatitis (HP). Expression of p63 is found in all investigated cases in all types of PEM and BCH.

This is the first attempt to investigate the associations between PEM in the context of basic pathology in TURP-material and enrich the available information about the histoepidemiology of prostatic metaplasias. The observed combination between PEMs and their association with BPH and HP in 100% probably reflects the final stage of a single morphogenetic chain.

Key words: prostate, metaplasia, transurethral resection, prostatitis.

Introduction

Metaplasia is a reversible change in which one adult cell type is replaced by another adult cell type, related to the first one [13]. It is a sign of tissue adaptation towards changed conditions or requirements to them.

The prostatic epithelium has an interesting but limited repertoire of responses against injury. These responses include a variety of metaplastic and proliferative lesions that may mimic prostatic adenocarcinoma (PCa) [1].

Prostatic epithelial metaplasia (PEM) is usually a secondary to inflammation, alteration in the hormonal milieu, or injury. The most common lesions in the everyday practice of the pathologists are – four major categories of PEM (squamous, urothelial, mucinous and eosinophilic) and basal cell hyperplasia (BCH). The diagnostic significance of PEM resides in its pseudoneoplastic status, but these metaplastic proliferations are not precursors for prostatic carcinoma [1, 9].

The frequency of PEM, investigated in specimens of prostatic needle biopsies, total prostatectomies, transurethral resection of the prostate (TURP) and autopsies, have been described up to now [1, 9]. Less well studied is their combination with benign prostatic hyperplasia (BPH) and National Institutes of Health (NIH) – category IV prostatitis (so-called histologic prostatitis (HP)) [1, 9, 12, 15].

No studies about the association of PEM in series of a single prostate specimen (TURP) are available so far.

The aim of the current investigation is to examine some histoepidemiological relationships of PEMs in the patient population from a general hospital, in the context of the basic prostate pathology (BPH, HP, PCa and BCH) in TURP-material.

Materials and Methods

A retrospective record review was performed on 61 TURP – specimens obtained at St. George University Hospital of Plovdiv, Bulgaria for the period of one year (2014). The study was approved by the Ethics Committee of the hospital. The age of the patients ranged from 54 to 88 years (mean 72.2 years). The leading clinical symptoms covered the so-called prostatic syndrome typical for BPH and represented a basic indication for surgical intervention. Neither radiation and hormonal treatment nor prostatic surgery and cryosurgery before TURP were performed. All specimens were routinely fixed in 10 % buffered formalin and embedded in paraffin for histological evaluation. Tissue sections from 1 to 10 paraffin blocks for each case, stained with hematoxylin-eosin (HE) and hematoxylin-phloxine-saffron (HPS), were examined retrospectively independently by two pathologists (MK and DD).

Simultaneously, BPH, PCa, HP [12, 14], and BCH were also evaluated. 3 cases of each PEM type and BCH were selected (15 in total). Standard 4-µm-thick consecutive tissue sections were cut and stained immunohistochemically with p63 (clone 4A4 ready-to-use; Ventana Medical Systems, Tucson, AZ).

Results

PEM is found in 37/61 cases (60.6%), localized in the transition zone of the prostate, seen in all investigated TURP specimens. Squamous metaplasia was detected in 7/61 (11.5%) cases. The changes may be focal or diffuse, appearing as intraductal syncytial aggregates of flattened cells with abundant eosinophilic cytoplasm or cohesive aggregates of glycogen-rich clear cells with shrunken hyperchromatic nuclei (**Fig.1A**). Keratinization is unusual except at the edge of infarcts or areas of acute inflammation. When it is in a combination squamous metaplasia is associated most commonly with urothelial metaplasia in 3/7 (42.8%) cases. Urothelial metaplasia was detected in 17/61 (27.9%) cases. Urothelial metaplasia occurs in the medium-sized and small ducts in the prostate beyond the normal transitional-columnar junction that apparently arises as a result of metaplastic change. It is difficult to identify because of variable location of the normal transitional-columnar junction. Microscopically, usually only a few glands are involved in a single focus, but extensive involvement may also be observed. The glands exhibit proliferation of elongated urothelial cells beneath a bland-appearing luminal secretory cell layer (**Fig. 1B**). When it is in a combination urothelial metaplasia is associated most commonly with squamous metaplasia, in 3/17 (17.6%) cases.

Mucinous metaplasia was detected in 3/61 (4.9%). Mucinous metaplasia refers to clusters of tall columnar cells or goblet cells with cytoplasm filled with blue-grey

mucin PAS/alcian blue positive that are infrequently observed in the prostatic acinar epithelium (**Fig. 1C**). We do not observe a combination of this type of metaplasia with another type.

Eosinophilic metaplasia was detected in 34/61 (55.7%) (consistent with previous studies) [11]. The apical portions of secretory epithelial cells were filled with eosinophilic cytoplasmic granules with different size (**Figs. 1D and 2A**). In 13/34 (38.2%) it is a separate process. Eosinophilic metaplasia is combined with urothelial metaplasia in 17/34 (50%), with squamous metaplasia in 7/34 (20.6%) and with BCH in 24/34 cases (70.6%)

Fig. 1A

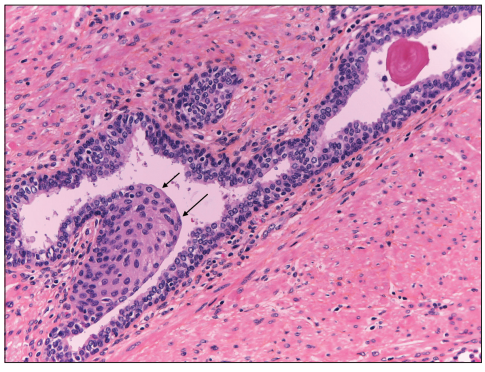

Fig. 1B

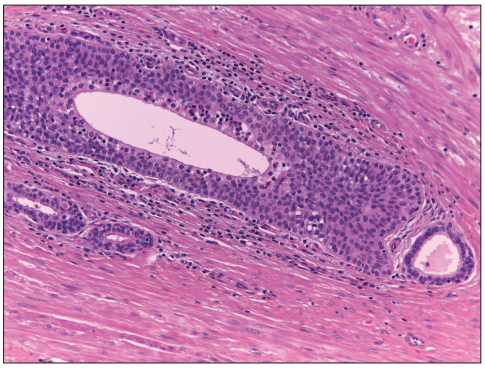

Fig. 1C

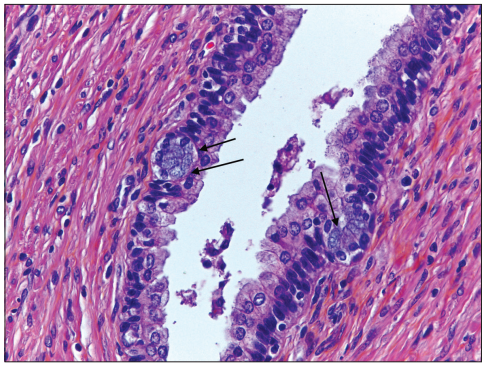

Fig. 1D

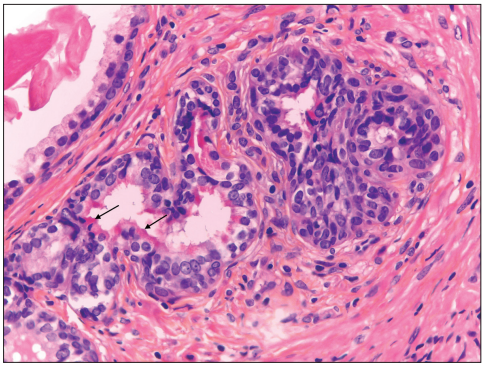

Fig. 1. Prostatic epithelial metaplasia: **(A)** Squamous metaplasia in ductal secretory epithelium on the left side of the image (arrows). **(B)** Urothelial metaplasia in ductal/secretory epithelium; moderate peri- and intra-glandular chronic histologic prostatitis are also observed. **(C)** Mucinous metaplasia (arrows) in ductal secretory epithelium. **(D)** Eosinophilic metaplasia is found in ductal and acinar structures on the left side of the image (arrows) in association with basal cell hyperplasia on the right side of the image: Hematoxylin-phloxine-saffron, (A) and (B) x200; (C) and (D) x400.

BCH was detected in 24/61 (39.3%). In all cases with BCH (100%), it is combined with other type PEM: with squamous metaplasia in 7/24 cases (29.2%), with urothelial metaplasia in 8/24 cases (33.3%), and with eosinophilic metaplasia in 24/24 cases (100%).

The coincidence of quadriple lesion: triple PEM (squamous, urothelial and eosinophilic) and BCH was observed in 3/61 cases (4.9%) (**Fig. 2A**).

Expression of p63 is found in all investigated cases and in all types of PEM and BCH (**Fig. 2B**). Both BCH and HP (of moderate to high grade with glandular, periglandular and stromal localization) were noted in all cases of PEM (100%) (**Figs. 1B and 2A**). There is no association with PCa.

Fig. 2A **Fig. 2B**

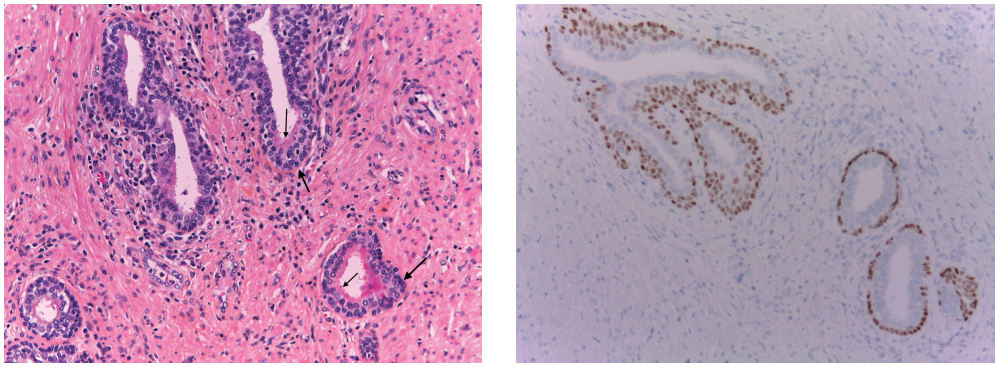

Fig. 2. Prostatic epithelial metaplasia's association in a serial sections: (**A**) Association between eosinophilic metaplasia (thin arrows) and basal cell hyperplasia (thick arrows); moderate periglandular chronic histologic prostatitis are also observed. (**B**) p63 expression in a focus of eosinophilic metaplasia (on the right side of the image) and basal cell hyperplasia (on the left side of the image): (A) Hematoxylin-phloxine-saffron, ×200 and (B) immunohistochemistry anti-p63, x200.

Discussion

Throughout adult life, new developmental commitment of adult stem cells causes frequent metaplastic conversion in some organs. These reversible epithelial replacements are almost always observed in association with chronic inflammation and persistent irritation [8].

Inflammatory mediators (cytokines) and other soluble factors released by both epithelial and inflammatory cells might alter the transcription-factor expression profile of stem cells and lead to the development of metaplasia [8].

The frequency of PEM varies from 0.6 (urothelial) to 94% (squamous metaplasia) depending on the material being investigated [1, 9].

Our results on TURP-specimens confirm this frequency, as we find PEM and BCH in 60.6% and 39.3% of TURP-cases.

Additionally, we show that the associations between different types of PEM is a frequent finding in TURP-specimens. On the other hand, PEM is associated always with BPH, HP and BCH.

PEM and BCH results from a variety of insults to the prostate, including acute and chronic inflammation, infarction, radiation therapy, and androgen deprivation therapy [15].

Squamous metaplasia commonly involves the prostatic urethra in patients with an indwelling catheter. It is a specific phenotype in response to estrogen, and ER α is required to mediate this response [2]. Also, transitional metaplasia may occur in the medium-sized and small ducts in the prostate, sometimes in association with inflammation [15].

Mucinous metaplastic cells in the prostate were found in the foci of atrophy, urothelial cell metaplasia, BCH and BPH [7]. In our single case, we did not find any combination with other types of PEM.

There are single observations showing variable degree of association of eosinophilic metaplasia with chronic inflammation [3, 11]. Cheng et al. describe eosinophilic metaplasia as a lesion that is frequently encountered in inflammatory conditions, suggesting a host response to an altered cellular milieu [6]. Gaudin P et al. describe eosinophilic metaplasia in benign prostate in 32% of the patients with post-radiation therapy for prostatic carcinoma, in close association with chronic inflammation [6]. We published two case reports revealing the association of chronic prostatic inflammation (nonspecific granulomatous prostatitis) with eosinophilic metaplasia in TURP-material [4, 5]. In the present study, we find a very common combination of eosinophilic metaplasia with other types of PEM, most commonly eith the urothelial metaplasia (50%) and BCH (70.6%).

Conclusion

Epithelial metaplasia is in general the result of an adaptive replacement of the cells sensitive to noxious environmental agents by other cells more capable of withstanding such injury [16]. Selecting histologically investigated by us patients (neither radiation and hormonal treatment nor prostatic surgery before TURP), our results indicate that the main pathogenetic factors for PEM are acute and chronic prostate inflammation and BPH. The expression of p63 by all types of PEM and BCH, as well as the frequent combination between them is in favour of stress factors, the transitional zone of the prostate glands increases due to the proliferation of p63+ basal progenitor stem cells. Similar to Barrett's oesophagus molecular pathogenesis, it could be speculated that there is an activation of specific transcription factors leading to the expression of an different metaplastic-type of genes which gives rise to PEM [10]. When the new genotype is more specific – squamous and urothelial metaplasias (direct metaplasia) are likely to develop, and when it is differentiated in a direction other than normal, mucinous or eosinophilic metaplasias (indirect, phenotypical type of metaplasia) develop [13].

References

1. **Bostwick, D. G., D. Hull, J. Ma, D. Hossain**. Nonneoplastic metaplasia. – In: *Urological surgical pathology: Nonneoplastic diseases of the prostate* (Eds. D. G. Bostwick, L. Cheng), Philadelphia, PA, USA, Elsevier Saunders Publishers, 2014, 379.
2. **Chen, M., C. R. Yeh, H. C. Chang, S. Vitkus, X. Q. Wen, N. A. Bhowmick, A. Wolfe, S. Yeh.** Loss of epithelial oestrogen receptor alpha inhibits oestrogen-stimulated prostate proliferation and squamous metaplasia via in vivo tissue selective knockout models. – *J. Pathol*., **226**, 2012, 17-27.
3. **Cheng, L, G. T. MacLennan, F. W. Abdul-Karim, A. Lopez-Beltran, R. Montironi.** Eosinophilic metaplasia of the prostate: a newly described lesion distinct from other eosinophilic changes in prostatic epithelium. – *Anal. Quant. Cytol. Histol.,* **30**, 2008, 226-230.
4. **Dikov, D., M. Koleva, J. Peshev, V. Belovejdov.** Nonspecific granulomatous prostatitis in association with eosinophilic epithelial metaplasia and prostatic adenocarcinoma: a case report. – *Indian J. Pathol. Microbiol.,* **60**, 2017, 409-411.
5. **Dikov, D., I. Vassilev, J. Dimitrakov**. Nonspecific granulomatous prostatitis with calculous ductal ectasia and extensive Paneth cell-like epithelial metaplasia. Case report. – *APMIS*. **113**, 2005, 564-567.
6. **Gaudin, P. B., M. J. Zelefsky, S. A. Leibel, Z. Fuks, V. E. Reuter.** Histopathologic effects of free-dimensional conformal external beam radiation therapy on benign and malignant prostate tissue. – *Am. J. Surg. Pathol*., **23**, 1999, 1021-1031.
7. **Grignon, D. J., F. P. O'Malley**. Mucinous metaplasia in the prostate gland. – *Am. J. Surg. Pathol.*, **17**, 1993, 287-290.

8. **Herfs, M., P. Hubert, P. Delvenne**. Epithelial metaplasia: adult stem cell reprogramming and (pre) neoplastic transformation mediated by inflammation? – *Trends Mol. Med*., **15**, 2009, 245-253.
9. **Humphrey, P.** Metaplasia. – In: *Urological Pathology: Nonneoplastic diseases of the prostate and seminal vesicles* (Eds. A. Amin, D. Grignon, J. Srigley, J. Eble J), Philadelphia, PA, USA: Wolters Kluwer/Lippincott Williams & Wilkins Publishers, 2013, 518-526.
10. **Jiang, M., H. Li , Y. Zhang, Y. Yang, R. Lu, K. Liu, S. Lin, X. Lan, H. Wang, H. Wu, J. Zhu, Z. Zhou, J. Xu, D. K. Lee, L. Zhang, Y. C. Lee, J. Yuan, J. A. Abrams, T. C. Wang, A. R. Sepulveda, Q. Wu, H. Chen, X. Sun, J. She, X. Chen, J. Que.** Transitional basal cells at the squamous-columnar junction generate Barrett's oesophagus. – Nature, **26**, 2017, 529-533.
11. **Koleva, M., D. Dikov, V. Belovejdov, V. Sarafian**. Eosinophilic metaplasia in transurethral resection of the prostate. – *Indian J. Pathol. Microbiol.,* 2019 (in press)
12. **Krieger, J. N., L. Nyberg, J. C. Nickel**. NIH consensus definition and classification of prostatitis. – JAMA, **282**, 1999, 236-237.
13. **Lugo, M., P. B. Putong.** Metaplasia. An overview. – *Arch. Pathol. Lab. Med.,* **108**, 1984, 185-189.
14. **Nickel, J. C., L. D. True, J. N. Krieger, R. E. Berger, A. H. Boag, I. D. Yong.** Consensus development of a histopathological classification system for chronic prostatic inflammation. – *BJU Int.,* **87**, 2001 797-805.
15. **Petraki, C. D., C. P. Sfikas.** Histopathological changes induced by therapies in the benign prostate and prostate adenocarcinoma. – *Histol. Histopathol*., **22**, 2007, 107-118.
16. **Rubio, C. A., Y. Kato.** Classification of vacuolated cells in the gastric mucosa. – *J. Surg. Oncol*., **34**, 1987, 128-132.

Institute of Experimental Morphology, Pathology and Anthropology with Museum
Bulgarian Anatomical Society

Acta morphologica et anthropologica, 26 (3-4)
Sofia ● 2019

ACE and ACE2 Protein Expression Changes with Tumour Grade in Invasive Ductal Carcinomas.

Desislava Ankova, Despina Pupaki, Pavel Rashev*

Institute of Biology and Immunology of Reproduction "Acad. Kiril Bratanov", Bulgarian Academy of Sciences, Sofia, Bulgaria

* Corresponding author e-mail: dessislava_ankova@abv.bg

Renin-angiotensin system is mainly known as a regulator of cardiovascular homeostasis. The aim of the present study was to determine the immunohistochemical expression of angiotensin-converting enzyme and angiotensin-converting enzyme 2 in non-tumorous breast tissue and in G1, G2 and G3 invasive ductal carcinomas, using immunoperoxidase method on formalin fixed paraffin embedded tissue sections from 10 samples of non-tumorous breast tissue and 30 cases of invasive ductal carcinoma. It was found that ACE was located only in ductal epithelium, while in invasive carcinomas, stromal cells were also positive for ACE. Intensity of staining increased with tumour grade. None of the examined invasive carcinomas showed positive staining for ACE2 in tumour epithelial cells, but weak staining was observed in stromal cells adjacent to tumour epithelial cells. In higher grade tumours, less stromal cells were positive for ACE2. These observations suggest that ACE and ACE2 may be involved in the pathogenesis of breast cancer.

Key words: breast cancer, ACE, ACE2

Introduction

The renin-angiotensin system (RAS) consists of systemic and local parts. The systemic RAS has been mainly perceived as an important regulator of cardiovascular homeostasis and as a key factor in the pathogenesis of hypertension and atherosclerosis. The local renin-angiotensin systems observed in various organs act mainly over a limited area. The first element of RAS is liver-derived angiotensinogen, a glycoprotein cleaved by renin to generate decapeptide angiotensin I (Ang I). The angiotensin-converting enzyme (ACE) is a protease capable of cleaving the inactive Ang I to active octapeptide angiotensin II (Ang II), which is regarded as the most active regulator of the systemic RAS [17]. The actions of Ang II are mediated predominantly through its specific receptors, Ang II receptor type 1 (AT1R) and Ang II receptor type 2 (AT2R) [6]. Most of the known effects of Ang II – such as its stimulation of angiogenesis, cellular proliferation, inflammatory and antiapoptotic responses – occur via AT1R [12, 13]. AT2R-mediated actions have been shown to oppose those elicited by AT1R [27, 29]. However, several lines of evidence

suggest that signalling via AT2R may also be proangiogenic and proinflammatory [26, 30]. Although Ang II is the most important effector of the RAS, there are also other products of aminopeptidase activity of ACE and angiotensin converting enzyme 2 (ACE2), such as angiotensin III (Ang III), angiotensin IV (Ang IV), and angiotensin-(1-7) [(Ang-(1-7)], which all show potent biological activity [19, 31, 16, 24]. Ang-(1-7) is an endogenous 7-amino-acid peptide hormone that exerts antiproliferative activity and counteracts the vasodilative and apoptotic properties of Ang II [2]. The specific effects of Ang-(1-7) are mediated by a recently identified receptor, the *mas* oncogene product (MAS) [14]. Ang-(1-7) may be formed from Ang I through cleavage of angiotensin-(1-9), or it may be generated directly from Ang II by the enzymatic activity of ACE2. ACE2, discovered almost a decade ago, is an ACE homologue and a zinc-metallopeptidase. It has been suggested that ACE2 may oppose the effects of ACE on the organ and tissue levels through the generation of Ang-(1-7) by the local RAS. The local RAS systems have been detected in various species and in diverse organs, such as the brain, the testes, the prostate, the pancreas, the adrenal gland, and the mammary gland [7, 11, 15, 21, 22, 25, 28]. The local RAS systems enable the generation of Ang II, and may therefore exert biological activity on an organ level. Recent studies suggest that, on a tissue level, the local RAS may influence cell proliferation and apoptosis, which are considered crucial in carcinogenesis [1, 18].

Invasive ductal carcinoma is the most common type of breast cancer. According to the degree of tubule formation, nucleus pleomorphism and mitotic index, invasive carcinomas are classified as well-differentiated (low-grade) – Grade 1 (G1), moderately differentiated (medium-sized) – Grade 2 (G2) and low-differentiated (high-grade) – Grade 3 (G3). Data on ACE and ACE2 protein expression in breast carcinomas are scarce and in none of these studies tumour grade was taken into account.

The aim of the current study was to investigate ACE and ACE2 protein expression in non-tumorous breast tissue and Grade 1 (G1), Grade 2 (G2) and Grade 3 (G3) invasive ductal carcinomas.

Materials and Methods

Thirty samples of invasive ductal carcinoma (10 cases of highly differentiated (G1) ductal carcinoma, 8 cases of moderately differentiated (G2) ductal carcinoma and 12 cases of low-differentiated (G3) ductal carcinoma) and 10 samples from non-tumorous breast tissue were included in the study.

Tissue samples were fixed in 10% buffered formalin, dehydrated and embedded in paraffin. Paraffin sections, 5 μm thick, were stained with hematoxylin and eosin for histopathological evaluation.

Immunohistochemistry was performed on paraffin embedded 5 μm tissue sections, following antigen retrieval in Citrate Buffer, pH 6.0 (ScyTek Laboratories Inc.,USA) at 95°C for 20 min. Endogenous peroxidase activity was blocked with 3% H_2O_2 for 10 min at room temperature. Subsequently, the sections were washed in TTBS (tris-buffered saline + 0,05% Tween 20) and incubated with primary antibodies against ACE (1:500, rabbit monoclonal, Abcam), ACE2 (1:150, Rabbit monoclonal, Abcam). Biotin-Streptavidin HRP detection system (ScyTek Laboratories Inc., USA) with DAB as chromogen was used.

Results

Immunohistochemical examination in non-tumorous tissue showed weak staining for ACE located only in ductal epithelial (**Fig. 1 a**). In invasive carcinomas, tumour epithelial cells were also stained, but intensity of staining increased in higher grade carcinomas (Fig. 1 c, d) with the most intense staining being observed in G3. While reaction for ACE was absent in stromal cells of non-tumourous tissue, in G1 invasive carcinomas staining reaction was observed in single stromal cells (**Fig. 1 b**) and in G2 and G3 invasive carcinomas there was intensive staining of stromal cells (**Fig. 1 c, d**).

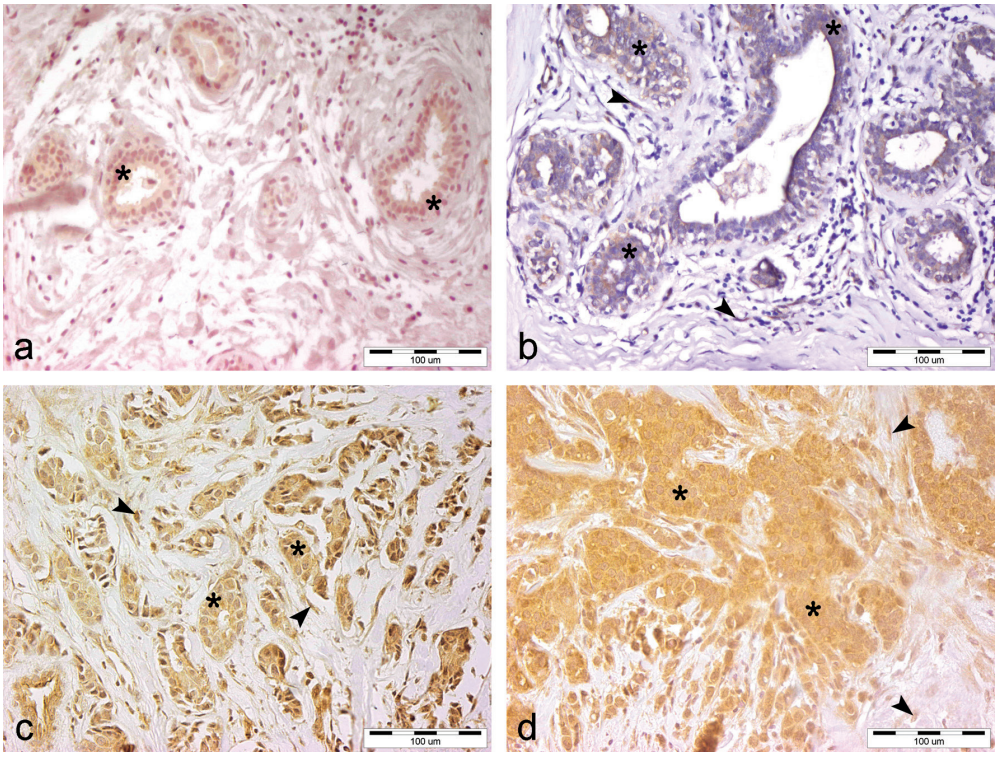

Fig. 1. Immunohistochemical localization of ACE in a) non-tumourous breast tissue; b) invasive highly differentiated (G1) ductal carcinoma; c) invasive moderately differentiated (G2) ductal carcinoma and d) invasive low differentiated (G3) ductal carcinoma. Positive staining for ACE in epithelial cells (asterisk) and stromal cells (arrowhead).

In non-tumourous breast tissue, ACE2 was predominantly located in ductal epithelium, showing intense apical staining and weaker cytoplasmic reaction, as well as in some of the stromal cells (**Fig. 2 a**). None of the examined invasive carcinomas showed positive staining for ACE2 in tumour epithelial cells, but weak staining was observed in stromal cells adjacent to tumour epithelial cells (**Fig. 2 b, c, d**). In higher grade tumours less stromal cells were positive.

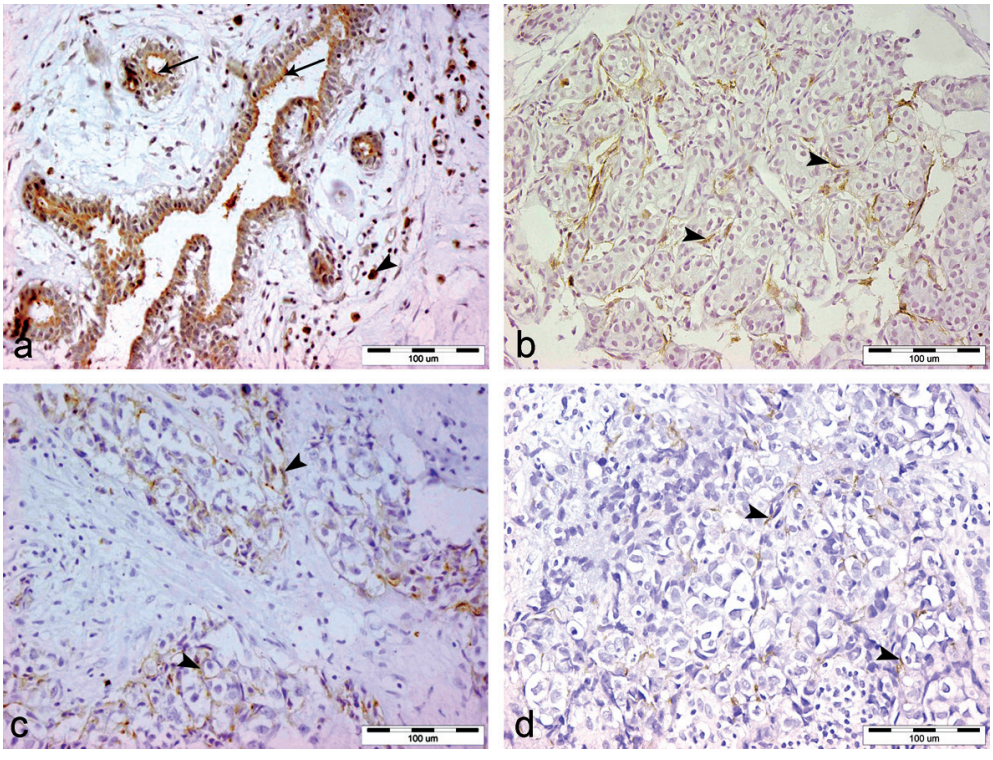

Fig. 2. Immunohistochemical localization of ACE2 in a) non-tumourous breast tissue; b) invasive highly differentiated (G1) ductal carcinoma; c) invasive moderately differentiated (G2) ductal carcinoma and d) invasive low differentiated (G3) ductal carcinoma. Apical reaction in ductal epithelium (arrow) and in stromal cells (arrowhead).

Discussion

Breast cancer is the most common spontaneously diagnosed malignancy and one of the leading causes of death in women. The role of the renin-angiotensin system (RAS) in the development of various malignancies has been extensively investigated in recent years and its impact and involvement in tumour growth, cell proliferation and migration have been demonstrated [5].

Current study showed a different trend in the expression of ACE and ACE2 in different grades of invasive ductal carcinomas. With the decrease in differentiation, ACE protein expression was increased, whereas for ACE2 an inverse relationship was observed. Increased ACE expression has been reported to be associated with enhanced tumour progression and metastasis, including in breast cancer. Similar correlation has been found in other types of tumours. Han C. et al. have reported that using qRT-PCR they had found significant increase in ACE expression in laryngeal cancer, which had been associated with unfavourable prognosis and higher risk of tumour metastases [10]. However, the level of ACE expression in malignant tumour cells does not always correlate with the intensity of Ang II formation due to the active chymase regulating the ACE-independent Ang II formation pathway [32].

Our immunohistochemical analysis of ACE2 showed lack of protein expression in tumour epithelial cells and reduction in the staining of the stromal cells in these tumours

with the increase of their grade. This is logical, since ACE2 is responsible for the conversion of Ang II to Ang-(1-7), which stimulates apoptosis and suppresses cell proliferation, exerting its regulatory effect via the MAS1 receptor. According to some authors, the reduction of ACE2 expression in breast cancer is considered to be a marker of severe disease with a high risk of metastases. Increased expression of the ACE2/Ang-(1-7)/MAS1 axis inhibits cell migration and invasion *in vivo* and *in vitro* in breast cancer, while the reduction in its expression enhances breast cancer metastases by activating PAK1/NF-κB/Snail1 pathways [4,33]. It has been reported that the level of expression of ACE2 negatively correlates with the intensity of neoangiogenesis in non-small cell lung carcinoma. The ACE2/Ang-(1-7)/MAS1 axis inhibits VEGFA secretion, while matrix metalloproteinases MMP-2 and MMP-9, help limit neoangiogenesis, increase tumour sensitivity to cytostatic drugs, and reduce the risk of metastases [3, 9]. Numerous studies have shown that hypoxia is a distinctive feature of solid tumours and that inadequate oxygen supply contributes to the pro-oncogenic effect of ACE/Ang II at the background of reducing the effects of the ACE2/Ang-(1-7)/MAS1 axis [8]. There is enough evidence that support the inclusion of Ang-(1-7) in clinical practice as a treatment option of triple-negative breast cancer [14, 20].

Conclusions

In conclusion, the present study demonstrated a different trend in ACE and ACE2 expression. ACE protein expression was increased in higher grade tumours, whereas the opposite was observed for ACE2 protein expression. These results further support the role of ACE and ACE2 in the progression of invasive ductal carcinomas and may be useful in the development of effective therapies using ACE inhibitors.

References

1. **Ager, E., J. Neo, C. Christophi.** The renin-angiotensin system and malignancy. – *Carcinogenesis*, **29**, 2008, 1675–1684.
2. **Campbell, D. J.** Vasopeptidase inhibition: A double-edged sword? – *Hypertension*, **41**, 2003, 383–9.
3. **Cheng, Q., L. Zhou, J. Zhou, H. Wan, Q. Li, Y. Feng.** ACE2 overexpression inhibits acquired platinum resistance induced tumor angiogenesis in NSCLC. – *Oncol. Rep*., **36**(3), 2016, 1403–1410.
4. **Clarke, N. E., A. J. Turner.** Angiotensin-ConvertingEnzyme2: The first Decade. – *Hyperten*, **12**, 2012, 307315.
5. **de Alvarenga, E.C., M. de Castro Fonseca., C. Coelho Carvalho, C. C. Carvalho, R. M. Florentino, A. França, E. Matias, P. B. Guimarães, C. Batista, V. Freire, A. K. Carmona, J. B. Pesquero, A. M. de Paula, G. Foureaux, M. F. Leite.** Angiotensin Converting Enzyme Regulates Cell Proliferation and Migration. – *PLoS One*, **11**(12), 2016, e0165371.
6. **Dinh, D. T., A. G., Frauman, S. P. Andrade.** Angiotensin receptors:distribution, signalling and function. – *Clin. Sci. (Lond.),* **100**, 2001, 481–492.
7. **Fallo, F., M. Pistorello, F. Pedini, D. D'Agostino, F. Mantero, M. Boscaro.** In vitro evidence for local generation of renin and angiotensin II/III immunoreactivity by the human adrenal gland. – *Acta Endocrinol.,* **125**, 1991, 319–330.
8. **Fan, L., Y. Feng, H. Y. Wan, L. Ni, Y. R. Qian, Y. Guo, Y. Xiang, Q. Y. Li.** Hypoxia induces dysregulation of local renin-angiotensin system in mouse Lewis lung carcinoma cells. – *Genet. Mol. Res.,* **13**(4), 2014, 10562–10573.
9. **Feng, Y., L. Ni., H. Wan, L. Fan, X. Fei, Q. Ma, B. Gao, Y. Xiang, J. Che, Q. Li**. Overexpression of ACE2 produces antitumor effects via inhibition of angiogenesis and tumor cell invasion in vivo and in vitro. – *Oncol. Rep.,* **26**, 2011, 1157–1164.
10. **Han, C., W. Ge.** Up-regulation of angiotensin-converting enzyme (ACE) enhances cell proliferation and predicts poor prognosis in laryngeal cancer. – *Med. Sci. Monit.,* **22**, 2016, 4132–4138.

11. **Leung, P. S., W. P. Chan, T. P. Wong, C. Sernia.** Expression and localization of renin-angiotensin system in the rat pancreas. – *J. Endocrinol.,* **160**, 1999, 13–19.
12. **Leung, P. S., P. M. Suen, S. P. Ip, C. K. Yip, G. Chen, P. B. Lai.** Expression and localization of AT1 receptors in hepatic Kupffer cells: its potential role in regulating a fibrogenic response. – *Regul. Pept.,* **116**, 2003, 61–69.
13. **Levy, B. I.** Can angiotensin II type 2 receptors have deleterious effects in cardiovascular disease? Implications for therapeutic blockade of the renin–angiotensin system. – *Circulation,* **109**, 2004, 8–13.
14. **Luo, Y., E. Tanabe, M. Kitayoshi, Y. Nishiguchi, R. Fujiwara, S. Matsushima, T. Sasaki, T. Sasahira, Y. Chihara, D. Nakae, K. Fujii, H. Ohmori, H. Kuniyasu.** Expression of MAS1 in breast cancer. – *Cancer Sci.,* **106**(9), 2015, 1240–1248.
15. **O'Mahony, O. A., S. Barker, J. R. Puddefoot, G. P. Vinson.** Synthesis and secretion of angiotensin II by the prostate gland in vitro. – *Endocrinology*, **146**, 2005, 392–398.
16. **Ochedalska, A. L., E. Rebas, J. Kunert-Radek, M. C. Fournie-Zaluski, M. Pawlikowski.** Angiotensins II and IV stimulate the activity of tyrosine kinases In estrogen-induced pituitary tumors. – *Biochem. Biophys. Res. Commun.,* **297**, 2002, 931–933.
17. **Peach, M.** Renin-angiotensin system: biochemistry and mechanismof action. – *Physiol. Rev*., **57**, 1977, 313–370.
18. **Piastowska-Ciesielska, A. W., J. Drobnik, J. Zarzyńska, K. Domińska, J. A. Russell, T. Ochędalski.** Influence of myocardial infarction on changes in the expression of angiotensin type 1 receptor in the rat prostate. – *Folia Histochem. Cytobiol*., **49**, 2011, 497–503.
19. **Reaux, A., M. C. Fournie-Zaluski, C. Llorens-Cortes**. Angiotensin III: a central regulator of vasopressin release and blood pressure. – *Trends Endocrinol. Metab*., **12**, 2001, 157–162.
20. **Regulska, K., B. Stanisz, M. Regulski.** The renin-angiotensin system as a target of novel anticancer therapy. – *Curr. Pharm. Des*., **19**, 2013, 7103–7125.
21. **Rice, G. I., D. A. Thomas, P. J. Grant, A. J. Turner, N. M. Hooper.** Evaluation of angiotensin-converting enzyme (ACE), its homologue ACE2 and neprilysin in angiotensin peptide metabolism. – *Biochem. J.,* **383**, 2004, 45–51.
22. **Saavedra, J. M.** Brain and pituitary angiotensin. – *Endocr. Rev.,* **13**, 1992, 329–380.
23. **Santos, R. A., A. J. Ferreira**. Angiotensin-(1-7) and the renin-angiotensin system. – *Curr. Opin. Nephrol. Hypertens.,***16**, 2007, 122–128.
24. **Santos, R. A., M. J. Campagnole-Santos, S. P. Andrade.** Angiotensin-(1-7): an update. – *Regul. Pept.,* **91**, 2000, 45–62.
25. **Santos, R. A., A. C. Simoes e Silva, C. Maric, D. M. Silva, R. P. Machado, I. de Buhr, S. Heringer-Walther, S. V. Pinheiro, M. T. Lopes, M. Bader, E. P. Mendes, V. S. Lemos, M. J. Campagnole-Santos, H. P. Schultheiss, R. Speth, T. Walther.** Angiotensin-(1-7) is an endogenous ligand for the G protein-coupled receptor. – *Proc. Natl. Acad. Sci. U.S.A.,* **100**, 2003, 8258–8263.
26. **Sarlos, R., B. Rizkalla, C. J. Moravski, Z. Cao, M. E. Cooper, J. L. Wilkinson-Berka.** Retinal angiogenesis is mediated by an interaction between the angiotensin type 2 receptor, VEGF, and angiopoietin. – *Am. J. Pathol.,* **163**, 2003, 879–887.
27. **Smith, G. R., S. Missailidis.** Cancer, inflammation and the AT1 and AT2 receptors. – *J. Inflamm. (Lond.)*, 1, 2004, 3.
28. **Tahmasebi, M., S. Barker, J. R. Puddefoot, G. P. Vinson.** Localization of renin-angiotensin system (RAS) components in breast. – *Br. J. Cancer.,* **95**, 2006, 67–74.
29. **Tamarat, R., J. S. Silvestre, M. Durie, B. I. Levy.** Angiotensin II angiogenic effect in vivo involves vascular endothelial growth factor-and inflammation-related pathways. – *Lab. Invest.,* **82,** 2002, 747–756.
30. **Wolf, G., U. Wenzel, K. D. Burns, R. C. Harris, R. A. Stahl, F. Thaiss**. Angiotensin II activates nuclear transcription factor-kappa B through AT1 and AT2 receptors. – *Kidney Int*., **61**, 2002, 1986–1995.
31. **Wright, J. W., L. T. Krebs, J. W. Stobb, J. W. Harding.** The angiotensin IV system: functional implications. – *Front Neuroendocrinol*., **16**, 1995, 23–52.
32. **Xie, G., Y. Liu, Q. Yao, R. Zheng, L. Zhang, J. Lin, Z. Guo, S. Du, C. Ren, Q. Yuan, Y. Yuan.** Hypoxia-induced angiotensin II by the lactate-chymasedependent mechanism mediates radioresistance of hypoxic tumor cells. – *Sci Rep.,* **7**, 2017, 42396.
33. **Yu, C., W. Tang, Y. Wang, Q. Shen, B. Wang, C. Cai, X. Meng, F. Zou**. Downregulation of ACE2/Ang-(1–7)/Mas axis promotes breast cancer metastasis by enhancing store-operated calcium entry. – *Cancer Letters*, **376**(2), 2016, 268-277.

Institute of Experimental Morphology, Pathology and Anthropology with Museum
Bulgarian Anatomical Society

Acta morphologica et anthropologica, 26 (3-4)
Sofia ● 2019

Expression of Hsp27 and Phosphorylated Hsp27 in 8 Weeks Old Human Embryo

Katerina Kavaldzhieva[1], Iliana Buteva-Hristova[2], Dora Marinova[3], Magdalena Pencheva-Demireva[1], Nikola Mladenov[1], Vladislav Lazarov[1], Tzvetanka Markova[4], Nedka Trifonova[1], Dimitrina Dimitrova-Dikanarova[1]*

[1] *Department of Biology, Medical Faculty, Medical University – Sofia, Bulgaria*
[2] *Department of Obstetrics and Gynaecology, St. Sofia Private Hospital, Bulgaria*
[3] *St. Sofia University Hospital for Pulmonary Diseases, Medical University – Sofia, Bulgaria*
[4] *Department of Pharmacology, Medical University – Sofia, Bulgaria*

*Corresponding author e-mail:kkavaldjieva@gmail.com

Heat shock proteins (Hsp) interact with many different molecules and play an important role in various cellular functions such as stress tolerance, protein folding, protein degradation, cytoskeletal integrity, signal transduction, cell cycle. The aim of our work is to register the expression of small heat shock protein (sHsp) member's – Hsp27 and phosphorylated Hsp27 (pHsp27), in different tissues and organs of 8-week old human embryo. Immunohistochemical evaluation of human embryo sample was performed using antibodies against Hsp27 and pHsp27, and polymer-based detection system. Results were read using light microscopy.The Hsp27 had cytoplasmic expression in the encephalon, medulla spinalis, skeletal muscles, heart, liver, intestinal epithelium and muscles. The phosphorylated Hsp27 was expressed in bones and muscles. Our results suggest that both forms of Hsp27 play an important specific role in the proliferation and differentiation of different tissue's cells during human embryo development.

Key words: human embryo, Hsp27, pHsp27, small heat shock proteins, immunohistochemistry

Introduction

During the evolution, the living forms created different mechanisms to protect their cells against stress conditions such as environmental, metabolic, pathophysiologic (e.g., heat, cold, oxidative stress, acidosis, ischemia, toxins, heavy metals) changes and abnormalities. The different types of stress forces inflict damage on the macromolecules (proteins denaturation and aggregation) and the cellular stress response is based on repairing the macromolecule structure without regard to the primary source [15]. The most ancient mechanism of cell protection which emerged in the course of evolution is the synthesis of stress proteins (heat shock proteins – Hsps). Hsps are highly conserved proteins, expressed in all organisms, from prokaryotes to man. They interact with many different molecules and play an important role in diverse cellular functions such as stress tolerance, protein folding, protein degradation, maintaining cytoskeletal integrity, cell cycle, autophagy, cell death, differentiation, signal transduction and development [3].

Heat shock proteins are grouped into five main families based on molecular weight, amino acid sequence and function: 100–110 kDa family; the 83–90 kDa family; the 70 kDa family containing Hsps ranging from 66–78 kDa; the 60 kDa family; and the small Hsps ranging from 15–30 kDa.

A prominent group of the stress proteins are the molecular chaperones. The small heat shock proteins are molecular chaperons present in all organisms - from bacteria to men. The most important members of this group are alpha crystallin (HspB5) and Hsp27 (HspB1). Proteins of this family are grouped together based on similar structural and functional properties. They have a conserved core domain, so-called alpha-crystallin-domain (ACD, Hsp20 domain), which is flanked by highly variable sequences that are very important for their chaperone functions, therefore they are the least conserved Hsps despite that they are present in all living organisms [11]. Hsp27 is expressed constitutively in many tissues and cell lines, and its expression increases at high levels after various types of stress. It modulates cell survival during the stress [1].

Bakthisaran et al. [3] suggested that circulating αB crystallin and Hsp27 in the blood plasma may exhibit immunomodulatory and anti-inflammatory functions.

Small Hsps share the ability to form oligomeric structures [2] and are often detected as phosphoproteins.

Phosphorylation of Hsp27 was shown to modulate the functional activity of the protein in a variety of studies. The role of Hsp27 phosphorylation in cell protection is not entirely clear. There are conflicting results in literature concerning this aspect. Some *in vitro* studies concluded that the unphosphorylated oligomeric Hsp27 protects protein against aggregation better, whereas others found no difference or better protection by phosphorylated Hsp27 [12].

Expression of multiple Hsps is required during the mammalian embryo development which is characterized by rapid cell growth and differentiation [27].The mammalian genome is activated during early cleavage, and production of proteins important for cleavage occurs. There are many investigations concerning embryonic expression of Hsp in mammals. Trifonova et al. [25] demonstrated the expression of another small Hsp – alpha crystalline in a variety of organs and tissues of human fetus, which serves as an example of the significance of this protein group in the embryo development.

The expression of small Hsp in significant quantities could be observed in adult as well. Mineva et al. [19] demonstrated pattern of Hsp in both normal and pathological thyroid glands. They proposed that Hsp plays a major role in cell differentiation. This notion is further confirmed by Pupaki et al. [22] which examined the role of Hsp in cell differentiation in pig embryos. On the other hand, Stamenova et al. [24] confirmed the presence of alpha crystalline in human placenta but found no significant differences in the expression or distribution when comparing normal or pathological organs (except a total of two cases).

Hsps are among the first proteins produced in the very early-stage embryos. In the mouse embryo, zygotic genome activation starts at 2-cell stage, and it's prooved that Hsp70.1 is one of first proteins, produced after activation of zygotic genome [4]. Small Hsps are far less studied in mammalian embryos. Due to ethical and technical difficulties, studies about Hsps are focused on early mammalian development.

Hsp27 are registered in murine zygote and 2-, 4-, 8-cells blastomeres [16]. Hsp27 is located in cytoplasm of zygotes and early embryos from the 2-cell stage to blastocyst stage and in the nuclei, but not in nucleoli [16].

Other authors investigated Hsp25 (murine Hsp27) in preimplantation stages and concluded that the highest expression of Hsp25 could be found in the blastocyst stage. In normal conditions, they observed cytoplasmic expression of Hsp25, and in chronic heat shock conditions they found that the investigated protein is located in the nucleus [14].

Data in literature are scarce and mainly relate to Hsp27's developmentally regulated manner of expression. The exact role of Hsp27 in unstressed physiological conditions

remains unclear. There are reports that chaperons could be involved in the keeping balance between differentiation and apoptosis, inhibiting apoptosis by regulating upstream signaling pathways [21, 23]. Some authors suggest that the transient expression of Hsp27 is essential for preventing apoptosis of differentiating embryonic stem cells [18].

Most of the knowledge about the function of sHsps in mammalian embryos is based on studies of animals or somatic cells, induced to differentiate. The precise role of Hsps during the human embryonic development is yet to be elucidated.

The aim of the present study is to describe the expression of a member of the sHsps – Hsp27 and his phosphorylated form in different tissues and organs of 8-week old human embryo.

Materials and Methods

In our experiments we investigated the expression of Hsp27 and pHsp27 in tissues of human 8 weeks old embryo using indirect immunohistochemical method, as described by Hristova et al. [13].

Formalin fixed and paraffin embedded embryo from a patient with elective abortion in the 8th gestation week was immunostained. Gestation age was determined with the patient history for last menstrual period, the ultrasound calculations, and the embryo size and morphology on the sections was checked according to the rules in literature [20]. Tissue sections of 3 μm were prepared and placed on an adhesive slides (VWR Micro Slides, Superfrost Plus, USA).

We used as primary antibodies rabbit polyclonal monospecific anti human anti Hsp27 antibody (Elabsience, code № E-AB-31748) and rabbit polyclonal monospecific anti human anti pHsp27 antibody (Santa Cruz Biotechnology, Inc code № ab1426). In negative control the primary antibody was omitted.

Deparaffinization was performed in xylene and ethyl alcohol following standard procedure.The visualisation method is the two-step polymer based En-Vision™ FLEX mini Kit, High pH (Dako, code №K8024). It includes a dextran "skeleton" to which were attached multiple enzyme molecules, and anti-mouse and anti-rabbit secondary antibodies.

The ready sections were observed by light microscope (Zeiss Axioscope 20) using a semiquantitative 4-level scale, including no expression, weak, moderate or strong expression [6].

All procedures were performed at the Laboratory of Reproductive Immunology, Department of Biology, Medical University of Sofia after institutional ethical board approval and in agreement with the Declaration of Helsinki for Medical Research Involving Human Subjects.

Results

After applied indirect immunohistochemical method we observed strong expression of Hsp27 in myocardium **(Fig.1A)** and skeletal muscles **(Fig.1C)**. Moderate to weak cytoplasmic expression of Hsp27 was observed in the centers of ossification**(Fig.1E)**, skin – epidermis and derma **(Fig. 1G)**, smooth intestinal muscle **(Fig. 1I)**, intestinal epithelium **(Fig. 1K)**. We obtained weak cytoplasmic expression of Hsp27 in the hepatocytes **(Fig. 1M)**, the encephalon (**Fig. 1O**) and medulla spinalis.

We registered strong staining of phosphorylated form of Hsp27 the myocardium **(Fig.1B)** and skeletal muscles **(Fig. 1D)**. Strong to moderate cytoplasmic expression of Hsp27 was observed in the centers of ossification **(Fig.1E).** Moderate to weak expression

we found in intestinal smooth muscles **(Fig. 1J)**. Negative immunohistochemical reaction with phosphorylated form of Hsp27 was registered in skin (epidermis and derma) **(Fig. 1H)**, intestinal epithelium **(Fig. 1L)**, liver cells **(Fig.1N)**, and in the encephalon **(Fig. 1P)**.

Nuclear expression of Hsp27 and phosphorylated Hsp27 was registered in single cells of the ossification centers in bones **(Fig. 1E, F)**.

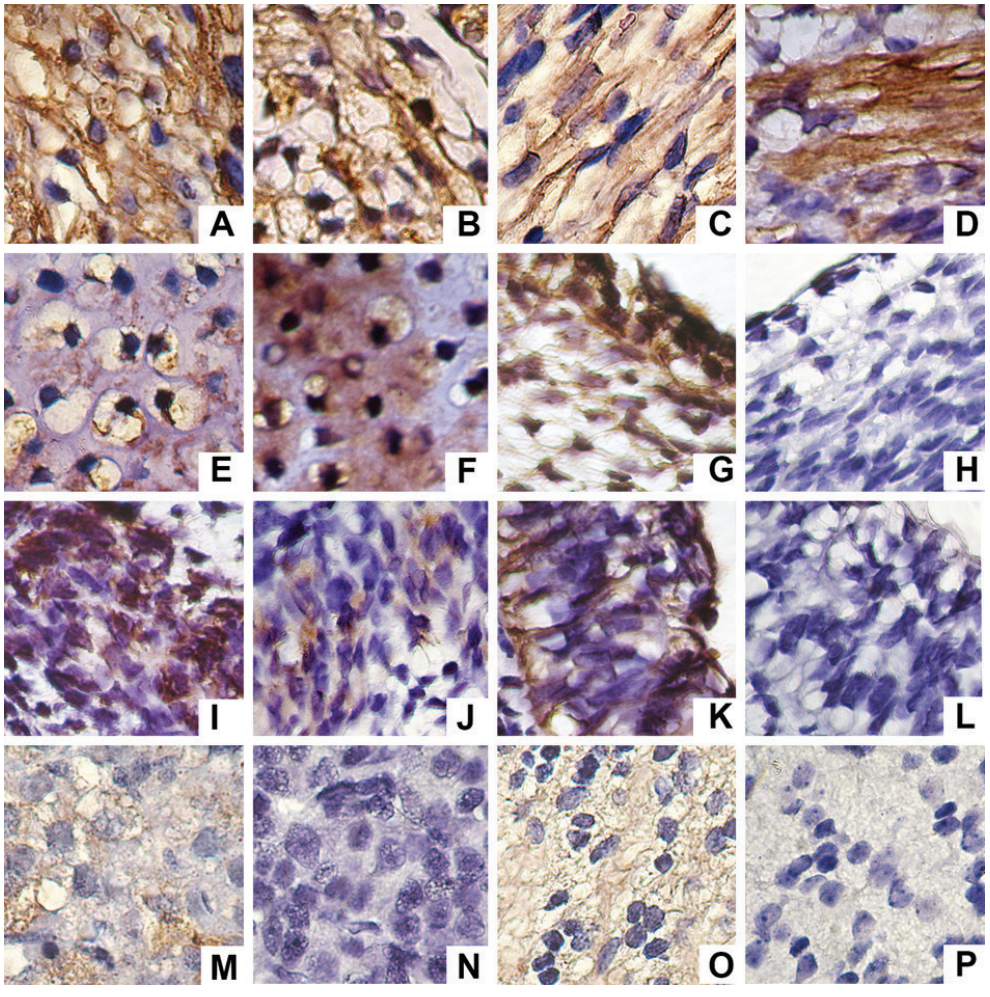

Fig. 1. (A – Hsp27, B – pHsp27) Immunohistochemical study on paraffin embedded tissues of 8 gw human emrbryo. Strong cytoplasmic expression in the myocardium, nuclear expression of the protein is not registered; (C – Hsp27, D – pHsp27) Strong cytoplasmic expression in the skeletal muscles, nuclear expression of the protein is not registered; (E – Hsp27, F – pHsp27) Moderate cytoplasmic and nuclear expression in single cells in ossification centres; (G) Weak cytoplasmic expression of Hsp27 in epidermis and derma of skin; (H) Negative immunohistochemical reaction with pHsp27; (I – Hsp27, J – pHsp27) Moderate to weak cytoplasmic expression in the intestinal smooth muscles, nuclear expression of the protein is not registered.; (K) Moderate to weak cytoplasmic expression of Hsp27 in the intestinal epithelium; (L) Negative immunohistochemical reaction with pHsp27; (M) Weak cytoplasmic expression of Hsp27 in hepatocytes; (N) Negative immunohistochemical reaction with pHsp27; (O) Weak cytoplasmic nevronal expression of Hsp27 in encephalon; (P) Negative immunohistochemical reaction with pHsp27.

Semiquantitative evaluation of immunohistochemical reaction is presented in **Table 1**.

Table 1. Semiquantitative evaluation of cytoplasmic expression of Hsp27 and pHsp27 proteins in organs and tissues of 8 gestation weeks (gw) old human embryo. + weak expression; ++ moderate expression, +++ strong expression; – lack of expression

Tissue	**Hsp27**	**pHsp27**
Skeletal muscles	+++	+++
Heart - myocardium	+++	+++
Bone/ossification center	+	++
Intestine smooth muscle	+	+
Intestinal epithelium	+	–
Encephalon	+	–
Medulla spinalis	+	–
Liver	+	–
Skin – epidermis and derma	+	–
Cartilage	–	–
Lungs	–	–
Kidney	–	–
Thymus	–	–
Nasal epithelium	–	–
Suprarenal gland	–	–
Gonads	–	–

Discussion

The mammalian embryonic development is a very complicated and strongly regulated process, in which Hsps play an important but not fully understood role.

Hsps are proteins, involved in processes of cell proliferation, differentiation and migration [7]. The genes of Hsps cannot be considered as developmental genes but they should be expected to intervene as modulators in the developmental process [7]. The Hsps expression and their functions during development are not yet well described. The central role of Hsps is to act as chaperones. Hsps can bind temporarily different protein molecules and influence their function. Hsp27 limits the activation of apoptosis cascade and reduces the programmed cell death [5]. Garrido C.[10] suggests that the antiapoptotic role of this protein is very important in the processes of proliferation and differentiation during the development of embryo. We admit that this protein has a role not only against stress condition but it plays role in the normal biological processes.

In the present study we investigated sagittal sections of whole 8-week old human embryo and we can observe immunohistochemical evaluation about expression of both forms of Hsp27.

In skeletal and smooth muscles, and myocardium, we registered both forms of Hsp27 – phosphorylated and unphosphorylated. The heart forms early during the embryonic development. It is the first functional organ - beats spontaneously by 4th week. Early expression of some sHSPs (especially orthologues of HSPB1, HSPB8, HSPB5, but also HSPB6 and HSPB2) during heart formation has been reported in a wide range of animal species such as *D. melanogaster*, sea squirt, *D.rerio*, mouse, pig and human. In model object *X. laevis* lack of Hsp27 at the subcellular level causes perturbation of the actin filament network and myofibril disorganization [9]. Some authors [8] assume that Hsp27 is involved in cardiomyocyte differentiation, which is in accordance with our results.

The activity of Hsp27 in skeletal muscles is closely connected with its phosphorylated and unphosphorylated state. Unphosphorylated Hsp27, in its large oligomeric state, is able to bind up to 30 actin monomers, whereas its phosphorylation leads to disintegration of the large complex [9].

An important step of muscle differentiation is fusion of mononucleated myoblasts in multinucleated muscle fibers. Several studies have shown that small HSPs are expressed during the key steps of muscle differentiation. Hsp27 and HspB5 (alpha-B crystallin) make a myotube-specific association with actin microfilaments, which confirms their cytoprotective role. Hsp27 is involved in protection of skeletal myoblasts against oxidative stress and may play an important role in regulating the glutathione system and resistance to Reactive oxygen species (ROS) in skeletal muscle cells [9].

We suggest that strong expression of both states of Hsp27 in skeletal muscles is related with fast growing and differentiation of muscle fibers and his moving activity in this stage.

Small Hsps are very important for connective tissue differentiation during embryonic development. Investigations of chondrogenesis in murine embryos (*in vivo* and *in vitro*) prove intensive expression of Hsp25 during transdifferentiation of chondrocytes in osteoblast-like cells [7]. Our results confirm this observation.

In other organs (liver, brain) we observed only Hsp27, but not phosphorylated form. In the cartilage we detected only phosphorylated form. In the lungs we obtained negative result for both forms of the protein.

Expression of Hsp25 (murine analog of Hsp27 in human) is registered in different stages in mouse embryonic development in brain, in the peripheral tracts and in longitudinal tracts of the ventral region of tegmentum, pons and medulla. Hsp25 is very selectively expressed in isolated or grouped neurons and it is most abundant in axons and dendrites [17]. We observed similar expression of Hsp27 in axons and dendrites.

We compared our results about 8-week embryo with data about expression of Hsp27 in tissues of adults [26] and we continued our previous experiments concerning expression of Hsp27 and pHsp27 in different tissues from human embryos in gestational age from 6 to 12 gestational weeks (gw). We detected the peak of cytoplasmic expression of Hsp27 in embryos in 10 and 11 gw in multiple organs and tissues, that gradually decreased in 12 gw [13]. The phosphorylated form of pHsp27 was weakly expressed from 11gw in single tissues – intestinal muscular layer, lung basal membrane, retinal basal layer, cartilage and nerves [13]. In our previous study we have scarce tissues from 8 gw embryo and information about Hsp27 expression in this age is insufficient.

We observed some differencein Hsp27 expression – in adults Hsp27 lacks in brain cells, according to the data in the literature [26]. In the skin we found a weak to moderate expression of Hsp27, but in adult strong expression is found.

Other difference is observed in gonads – in adults [26] there is a weak expression of Hsp27 in Leydig cells, moderate to strong expression in epididymis glandular cells. In ovaries was observed moderate to strong expression of Hsp27 in follicle cells. We suppose that this result is due to the fact that gonads in 8-week embryo are not yet differentiated as ovary or testis and are not yet functioning.

Conclusions

The present results of the expression of Hsp27 in the tissues and organs of 8 week old human embryo, compared to the results from our previous investigation of tissues and organs from embryos, fetus and adult human give us reason to suppose stage specific expression of Hsp27. This may be due to different needments of the cells during the various stages of their development and function. We suggest that our result will be useful for arranging the complex expression pattern of this protein during embryonic development.

References

1. **Arrigo A-P., J. Landry.** Expression and function of the low-molecular-weight heat shock proteins. – In: *Cold Spring Harbor Monograph Series: The Biology of Heat Shock Proteins and Molecular Chaperones*. (Eds. R. Morimoto, A. Tissieres, C. Georgopoulus) Ed 26. Cold Spring Harbor, NY: Cold Spring Harbor Laboratory Press; 1994, 335–373.
2. **Arrigo, A.-P., J. P. Suhan, W. J.Welch.** Dynamic changes in the structure and intracellular locale of the mammalian low-molecular-weight heat shock protein. – Mol. Cell. Biol. **8**, 1988, 5059–5071.
3. **Bakthisaran, R., R. Tangirala, Ch. Mohan Rao**. Small heat shock proteins: Role in cellular functions and pathology. –Biochim. Biophys. Acta,**1854**, 2015, 291–319.
4. **Bensaude, O., C. Babinet, M. Morange, F. Jacob.** Heat shock proteins, first major products of zygotic gene activity in mouse embryo. – Nature **305**, 1983, 331–333.
5. **Bruey, J. M., C. Ducasse, P. Bonniaud, L. Ravagnan, S. A. Susin, C. Diaz-Latoud, S. Gurbuxani, A. P. Arrigo, G. Kroemer, E. Solary, C. Garrido. Hsp27 negatively regulates cell death by interacting with cytochrome c.** – Nat. Cell. Biol., **2**, 2000, 645–652.
6. **Cherneva, R., O. Georgiev, D. Petrov, Y. Slavova, D. Toncheva, B. Bechev, M. Stamenova, N. Trifonova.** Expression of small Heat shock protein aB crystallin in non-small cell lung cancer. – Compt. Rend. Acad. Bulg. Sci., **62**, 2009, 11, 1483–1488.
7. **Christians, E., Q. Zhoub, J. P. Renard, I. J. Benjamin.** Heat shock proteins in mammalian development. – Seminars in Cell & Developmental Biology,**14**, 2003, 283–290.
8. **Davidson, S.M., M.Morange.** Hsp25 and the p38 MAPK pathway are involved in differentiation of cardiomyocytes. – Dev. Biol., **218**, 2000, 146–160.
9. **Dubińska-Magiera, M., J. Jabłońska, J. Saczko, J. Kulbacka, T. Jagla, M. Daczewska.** Contribution of small heat shock proteins to muscle development and function. – FEBS Lett.,588, 2014, 517–530.
10. **Garrido, C., M. Brunet, C. Didelot, Y. Zermati, E. Schmitt, G. Kroemer**. Heat Shock Proteins 27 and 70: Anti-Apoptotic Proteins with Tumorigenic Properties. – Cell Cycle, 5, 2006, 2592–2601.
11. **Haslbeck, M., E. A. Vierling**. First line of stress defense: small heat shock proteins and their function in protein homeostasis. – J. Mol. Biol., **427**, 2015, 1537–1548.
12. **Hayes, D., V. Napoli, A. Mazurkie, W. F. Stafford, P. Graceffa.** Phosphorylation Dependence of Hsp27 Multimeric Size and Molecular Chaperone Function. – J. Biol. Chem. **284**, 2009, 18801–18807.
13. **Hristova, I., V. Novachkov, S. Petrov, I. Vatev, D. Dimitrova, D. Marinova, Y. Slavova, N. Trifonova.** Immunohistochemical study of Hsp27 in human embryos. – Compt. Rend. Acad. Bulg. Sci., **67**, 2014, 3, 367–372.

14. **Kim, M., D. Geum, I. Khang, Y. M. Park, B. M. Kang, K. A. Lee, K. Kim.** Expression pattern of HSP25 in mouse preimplantation embryo: heat shock responses during oocyte maturation. – Mol. Reprod. Dev., **61**, 2002, 3–13.
15. **Kueltz, D.**, Molecular and evolutionary basis of the cellular stress response. – Ann. Rev. Physiol., **67**, 2005, 225–257.
16. **Liu, S., X. Dai, L. Cai, X. Ma, J. Liu, S. Jiang, J. Liu, Y. Cui.** Effect of Hsp27 on early embryonic development in the mouse. – Reproductive BioMedicine Online, **26**, 2013, 491–499
17. **Loones, M. T., Y. Chang, M. Morange.** The distribution of heat shock proteins in the nervous system of the unstressed mouse embryo suggests a role in neuronal and non-neuronal differentiation. – Cell Stress & Chaperones, **5**, 2000**,** 291–305.
18. **Mehlen, P., A. Mehlen, J. Godet, A. P. Arrigo.** Hsp27 as a switch between differentiation and apoptosis in murinee stem cells. – J. Biol. Chem., **272**, 1997, 31657–31665
19. **Mineva I., M. Stamenova, S. Popovska, T. Betova, P. Rashev, E. Sapundzhiev, M. Simeonova, N. Trifonova.** Localization of low molecular weight stress protein (sHsp) alpha B-crystalin in human thyroid gland. – Compt. Rend. Acad Bulg Sci. (2007) **60**, 4, 449–452.
20. **Moore, K.L., T.V.N. Presaud, M.G. Torchia.** The Developing Human. Clinically oriented embryology. Ninth edition, Elsevier, 2013, 77-91.
21. **Morange, M., A. Diu, O. Bensaude, C. Babinet**. Altered expression of heat shock proteins in mouse embryonal carcinoma cells and mouse early embryonic cells. – Mol. Cell Biol., **4**, 1984, 730–735.
22. **Pupaki D., E. Sapundzhiev, P. Rashev, M. Stamenova**. Expression of small heat shock proteins in tissue differentiation of pig fetuses. – Acta Morphol., Antropol. 15(2010) 92–95.
23. **Schmitt, E., M. Gehrmann, M. Brunet, G. Multhoff, C. Garrido.** Intracellular and extracellular functions of heat shock proteins: repercussions in cancer therapy. – J. Leucoc. Biol., **81**, 2007, 15–27.
24. **Stamenova, M., S. Popovska, T. Betova, P. Rashev, E. Sapundzhiev, M. Simeonova, N. Trifonova.** Expression of low molecular stress proteins (sHsps) alpha-crystallins in human placenta in different types of pathology. – Embryology **2**, (2007), 3-8 [in Bulgarian].
25. **Trifonova N., B.Angelov, P. Rashev, E. Sapundzhiev, I. Buteva, M. Stamenova.** Expression of eye lens antigens – alpha crystallins in extra-ocular human fetal tissues. Bulg. review of ophtalmology, **1**, 2007, 49–54 [in Bulgarian].
26. **Uhlén M., L. Fagerberg, B.M. Hallström, C. Lindskog, P. Oksvold, A. Mardinoglu, Å. Sivertsson, C. Kampf, E. Sjöstedt, A. Asplund, I. Olsson, K. Edlund, E. Lundberg, S. Navani, C. A. Szigyarto, J. Odeberg, D. Djureinovic, J. O. Takanen, S. Hober, T. Alm, P. H. Edqvist, H. Berling, H. Tegel, J. Mulder, J. Rockberg, P. Nilsson, J. M. Schwenk, M. Hamsten, K. von Feilitzen, M. Forsberg, L. Persson, F. Johansson, M. Zwahlen, G. von Heijne, J. Nielsen, F. Pontén.** Tissue-based map of the human proteome.Science, **347**, 2015,Available at https://www.proteinatlas.org/ENSG00000106211-HSPB1/tissue
27. **Witkin S. S., I. M. Linhares.** Heat Shock Proteins and Fertility. – In: *Heat Shock Proteins and Whole Body Physiology.Heat Shock Proteins, vol 5* (Eds. A. Asea, B. Pedersen) Dordrecht, Springer, 2010, 151–162.

Institute of Experimental Morphology, Pathology and Anthropology with Museum
Bulgarian Anatomical Society

Acta morphologica et anthropologica, 26 (3-4)
Sofia ● 2019

Morphological Characteristics and Cytoarchitecture of the Myenteric Ganglia in the Rat Proximal Colon

Todor Kirov[1], Dimitrinka Atanasova[2,3], Lina Malinova[1], Lazar Jelev[1], Nikolai Lazarov[1,3]

[1] *Department of Anatomy and Histology, Medical University of Sofia, Sofia, Bulgaria*
[2] *Department of Anatomy, Faculty of Medicine, Trakia University, Stara Zagora, Bulgaria*
[3] *Institute of Neurobiology, Bulgarian Academy of Sciences, Sofia, Bulgaria*

* Corresponding author e-mail: tvkirov@gmail.com

The myenteric plexus, which consists of interconnected ganglia, has been a subject of interest since its discovery in the late nineteenth century. In our study we focus on the morphology of these ganglia, when observed on routine sections through the rat intestinal wall of a randomly chosen segment, in this case the proximal colon. After applying routine histological methods, we found myenteric neurons of variable shape and size, interspersed between enteric glial cells and nerve fibers. Although the exact morphological type cannot be surely determined, the presence or absence of short and broad neuronal processes may lead the examiner to a conclusion about the major morphological group, which it belongs to. In conclusion, the sections are still one of the simplest and, therefore, frequently used methods of examination of the enteric nervous system, because they provide basic, but valuable information about the cytoarchitecture of the enteric ganglia.

Key words: enteric neurons, myenteric plexus, morphology, cytoarchitecture.

Introduction

The myenteric plexus (plexus of Auerbach) is one of the two major components of the enteric nervous system and consists of variably sized ganglia, interconnected by nerve fiber bundles (inter-ganglionic strands). The structure of the plexus has been a subject of intense scientific interest since its first description by Auerbach in the distant 1864. The most widely accepted classification of its constituent neurons is that of Dogiel, who subdivided them into three morphological classes, now called Dogiel-type-1, 2 and 3 [2]. Other classification schemes have also been proposed [5], as well as extensions of the one of Dogiel [1]. However, even though it is oversimplified, the original classification is still widely used, which is mostly due to the extensive research in the area, which has proven that there is a strict correlation between the structural type and the electrophysiological and neurochemical properties of the neurons [3].

Over time, Dogiel-type-1 and 2 morphological subtypes have become major checkpoints during primary investigation of unexamined material, perhaps due to their

distinct outlook and opposing functions. Dogiel-type-1 neurons have a single long process (an axon) and several short and broad processes (lamellar dendrites), emerging from the soma [2]. Functionally, these neurons serve as inhibitory and excitatory motor neurons for the circular and longitudinal musculature and also as interneurons. The Dogiel-type-2 neurons are perhaps the best example of correlation between morphology and function and, therefore, there is hardly any disagreement between researchers regarding their nature. These neurons are often regarded structurally as "multiaxonal", i.e. their neuronal somata have oval, smooth contours and give rise to several long processes, all of which functionally are proven to be axons. The role they play in enteric circuitry has also well established. In particular, these belong to the so-called intrinsic primary afferent neurons (IPAN), a major sensory component of the enteric reflex circuitry.

However, despite their structural and functional differences, most of the enteric neurons share a common morphological feature: their bodies and processes are more or less flattened in a plane that is parallel to the intestinal external surface, i.e. to the interface between the two muscle layers [4]. Therefore, for specific scientific purposes, the most beneficial methodology includes whole-mount preparations or at least tangential (oblique) sections through the enteric muscle layers, so as to observe the larger neuronal surface or cross-section, respectively. The contours of this surface are the main factor, which the morphological classification of the enteric neurons is based on.

Nevertheless, the sections, either cross- or longitudinal, through the organs of the digestive tract remain the first and sometimes only method for visualization of a variety of structures, both for scientific purposes and student education. Therefore, in this article we have aimed to describe the appearance of the myenteric ganglia on cross- and longitudinal sections of a specific enteric segment (in this particular case the proximal colon), using several of the most common staining techniques.

Material and methods

In our study we used 20 adult (3-month-old) Wistar rats of both sexes with average weight (200-300 g). The entire array of experiments was carried out at the Medical University of Sofia in accordance with its ethical principles for the care and use of laboratory animals. We performed a routine transcardial perfusion with 4% paraformaldehyde in 0.1 M phosphate buffer (PB), pH 7.2-7.4. This neutral buffered fixative penetrates rapidly and does not cause excessive tissue shrinking or distortion of the cellular structure. After perfusion, we collected specimens from the region of the proximal colon, each measuring approximately 10 mm, which were postfixed in the same fixative overnight, at 4°C. Thereafter, the tissue blocks were washed in tap water and then in distilled water, dehydrated with alcohol series, embedded in paraffin and cut into7 μm and 10 μm (for the impregnation technique) thickcross- and longitudinal sections. Then we applied standard protocols of hematoxylin and eosin (H&E) staining, Nissl staining and the Gomori method of silver nitrate impregnation.

Results

In most cases, the cross-sections reveal myenteric ganglia that appear as small clusters of cells, populated only by a few neurons with unimpressive dimensions (**Fig. 1A**). Neurons with larger sectional surface were very rare. On the longitudinal sections, the myenteric plexus acquires the form of larger clusters of neurons, occupying a cleft-like space, lying between bundles of the circular and longitudinal muscle layers (**Fig. 1B,**

C and D). The shape of the ganglia appears to be variable, including circular, oval, egg-shaped and polygonal shapes. The same is also valid for the number of neurons per ganglion and the shape of their bodies. The nerve cell count ranges from five to more than twenty per ganglion. The contours of the perikarya vary largely; we registered rounded, oval, fusiform and stellate shapes. The differences that the neurons show, when applying the different staining techniques, are few, but readily noticeable.

Whenever the cut engages neuronal nuclei, with the routine H&E staining they appear to be quite euchromatic, slightly eccentrically placed and with vesicular appearance. Should the nucleolus be also present, it usually lies centrally (**Fig. 1B**). A regular finding in the vicinity of the neuronal bodies are the nuclei of the supporting enteric glial cells. They are usually oval or fusiform, intensely heterochromatic, and relatively small in size, especially in comparison to the neuronal ones. The cellular boundaries of those cells are poorly demarcated and their cytosol is practically indistinguishable, due to their poor staining capabilities and the cellular interposition. The intercellular spaces are occupied by nerve fibers, which give it a reticular appearance.

With the Nissl staining, the findings are slightly different, because the cresyl-violet has high affinity to neurons only (**Fig. 1C**). There, we can still observe the aforementioned neuronal shapes and nucleoli, but the nucleus itself remains relatively unstained. The latter is not true for the glial cells, as their nuclei are still readily recognizable, whereas the rest of the cellular structure is lost.

When applying the silver impregnation technique, determining the exact neuronal borders is not always easy, because there is significant interposition of cellular structures (**Fig. 1D**). Nevertheless, there is significantly more reduction of silver ions in the cytosol of the neurons, when compared with the glial cells. Combined with their overall bigger size, this is usually enough to distinguish the two cellular types. The nerve fibers are not stained with this technique, so the ganglionic intercellular spaces appear to be empty.

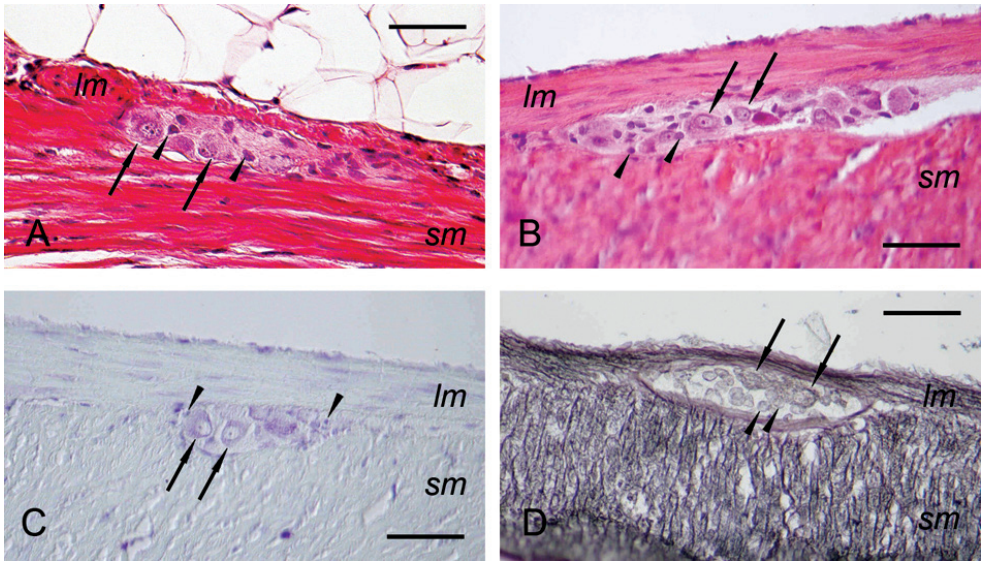

Fig.1. Demonstration of myenteric ganglia in the rat proximal colon on sections through the smooth muscle layer. Note the variable shape of the neuronal perikarya. lm – longitudinal muscle; cm – circular muscle; arrows – perikarya of myenteric neurons; arrowheads – nuclei of enteric glial cells. Scale bar: 50μm. (A) Cross section, H&E; (B) Longitudinal section, H&E; (C) Longitudinal section, Nissl staining; (D) Longitudinal section, Gomori silver nitrate impregnation.

Discussion

The sections through the intestinal wall reveal significant, but sometimes insufficient information about the exact neuronal morphology. This is especially true for cross-sections, in which the plane of the cut passes quite unfavorably through the myenteric ganglia. In those sections the ganglia appear to be falsely small and the neurons quite difficult to be distinguished. Naturally, this is due to the fact, that the longer axis of the myenteric ganglia is parallel to the longitudinal axis of the gut. Moreover, for similar reasons the sectional surface of the cells is severely reduced. That is why, in terms of tissue sections, a much more beneficial approach is the series of longitudinal sections, which is the main substrate of our current study.

As mentioned previously, the shape and size of the ganglia appears to be variable. This is hardly a surprise because, naturally, they would depend on the extent to which the ganglia are affected by the cut. Moreover, the ganglia are prone to be more or less deformed, depending on the state of intestinal distension. In our study, we have put all the specimen under the same conditions (appr. 10% stretching), but when evaluating results from different sources, this factor should be taken into consideration. This factor is also valid when attempting to calculate the nerve cell count and density. Consequently, even in adjacent ganglia the cell count is greatly variable, as reported above.

In terms of neuronal morphology, it is only sometimes possible to determine the exact morphological subtype, according to the universal classification of Dogiel. Should the general shape of the neuronal soma be close to that of a multipolar neuron, one may be inclined to accept that this is a motor neuron, innervating the smooth muscle (since they have been proven to express Dogiel-type-1 morphology). Conversely, the IPANs, which in most cases show Dogiel-type-2 morphology, are expected to present themselves with oval perikarya, devoid of any broader cellular processes. However, without confirmation via specific staining methods (e.g. immunohistochemical reaction), solid conclusions regarding the morphologic affiliation should be avoided, because findings on sections might be misleading.

Conclusions

The myenteric ganglia are a common occurrence on cross- and longitudinal sections through the enteric wall, regardless of the examiner's intentions, educational or scientific. Despite providing only partial information about the neuronal morphology, these sections remain one of the simplest and most frequent means of tissue observation and, therefore, correct interpretations of the structures found is crucial. Thus, this study is simply done to emphasize on the basic checkpoints, needed for successful evaluation of looked for or random findings in the myenteric ganglia.

References

1. **Brehmer, A., F. Schrödl, W. Neuhuber.** Morphological classification of enteric neurons – 100 years after Dogiel. – *Anat. Embryol. (Berl),* **200**(2), 1999, 125–135.
2. **Furness, J**. *The Enteric Nervous System*. Blackwell Publishing, Oxford, 2006, 29–78
3. **Gershon, M., A. Kirchgessner, P. Wade**. Functional anatomy of the enteric nervous system. – In: *Physiology of the Gastrointestinal Tract*. Raven Press, New York, 1994, 381–422.
4. **Hanani, M., L. Ermilov, P. Schmalz, V. Louzon, S. Miller, J. Szurszewski**. The three-dimensional structure of myenteric neurons in the guinea-pig ileum. – J. *Auton. Nerv. Syst.*, **71**(1), 1998, 1–9.
5. **Stach, W.** A revised morphological classification of neurons in the enteric nervous system. – In: *Nerves and the Gastrointestinal Tract*. MTP Press, Lancaster, 1989, 29–45.

Institute of Experimental Morphology, Pathology and Anthropology with Museum
Bulgarian Anatomical Society

Acta morphologica et anthropologica, 26 (3-4)
Sofia ● 2019

Comparative Immunohistochemical Study on Collagen Types in Kidney during Aging and Hypertension

Stancho Stanchev, Alexandar Iliev, Boycho Landzhov*

Department of Anatomy, Histology and Embryology, Medical University of Sofia, Bulgaria

*Corresponding author e-mail: stanchev_1989@abv.bg

Renal fibrosis is characterized by increased synthesis of collagen molecules in the renal parenchyma and interstitium. In the present study, we demonstrated the expression of collagen types I and V and procollagen type III in the renal structure of 12-month-old spontaneously hypertensive rats and age-matched Wistar rats. The main findings included higher immunoreactivity of the examined molecules under hypertensive conditions. The results were obtained by semi-quantitative analysis of the immunohistochemical expression. We found pronounced intraglomerular expansion of collagen type III and V in spontaneously hypertensive rats compared to the normotensive group. In addition, the accumulation of collagen fibers in the renal parenchyma and interstitium was also represented by Mallory's trichrome method. We analyzed the severity of the renal fibrosis as a result of aging as well as in a case of essential hypertension. In conclusion, the development of renal fibrosis is more severe under hypertensive conditions and is associated with specific distribution of the analyzed collagen types.

*Key words:*collagen, kidney, hypertension, aging

Introduction

Renal fibrosis is a nonspecific process, which can be observed as a result of aging, as well as various pathological conditions. In addition, hypertensive kidney damage is accompanied by pronounced expansion of extracellular molecules both in the renal cortex and medulla [8]. It seems that the severity of interstitial fibrosis rather than the glomerular changes correlates better with the renal functional capacity [19]. The development of renal fibrosis depends on the activity of renal interstitial fibroblasts, inflammatory cells, cytokines and matrix metalloproteinases [4]. The accumulation of collagen fibers can be represented by different histological techniques, which include Masson's trichrome method, Sirius Red, which are strongly specific for collagen types I and III, as well as immunohistochemical methods [17]. Many studies reveal that the fibrous skeleton of the kidney contains various collagen molecules with specific distribution in the renal structure. It is well known that collagen types I, III and V are all expressed in the renal interstitium [6]. Collagen types I and III are not found in the glomeruli under physiological conditions, which suggests that the altered expression of these molecules may serve as indicator of glomerular injury [6, 7]. Collagen type V is

also found in the glomerular and extraglomerular mesangial matrix [6]. Renal fibrosis is usually associated with increased synthesis of collagen types I and III, where cellular phenotypic changes may play a crucial role in the process [4]. On the other hand, there is insufficient information regarding the changes in the expression of collagen type V during the development of renal fibrosis due to hypertensive kidney damage.

The spontaneously hypertensive rat (SHR) is a widely used model for essential hypertension. In this strain, the hypertensive-induced renal morphological alterations correlate well with these observed in the human population [10].

The aim of the current study was to demonstrate the hypertension-induced renal fibrosis in SHR and to establish the distribution of collagen types I and V and procollagen III in the renal structure. We have also shown the altered expression of these molecules in cases of hypertensive and age-related renal fibrosis.

Materials and Methods

Experimental animals and tissue preparation

Male SHR and Wistar rats (WR), available at the Medical University of Sofia, aged 12 months (n=3; per group) were used for this study with the approval of the University Committee on Animal Resources. The rats were anesthetized intraperitoneally with Thiopental 40 mg/kg b.w. The chest cavity was opened and transcardial perfusion was made with 4% paraformaldehyde in 0.1 M phosphate buffer, pH 7.2. The kidneys were quickly removed and fixed in 10% neutral buffered formalin. After routine paraffin embedding, 5 μm thick sections were cut and stained with Mallory's trichrome method. The paraffin was removed, after which the slides were placed in 0.1% fuchsin for 1-2 minutes, washed and placed in 1% solution of phosphomolybdic acid for 3-5 minutes. After thorough rinsing, the slides were placed in a mixture of aniline blue, orange G and oxalic acid for 2 minutes, washed again and embedded in entellan.

Immunohistochemistry

For the immunohistochemical analysis, the 5 μm-thick sections mounted on gelatin-coated slides were preincubated for one hour in 5% normal goat serum. After that, incubation with a primary antibody was done for 24 h at room temperature. The following reagents were used: mouse monoclonal anti-collagen type I IgG antibody (Santa Cruz Biotechnology Catalogue No. sc-293182, Santa Cruz Biotechnology, Inc., Heidelberg, Germany); mouse monoclonal anti-procollagen type III IgG antibody (Santa Cruz Biotechnology Catalogue No. sc-166316); mouse monoclonal anti-collagen type V IgG antibody (Santa Cruz Biotechnology Catalogue No. sc-166155); all antibodies were used at concentration 1:500. After rinsing in PBS, incubation in biotinylated goat anti-mouse IgG antibody at concentration 1:500 for two hours was performed. The sections were washed in PBS and incubated in avidin-biotin peroxidase complex for 1 h. This step was followed by rinsing in PBS and then in 0.05 M Tris−HCl buffer, pH 7.6, which preceded incubation in 0.05% 3,3-diaminobenzidine (DAB) containing 1% hydrogen peroxide (H_2O_2) (1:100) for visualization of the reaction. Sections were briefly washed in 0.05 M Tris−HCl buffer, pH 7.6. The slides were air-dried for 24 h, then rinsed in distilled water for five minutes, three times, contrastained with hematoxylin, air-dried again and coverslipped with Entellan. One section per animal from the kidney (a total of twelve sections) were used as controls. All were incubated in the way previously described, but omitting the primary or secondary antibody. All controls were negative.

Semi-quantitative analysis of the immunohistochemical expression

For semi-quantitative analysis of the expression of collagen types I and V and procollagen type III, we used software ImageJ 1.52a, freely downloaded from the website of the National Institute of Health (NIH) (http://imagej.nih.gov/ij/). The intensity of staining was assessed through the IHC Profiler plugin, freely downloaded from the Sourceforge website (https://sourceforge.net/projects/ihcprofiler/). The IHC Profiler assigned a score to each visual field in a four tier system – high positive (3+), positive (2+), low positive (1+) and negative (0). Five slides were used from each organ. We analyzed at least ten randomly selected visual fields on each slide. The final score was the average of the scores of all visual fields as calculated by the IHC Profiler.

Results

Histological findings

In 12-month-old WR, we found moderate expansion of collagen fibers among the renal parenchyma and interstitial connective tissue, stained in blue color by Mallory's trichrome method. In the renal cortex, accumulations of collagen fibers were described in the region of the parietal layer of the glomerular capsule and glomerular capillary tufts of the three main types of nephrons. Perivascular fibrosis was represented by concentric layers of collagen fibers around interlobular and intralobular blood vessels. Interstitial fibrosis was established among various sections of proximal and distal tubules (**Fig. 1**).

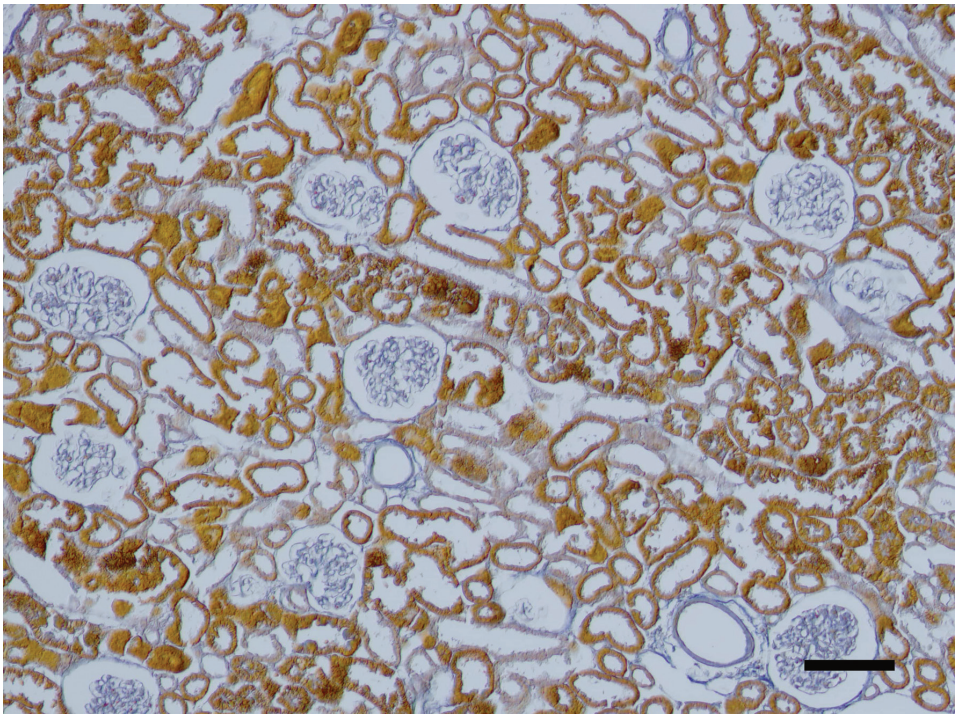

Fig. 1. Photomicrograph of kidney stained with Mallory's trichrome method. WR, age – 12 months. Scale bar – 150 μm.

In 12-month-old SHR, we established more pronounced expansion of collagen fibers in the interstitial connective tissue and the structural elements of the renal corpuscles in SHR compared to the normotensive rats. The renal fibrosis was more severe in the inner cortex and medulla in the hypertensive rats. Mallory's trichrome method revealed extensive areas of collagen accumulations in the region of the parietal layer of the glomerular capsule and glomerular capillary tufts of the midcortical and juxtamedullary nephrons as well as around the tubular epithelial cells. The described morphological alterations showed characteristics of advanced glomerulosclerosis and tubular atrophy. We didn't find such selectivity of the renal injury in WR (**Fig. 2**).

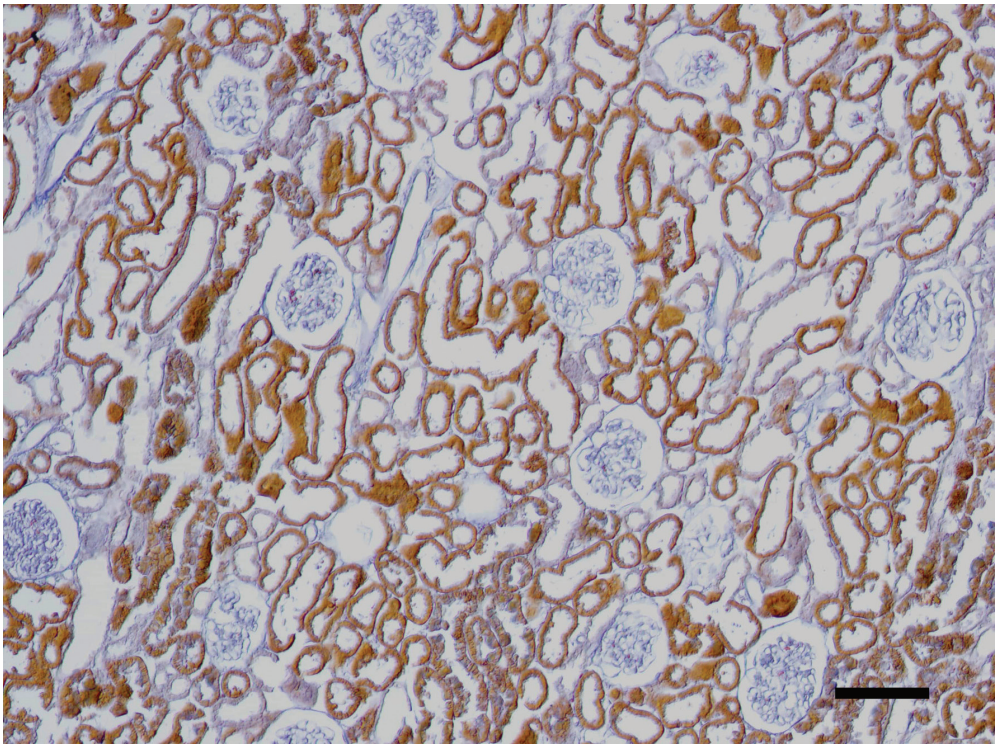

Fig. 2. Photomicrograph of kidney stained with Mallory's trichrome method. SHR, age – 12 months. Scale bar – 100 μm.

Expression of collagen type I and V and procollagen type III in the kidney of WR

In 12-month-old WR, we described heterogeneous distribution of the collagen types I and V and procollagen type III. Collagen type I was found along the proximal and distal convoluted tubules and moderate expression in the renal corpuscles of the three types of nephrons. Collagen type V showed high positive reaction in the glomeruli as well as the interstitial connective tissue. Procollagen type III was found mainly in the interstitial connective tissue and low positive reaction in the renal corpuscles (**Fig. 3A, 3B, 3C**).

Expression of collagen type I and V and procollagen type III in the kidney of SHR

The immunohistochemical study on the distribution of collagen types I and V and procollagen type III in the renal structure showed higher expression of the examined molecules in SHR. The results showed that the progression of the renal fibrosis under

hypertension is associated with increased expansion mainly of collagen type V and procollagen type III. We found increased proportion of intraglomerular distribution of collagen type V and procollagen type III in SHR compared to the normotensive rats. In WR, the renal medulla showed low positive to positive immunoreactivity for collagen type I and procollagen type III, while in SHR quite positive reaction for collagen type I and V was established (**Fig. 3D, 3E, 3F**).

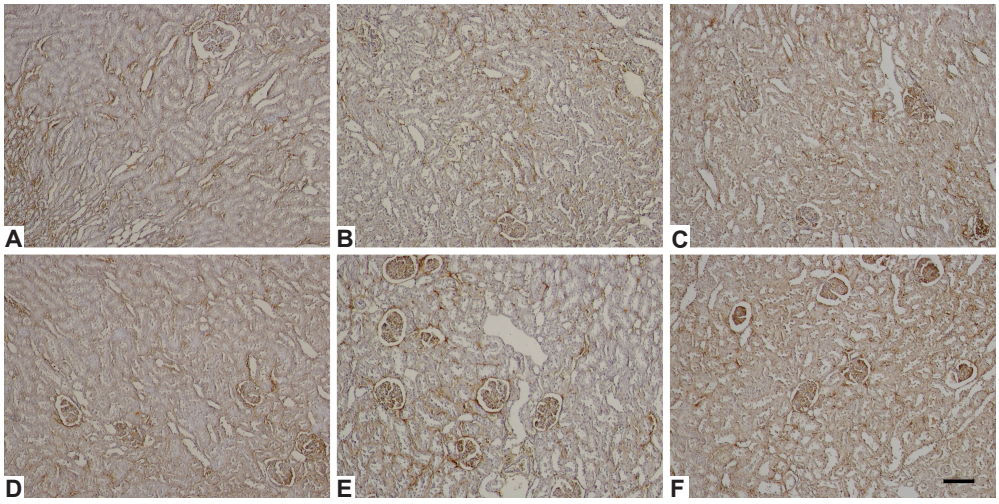

Fig. 3. Immunohistochemical expression of collagen type I and V and procollagen type III in the kidney of WR and SHR. **A**. Collagen type I in 12-month-old WR; **B.** Procollagen type III in 12-month-old WR; **C**. Collagen type V in 12-month-old WR; **D**. Collagen type I in 12-month-old SHR. **E**. Procollagen type III in 12-month-old SHR; **F.** Collagen type V in 12-month-old SHR. Scale bar – 100 μm.

Semi-quantitative analysis

The intensity of the immunohistochemical reaction varied between the kidney of SHR and WR and between the studied types of collagen and procollagen type III. In order to objectify these findings, we calculated the expression semi-quantitatively using the IHC Profiler. Results are summarized in **Table 1**.

Table 1. Semi-quantitative analysis of the immunohistochemical expression of collagen type I and V and procollagen type III in kidney of SHR and WR. The percentage for each score represents the percentage of visual fields that the IHC Profiler assigned this score to.

Type of collagen/procollagen	Kidney	
	SHR	WR
Collagen type I	Positive (2+) (48%)	Positive (2+) (33%)
	Low-positive (1+) (34%)	Low-positive (1+) (31%)
	Negative (0) (18%)	Negative (0) (36%)
Procollagen type III	High-positive (3+) (63%)	High-positive (3+) (49%)
	Positive (2+) (21%)	Positive (2+) (31%)
	Low-positive (1+) (16%)	Low-positive (1+) (20%)
Collagen type V	High-positive (3+) (57%)	High-positive (3+) (41%)
	Positive (2+) (21%)	Positive (2+) (34%)
	Low-positive (1+) (22%)	Low-positive (1+) (25%)

Discussion

It has been proved beyond doubt that the prolonged and untreated essential hypertension is a primary risk factor for chronic kidney disease [16]. Our results show that renal fibrosis in SHR compared to normotensive controls is associated with increased expression of the examined collagen molecules, mainly collagen types III and V. A number of authors have shown that the progression of renal fibrotic changes is usually associated with accumulation of collagen types I and III [1, 4]. In addition, we established a significantly higher expression of collagen type V in SHR, which suggests that this molecule may play a key role in the development of hypertension-induced renal fibrosis. The elevated blood pressure causes glomerular injury and leads to increased number of sclerotic glomeruli [5]. Glomerulosclerosis is characterized by accumulation of collagen types I and III in the glomerular capillary tufts, which is demonstrated in the present study. As a structural element of the glomerular mesangium, collagen type V showed positive reaction in the region of the renal corpuscles in SHR and WR. The immunohistochemical expression for collagen type V was higher in SHR compared to normotensive controls, which indicates that this extracellular molecule is also involved in the development of the glomerular damage. On the other hand, there is contradictory evidence regarding the effect of interstitial fibrosis on the development of renal morphological changes in the structural elements of the nephrons. Some authors have demonstrated intact tubular segments of the nephrons, which are surrounded by an extensive mass of collagen fibers and areas of tubular degeneration [13, 14]. However, the influence of prolonged interstitial fibrosis as a possible harmful factor for chronic kidney damage has not been excluded [13, 14].

In the present study, we also found that the expansion of collagen molecules in SHR is more pronounced in the inner rather than the outer cortex. Some authors have tried to explain the described selectivity of renal alterations with the higher glomerular capillary pressure of midcortical and juxtamedullary nephrons under hypertensive conditions [11]. On the other hand, the aging kidney is characterized by numerous inevitable morphological changes, similar to those observed in essential hypertension, such as tubular atrophy, glomerulosclerosis and tubulointerstitial fibrosis [3]. Unfortunately, the lack of strongly specific alterations makes it difficult to determine the etiology of the kidney damage. Jenkins et al. reported periglomerular fibrosis in glomeruli characterized by open capillary loops and the presence of concentric layers of collagen fibers in the region of the basement membrane of glomerular capsule. Moreover, the authors termed the expansion of interstitial collagen as renal 'fibrosis', and the increase of the structural elements of the basement membrane as 'sclerosis' [12]. It is well known that collagen type IV is mainly found in the basement membranes. In our study, the higher expression of collagen type V in SHR in the parietal and visceral layer of glomerular capsule may contribute to the progression of sclerosis. In rat kidney, the complete degeneration of a single nephron is accompanied by $40 \times 10^6\ \mu m^3$ lack of epithelial tissue, which is replaced by extracellular fibers [18].

Indeed, the development of renal interstitial fibrosis is a multifactorial process, which is closely associated with the increased activity of various cell types. It is well known that renal interstitial fibroblasts play a key role in the synthesis of extracellular molecules. However, the examination of these cells is usually difficult, because of the lack of strongly specific expression of marker molecules [2]. The demarcation of fibroblasts from other interstitial cells is based on the presence of F-actin in their cytoskeleton and a well-developed rough endpolasmatic reticulum [13]. Many studies have suggested the primary role of myofibroblasts in the course of hypertensive induced renal fibrosis. There are several hypotheses for the origin of these cells, including from

interstitial fibroblasts [4]. It seems that interstitial dendritic cells are also involved in the development of renal injury, because some authors have demonstrated a positive correlation between the abundance of these cells and the tubulointerstitial changes [9]. As aging progresses, the tubular epithelial cells may acquire secretory phenotype properties, which are associated with increased production of proinflammatory cytokines [20]. Morphometric studies have demonstrated the evaluation of renal fibrosis on slides stained by trichrome and immunohistochemical methods [15]. Unfortunately, these methods have some limitations concerning the renal biopsy technique.

Conclusion

In conclusion, hypertensive kidney damage is associated with more severe morphological changes in the renal parenchyma and interstitium compared to the physiologically aging kidney. Renal fibrosis is characterized by an increased synthesis of collagen types I and III, as confirmed by our results. The observed high positive immunoreactivity for collagen type V in the present study shows that this molecule likely also plays a crucial role in this process.

Acknowledgement: This work is supported by the Bulgarian Ministry of Education and Science under the National Program for Research "Young Scientists and Postdoctoral Students".

References

1. **Alexakis, C., P. Maxwell, G. Bou-Gharios.** Organ-specific collagen expression:implications for renal disease. – *Nephron Exp. Nephrol.,***102**, 2006, e71–e75.
2. **Boor, P., T. Ostendorf, J. Floege.** Renal fibrosis: novel insights into mechanisms and therapeutic targets. – *Nat. Rev. Nephrol.,***6**, 2010,643–656.
3. **Denic, A., R. J. Glassock, A. D. Rule.** Structural and functional changes with the aging kidney. – *Adv. Chronic. Kidney Dis.,* **23**, 2016, 19–28.
4. **Farris, A. B., R. B. Colvin.** Renal interstitial fibrosis: mechanisms and evaluation. – *Curr. Opin. Nephrol. Hypertens.,* **21**, 2012, 289–300.
5. **Fukuda, K., A. Shimizu, T. Kaneko,Y. Masuda, F. Yasuda, M. Fukui, S. Higo, A. Hirama, A. Mii, S. Tsuruoka, R. Ohashi, Y. Iino, Y. Fukuda, Y. Katayama.**A case of secondary focal segmentalglomerulosclerosis associated with malignant hypertension. – *CEN Case Rep.,* **2**, 2013, 68–75.
6. **Genovese, F., A. A. Manresa, D. J. Leeming, M. A. Karsdal, P. Boor.** The extracellularmatrix in the kidney: a source of novel non-invasive biomarkers of kidneyfibrosis? – *Fibrogenesis Tissue Repair,* **28**, 2014, 4.
7. **He, J. S., K. Hayashi, S. Horikoshi, K. Funabiki, I. Shirato, Y. Tomino.** Identificationof cellular origin of type I collagen in glomeruli of ratswith crescenticglomerulonephritis induced by anti-glomerular basementmembrane antibody. – *Nephrol.Dial. Transplant.,* **16**, 2001, 704-711.
8. **Hewitson, T. D.** Fibrosis in the kidney: is a problem shared a problem halved? – *Fibrogenesis Tissue Repair,* **5**, 2012, S14.
9. **Heymann, F., C. Meyer-Schwesinger, E. E. Hamilton-Williams, L. Hammerich, U. Panzer, S. Kaden, S. E. Quaggin, J. Floege, H. J. Gröne, C. Kurts.** Kidney dendritic cell activation is required for progression of renal disease in a mouse model of glomerular injury. – *J. Clin. Invest.,* **119**, 2009, 1286–1297.
10. **Huang, C., Y. Y. Lin, A. L. Yang, T. W. Kuo, C. H. Kuo, S. D. Lee.** Anti-Renal Fibrotic Effect of Exercise Training in Hypertension. – *Int. J. Mol. Sci.,***19**, 2018, E613.
11. **Iversen, B. M., K. Amann, F. I. Kvam, X. Wang, J. Ofstad.** Increasedglomerular capillary pressure and size mediate glomerulo-sclerosis in SHR juxtamedullary cortex. – *Am. J. Physiol.,* **274**, 1998, F365-F373.

12. **Jenkins, J., S. V. Brodsky, A. A. Satoskar, G. Nadasdy, T. Nadasdy.** The relevance of periglomerular fibrosis in the evaluation of routine needle core renal biopsies. – *Arch. Pathol. Lab. Med.,* **135**, 2011, 117–122.
13. **Kaissling, B., M. Le Hir.** The renal cortical interstitium: morphological and functional aspects. – *Histochem. Cell. Biol.,* **130**, 2008, 247–262.
14. **Kaissling, B., M. Lehir, W. Kriz.** Renal epithelial injury and fibrosis. – *Biochim. Biophys. Acta.,* **1832**, 2013,931–939.
15. **Servais, A., V. Meas-Yedid, O. Toupance, Y. Lebranchu, A. Thierry, B. Moulin, I. Etienne, C. Presne, L. B.de Hurault, P. Le Pogamp, Y. Le Meur, D. Glotz, C. Hayem, J. C. Olivo Marin,E. Thervet.** Interstitial fibrosis quantification in renal transplant recipientsrandomized to continuecyclosporine or convert to sirolimus. – *Am. J. Transplant.,* **9**, 2009, 2552–2560.
16. **Sternlicht, H., G. L. Bakris.** The kidney in hypertension. – *Med. Clin. North. Am.,* **101**, 2017, 207–217.
17. **Street, J. M., A. C. Souza, A. Alvarez-Prats,T. Horino, X. Hu, P. S. Yuen, R. A. Star.** Automated quantification of renal fibrosiswith Sirius Red and polarization contrast microscopy. – *Physiol. Rep.,* **2**, 2014, e12088.
18. **Venkatachalam, M. A., K. A. Griffin, R. Lan, H. Geng, P. Saikumar, A. K. Bidani.** Acute kidney injury: a springboard for progression in chronic kidney disease. – *Am. J. Physiol. Renal Physiol.,* **298**, 2010, F1078-F1094.
19. **Vleming, L. J., J. W. de Fijter, R. G. Westendorp, M. R. Daha, J. A. Bruijn, L. A. van Es.** Histomorphometric correlates of renal failure in IgA nephropathy. – *Clin. Nephrol.,***49**, 1998, 337–344.
20. **Yang, L., T. Y. Besschetnova, C. R. Brooks, J. V. Shah, J. V. Bonventre.** Epithelial cell cyclearrest in G2/M mediates kidney fibrosis after injury. – *Nat. Med.,* **16**, 2010, 535–543.

Institute of Experimental Morphology, Pathology and Anthropology with Museum
Bulgarian Anatomical Society

Acta morphologica et anthropologica, 26 (3-4)
Sofia ● 2019

Cytoarchitecture of the Spinal Trigeminal Nucleus in Rats

Andrey Ivanov[1], Dimitrinka Atanasova[1,2], Nikolai Lazarov[1,3]*

[1] *Institute of Neurobiology, Bulgarian Academy of Sciences, Sofia, Bulgaria*
[2] *Department of Anatomy, Faculty of Medicine, Trakia University, Stara Zagora, Bulgaria*
[3] *Department of Anatomy and Histology, Medical University of Sofia, Sofia, Bulgaria*

* Corresponding author e-mail: andr92123@gmail.com

The spinal trigeminal nucleus (SpV) is one of the three nuclei in the trigeminal sensory nuclear complex which extends over the whole length of the brainstem. The SpV travels adjacent to the spinal trigeminal tract and is responsible for relaying various sensory modalities including temperature, deep or crude touch, and pain from the ipsilateral portion of the face. It is continuous with the substantia gelatinosa, while the tract is continuous with Lissauer‘s tract. The purpose of the study is to scrutinize the structure and cytoarchitecture of this nucleus in the rat. The SpV is the largest trigeminal nucleus and is found in the lateral tegmentum of the medulla and caudal pons. Spinal trigeminal neurons are composed of soma with sporadic Nissl bodies surrounded by a network of myelinated axons. Our results show that its three structural divisions, i.e. the oral, interpolar, and caudal subnuclei, share a common neuronal organization though they are associated with the transmission of different kind of sensory information from the orofacial region.

Key words: spinal trigeminal nucleus, hematoxylin staining, neutral red staining, toluidine blue

Introduction

The trigeminal nerve (the fifth cranial nerve, CN V) is the nerve responsible for facial sensation and motor functions such as biting and chewing. This nerve is the largest of the cranial nerves. Its name („trigeminal“ = tri-, or three and – geminus, or twin: three twins) derives from the fact that each of the two nerves (one on each side of the brain bridge) has three main branches: the ophthalmic nerve (NOpth – nerve ophthalmicus, V1), maxillary nerve (NMax – nervus maxillaris, V2) and mandibular nerve (NMan – nervus mandibularis, V3) [7].

In embryonic development, the motor division of the trigeminal nerve originates from the basal plate of embryonic ridges, and sensory division originates from the

cranial neural crest. Sensory information from the face and body is processed by parallel pathways in the central nervous system [7].

The trigeminal sensory nuclei comprising the trigeminal sensory nuclear complex are divided into three parts. From caudal to rostral direction (ascending from the medulla to the midbrain), they are the spinal trigeminal nucleus, principal sensory and mesencephalic trigeminal nuclei. Parts of the trigeminal nucleus receive different types of sensory information; the spinal trigeminal nucleus receives fibers associated with pain and temperature signals, the main sensory nucleus receives fibers with contact information, and the mesencephalic nucleus receives fibers from the proprioceptors and mechanoreceptors of the jaws and teeth. The fibers associated with pain from the peripheral nociceptors are transferred to the cranial nerves V, VII, IX and X. Upon entering the brain stem, the sensory fibers are grouped and sent to the spinal trigeminal nucleus [5].

The spinal trigeminal nucleus contains the sensory map of pain and temperature of the face and mouth. From this nucleus, the secondary fibers intersect the midline and ascend in the trigeminothalamic tract to the contralateral thalamus. The fibers for pain and temperature are sent to multiple thalamic nuclei [2].

Inside the spinal trigeminal nucleus, information is presented in the form of layer analogy. The lower parts of the nucleus (in the upper cervical part of the spine and lower medulla) represent the peripheral areas of the face (scalp, ears and chin). The higher levels (in the upper medulla) represent the central areas (nose, cheeks and lips). The highest levels (in the pons) are the mouth, teeth and pharyngeal cavity areas [4].

The purpose of the study is to scrutinize the structure of the spinal trigeminal nucleus in rats.

Materials and Methods

The experiments in this study were performed on adult (12-week-old; n= 6) normotensive rat material, the Wistar breed. The experimental procedures were consistent with the European Communities Council Directive 2010/63 /EU, were conducted in accordance with national rules on animal experiments, and were approved by the Ethics Committee of the Institute of Neurobiology, Bulgarian Academy of Sciences. The experimental animals were anaesthetized with ether followed by intraperitoneal injection of thiopental (40 mg/kg body weight). After anesthesia, they were perfused through the ascending aorta with the cannula inserted through the left ventricle of the heart. Initially, the circulatory system was flushed for about 5 minutes with 0.05 M phosphate-buffered sodium chloride solution (PBS) at pH 7.36. After washing, the system was started with a retainer consisting of 4% paraformaldehyde (Merck) in 0.1 M phosphate buffer (PB) for about 20 minutes. After perfusion, we removed under a magnifying glass the area from the midbrain to the cervical part of the spinal cord. The formed tissue blocks were left overnight in the same retainer at 4 ° C. After fixing, the material was washed from the rest of the retainer until the next day with tap water. The incorporation of the material into paraffin necessitates its dehydration through an ascending series of alcohols, starting with placing it in 50% ethanol for 2 h, after which the tissue is transferred to 70% ethanol until the next day, followed by 80% ethanol for 2 h, 96 % ethanol – 2×20 min, 100% ethanol – 2×15 min. The next step involves clarifying the material in cedar oil in penicillin vials, which are left open to allow the ethyl alcohol to evaporate. The material remains in cedar oil until it becomes amber or until it sinks to the bottom of the bottle, which may take several days. After washing twice with xylene (2 times for 10 minutes), the material was paraffin embedded.

Routine staining with Neutral red

This method of staining is the most widespread in histological practice, because, thanks to the appropriate combination of colorants, belonging to two opposite groups - basic and acidic dyes, it gives a general idea of the state of the structure under study [3].

Neutral Red is a weak cationic azine dye that is used extensively as a nuclear stain in a variety of biological stain applications. Standard protocol has been used for dewaxing and rehydration after which Neutral Red staining solution has been added and samples incubated for 5 minutes at room temperature followed by 2-minute wash with distilled water. Sections have been dehydrated, cleared in xylene and mounted.

Staining with Toluidine blue

Toluidine blue staining is another method of demonstrating acidic tissue components (Davidoff). The dewaxed and water-driven sections were transferred to a 0.5% solution of toluidine blue for 5-10 min. The sections were rinsed in distilled water and then differentiated in 70% ethanol until the excess paint was washed, observing under a microscope. This is followed by dehydration, treatment with xylene and incorporation into Entellan.

Results and Discussion

This nucleus is the largest trigeminal nucleus and is found in the lateral tegmentum of the medulla and caudal pons. The SpV travels adjacent to the spinal trigeminal tract. The SpV is continuous with the substantia gelatinosa, while the tract is continuous with Lissauer‘s tract (**Fig. 1**) [6].

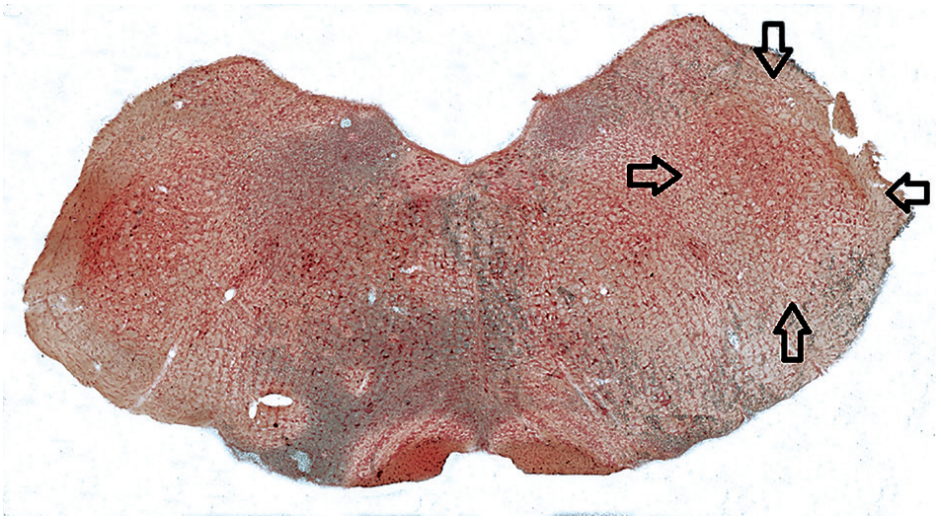

Fig. 1. Neutral red stained coronal section of the medulla oblongata showing cell types of the spinal trigeminal nucleus outlined from the spinal trigeminal tract laterally. The arrows indicate the boundaries of the spinal trigeminal nucleus. Magnification: 50×.

The spinal trigeminal neurons have a distinct cell body, soma with sporadic Nissl bodies surrounded by a network of myelinated axons (**Fig. 2**). Around the nucleus, myelinated fibers may be observed. These fibers are associated with pain signaling from the peripheral nociceptors which are transferred to the cranial nerves V, VII, IX and X [1]. Upon entering the brain stem, the sensory fibers are grouped and sent to the spinal trigeminal nucleus. This incoming fiber bundle can be identified in pons- and medulla-cross sections as the spinal tract of the trigeminal nucleus, which is parallel to the spinal trigeminal nucleus. The spinal tract of the fifth cranial nerve is analogous to dorsolateral fasciculus in the spinal cord.

Furthermore, along the caudal-rostral direction, three separate parts of the spinal nucleus may be distinguished – the oral part, the caudal part and the interpolar part. The differentiation of the three anatomical parts of the nucleus may be associated with their different functions [8]. The first part is associated with the transmission of discriminative (fine) tactile sensations from the orofacial area and is an extension of the main sensory nucleus of the fifth cranial nerve. The interpolar nucleus' function is also associated with the transmission of tactile information as well as tooth pain, while the caudal part transmits information on nociception and thermal sensations from the head [9, 10].

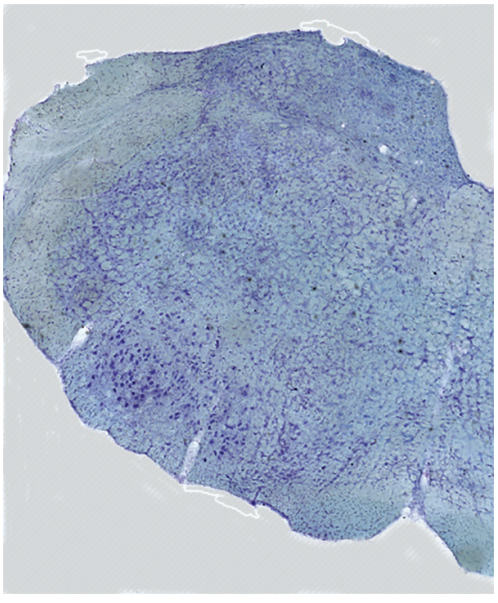

Fig. 2. Coronal section of the medulla oblongata with toluidine blue staining depicting neuronal organization of the spinal trigeminal nucleus. Magnification: 50×.

Taking into account the achievements in recent years in elucidating the morphology of the spinal nucleus, there is still scope for more investigation revealing the neurotransmitter affiliation of its cell population. The receptor profile of the neurons in the spinal nucleus, the role of endogenous neurotransmitters and neuromodulators has not been fully scrutinized. Therefore, more studies will be needed in order to better fathom the anatomy of the spinal trigeminal nucleus and its association with the functions it executes.

References

1. **Brodal, P.** *The central nervous system: Structure and function*, 3rd edition, New York, NY, US: Oxford University Press, 2004.
2. **Carpenter, M. B., J. Sutin.** *Human Neuroanatomy*, 8th edition, Williams and Wilkins, 1983.
3. **Davidoff, M., P. Galabov.** *Contemporary histochemical methods for investigation of the Nervous system*, 1981 (in Bulgarian).
4. **Lübbert, M., J. Kyereme, N. Schöbel, L. Beltrán, C. H. Wetzel, H. Hatt.** Transient receptor potential channels encode volatile chemicals sensed by rat trigeminal ganglion neurons. – *PLoS ONE*, **8**(10), 2013, e77998.
5. **Martin, J. H.** *Neuroanatomy: Text and Atlas*, 3rd edition, McGraw-Hill, New York, 2003.
6. **Paxinos, G.** *The Rat Brain in Stereotaxic Coordinates*, 5 edition, Academic Press, 2004.

7. **Wilson-Pauwels, L., E. J. Akesson, P. A. Stewart.** *Cranial Nerves: Anatomy and Clinical Comments*, B. C. Decker, 1998.
8. **Olszewski, J.** On the anatomical and functional organization of the spinal trigeminal nucleus. – *J. Comp. Neurol.,* **92**, 1950, 401-413.
9. **Huff, T., D. T. Daly.** *Neuroanatomy, Cranial Nerve 5 (Trigeminal*), StatPearls [Internet] StatPearls Publishing; Treasure Island (FL), 2018.
10. **Rusu, M.** C. The spinal trigeminal nucleus – Considerations on the structure of the nucleus caudalis. – *Folia Morphol. (Warsz.),* **63**, 2004, 325-328.

Institute of Experimental Morphology, Pathology and Anthropology with Museum
Bulgarian Anatomical Society

Acta morphologica et anthropologica, 26 (3-4)
Sofia ● 2019

Statistical Analysis of ZAP-70 And CD38 Expression in Chronic B-cell Leukemia Patients

Elza Azmaiparashvili, Vladimer Kuchava

[1] *Institute of Clinical Oncology, Tbilisi, Georgia.*
[2] *Institute of Clinical Oncology, Tbilisi, Georgia.*

* Corresponding author e-mail: E.Azmaipharashvili@gmail.com

Chronic lymphocytic leukemia (CLL) cells with unmutated immunoglobulin heavy chain gene (U-IGHV) differs from those with mutated IGHV (M-IGHV) in the expression levels of a relatively small subset of genes. It is observed heterogeneous clinical behavior of patients with chronic lymphocytic leukemia according to gene expression profile: a) indolent disease and a lack of disease-related complications for a long period; b) progressive and/or symptomatic disease which requires therapy relatively soon after the diagnosis. Most clinically relevant markers, which can be used as a surrogate marker for expression of U-IGHV are zeta-chain associated protein of 70 kDa (ZAP-70) and CD38. The aim of our study is to evaluate whether expression profiles of these markers differ in different countries. Based on our results we concluded that ZAP-70 and CD38 have differential expression.

Key words: CLL, U-IGHV, M-IGHV, ZAP-70.

Introduction

The clinical behavior of patients with chronic lymphocytic leukemia (CLL) is heterogeneous [1]. Some patients have indolent disease and lack of disease-related complications for many years; others develop progressive and/or symptomatic disease requiring therapy within in a relatively short time after diagnosis. Early treatment of the CLL could put patients at risk for therapy-related complications that might compromise their quality of life and/or survival [4].

Traditional staging systems could not distinguish an aggressive disease course from the good prognosis in patients.

In our research we are focusing on the new and most clinically relevant markers: zeta-associated protein 70 (ZAP-70) and CD38 expression. Gene expression analyses found out that CLL cells with unmutated immunoglobulin heavy chain gene (U-IGHV) are different from CLL cells with mutated IGHV (M-IGHV) in the expression levels of a relatively small subset of genes, one of which encodes the zeta-chain associated protein of 70 kDa [4]. The same finding was revealed for U-IGHV leukemia-cell which are known to express CD38. In this respect, ZAP-70 and CD38 expression analyses

can provide complementary prognostic information identifying three patient subgroups with good, intermediate and poor prognosis [3].

Comparing two markers, ZAP-70 has been emerged as the most promising surrogate marker for the IGVH mutation status. However, the combination of ZAP-70 and CD38 increases the prognostic power than usage each separately.

Most patients with CLL that express U-IGHV and/or CD38, but lack expression of ZAP-70, will not require therapy by current criteria for many years after diagnosis [1, 3].

Patients who have CLL cells with M-IGHV, apparently lack leukemia-cell expression of ZAP-70. Such patients have a relatively indolent clinical course and might not have the same risk-benefit ratio with early therapy as patients with CLL cells that express ZAP-70, who on average require therapy within 3 years after the diagnosis [4].

Prognostic predictions in B-cell chronic lymphocytic leukemia (B-CLL) at early clinical stage are based on biological disease parameters, such as ZAP-70 and CD38 protein levels, genomic aberrations as well as IGVH mutation status. The levels of ZAP-70 and CD38 stays sustainable over the time in the majority of patients [2].

The use of these prognostic markers could not obviate clinical monitoring for other features associated with disease progression, such as lymphocyte doubling time, progressive lymphadenopathy, measurement of beta-2-microglobulin levels, or development of disease-related symptoms or disease-associated cytopenia [4, 7].

Average treatment-free survival time in patients whose leukemic cells were ZAP-70(+)/CD38(+) was 30 months compared to 130 months in patients with a ZAP-70(-)/CD38(-) status. In patients with discordant ZAP-70/CD38 results, the average treatment-free survival time was 43 months [6, 7].

The aim of our study was to estimate the difference of expression profiles of these markers in different countries.

Materials and Methods

To evaluate expression rate of ZAP-70 and CD38 markers we applied flow cytometry and immunocytochemistry in 320 B-CLL patients.The median age of the patients while diagnosis was 56 (42-96years). We performed flow cytometry and Immunocytochemistry to detect expression of ZAP-70 and CD38. CLL cells also were analyzed for CD19, CD20, CD23, and CD38, using monoclonal antibodies (mAbs) conjugated to allophycocyanin (APC), peridinin-chlorophyll-protein (PerCp), fluorescein isothiocyanate (FITC), or phycoerythrin (PE) (Becton Dickinson, Pharmingen, Dako). ZAP-70 expression is thought to be positive if the percentage of CLL cells expressing ZAP-70 is greater than 20% and the optimal threshold for CD38 (+) equals 35% or more of the CLL cells.

We performed comparison of expression profiles of two prognostic markers in different countries: Germany, USA, Egypt, India and Georgia [1, 4, 5, 6, 8, 9].

Results and Discussion

We revealed, that the percentage of both ZAP-70/CD38 negative expression levels were close in all three countries: Germany, Egypt and Georgia: 47,6%, 48,0% and 49,5 % respectively. Both ZAP-70/CD38 positive expression levels appeared highest in India (56,0%) compared to other countries as Germany (23,4%), USA, Mississippi (35,3%), Georgia (35,3%) and Egypt (48,0%). This fact also was mentioned by Indian researchers, however they did not give explanation [5]. Discordant expression of these two markers showed lowest levels in Georgia (17,2%) compared to Germany (29,0%)

and Egypt (42%). In our opinion it was caused by technical aspects of estimating marker expression. According to some authors FCI (Flow Cytometry) technique is sensitive, more objective and quantitative in comparison with microscopic detection of manual absorbance-based enzyme immunohistochemistry products [10]. We started to use flow cytometry later then immunocytochemistry, after that we revealed, flow cytometry was more sensitive and precise comparing to immunocytochemistry.

Immunocytochemistry expression of CD38 (total expression level is negative) and ZAP-70 (total expression in CLL cells is positive) is shown on figures 1 and 2, respectively (**Figs. 1, 2**).

Results from flow cytometry were shown on figure 3 and 4. It was demonstrated CD 38 positive cell percentage on CD19(+)CLL cells (**Fig. 3**) and ZAP-70 expression level estimated on CD20(+)CLL cells (**Fig. 4**)

As it was shown above data for these marker expressions differ between countries.

With the respect of value of prognostic markers we included ZAP-70(+)/CD19(+)/CD5(+) and percentage of CD38(+)/CD19(+)/CD5(+) B-CLL cells into a routine diagnostic B-CLL panel to predict outcome.

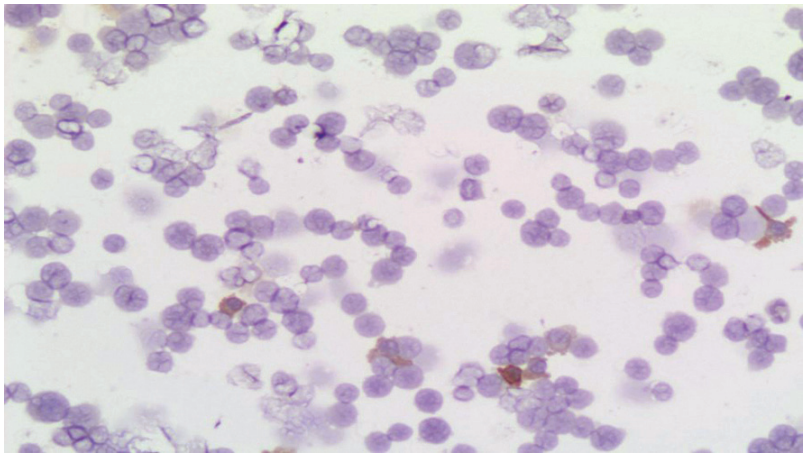

Fig. 1. Expression of CD38 by immunocytochemistry

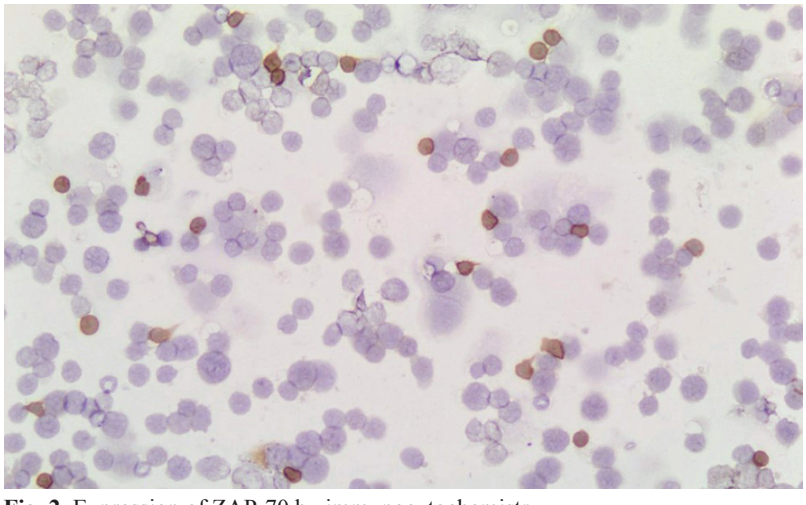

Fig. 2. Expression of ZAP-70 by immunocytochemistry

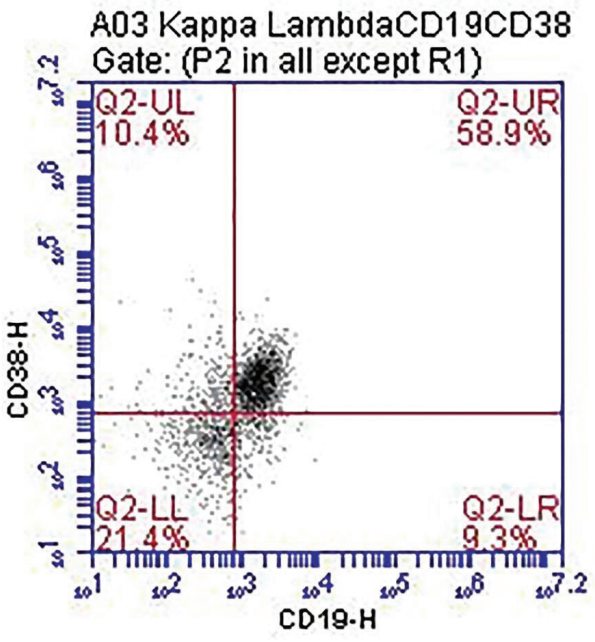

Fig. 3. Flow Cytometry image of CD19/CD38 expression

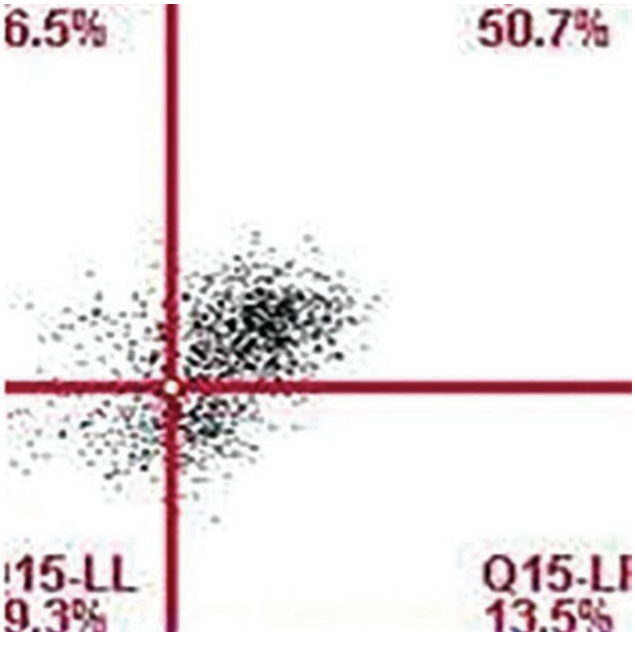

Fig. 4. Flow Cytometry image of CD20/ZAP-70 expression

Clinical studies are in progress to evaluate the potential benefit of early therapy in newly diagnosed patients who have adverse prognostic markers. Such studies might determine whether patients at high risk for early disease progression benefit from therapy administered soon after diagnosis. Also we continue working to reveal the reasons for differences of disease outcome [7].

References

1. **Schroers, R., F. Griesinger, L. Trümper, D. Haase, B. Kulle, L. Klein-Hitpass, L. Sellmann, U. Dührsen, J. Dürig.** Combined analysis of ZAP-70 and CD38 expression as a predictor of disease progression in B-cell chronic lymphocytic leukemia. – *Leukemia*, **19**(5), 2005, 750-758.
2. **Deaglio, S., T. Vaisitti, S. Aydin, G. D'Arena, L. Bonello, P. Omedé, M. Scatolini, O. Jaksic, G. Chiorino, D. Efremov, F. Malavasi.** CD38 and ZAP-70 are functionally linked and mark CLL cells with high migratory potential. - *Blood,* **110**, 2007, 4012-4021 .
3. **Hus, I., M. Podhorecka, A. Bojarska-Junak, J. Roliński, M. Schmitt, M. Sieklucka, E. Wasik-Szczepanek, A. Dmoszyńska.** The clinical significance of ZAP-70 and CD38 expression in B-cell chronic lymphocytic leukaemia. – *Oncology*, **17**(4), 2006, 683-690.
4. **Rassenti, L. Z., S. Jain, M. J. Keating, W. G. Wierda, M. R. Grever, J. C. Byrd, N. E. Kay, J. R. Brown, J. G. Gribben, D. S. Neuberg, F. He, A. W. Greaves, K. R. Rai, T. J. Kipps.** Relative value of ZAP-70, CD38, and immunoglobulin mutation status in predicting aggressive disease in chronic lymphocytic leukemia. - *Blood*, **112**(5), 2008, 1923–1930.
5. **Gogia, A, A. Sharma, V. Raina, L. Kumar, R. Gupta, R. Kumar.** Prevalence of ZAP-70 and CD 38 in Indian chronic lymphocytic leukemia patients. – *Indian J Cancer*, **50**(4), 2013, 333-336.
6. **El-Sharnouby, J. A., A. A. El-Shakankiri, O. M. Hendy, L. M. Ahmed, A. M. Taha.** Significance of zeta-associated protein (ZAP-70) and CD38 expression in chronic lymphocytic leukemia. – *Egypt J. Immunol.,* **13**(2), 2006, 69-84.
7. **Robak, T.** Staging and prognostic factors in chronic lymphocytic leukemia: Current status. – *J. Leuk (Los Angel),* **2**, 2014, e111.
8. **Assem, M., A. T. Hamid, S. Kohla, S. Arsanyos.** The Prognostic significance of combined expression of ZAP-70 and CD38 in chronic lymphocytic leukemia. – *J. Egypt Natl. Canc. Inst.* **21**(4), 2009, 287-297.
9. **Liu, Y., Y. Wang J. Yang, Y. Bi, H. Wang.** ZAP-70 in chronic lymphocytic leukemia: A meta-analysis. – *Clinica Chimica Acta,* **483**, 2018, 82-88.
10. **Brahmi, U., A. Rajwanshi, K. Joshi, P. Dey, H. Vohr, N. K. Ganguly, S. K. Gupta.** Flow cytometric immunophenotyping and comparison immunocytochemistry in small round cell tumors. – *Ann. Quant. Cytol. Histol.*, **23** (6), 2001, 405-412.

Institute of Experimental Morphology, Pathology and Anthropology with Museum
Bulgarian Anatomical Society

Acta morphologica et anthropologica, 26 (3-4)
Sofia ● 2019

Relapsing remitting multiple sclerosis in patients under treatment with laquinimod

Vera Kolyovska[1], Dimitar Maslarov[2]*

[1] *Institute of Experimental Morphology, Pathology and Anthropology with Museum, BAS, Sofia, Bulgaria*
[2] *Medical University of Sofia, Neurology Clinic of First MHAT "St. John the Baptist", Sofia, Bulgaria*

*Corresponding author e-mail: verakol@abv.bg

Multiple sclerosis (MS) is a chronic autoimmune disease of the central nervous system (CNS), which is pathophysiologically characterized by both inflammatory demyelination and neurodegeneration. Laquinimod is a small molecule, an investigation for oral drug administration being developed for the treatment of relapsing-remitting multiple sclerosis (RRMS). We explore serum IgG antibodies to GM1, GM3 and GD1a gangliosides in our patients under laquinimod treatment. The results show high IgG titers of anti-GM1 antibodies, but low titers of anti-GM3 and anti-GD1a antibodies. There are no data laquinimod to affect the demyelinisation - in almost all patients the anti-GM1 antibodies titer is positive. It can be concluded that laquinimod has a neuroprotective action. Oral application of laquinimod against MS may reduce brain damage caused by neurodegeneration. Laquinimod has dual properties of immunomodulation and neuroprotection, and is a potentially promising oral treatment of RRMS.

Key words: serum anti-ganglioside antibodies, laquinimod, relapsing–remitting multiple sclerosis, neuronal damage, neuroprotection.

Introduction

Multiple sclerosis (MS) is a chronic, progressive disease affecting the central nervous system (CNS) (both brain and spinal cord). The symptoms are caused by the body's own immune system attacking and damaging the myelin sheaths surrounding nerve fibers. This leads to inflammation within the CNS making the patient to suffer relapses and disease progression. The etiology of the disease is unknown, but it is assumed to depend, like other autoimmune diseases on both genetic and environmental factors [9]. Histopathologically, MS has been characterized by focal inflammatory infiltrates, demyelination, but in some cases remyelination, astrogliosis and variable axonal damage within the CNS [19]. One hallmark of the pathology of MS is inflammation involving B-cells, T-cells, and macrophages, which results in damage of the CNS tissue.

The treatment and the management of MS should be targeted toward relieving symptoms of the disease, treating acute exacerbations, shortening the duration of acute relapse, reducing frequency of relapses and preventing disease progression [12].

The treatment of the disease has two aspects: immunomodulatory therapy (IMT) for underlying the immune disorder and therapies to relieve or modify symptoms. IMT is directed toward reducing the frequency of relapses and slowing progression. Currently, the most disease-modifying agents have been approved for use only in the relapsing forms of MS [12].

Laquinimod may be considered as an immunomodulatory drug. However, murine studies of experimental autoimmune encephalomyelitis (EAE) and results from MRI suggest that this drug may also exhibit indirect and potentially direct neuroprotective effects. In adults with relapsing-remitting multiple sclerosis (RRMS), laquinimod has demonstrated ability to slow disease progression; its beneficial effects have been demonstrated on both clinical endpoints and MRI surrogate markers. It shows a favorable safety profile [5, 7, 8]. Its unique profile together with the convenience of an orally-administered drug, make laquinimod an attractive agent for patients with MS. In order to improve MS therapy, agents are needed to protect effectively against both inflammatory and neurodegenerative components of this disease [9]. Positive results have been reported for five new oral drugs for RRMS: fingolimod, cladribine, teriflunomide, laquinimod and dimethyl fumarate - in phase 3 studies. Several new oral drugs are likely to be approved for RRMS in the near future. Some oral treatments have shown benefit and would generate much interest because of the convenience of such administration. However, the availability of convenient oral drugs will not necessarily translate into clinical effectiveness and safety [10].

Laquinimod (ABR-215062; Molar mass: 356.803 g/mol) is an orally administered quinoline-3-carboxamide small-molecule derivative of the parent compound, the immunomodulator linomide. It was developed as a therapeutic agent against MS because of lack of safety concerns seen with the parent compound. In preclinical studies, evidence has accumulated suggesting that laquinimod may exhibit immunomodulatory and potentially neuroprotective properties [19]. This drug has a high level of oral bioavailability, a small distribution volume and a low rate of total clearance. As a small molecule, laquinimod diffuses freely across the blood–brain barrier (BBB) without any known active transport by extra- and/or intracellular receptors [4]. As such, it can reach the CNS and may exert direct or indirect neuroprotective effects [17]. Mechanisms that have been proposed for neuronal and axonal damage in EAE and MS include effects driven by an inflammatory milieu, mitochondrial dysfunction, and glutamate toxicity. The actual cause of damage may be one or another combination of the described above. Experimental evidence suggests that laquinimod may be able to inhibit some of these effects. Laqunimod's influence on EDSS scores may possibly be due to its ability to affect the CNS directly, thereby reducing the diffuse neurodegenerative effects of MS, which are linked to long-term disability progression rather than peripherally initiated, T-cell-mediated focal lesions that are linked to relapses [9]. Clinical data show laquinimod to be well tolerated in patients with RRMS. In order to clarify of laquinimod's proved neuroprotective effects, the manufacturer is planning to investigate its use in a population with primary progressive MS. Laquinimod also exhibits the effects of cell migration. It may reduce the entry of proinflammatory monocytes into the CNS by lowering the levels of matrix metalloproteinase 9, which regulates the trafficking of monocytes into inflamed tissues [14]. It has a high level of oral bioavailability, a small distribution volume and a low rate of total clearance. The maximum plasma concentration is reached within the first hour following its administration and is less than 5 μM after the administration of 0.05 – 2.4 mg of the drug [6]. The experimental studies have shown that laquinimod decreases the activation of microglia [3]. Modulation of astrocytic activation has been postulated as yet another mechanism of action of laquinimod. Downregulation of the astrocytic proinflammatory response appears to

preserve oligodendrocytes, axons and myelin. Laquinimod was also able to regulate synaptic transmission by increasing inhibitory postsynaptic currents and, at the same time, by reducing excitatory postsynaptic currents, pointing to its novel, potentially neuroprotective properties [17]. Since MS patients must be on medication throughout their lifetime, an oral treatment creates a substantial advantage compared with existing products in the market, all of which must be injected. If applied once daily, an oral tablet of investigated laquinimod (Nerventra) acts as a CNS-active immunomodulator with a novel mechanism of action being developed for the treatment of RRMS. The global Phase III clinical development program which evaluates oral laquinimod in MS includes two pivotal studies, ALLEGRO and BRAVO. Phase III of laquinimod trial, CONCERTO, is evaluating two doses of the investigational product (0.6 mg and 1.2 mg) in approximately 1,800 patients for up to 24 months. Following late-stage studies, Teva™ is conducting this phase of the trial, CONCERTO, evaluating two doses of (0.6 mg and 1.2 mg) in 2,100 patients for up to 24 months. The primary outcome measure is the time to confirm disability progression as measured by the Expanded Disability Status Scale (EDSS). Treatment with laquinimod reduces development of active MRI lesions in relapsing MS [15].

MS treatment needs accessible markers for early neuronal injury and rapid onset of therapy. Over the past ten years the importance of potential applicability of antibodies as biological markers for the diagnosis, classification, disease activity and prediction of clinical courses in MS has evolved [1]. Gangliosides are a family of acidic glycosphingolipids highly concentrated in the nervous system, where they represent about 10% of the total lipid content [21]. GM1 is a main myelin ganglioside and the GD1a is one of the major ganglioside fractions in the CNS [22]. MS treatment needs accessible markers for early neuronal injury and rapid onset of the therapy. Therefore, the MS therapy should include the prevention of neuronal degeneration and dysregulation of neuron-glia interactions, as soon as the diagnosis is made. In the last decade an enormous effort has been applied to discover biological markers of neuronal damage capable to predict the course of the disease and effective response to therapy [2, 13]. Over the past ten years the importance of potential application of antibodies as biological markers for the diagnosis, classification, disease activity and prediction of clinical courses in MS has evolved [1].

The aim of the present study was to correlate the neuronal injury with serum levels of anti-GM1, anti-GM3 and anti-GD1a antibodies in patients with RRMS under treatment with laquinimod.

Materials and Methods

The samples are from Neurology Clinic of First MHAT, Sofia. Sera were obtained from 10 patients with clinically defined MS with relapsing – remitting form of the disease. They were with a long duration of the disease and in clinical relapse during sample collection. None of MS patients received another immunosuppressive treatment at the time of venipuncture. An informed consent was obtained from each patient. Because our Laquinimod patients are in chronic relapsing remitting form of the disease in our experiments we worked with anti-gangliosides IgG antibodies.

ELISA Protocol. The serum anti-GD1a, GM1, GM3 IgG antibodies were estimated by the enzyme-linked immunosorbent assay (ELISA) [16]. We determined antiganglioside antibodies (AGAs) of the IgG class against GD1a ganglioside. AGAs were found in low titers in some healthy subjects we estimated a reference range for the healthy controls. MS patients were considered strongly positive only if the optical density of their sera exceeded

x ± 2 SD of the healthy controls. Briefly, 1000 ng of GD1a, GM1 and GM3 ganglioside in 100 ml of methanol were separately pipetted into three 96 well microtitre plates. After air drying, the wells were blocked with BSA-PBS (1% bovine serum albumine in phosphate-buffered saline) for 1h. After washing six times with PBS, 100 ml of sera diluted 1:20 to 1:5000 in BSA-PBS, were added to each well and incubated overnight. After that the plates were washed thoroughly six times with PBS. Binding was detected following a 2h incubation period with BSA-PBS diluted (1/3200) peroxidase-conjugated goat anti-human IgG antibodies and with BSA-PBS diluted (1/4800) peroxidase conjugated goat anti-human IgM antibodies. All incubation steps were performed at 4°C. After washing with PBS, colour development was achieved in a substrate solution containing 15 mM 0-phenilendiamine and 0.015% H_2O_2 in 0.1M sodium acetate buffer, pH 5.0 at room temperature. The reaction was stopped after 30 min by addition of 50 ml of 1N H_2SO_4 and the optical density (OD) was measured and read spectrometrically at 490 nm with an ELISA reader (TECAN, Sunrise TM, Austria). Non specific antibody binding (OD value in a well not containing GD1a ganglioside) was subtracted for each measurement. Adult patients were considered strongly positive only if the mean OD of their sera exceeded x ± 2SD (standard deviation) of the healthy controls. Determinations were carried out in triplicate. The Student's test was used to determine statistical differences between the groups using p value of less than 0.05 as the level of confidence. The data were presented as a mean value (M) ± standard error of mean.

Results and Discussion

Our observations in the titers of the anti-gangliosides GM1, GM3 and GD1a antibodies in sera of patients under treatment with laquinimod show elevated titer of anti-GM1 antibodies but lack of anti-GM3 and anti-GD1a antibodies **(Table 1).** There are no data laquinimod to affect the demyelination.

As we know from our previous studies, the presence of anti-GM1 IgG antibodies in the patient sera is in correlation with demyelination and of IgG anti-GD1a - with neurodegeneration, respectively [23, 24]. There are three hypotheses about the presence of anti-GM3 IgG antibodies in the patient sera. The increased titers of the last are usually considered to indicate neurodegeneration and BBB damage. It is correlated with BBB destruction, which may lead to severe metabolic abnormalities (e. g. diabetes) or with appearance of cancer cells [11].

A considerable increase of GD1a in the serum after the first attacks of RRMS and primary progressive MS (PPMS) was determined and is generally connected with neuronal damage [11, 23, 24]. Autoantibodies against gangliosides GM1 and/or GD1a are associated with acute motor axonal neuropathy and acute motor-sensory axonal neuropathy, whereas antibodies to GD1b ganglioside are detected in acute sensory ataxic neuropathy. Antibodies to GM1 and GD1a gangliosides have been proposed to disrupt the nodes of Ranvier in motor nerves via complement pathway [18]. Serum antibodies to different gangliosides have also been identified in some subtypes and variants of Guillain-Barré Syndrome (GBS). These observations, correlated and integrated with electrophysiological and pathological findings in humans indicate that the GBS subtypes acute motor conduction block neuropathy, acute motor axonal neuropathy, acute motor and sensory neuropathy, but also acute sensory neuropathy and possibly also a chronic disorder as multifocal motor neuropathy represent a spectrum of the same immunopathologic process. Being nodal axolemma and paranode the focus to the nerve injury, these immune-mediated neuropathies could be more properly classified as nodo-paranodopathies [20].

Table 1. Titers of the anti-gangliosides GM1, GM3 and GD1a antibodies in sera of patients under treatment with laquinimod. Only patients from 1 to 7 with GM1 antibody titer show very high OD with p value < 0.05. Their sera are considered highly positive.

Patients	serum anti-GM1 antibody titer	serum anti-GM3 antibody titer	serum anti-GD1a antibody titer
1.RRMS without relapse	+	-	+/-
2. RRMS without relapse	+	-	+/-
3. RRMS without relapse	+	-	+/-
4. RRMS without relapse	+	-	-
5. RRMS without relapse	+	-	-
6. RRMS without relapse	+	-	-
7. RRMS without relapse	+	-	-
8. RRMS without relapse	+/-	-	-
9. RRMS without relapse	+/-	-	-
10. RRMS without relapse	+/-	-	-

Numerical value of the titer: (-) $\leq$ 0.047; normal is 0.047; (±) is 0.062; (+) is 0.077; (++) is 0.107

Conclusions

In conclusion, our study indicates, for the first time, that the changes in serum IgG anti-GM1, anti-GM3 and anti-GD1a ganglioside antibodies in MS patients under treatment with laquinimod reflect with the CNS neuronal injury. Increased relative anti-GD1a portion in the serum of patients with MS indicates continuous neuronal damage. Therefore, GD1a and GT1b gangliosides can serve as biomarkers for these early pathological CNS changes in MS. The results from these trials could further inform about the clinical benefit of laquinimod in patients with a persisting, but still insufficient need of safe and at the same time effective oral compounds with neuroprotective effects. Reflecting the results, we conclude that some patients may proceed to make relapses, regardless of the fact that they are continuously treated with a suitable medicine, and the serum titers of GM1, GM3 and GD1a IgG anti-ganglioside antibodies demonstrate that all these medicines are not 100% effective. The admission of laquinimod should not be interrupted. Laquinimod should be admitted for long period of time. So far we do not have enough patients receiving laquinimod. We continue to follow our patients and to look for new ones. There are no data for laquinimod to affect the demyelinisation – almost all patients are positive on GM1. It can be concluded that laquinimod has a neuroprotective action. Oral laquinimod for MS may reduce brain damage caused by neurodegeneration. For the first time, IgG antibodies against GM3 ganglioside in serum were examined and it could be concluded that patients before, during and after this therapy have no metabolic disorders. Laquinimod had potential benefits in reducing relapse rates and was safe for most of the patients with RRMS, subjected on short-term treatment. The most common adverse events included headache, back pain, arthralgia, diarrhea, cough, urinary tract infection, elevated alanine aminotransferase, insomnia, nausea, abdominal pain and sinusitis.

References

1. **Berger, T., M. Reindl.** Emergence of antibodies as biomarkers in multiple sclerosis. – *Future Neurology*, **1**(1), 2006, 57-66.

2. **Brettschneider, J., A. Petzold, A. Junker, H. Tumani.** Axonal damage markers in the cerebrospinal fluid of patients with clinically isolated syndrome improve predicting conversion to definite multiple sclerosis. – *Mult. Scler.*, **12**(2), 2006, 143-148.
3. **Brück, W., C. Wegner.** Insight into the mechanism of laquinimod action. – *J. Neurol. Sci*., **306**(1-2), 2011, 173-179.
4. **Brück, W., R. Pförtner, T. Pham, J. Zhang, L. Hayardeny, V. Piryatinsky, U.K. Hanisch, T. Regen, D. Van Rossum, L. Brakelmann, K. Hagemeier, T. Kuhlmann, C. Stadelmann, G. John, N. Kramann, C. Wegner.** Reduced astrocytic NF-kappaB activation by laquinimod protects from cuprizone-induced demyelination. – *Acta Neuropathol*., **124**(3), 2012, 411-424.
5. **Comi, G., D. Jeffery, L. Kappos, X. Montalban, A. Boyko, M. A. Rocca, M. Filippi.** Placebo-controlled trial of oral laquinimod for multiple sclerosis. – *New Engl. J. Med*., **366**(11), 2012, 1000-1009.
6. **Fernández, O.** Oral laquinimod treatment in multiple sclerosis. – *Neurologia*, **26**(2), 2011, 111-117.
7. **Giacomini, P.S., A. Bar-Or.** Laquinimod in multiple sclerosis. – *Clin Immunol*., **142**(1), 2012, 38-43.
8. **He, D., K. Han, X. Gao, S. Dong, L. Chu, Z. Feng, S. Wu.** Laquinimod for multiple sclerosis. – *Cochrane Database Syst Rev*., **6**(8), 2013, CD010475. doi: 10.1002/14651858.
9. **Kieseier, B. C.** Defining a role for laquinimod in multiple sclerosis. – *Ther. Adv. Neurol. Disord*., **7**(4), 2014, 195-205.
10. **Killestein, J., R. Rudick, C. Polman**. Oral treatment for multiple sclerosis. - *Lancet Neurol*., **10**(11), 2011, 1026-1034.
11. **Kolyovska, V., I. Sainova, S. Dimitrova, I. Ivanova-Pandourska, R. Eneva, S. Engibarov, Tz. Markova, D. Maslarov.** Presence and levels of anti-GM3 antibodies and GM3 ganglioside molecules in probes from experimental *in vitro*-models. – *Biochem. Molec. Biol. J*., **4**(2), 2018, 18.
12. **Luzzio, C., F. Dangond.** Multiple Sclerosis. – Chief Editor: Keegan B.M. MEDSCAPE, 2014.
13. **Malmeström, C., S. Haghighi, L. Rosengren, O. Andersen, J. Lycke.** Neurofilament light protein and glial fibrillary acidic protein as biological markers in MS. – *Neurology*, **61**(12), 2003, 1720-1725.
14. **Mishra, M., J. Wang, C. Silva, M. Mack, V. Yong.** Kinetics of proinflammatory monocytes in a model of multiple sclerosis and its perturbation by laquinimod. – *Am. J. Pathol*., **181**, 2012, 642–651.
15. **Polman, C., F. Barkhof, M. Sandberg-Wollheim, A. Linde, O. Nordle, T. Nederman.** Treatment with laquinimod reduces development of active MRI lesions in relapsing MS. – *Neurology*, **64**(6), 2005, 987-991.
16. **Ravindranath, M., S. Muthugounder, T. Saravanan, N. Presser, D. Morton.** Human antiganglioside autoantobodies: validation of ELISA. – *Ann. N. Y. Acad. Sci*., **1050**, 2005, 229–242.
17. **Ruffini, F., S. Rossi, A. Bergamaschi, E. Brambilla, A. Finardi, C. Motta, V. Studer, F. Barbieri, V. De Chiara, L. Hayardeny, G. Comi, D. Centonze, G. Martino.** Laquinimod prevents inflammation-induced synaptic alterations occurring in experimental autoimmune encephalomyelitis. – *Mult. Scler*., **19**(8), 2013, 1084–1094.
18. **Susuki, K., N. Yuki, D. Schafer, K. Hirata, G. Zhang, K. Funakoshi, M. Rasband.** Dysfunction of nodes of Ranvier: a mechanism for anti-ganglioside antibody-mediated neuropathies. – *Exp. Neurol*., **233**(1), 2012, 534-542.
19. **Thöne, J., R. Gold.** Review of laquinimod and its therapeutic potential in multiple sclerosis. – *Expert Opin. Pharmacother*., **14**(18), 2013, 2545-2552.
20. **Uncini, A.** A common mechanism and a new categorization for anti-ganglioside antibody-mediated neuropathies. – *Exp. Neurol*., **235**(2), 2012, 513-516.
21. **Wiegandt, H.** Gangliosides: a review with 677 references. – *New Compr. Biochem*., **10**, 1985, 199.
22. **Yu, R., K. Iqbal.** Sialosylgalactosyl ceramide as a specific marker for human myelin and oligodendroglial perikarya: gangliosides of human myelin, oligodendroglia and neurons. – *J. Neurochem*., **32**, 1979, 293-300.
23. **Zaprianova, E., K. Majtenyi, D. Deleva, O. Mikova, A. Filchev, B. Sultanov, V. Kolyovska, E. Sultanov, L. Christova, X. Kmetska, D. Georgiev.** Serum IgG and IgM ganglioside GM1 antibodies in patients with multiple sclerosis. – *Clin. Neurosci.,* **57**, 2004, 94-99.
24. **Zaprianova, E., D. Deleva, V. Kolyovska, B. Sultanov.** Clinical significance of serum anti-ganglioside antibodies in multiple sclerosis. – *Acta morphol. anthropol.,* **17**, 2011, 19-24.

Institute of Experimental Morphology, Pathology and Anthropology with Museum
Bulgarian Anatomical Society

Acta morphologica et anthropologica, 26 (3-4)
Sofia ● 2019

Genetic Variability Patterns of Haemonchus Species Affecting Small Ruminants in Egypt and Bulgaria

Omnia M. Kandil[1], Khaled A. Abdelrahman[1], Noha M. F. Hassan[1], Veselin Nanev[2], Ivelin Vladov[2], Margarita Gabrashanska[2].*

[1] Department of Parasitology and Animal Diseases, National Research Centre (NRC), Cairo, Egypt.
[2] Institute of Experimental Morphology, Pathology and Anthropology with Museum, Bulgarian Academy of Sciences, Sofia, Bulgaria

* Corresponding author e-mail: kandil_om@yahoo.com

The current study was carried out to study the impact of disparate geographical regions on genetic structures variability of *Haemonchus* species populations among small ruminants from Egypt and Bulgaria using mtDNA markers and to diagnose the predominant *Haemonchus* species isolated from the naturally infected sheep and goats through studying the genetic characterization and the phylogenetic relationships of such isolates. This study disclosed that the nucleotide sequences of PCR products belonged to the Cytochrome Oxidase subunit 1 gene of *H. contortus*. The dendrogram elucidated a close relation between Egyptian and Bulgarian goat isolates where they were located in the same sub genotype group. Thus goats' nucleotide sequences from Egypt and Bulgaria showed little variations among all published sequences with one substitution. Contrariwise, the Egyptian and Bulgarian sheep isolates are in two varied sub genotypes where sheep nucleotide sequences from Egypt and Bulgaria demonstrated great variation with others including five substitutions. The data obtained bring out the level of genetic variability among populations of *H. contortus* isolates of small ruminants in Egypt and Bulgaria. Thus, the current results could be a starting point for applying potent diagnosis and control measures and assaying the consequences of altering environment and management conditions.

Key words: Haemonchus, genetic variability, PCR, COI, small ruminants, Egypt, Bulgaria.

Introduction

Haemonchosis represents a serious global parasitic disease that adversely affects livestock production [1]. The blood feeding abomasal nematode *Haemonchuscontortus* (*H. contortus*); the causative agent of the disease is extremely pathogenic and the most economically vandal parasite of sheep and goats all over the world [15]. In Egypt, sheep and goats represent a significant source of the meat, milk and wool/hair industry. Similarly, in Bulgaria, sheep and goats are maintained in small private farms under

extensive conditions and sheep breeding considers one of the most important livestock industries. The pathological, epidemiological and economical impacts of the disease trigger various studies how to control the disease, thus, studying the genetic diversity and genetic relationships of this nematode via phylogenetic trees is indispensable [9]. Also, precise identification and genetic characterization is essential for valid diagnosis and increasing the efficacy of the control programs of parasitic nematodes [5]. Recently, various molecular markers have often been utilized for studying population genetics and phylogenetic analysis in different species [20]. Among the mtDNA, cytochrome oxidase subunit 1 (COI) genes have proved efficacy in various population genetic studies [8]. Furthermore, the rate of the substitution of the mtDNA was higher than the nuclear DNA [3, 6], so it is used to differentiate between firmly related individuals. Thus, the current study was fulfilled to study the comparative genetic diversity of *Hamonchus* species population among small ruminants in Egypt and Bulgaria and diagnose the predominant *Haemonchus* species isolated from the naturally infected Egyptian and Bulgarian sheep and goats through studying the genetic characterization and the phylogenetic relationships of such isolates that provide insight to improve diagnostics, comprehend the relationships between parasites, hosts, and geographic regions participating proactively in determining the potential for disease dissemination.

Material and Methods

Animals

Rapid clinical investigation of the suspected naturally infected sheep and goats was done prior slaughtering process at the abattoirs of Cairo, Giza and Qalubia in Egypt and Sofia in Bulgaria.

Parasite

Haemonchus species worms were harvested from the abomasa of the suspected naturally infected animals. Individual male worms were separated, washed extensively in PBS buffer pH 7.2 (37 °C) identified as stated by [14] and fixed in 70% ethyl alcohol.

DNA extraction

Twenty–two adult male worm specimens (18 samples as 3 of both species from three localities from Egypt and four samples; two from sheep and two from goats from Bulgaria), were prepared. DNA extraction kits (Qiagen) were utilized, as adopted by the manufacturer's protocols. DNA extracts were stored at −20°C.

PCR

The primer set utilized to amplify partially the COI gene of the *H. contortus* genome was, COIF:5′CCTACTATAATTGGTGGGTTTGGTAA–3′,COIR: 5′–TAGCCGCAGTAAAATAAGCACG–3′, as adopted by [12] PCR was done according to [10]. A total volume of 50 µl containing 1 × PCR buffer (20mM Tris–HCl and 50mMKCl at pH 8.4), 1.5mM MgCl2, 0.2mM deoxynucleoside triphosphate mixture (dATP, dCTP, dGTP and dTTP), 100 pmol of each primer, 2.5 units (U) of proof reading Thermusaquaticus (*puf*Taq) polymerase, 0.1 µg of extracted parasite genomic DNA and nuclease–free sterile double–distilled water up to 50.0 µl were used to perform PCR. Thermal profile was utilized through (Biometra thermocycler) as follows: an initial

denaturation was done at 95°C for 120 s; 35 cycles at 95°C for 50 s, 55°C for 45 s and 72°C for 60 s and the final extension at 72°C for 600 s. Agarose gel electrophoresis of 1.5% was used for analysis of the resulting PCR amplicons, as outlined by [16]. To visualize the resulted DNA bands, gel staining using ethidium bromide was used (0.5 µg/ml) against Gene Ruler 100 bp Plus ready–to–use DNA ladder (molecular weight marker) (Fermentas). Gel purification of the PCR products were processed utilizing a DNA gel purification kit (AB gene).

DNA sequencing

The PCR DNA products were sequenced with the previous primers, employing the BigDye Terminator v.3.1 Cycle Sequencing Kit on an automatic sequencer (3500 Genetic Analyzer; Applied Biosystems) [17]. The resulted data of nucleotide sequence of the COI gene of *H. contortus* from local Egyptian sheep and goats were presented to Gen Bank (KT826575, and KT826574) while that of Bulgarian sheep and goats were (KX379142 and KX379143). These sequence data were compared to other related isolates obtained by Gen Bank. The ClustalW (1.82) program of the European Bioinformatics Institute was used to align the nucleotide sequences.

Phylogenetic analysis

The analysis of the obtained nucleotide sequence involved multiple and pair–wise sequence alignments was constructed utilizing the un-weighted pair group method with arithmetic mean (UPGMA), distance method relied on Kimura 2-parameter model [13]. All trees were built utilizing the MEGA 6 program [19] and *H. placei* reference was appended as out groups.

Results and Discussion

In this study, the clinical investigation of the suspected infected animals has cleared that they suffered from weakness, loss of wool/hair, pale anemic mucosal membranes which may be due to infection by haemonchosis [5, 14]. The adult male *haemonchus* worms were selectively utilized for application of PCR to exclude the changeful DNA reinforcement which may have resulted from the eggs existed in the characteristic twisted uterine of the prolific female adult worms [6]. It is found that the mtDNA could define contrasts among closely related individuals due to its high rate of substitution in comparison with nuclear DNA [3]. So the COI gene has been used in determination of population genetic diversity in Brazil [4], in Pakistan [8] and in Egypt [10]. The analysis of PCR products has revealed about 213 bp length of a partial COI gene from the small ruminants under experiment. A particular band to *Haemonchus* species was detected in all reactions using COI specified primers. To explicate the population structure, comparison of the resulted sequences from Egypt and Bulgaria was performed with that of *Haemonchus* isolates from other nations recorded in gene bank. The obtained nucleotide sequences were recorded via MEGA 6.0 program revealing a 213 bp length of target size that coincided to nucleotide position 288 to 547 of *Haemonchus* mitochondrial genome and presented in Gene Bank with accession numbers (KT826575, KT826574, KX379142 and KX379143) from sheep, goats, of Egypt and Bulgaria, respectively. The results disclosed that the nucleotide sequence of PCR products belonged to the *H.contortus* COI gene in small ruminants. This goes in parallel with the finding obtained by [18] who mentioned that small ruminants consider the primary susceptive host that extremely infected by this hematophagus helminthes. The 9 Egyptian sheep isolates showed the

same sequence alignment with no variation so they are considered as one Egyptian sequence for sheep, as well as the 9 Egyptian goat isolates have also recorded similar sequence alignment. On the other side, the two Bulgarian isolates for the sheep were typically the same as well as, the two Bulgarian goats were also similar that may be due to the origin of the ruminants [2].

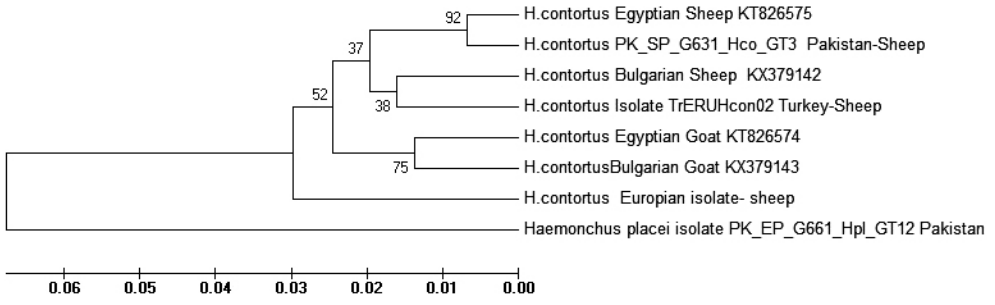

Fig. 1. Rooted Phylogenetic Tree of the Egyptian and Bulgarian *Haemonchus* species isolates with other related *Haemonchus*family and other nations isolates planned from nucleotide sequences encoding for COI gene of the analyzed *Haemonchus* genomes. A weighted pair group method with arithmetic mean dendrogram.

This suggested that the adult worms isolated from each species in each country were identical. The dendrogram showed close relation between Egyptian goat isolates and Bulgarian goat isolates where they are in the same sub genotype group; they have exhibited little diversities among all recorded sequences with one substitution (**Fig. 1**) that may be owing to the animal movement between countries which is an important determinant of population genetic structure in these nematodes [3]. While the Egyptian and Bulgarian sheep isolates are in two different sub genotypes so a major difference was noticed between sheep sequence from both countries with others in 5 substitutions that agree with the result obtained by [8, 12], who recorded variation in COI gene loci with high rate of gene flow among *Haemonchus* species from various hosts worldwide. In other context, [11] outlined that sheep were more susceptible to the heavy infection of helminthes than goats that may be owing to their various feeding behavior. While feeding of sheep and goats together, goats evade the 3rd stage infective nematode larvae as they intake usually woody plants, minimizing the larval swallowing, which usually are still on the grass preferred by sheep [7]. Thus this difference among the sheep nucleotide sequence from Egypt and Bulgaria isolates may be attributed to the repeated exposure of infection to *haemonchus* and other parasites that increase the opportunity of mutation and variation in genetic structure. Concerning more understanding of structural populations, the partial genomic sequences (213bp) of *Haemonchus* COI gene obtained from different Egyptian and Bulgarian sheep and goats was compared with that of four reference genotype sequences recovered from the Gen Bank from other nations and genus (**Fig.1**). The results declared that the Egyptian sheep isolates were more related to Pakistani isolate while Bulgarian sheep isolates were more related to the Turkish isolate. This might be due to several factors including the possible transportation of host via the different geographic areas as explained by [2], beside that both species in the different countries may have originated from the same ancestor during their developmental history [4]. This study has confirmed the *H. contortus* dominance and prevalence in both sheep and goats in Egypt and Bulgaria. The current work revealed

apparition of the homology between goat nucleotide sequences from Egypt and Bulgaria *Haemonchus* isolates among all published sequences while great variation was noticed in sheep sequence from Egypt and Bulgaria *Haemonchus* isolates. Our results declared that the migration of various hosts between the different geographical areas could affect the population genetic structure and facilitate the cross infection between variant hosts. The phylogenetic analysis of *H. contortus* separated from the Egyptian and Bulgarian small ruminants, could be an important aid in proceeding of proper management and control programs.

Acknowledgements: This work was funded from a bilateral project between the Academy of Scientific Research in Egypt and the Bulgarian Academy of Sciences, entitled "Recent methods for diagnosis of haemonchosis".

References

1. **Abdo, B., A. Nur, B. Abera, D. Lemma, E. Eticha.** Prevalence and associated risk factors of haemonchosis among small ruminants slaughtered in BishoftuElfora export abattoir, Ethiopia. – *Acta Parasitologica Globalis*, **8**, 2017, 73-78.
2. **Akkari, H., J. Jebali, M. Gharbi, M. Mhadhbi, S. Awadi, M. A. Darghouth.** Epidemiological study of sympatric Haemonchus species and genetic characterization of H. contortus in domestic ruminants in Tunisia. – *Vet. Parasitol.*, **193**, 2013, 118-125.
3. **Blouin, M. S.** Molecular prospecting for cryptic species of nematodes: mitochondrial DNA versus internal transcribed spacer. – *Int. J. Parasitol.,* **32**, 2002, 527-531.
4. **Brasil, B. S., R. L. Nunes, E. Bastianetto, M. G. Drummond, D. C. Carvalho, R. C. Leite, M. B. Molento, D. A. Oliveira.** Genetic diversity patterns of H. placei and H. contortus populations isolated from domestic ruminants in Brazil. – *Int. J. Parasitol.*, **42**, 2012, 469-479.
5. **Gasser, R. B., N. J. Bott, N. B. Chilton, P. Hunt, I. Beveridge.** Toward practical, DNA–based diagnostic methods for parasitic nematodes of livestock – bionomic and biotechnological implications. – *Biotechnol. Adv.*, **26(4),** 2008, 325-334.
6. **Gharamah, A. A., M. N. Azizah, W. A. Rahman.** Genetic variation of Haemonchuscontortus (Trichostrongylidae) in sheep and goats from Malaysia and Yemen. – *Vet. Parasitol.*, **188**, 2012, 268-276.
7. **Hoste, H., J. F. J. Torres–Acosta, V. Paolini, A. J. Aguilarcaballero, E. Etter, Y. Lefrileux, C. Chartier, C. Broqua.** Interactions between nutrition and gastrointestinal infections with parasitic nematodes in goats. – *Small Rumin. Res.*, **60**, 2005, 141-151.
8. **Hussain, T., K. Periasamy, A. Nadeem, M. E. Babar, R. Pichler, A. Diallo.** Sympatric species distribution, genetic diversity and population structure of Haemonchus isolates from domestic ruminants in Pakistan. – *Vet. Parasitol.*, **206**, 2014, 188-199.
9. **Jacquiet, P., J. F. Humbert, A. M. Comes, J. Cabaret, A. Thiam, D. Cheikh.** Ecological, morphological and genetic characterization of sympatric Haemonchus spp. parasites of domestic ruminants in Mauritania. – *Parasitology*, **110**, 1995, 483-492.
10. **Kandil, O. M., K. A. Abdelrahman, H. A. Fahmy, M. S. Mahmoud, A. H. El Namaky, J. E. Miller.** Phylogenetic patterns of Haemonchus contortus and related trichostrongylid nematodes isolated from Egyptian sheep. – *J. Helminthol.*, **91(5),** 2017, 583-588.
11. **Kanyari, P. W. N.** The relationship between coccidial and helminth infections in sheep and goats in Kenya. – *Vet. Parasitol.*, **51**, 1993, 137-141.
12. **Kanzaki, N., K. Futai.** A PCR primer set for determination of phylogenetic relationships of Bursaphelenchus species within the xylophilus group. – *Nematology*, **4**, 2002, 35-41.
13. **Kimura, M.** A simple method for estimating evolutionary rates of base substitutions through comparative studies of nucleotide sequences. – *J. Mol. Evol.*, **16**, 1980, 111-120.
14. **MAFF** (Ministry of Agriculture, Fisheries and Food). *Manual of veterinary parasitological laboratory techniques.* London, UK, ADAS, HMSO. *Veterinary parasitology* – 1986, 160pp
15. **O'Connor, L. J., S. W. Walkden–Brown, L. P. Kahn.** Ecology of the free-living stages of major trichostrongylid parasites of sheep. – *Vet. Parasitol.*, **142**, 2006, 1-15.

16. **Sambrook, J., D. W. Russell** Molecular cloning: a laboratory manual. Plain view, New York*, Cold Spring Harbor Laboratory Press*, 2000, 2001pp.
17. **Sanger, F., S. Nicklen, A. R. Coulson.** DNA sequencing with chain-terminating inhibitors. – *Proc. Nat. Acad. Sci., USA,* **74**, 1977, 5463-5467.
18. **Sutherl, I., I. Scott**. Gastrointestinal nematodes of sheep and cattle: *Biology and Control. Chichester, UK*, 2010, Wiley – Blackwell, 242p.
19. **Tamura, K., D. Peterson, N. Peterson, G. Stecher, M. Nei, S. Kumar**. MEGA5: Molecular evolutionary genetics analysis using maximum likelihood, evolutionary distance, and maximum parsimony methods. – *Mol. Biol. Evol.*, **28**, 2011, 2731-2739.
20. **Troell, K., A. Engstrom, D. A. Morrison, J. G. Mattsson, J. Hoglund.** Global patterns reveal strong population structure in H. contortus, a nematode parasite of domesticated ruminants. – *Int. J. Parasitol.,* **36**, 2006, 1305-1316.

Institute of Experimental Morphology, Pathology and Anthropology with Museum
Bulgarian Anatomical Society

Acta morphologica et anthropologica, 26 (3-4)
Sofia ● 2019

Histological Gastric Structure of Badger (Meles meles)

Emil Sapundzhiev, Mihail Chervenkov, Lubomir Hristakiev*
Department of Anatomy, Histology and Physiology, Faculty of Veterinary Medicine, University of Forestry, Sofia, Bulgaria

* Corresponding author e-mail: emisapun@yahoo.com

The aim of this study was to investigate histologically the stomach of a male badger (Meles meles) which was found on the road after car accident and to compare it with another carnivorous animals as dog, fox, wolf, jackal, bear, cat and tiger. In carnivores, for comparison aspect as nomenclature prescription, the mucosal layer of the stomach has a collagen like membrane layer - *stratum compactum mucosae,* just under the funduses of the glands. Previously it was called - *lamina subglandularis,* and its thickness in mature animals varies between 15-40 μm. Actually the layer in badger stomach was not presented in observed slides although the animal belongs to carnivorous order. It is similar situation as in animals of canine family unlike of animals from feline family which usually have layer - *stratum compactum mucosae*, between bottom of the glands and muscular mucosal lamina.

Key words: histology, carnivorous, badger, stomach

Introduction

The badger (*Meles meles*) belongs to Class Mammalia, Order Carnivora of the family Mustelidae. It is distributed in mountain areas that are less urbanized, and although it avoids contact with people, it is subject to taming. The badger is the only animal that allows in their labyrinthine hollow "renters", nevertheless they are other animal species.

As a wild animal it has been recorded consuming the greatest variety of foods, but also supplemented the diet with fruits, small vertebrates, various invertebrates (worms, molluscan and others).

The badger has been subjected to various genetic and ecological studies on its origin, structure distribution and behaviour. In our country there are little scientific reports that are related to badgers' investigations and treatment and they are concentrated generally on similar wild animals [1, 4, 5, 6]. Furthermore, there are small morphological investigations focusing on specific comparative morphofunctional explanation of badger organism or in comparison [4]. The animal is the object of hunting because of his precious skin and some subproducts of it. Stuffed specimens serve not only for ornamentation, but also for beautiful accessories, souvenirs and even clothes.

According manner of eating carnivorous must bite and rip their food off and probably because their teeth are brachidont, as herbivores chew side to side and their teeth are hypsodont [7, 9]. Unlike humans, their saliva does not contain digestive enzymes. Carnivores have a shorter digestive tract. This is because their meat is rich of nutrients and they can extract them easier. The actual size of a carnivorous stomach is significantly larger than herbivores. Their stomachs encompass roughly 60 to 70% of their digestive tracts. Within their stomach they have powerful digestive enzymes. They have roughly 10 times more the excretion of hydrochloric acid in their stomach than humans or herbivores. Their caecum, however is much smaller in comparison of other animals.

Anatomically, the stomach of the carnivores resembles a lot of human, both in shape and in a device where the entire mucosal surface is glandular, unlike that of the horse and the pig, in which animals about 1/3 of the surface has an aglandular cutaneus mucosa. Furthermore, ruminants have specific aglandular forstomach with three parts, respectively rumen, reticulum, omasum, and then follow a glandular abomasum, corresponding to ventriculus [7, 13, 14].

In histological literature there are data for specific lamina subglandularis in carnivorous stomach wall which presences into the propria of mucous layer. Some other histologists demonstrate double-layered structure of this lamina subglandularis, which is underneath the bases of the stomach glands. According to them the first layer which is situated closer to the bottoms of the glands and it is designated as stratum granulosum due to the fact that it is rich of connective tissue cells and their nuclei give impression for granulation. The second layer they call *stratum fibrosum*, consisting of thick collagen fibers and which actually is typical *stratum compactum mucosae* [2, 3, 8]. According to other authors and by Nomina Histologica only a single collagenous acellular layer *stratum compactum mucosae* exists in carnivorous stomach mucosa, which hypothetically protects the wall of perforations [10].

The aims of this study are investigation of the histological structure of the badger stomach wall and comparing it with other carnivorous animals as dog, fox, jackal, wolf, bear, cats and tiger, respectively which were surveyed previously and to comment this specific fact on the physiological reason for this.

Materials and Methods

The stomach of a male badger which was found on the road after car accident was investigated. After laparotomy the stomach was removed and pieces from the wall were cut. The histological slides were prepared by conventional method and after paraffin impregnation, the sections 7 μm thin were cut by microtome and stained with Hematoxylin and Eosin. Then the samples were examined microscopically and morphometry was done as well. For observation, measurement and picture documentation a microscope with computer system „Olympus“ (Japan) was used.

Results and Discussion

Almost 1/3 of the wall thickness of badger stomach is covered by mucosa (**Fig. 1**). Superficial mucosal epithelium has columnar form in one layer and weak eosinophily was demonstrated. Glandular tubules have transversal diameter around 25 μm and into the thin space between tubules in loose connective tissue of the propria an individual smooth muscle cells exist that are arisen by three layered structure of *lamina muscularis*

mucosae as it was described for another animals [3]. In stomach glandulocytes are shown, respectively basophilic chief cells (*exocrinocytes principales*) and eosinophilic parietal cells (*exocrinocytes parietales*) but less mucocytes are observed. Furthermore, as in many other investigated by us carnivorous species belonging to canine family the subglandular mucosal layer – *stratum compactum mucosae*, was not established [11, 12, 13, 16, 17].

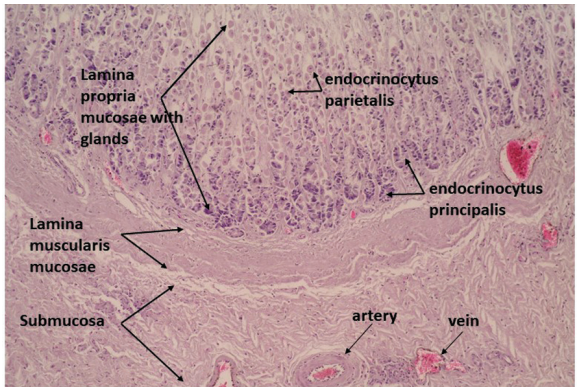

Fig. 1. Mucosal and submucosal layers of badger stomach (magn. × 100).

Opposite to this fact in felines species stomach the layer *stratum compactum mucosae* was always presented (**Table 1**). This distinctive feature is only commented by some authors [2], who report that the cat stomach has layer *stratum compactum mucosae*, but the latter may be absent in dog's stomach.

Submucosa is quite thicker in comparison of other large animals [7, 13, 14] and varies almost 500 μm. It includes between tissue composition well developed myotypical blood vessel plexus and masses of diffusely distributed lymphocytes. Submucosal autonomic nervous plexus – Meisneri, is very well presented in sites rich in white adipose tissue.

Table 1. Stratum compactum existence layer in stomach mucosa of investigated animals.

Family of Order Carnivores	Species	Total (n)	Male (n)	Female (n)	*Stratum compactum mucosae* (μm)
Canidae	Dog *(Canis familiaris)*	15	9	6	-
	Fox *(Vulpes vulpes)*	1	-	1	-
	Jackal *(Canis aureus)*	2	2	-	-
	Grey Wolf *(Canis lupus)*	2	2	-	-
Ursidae	Brown Bear *(Ursus arctus)*	1	-	1	-
Felidae	Domestic Cat *(Felis domestica)*	8	3	5	32.5 – 37.5
	Wild Cat *(Felis silvestris)*	2	1	1	15 – 25
	Tiger *(Panthera tigris)*	2	1	1	40 – 42.5
Mustelidae	Badger *(Meles meles)*	1	1	-	-

Thickness of muscular wall layer varies 200-300 μm and bundles are surrounded by delicate perimysium. Longitudinally cut smooth muscle cells have a worm-like nuclei as a result of suddenly cause death. The autonomic intramural myenteric nervous plexus containing multipolar neurons is found between muscular fascicles (**Fig. 2**).

The peritoneum has common compound [3, 7, 10] and its proper layer consists of dense irregular connective tissue covered outside with mesothelium.

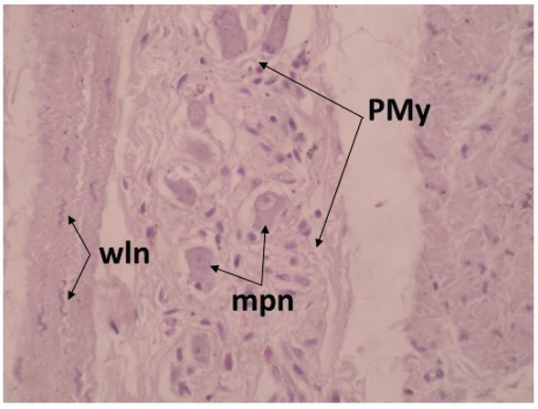

Fig. 2. Part of the muscular layer from badger stomach. PMy – *plexus nervous myentericus*, wln – worm-like nuclei, mpn - multipolar neurons (magn. × 400).

Conclusion

Dismissing of the layer *stratum compactum mucosae* in a badger stomach is a similar fact as in another canine carnivorous species like dog, fox, jackal, wolf and bear, but it differs in feline animals – cats (wild and domestic) and tiger, where it was demonstrated. This fact supports the hypothesis that the mucosal layer *stratum compactum mucosae* permanently exists in *Felidae family* animals, but it is not usually presented in animals belonging to *Canidae, Ursidae* and *Mustelidae family*, nevertheless that these three families belong to animals of *Order Carnivorae*.

Acknowledgements: The financial support by the National Program of Ministry of Education and Science for Young Scientists and Postdoctoral investigators 2018-2020 is acknowledged.

References

1. **Alexandrova, V., Y. Kostov.** The language of some wild predators in soundgrams (spectrograms). – *BJAS*, **18,** 2012, 133-137.
2. **Bacha, W. Jr., L. M. Wood.** Digestive system. - In: *Color atlas of veterinary histology* (Eds. Bacha, W. Jr., L. M. Wood), Philadelphia, USA, Williams & Wilkins Scientific Publishers, 1990, 111-150.
3. **Frappier, B. L.** Digestive system. - In: *Dellmann's Textbook of veterinary histology,* (Eds. H. D. Dellmann, J. A. Eurell), Ames, Iowa, USA, Blackwell Publishing, 2006, 170-211.
4. **Georgiev, G. I.** Characteristic features of the skeleton in different animals. **–** In: *Veterinary Osteology* (Ed. M. Stefanova), Sofia, D. V. Disign, 2015, 144-184 slides.
5. **Kostov, Y., V. Alexandrova.** *Principles of animal etiology* (Ed. V. Alexandrova), Sofia, Enovche, 2004, 176 p. [in Bulgarian]
6. **Kostov, Y., V. Alexandrova.** How to recognize (decode) animal language. – *BJAS*, **15**, 2009, 475-477.
7. **Kovachev, G., G. Georgiev, A. Vodenicharov.** Internal organs (v. II). In: *Anatomy of domestic animals* (Ed. I. Stoykov), KOTA, Stara Zagora, 2016, 167-169. [in Bulgarian].
8, **Krystev, H., S. Vitanov**. *Citologia i Histologia* (Ed. G. Kondov), Sofia, Zemizdat Scientific Publishers, 1993, 251-255 [in Bulgarian].
9. **Nikolova, N., I. Rumenova, M. Stefanova, G. I. Georgiev.** Differences of the skeleton and teeth in the badger (Meles meles L., 1758) – *Suppl. Management and sustainable use of biological resources, V-th National Student Scientific Conference*, University of Forestry, Sofia, 2013, 47.

10. **Nomina histologica**. Histologia generalis. International Committee on Veterinary Histological Nomenclature, Gent, 1992, 15-37.
11. **Sapundzhiev, E., P. Zahariev, D. Pupaki**. Morphologic investigation of the stomach mucosa characteristics in dogs and cats. – *Suppl. XVII Europ. Congress Vet. Anat., Budapest,* 2008, 32.
12. **Sapundzhiev, E., P. Zahariev, S, Stoyanov.** Histological structure of the grey wolf (Canis lupus) stomach. – *J. Tradition and Modernity in Vet. Med*., **2,** 2017, 66-68.
13. **Sapundzhiev, E., M. Chervenkov, Y. Iliev, S. Mustafa, M. Dimitrova.** Morphofunctional investigation of brown bear (Ursus arctus) stomach. – *J. Tradition and Modernity in Vet. Med*., **3,** 2018, 50-54.
14. **Smollich, A.** *Mikroskopische Anatomie* (Ed. H. Shultze), S. Hirzel Verlag, Leipzig, 1972, 166-188 [in German].
15. **Stinson, A. W., M. Lois, Calhoun.** Digestive system. – In: *Textbook of Veterinary Histology.* (Ed. H-D. Dellmann), Philadelphia, Lea & Febiger, 1993, 153-193.
16. **Zahariev, P., E. Sapundzhiev, D. Pupaki, P. Rashev, A. Palov, T. Todorov.** Morphological characteristics of the canine and feline stomach mucosa. – *J. Anatomia, Histologia, Embryologia*, **39, 6**, 2010, 563-568.
17. **Zahariev, P., D. Pupaki, S. Stoyanov, E. Sapundzhiev.** Histological investigation of jackal (Canis aureus) stomach.– *J. Anatomia, Histologia, Embryologia*, **43**, 2014, 99-100.

Institute of Experimental Morphology, Pathology and Anthropology with Museum
Bulgarian Anatomical Society

Acta morphologica et anthropologica, 26 (3-4)
Sofia ● 2019

Profile of Cell-Surface Glycopeptides and Role of Guerin 51 kDa gCBP for Tumor Cell Adhesion

*J. Stoyloff**

Institute of Experimental Morphology, Pathology and Anthropology with Museum, Bulgarian Academy of Sciences, Sofia, Bulgaria

* Corresponding author e-mail: info.jstoyloff@gmail.com

We found mainly tri-antennary and small amount of tetra-antennary glycopeptides with terminal galactose at the cell surface of Guerin 'heavy' cell's subpopulation (GH). On the other hand, Guerin 'light' cells (GL) contained oligomannoside and hybrid type oligosaccharides with terminal galactose and glucose. Next we used isolated cell-surface glycopeptides from GH cells in solid-phase inhibition assay. We found drastic reduction of adhered GH cells on laminin-coated plates in the presence of tri- and tetra-antennary cell-surface glycopeptides. We also saw drastic reduction of adhesion of GH cells on fibronectin-coated plates in presence of tri- and tetra-antennary cell-surface glycopeptides. Macromolecular ligand asialofetuin (AsFet) was also potent at inhibiting GH adhesion to fibronectin-coated plates. On collagen-coated plates most potent inhibition was observed by tri-antennary cell-surface glycopeptides, followed by tetra-antennary glycopeptides and asialofetuin.

Key words: galectin, cancer, adhesion

Introduction

Galectins participate in carbohydrate-mediated adhesion of tumor cells to extracellular matrix (ECM), as well as in homo- and heterotypic adhesions of tumor cells. Glycoproteins of the matrix are N-glycosylated and potential ligands for galectins. These ligands include laminin, fibronectin and collagen IV [9].

Secreted galactose-binding proteins could participate in cell-to-extracellular matrix (ECM) adhesion through bridging carbohydrate moieties of cell-surface glycoproteins and ECM glycoproteins. For example, galectin-1 is secreted outside colon cancer (Colo201) cells where it helps adhesion and spreading of these cells to fibronectin-, laminin-, and collagen-coated plates [6].

Review of the literature shows two models of oligomerization of lectins. In the ligand-induced oligomerization model, galectins bind cell-surface glycoproteins, followed by oligomerization. The other model of oligomerization postulates that oligomerization takes place before binding of ligands. Cell-surface N-linked

glycans are potential ligands for galectins with implications for oligomerization and adhesion. Galectin-3 binds to cell surface glycoproteins, including branched N-glycans [3]. Another report shows that Gal-3 binds specifically to beta-galactoside residues of cell surface glycoproteins [4].

The aim of the present study was to characterize adhesion of subpopulations of Guerin tumor cells to solid-phase immobilized glycoproteins of ECM. We also investigated the composition of cell-surface glycoproteins of Guerin tumor cells (GTC), in order to reveal the role of branching in adhesion. Finally, we present data of ligand-induced oligomerization of 51 kDa gCBP and implications of this oligomerization for adhesion of GTC.

Materials and Methods

Separation of Guerin tumor cells (GTC) subpopulations

Guerin tumor cells were separated according to their buoyant densities as described in [13].

Metabolic labeling of cell-surface glycoproteins with radioactive sugars

Monolayer of GH cells were detached by trypsinization, resuspended in complete RPMI medium containing 1 μCi/ml D-[14C] glucosamine (45 to 60 mCi/mmol), and grown for two days. Then Guerin tumor cells were labeled in a solution containing 0.01 mCi/ml [3H] mannose.

Isolation of cell-surface glycopeptides from GTC

Guerin tumor cells were washed with 0.15M NaCl/0.01M sodium bicarbonate, pH 7.5 and then incubated in the same buffer containing 0.05% tripsin (type III, Sigma) for 20 min at 37°C. The reaction was stopped with 0.003% soy trypsin inhibitor and the supernatant was used for lectin affinity chromatography.

Lectin affinity chromatography

Affinity chromatography was performed as described in [5].

Isolation of secreted 51 kDa gCBP from Guerin tumor cells

GTC in cell culture medium were incubated for 3 h at 37°C with radioactive ^{35}S methionine (500 μCi). Cell were washed and incubated in cell culture medium for 24 h [12] to allow maximum secretion of 51 kDa gCBP. Secreted 51 kDa gCBP was then isolated by gel filtration.

Inhibition assay

Inhibition of adhesion of GTC to solid-phase immobilized glycoproteins of ECM was done as described by Horiguchi [6]. Laminin, fibronectin or collagen (5 μg/ml in 0.1M carbonate buffer, pH 9.6) were added to microtiter plates and incubated for 3 h at 37°C. After washing with PBS, a solution of ^{35}S 51 kDa gCBP was added and incubated for 2 h in the presence of tri- and tetra-antennary cell-surface glycopeptides.

Results

We found mainly tri-antennary and small amount of tetra-antennary glycopeptides with terminal galactose at the cell surface of Guerin heavy (GH) cells (**Fig. 1**). Guerin light (GL) cells contained predominantly oligomannoside and hybrid type oligosaccharides with terminal galactose and glucose.

Cell-surface glycopeptides from GH cells are ligands of 51 kDa gCBP, as observed in inhibitory experiments shown in Figs. 2, 3 and 4. Approximately 9 × 10^5 GH cells/well adhere to laminin-coated plates. However, we see a drastic reduction of adhered cells in the presence of tri- and tetra-antennary cell-surface glycopeptides (**Fig. 2**).

Adhesion of GH cells to fibronectin-coated plates is shown in **Fig. 3**. Here we can also see a drastic reduction of adhesion in the presence of tri- and tetra-antennary cell-surface glycopeptides. Macromolecular ligand asialofetuin (AsFet) is also a potent inhibitor of GH adhesion to fibronectin-coated plates. It is evident that the most potent inhibition is by tetra-antennary cell-surface glycopeptides, followed by tri-antennary glycopeptides and asialofetuin.

Finally we investigated the inhibition of adhesion of GH cells on collagen IV-coated plates. Here most potent inhibition was observed by tri-antennary cell-surface glycopeptides, followed by tetra-antennary glycopeptides and asialofetuin (**Fig. 4**).

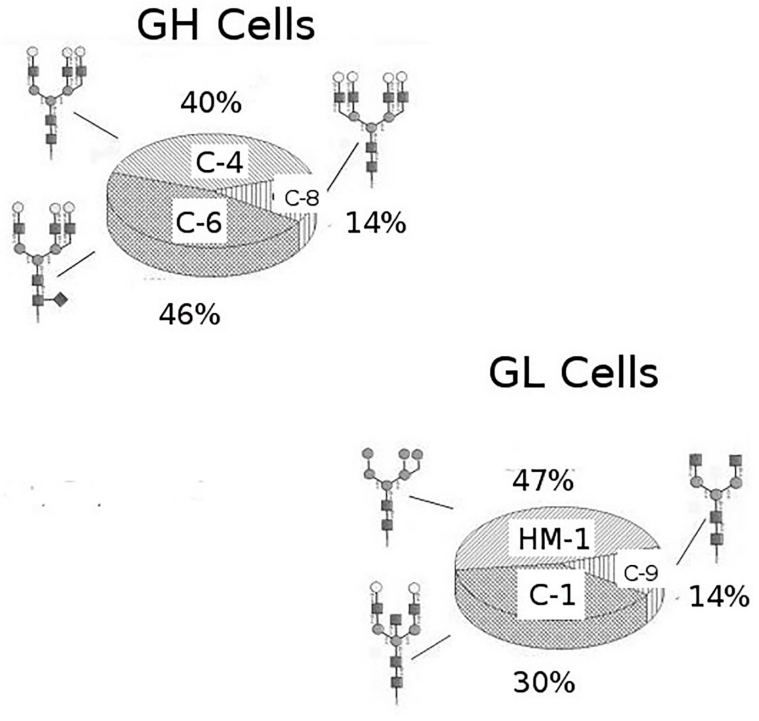

Fig. 1. Glycoprofile of cell surface glycoproteins of Guerin tumor cell's subpopulations

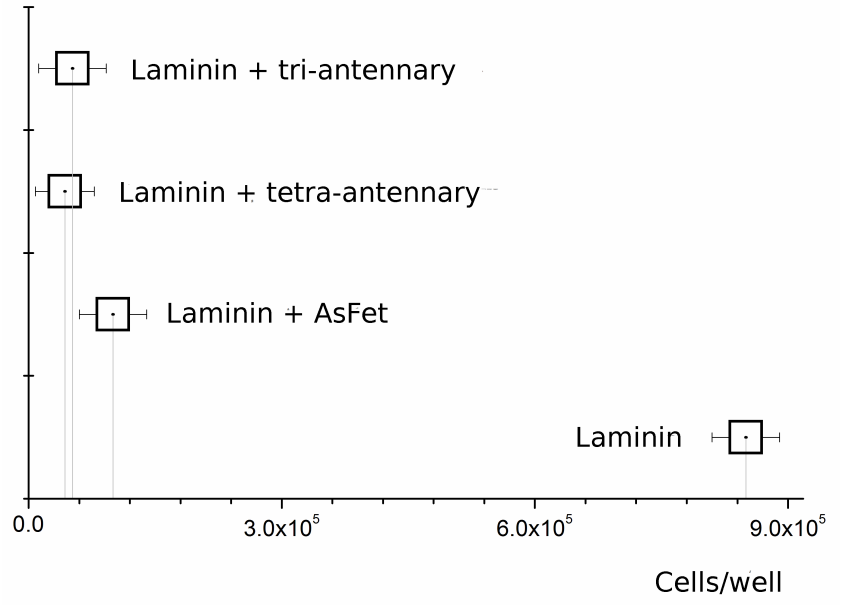

Fig. 2. Adhesion of Guerin "heavy" (GH) subpopulation to laminin. **Laminin** – adhesion of GTC to laminin, **Laminin + AsFet** – inhibition of adhesion with AsialoFetuin, **Laminin + tri-antennary** – inhibition of adhesion with tri-antennary cell-surface glycopeptides, **Laminin + tetra-antennary** – inhibition of adhesion with tetra-antennary cell-surface glycopeptides

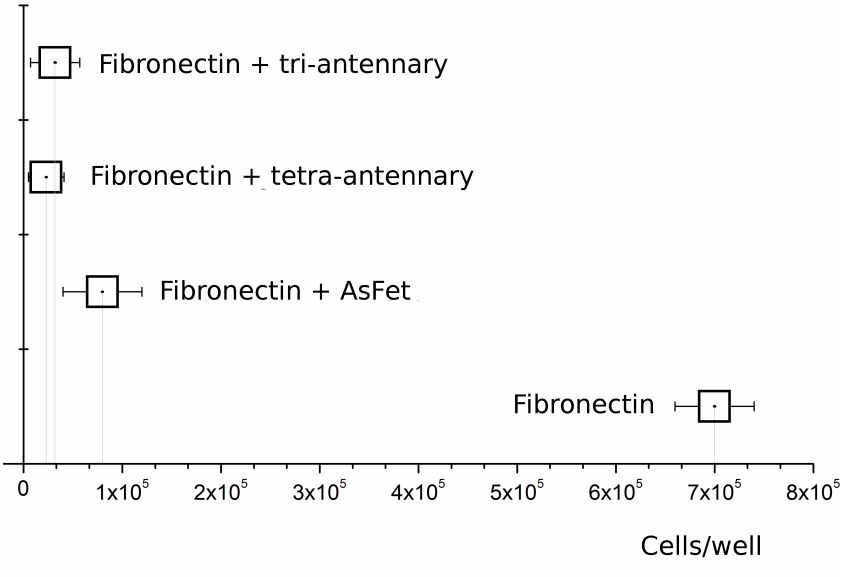

Fig. 3. Adhesion of Guerin "heavy" (GH) subpopulation to fibronectin. **Fibronectin** – adhesion of GTC to laminin, **Fibronectin + AsFet** – inhibition of adhesion with AsialoFetuin, **Fibronectin + tri-antennary glycopeptides** – inhibition of adhesion with tri-antennary cell-surface glycopeptides, **Fibronectin + tetra-antennary glycopeptides –** inhibition of adhesion with tetra-antennary cell-surface glycopeptides.

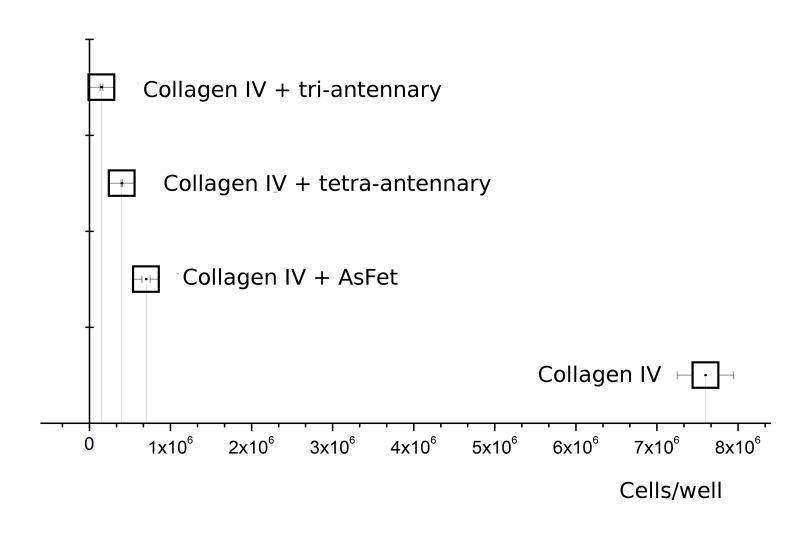

Fig. 4. Adhesion of Guerin "heavy" (GH) subpopulation to collagen IV. **Collagen IV** - adhesion of GTC to laminin, **Collagen IV + AsFet** - inhibition of adhesion with AsialoFetuin, **Collagen IV + tri-antennary glycopeptides** - inhibition of adhesion with tri-antennary cell-surface glycopeptides, **Collagen IV + tetra-antennary glycopeptides -** inhibition of adhesion with tetra-antennary cell-surface glycopeptides.

Comparing the inhibition of adhesion on laminin, fibronectin and collagen IV-coated plates, we found that the most potent inhibition in the case of laminin and fibronectin was brought about by tetra-antennary glycopeptides, whereas for collagen IV the most potent inhibition was caused by tri-antennary cell-surface glycopeptides.

Discussion

Analysis of membrane glycoproteins of 3T3 cells shows a decrease in bi-antennary glycopeptides, with a simultaneous increase in tri- or tetra-antennary glycopeptides [10]. Membrane subfractions of rat pheochromocytoma (PC12) cells consist of large tri- and tetra-antennary complex oligosaccharides accounting for 82 to 97% of the membrane glycoproteins [7]. The increase in antennae number of glycoproteins leads to increased binding to galectins [9]. Glycan branching of glycoproteins also correlates with the metastatic potential of oral squamous carcinoma [14]. Increased branching leads to increased binding to galectins, as showed by Andre et al. [1].

In situ oligomerization of galectins is shown by Nieminen et al. [8] in binding of galectin-3 to solid-phase immobilized asialofetuin. *In situ* oligomerization of galectin-3 on cell surface leads to cluster formation of receptors, as shown by FRET technique [8]. Oligomerization is a unique feature of secreted galectin-3, leading to formation of ordered galectin-glycan lattices on the cell surface. Balan et al. [6] show that galectin-3 is monomer in solution but in the presence of a ligand, galectin-3

polymerizes up to pentamers. Oligomerization of galectin-3, after ligand binding, occurs on cell surfaces within the physiological concentrations of the lectin. It has thus been proposed that oligomerization of the N-terminal domains of galectin-3 molecules, after ligand binding by the C-terminal domain, is responsible for adhesion of tumor cells to solid-phase immobilized glycoproteins [8]. Recombinant galectin-3, with missing N-domain, does not mediate adhesion between neutrophils and endothelial cells [11], pointing to the role of N-domain in oligomerization.

Conclusion

Our data show mainly tri-antennary and small amount of tetra-antennary oligosaccharides at the cell surface of Guerin heavy cells.

Guerin tumor cells secrete 51 kDa gCBP, which is involved in adhesion of GTC to plates coated with laminin, fibronectin and collagen IV. Inhibition experiments with cell-surface glycopeptides, isolated from Guerin cells, point to the role of these glycopetides as ligands for 51 kDa gCBP. We can assume that the secreted protein binds to laminin (fibronectin, collagen IV) and oligomerizes *in situ***.** According to the 'ligand-induced' model, receptors oligomerize only in the presence of their ligands. The low MW ligand galactose was able to induce oligomerization of 51 kDa gCBP. We found also that multivalent ligands were able to induce di- and trimers, but not tetramers of 51 kDa gCBP. It can be concluded that adhesion of GTC is mediated by 51 kDa gCBP, which form ligand-induced oligomers.

References

1. **André, S., S. Kojima, G. Gundel, R. Russwurm, X. Schratt.** Branching mode in complex-type tri-antennary N-glycans as regulatory element of their ligand properties. – *Biochim. Biophys. Acta*, **176**(5), 2006, 768-782.
2. **Balan, V., P. Nangia-Makker, D. Kho, Y. Wang, A. Raz.** Tyrosine-phosphorylated galectin-3 protein is resistant to prostate-specific antigen (PSA) cleavage. – *J. Biol. Chem.*, **287**(8), 2012, 5192-5198.
3. **Boscher, C, Y. Z. Zheng , R. Lakshminarayan, L. Johannes, J. W. Dennis.** Galectin-3 protein regulates mobility of N-cadherin and GM1 ganglioside at cell-cell junctions of mammary carcinoma cells. – *J. Biol. Chem.*, **287**(39), 2012, 32940-32952.
4. **Chiu, C., S. Strugnell, O. Griffith, S. Jones, A. Gown.** Diagnostic utility of galectin-3 in thyroid cancer. – *Am. J. Pathol.*, **176**(5), 2010, 2067-2081.
5. **Cummings, R., S. Kornfeld.** Fractionation of asparagine-linked oligosaccharides by serial lectin-Agarose affinity chromatography. A rapid, sensitive, and specific technique. – *J. Biol. Chem.*, **257**(19), 1982, 11235-11240.
6. **Horiguchi, N., K. Arirnota, A. Mizutani, Y. Endo-Ichikawa, H. Nakada.** Galectin-1 induces cell adhesion to the extracellular matrix and apoptosis of nonadherent human colon cancer Colo20J cells. – *Biochem. (Tokyo)*, **134**(6), 2003, 869-874.
7. **Margolis, R., S. Salton, U. Margolis.** Complex carbohydrates of cultured PC12 pheochromocytoma cells. Effects of nerve growth factor and comparison with neonatal and mature rat brain. – *J. Biol. Chem.*, **258**(7), 1983, 4110-4117.
8. **Nieminen, J., A. Kuno, J. Hirabayashi, S. Sato.** Visualization of galectin-3 oligomerization on the surface of neutrophils and endothelial cells using fluorescence resonance energy transfer. – *J. Biol. Chem.*, **282**(2), 2007, 1374-1383.
9. **Ozeki, Y., T. Matsui, Y. Yamamoto, K. Titan**i. Tissue fibronectin is an endogenous ligand for galectin. – *Glycobiology*, **5**, 1995, 255-261.
10. **Santer, U., F. Gilbert, M. Glick.** Change in glycosylation of membrane glycoproteins after transfection of NIH 3T3 with human tumor DNA. – *Cancer Res.*, **44(9)**, 1984, 3730-3735.

11. **Sato, S., N. Ouellet, I. Pelletier, M. Simard, A. Rancourt, M. G. Bergeron.** Role of galectin-3 as an adhesion molecule for neutrophil extravasation during streptococcal pneumonia. – *J. Immunol.*, **168**(4), 2002, 1813-1822.
12. **Stoyloff, J., S. Ivanov.** Isolation and characterization of galactose-specific carbohydrate-binding protein from Guerin tumor cells. – *Brain Res. Bull.*, **83**(1-2), 2010, 65-75.
13. **Stoyloff, J., S. Ivanov.** Guerin tumour cells have different isoprofile and cellular distribution of 51 kDa galactose-binding protein and different activity of the thermostable Regan enzyme. – *Comp. Rend. Acad. Bulg. Sci.*, **65**(3), 2012, 353-358.
14. **Tanda, N., S. Mori, M. Nose, T. Saito, S. Song.** Expression of Phaseolus vulgaris leukoagglutinin-binding oligosaccharides in oral squamous cell carcinoma: possible association with the metastatic potential. – *Pathol. Int.*, **46**(9), 1996, 639-645.

Institute of Experimental Morphology, Pathology and Anthropology with Museum
Bulgarian Anatomical Society

Acta morphologica et anthropologica, 26 (3-4)
Sofia ● 2019

Anthropology and Anatomy

Influence of Age and Sex on the Growth of Different Body-segments in 9-15-Year-old Schoolchildren from Sofia (Bulgaria)

Zorka Mitova

Institute of Experimental Morphology, Pathology and Anthropology with Museum, Bulgarian Academy of Sciences, Sofia, Bulgaria

* Corresponding author e-mail: mitovaz@bas.bg

During the intensive morphological growth in the puberty, the age and sex (both as main effects and in their interactions) play an important role in the phenotypic trait development. In the present report we analyze data on the influence of age and sex on the dimensionality of 15 main height-length, width, and circumferential anthropometric features in 9-15-year-old boys and girls from Sofia (Bulgaria). The influence of both factors on the morphological growth was estimated by MANOVA. The results indicate that almost all of the morphological features are statistically significantly influenced by age and sex. The interaction of these factors has been found to be statistically significant for 10 of the measured features. So the growing boys are on average higher, have longer body parts, as well as larger chest circumference and breadth, wider shoulder and pelvic girdles, and a larger forearm circumference compared to the growing girls.

Key words: adolescents, age, sex, interactions, growth, anthropometric features.

Introduction

The age and sex of an individual are important factors for its anthropological characterization during the various periods of its ontogenetic development. During the growth phase these factors play an important role in the formation of the specific features of the male and female body composition type [4,11, 12, 13,14, 20, 30, 31, 33]. The processes of growth and development at a young age are important for changes occurring in the aging of the body – involutive processes, functional specificity and morbidity [1, 16, 17, 18]. Significant role in the formation of somatic features of the organism during growth and development play various genetic and exogenous factors – biogeographical,

socio-economic and demographic, nutrition and physical activity [1, 3, 8,11, 24, 25, 26, 27, 28, 30, 32]. Under favorable conditions, the possibility of full realization of the hereditary potential of the organism is better. A number of authors have sought to find the link between human morphology and disease, to identify those external factors and habits that are at risk for human health and cause premature aging [1, 3, 16,17,18, 19]. Somatometric sex differences are also known to be present in newborns and continue to exist throughout the growth period [12, 13, 15, 21, 24, 27, 28]. Most vividly, however, they emerge during pubertyinmajor length-, width-, and circumference-based features of the body [2, 5, 6, 9, 13,14, 22, 23, 29, 31]. Based on the fact that one of the main characteristics of the growth process that reflects age dynamics well is speed, many authors estimate the growth rate by the absolute and relative annual growth of a number of anthropometric features and indices [11, 12, 13, 14, 20, 21, 22, 31].

From a mathematical point of view, a well-suited statistical approach forcapturing the influences of two or more factors (and in their interaction) on several biometric features is the multifactorial variant of ANOVA – MANOVA. In the available literature we have not encountered studies using such analysis of the influence of age and sex as independent factors and in their interaction.

The **aim** of the present work is to assess the morphological specificity of the growth process of the different body parts and areas in the studied subjects, depending on their age and sex (incl. their interaction) by MANOVA in 9-15-year-old children and adolescents from Sofia.

Material and methods

The data analyzed are part of a complex cross-sectional anthropological study including 1142 schoolchildren (569 boys and 573 girls) aged 9-15 years from three schools in Sofia city, carried out during the years 2001 and 2002 [10]. The schoolchildren and their parents volunteered for the research and gave their written informed consent. The boys and girls under investigation were separated uniformly each sex in seven age groups – mean ages of 9.5, 10.5, 11.5, 12.5, 13.5, 14.5 and 15.5 years. The groups of the 9-year-old children comprise 81 boys and 81 girls, aged from 9.00 years to 9.99 years. The rest investigated boys and girls were ranged according to the same age affiliation.

We included in the MANOVA analysis data on 15 directly measured anthropometric features (**see Table. 1**) of the trunk and extremities measured by standard anthropometric method [7]. All measurements were made on the right side of the body by standard anthropometric instruments in centimetres (cm).

The significance of the influence of both factors individually, and in their interaction (noted as **age & sex**) on the metric differences in the anthropometric features included in our MANOVA-model has been objectified by the respective levels of statistical significance as expressed by the F-ratio of the Pillai's test ($p<0.010$) and by SPSS software, version 16.0.

Results and Discussion

Validating the differences in the corresponding mean values between the groups in both the growth- as well as in the main lengths, breadths and circumferential features of the body in 9–15-year old children and adolescents, statistically reliable dependencies (at a very high level of statistical significance, $p < 0.000$) have been found even by using the Pillai's test (**Table 1**).

Table 1. Statistically significant levels concerning the effect of the tested factors on the size of various anthropological features.

	Factors	***Sex***		***Age***		***Sex & Age***	
№	***Features***	***F***	***p<***	***F***	***p<***	***F***	***p<***
1	Stature- **St**	19.357	0.000	322.685	0.000	13.632	0.000
2	Anteriortrunk length – **ATrL**	48.728	0.000	206.694	0.000	10.816	0.000
3	Upper extremity length – **Upp.EL**	53.992	0.000	230.697	0.000	11.359	0.000
4	Lower extremity length – **Low.EL**	29.376	0.000	237.460	0.000	14.664	0.000
5	Biacromial breadth – **BAB**	59.750	0.000	218.989	0.000	12.631	0.000
6	Bicristal breadth – **BCB**	12.139	0.001	118.191	0.000	3.215	0.004
7	Chest breadth on the level of *mst* – **ChB**	43.936	0.000	99.630	0.000	4.046	0.001
8	Sagittal chest breadth (Chest depth) – **SChB**	45.370	0.000	66.790	0.000	5.048	0.000
9	Chest circumference in pause – **ChCP**	76.092	0.000	61.613	0.000	7.846	0.000
10	Waist circumference – **Waist C**	38.471	0.000	29.785	0.000	1.900	0.078
11	Hip circumference – **Hip C**	24.666	0.000	108.412	0.000	0.592	0.737
12	Thigh circumference – **Thigh C**	22.756	0.000	57.454	0.000	0.370	0.898
13	Upper arm circumf. (relaxed) – **Upp.AC**	6.642	0.010	43.031	0.000	1.943	0.071
14	Forearm circumference – **FAC**	58.429	0.000	81.850	0.000	5.295	0.000
15	Middle calf circumference – **Mid. Calf C**	0.321	0.571	64.525	0.000	1.167	0.322

Pillai's test (p < 0.010)

Results show that all anthropometrical features analyzed were significantly influenced by the **age** factor. Of the **sex** factor were significantly influenced all, except middle calf circumference.

Of the fifteen anthropometric features tested by our MANOVA model, only ten – St, ATrL, Upp.EL, Low. EL, BAB, BCB, ChB, SChB, ChCP и FAC – have been found to be influenced by the interaction of **age & sex**.

Globally, this means that adolescents of one sex (i.e., males) aged between 9 and 15 years normally reach a greater body-height and generally larger sizes of: 1) the chest (incl. chest circumference in pause), 2) width of shoulders and pelvis, 3) anterior trunk length, 4) upper and lower extremities, and 5) forearm circumference, as compared to their teenage peers of the opposite sex – females.

The established relationship is considered to be genetically determined and has been associated with the longer duration of puberty in boys, as well as with their greater motor activity [5, 28, 29]**.**

The remaining circumference-based features Hip C, Thigh C, Upp.AC and Mid. Calf C as examined in adolescents between 9 and 15 years of age were reliably influenced by the specific effects of age and sex (separately, as individual factors), except for Mid. Calf C, where growth-changes according to the MANOVA-analysis were influenced only by age.

Interestingly, the consistency of the magnitude of differences between the minimum and maximum mean values of the features in our sample of schoolchildren aged from 9 to 15 years (i.e., the absolute increase in the feature between the 9th and 15th year) reflected the impact of age on metric differences in each individual characteristic.

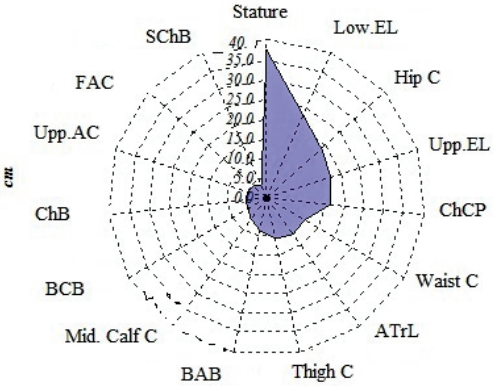

Fig. 1. Sequence of features in boys between 9 and 15 years of age according to the influence of the age factor.

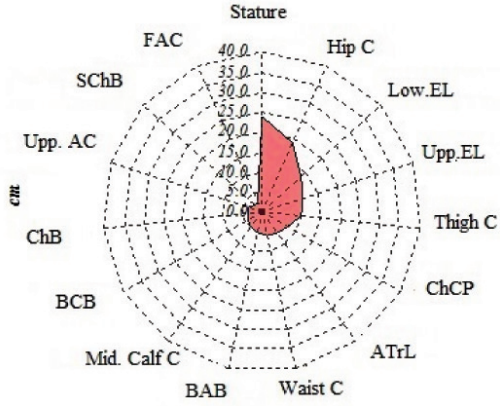

Fig. 2. Sequence of features in girls between 9 and 15 years of age according to the influence of factor age.

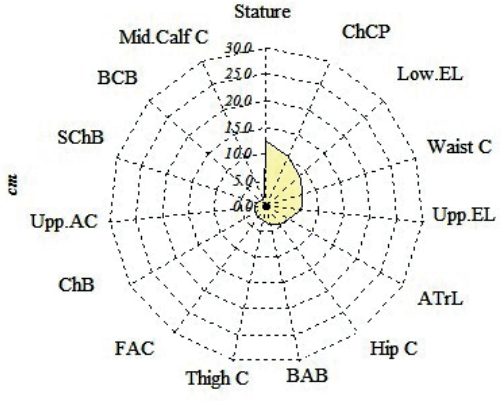

Fig. 3. Sequences of features inter both sexes (between 9 and 15 years of age) according to their minimum and maximum average difference.

In **boys** we found the sequence of features to be as follows **(Fig. 1)**: St > Low.EL > Hip C > Upp.EL > ChCP > Waist C > ATrL > Thigh C > BAB > Mid. Calf C > BCB > ChB > Upp.AC > FAC > SChB.

In **girls** the sequence was **(Fig. 2)**: St > Hip C > Low.EL > Upp.EL > Thigh C > ChCP > ATrL > Waist C > BAB > Mid. Calf C > BCB > ChB > Upp. AC > SChB > FAC.

The sequence of features, according to their maximum differences in mean values **between sexes** across the surveyed age-range, thus reflecting the influence of sex on the growth-changes at each individual size-class, is as follows **(Fig. 3)**: St > ChCP > Low. EL > Waist C > Upp.EL > ATrL > Hip C > BAB > Thigh C > FAC > ChB > Upp. AC > SChB > BCB > Mid. Calf C.

The analysis of the results shows that in the formation of inter-age morphological differences in adolescents of both sexes, along with the growth and the length-based measurements, the circumferential features in the area of the hip, thigh, chest and waist were also decisive. In adolescents of both sexes, the measurements of the shoulder girdle, the chest and the pelvis, the circumferences of the upper and the lower extremities, respectively, had a relatively smaller but important role in the formation of the inter-age differences.

For the formation of differences between the sexes in respect to the anthropometric characteristics, most decisive were the stature as well as the circumferential measurement of the chest, waist and hip, along with the other length-based measurements (Low. EL, Upp.EL, and ATrL, respectively), followed by the biacromial breadth. According to the MANOVA analysis, the middle calf circumference didn't contribute significantly to the differentiation between sexes as measured in the studied population of schoolchildren of age between 9 and 15 years.

When comparing the influence of age and sex (over the period between 9 and 15 years of age), roughly equal influence among both sexes were found to have only the circumferential dimensions in the area of the hip and thigh.

From the illustration in **Fig. 4** it can be seen that among the rest of the features, age has a significantly greater impact on boys than on girls **(see also Table 1)**.

In addition, we found that sex has a greater impact on growth changes in the hip circumference than in the thigh circumference, and that the increase in both body measurements was independent of the joint influence of sex and age. This fact most probably determines the larger circumferential dimensions of the hip and thigh in girls and the tendency to reduce age-related differences in thigh circumference in adolescents [10].

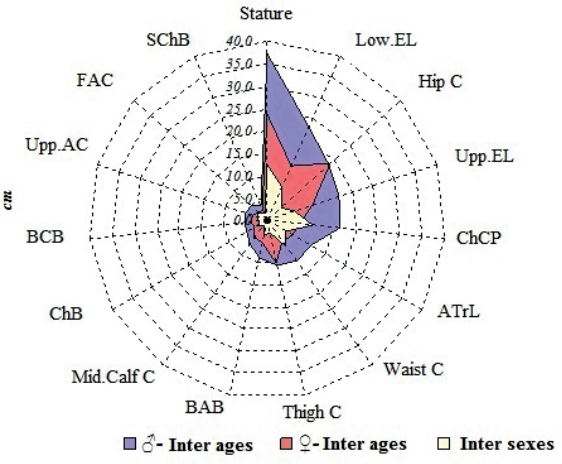

Fig.4. Comparison of the influence of age between 9 and 15 years in the formation of basic metric differences in adolescent boys and girls, and in them inter sexual differences from 9 to 15 years of age.

The results of our study are in line with the results of a number of foreign and Bulgarian researchers, who conducted transversal and/or longitudinal investigates [2, 4, 5, 11, 12, 13, 14, 19, 20, 21, 22, 23, 29, 31, 33]. In general, the authors estimate the growth rate by absolute and relative annual growth of a number of anthropometric features over a broad generalized age range (0 to >22 years), taking into account that, with the exception of pre-pubertal age groups, boys have a greater absolute increase in most of the studied features from that of the girls. High growth velocity was found in both sexes in weight, height, limb length, anterior trunk length, and shoulder width, while width and circumference of the chest and pelvic width showed less growth. Some studies seek for the relationship between puberty, initial body height and limb growth, the latter of which most strongly change their proportions as they grow. The conclusion is that in late puberty and low initial growth, the growth of the limbs and their segments is large, and in early puberty with high initial stature the growth is small.

In conclusion, the scientific contribution of the applied analysis to our study is that **1)** it provides an opportunity to assess separately and in interaction the role of the keys factors responsible for growth and development – age and sex and **2)** to evaluate the phenotypic effect of their impact in the formation of sexual differences in the transformation of the body during pre-puberty and puberty.

The results show that:

- All anthropometrical features analyzed were significantly influenced by the **age** factor;
- Of the **sex** factor were significantly influenced all, except middle calf circumference;
- The interaction between **age & sex** additional determines that male adolescents reach significantly larger height and length-based dimensions of the body, larger diameter and circumference of the chest, shoulder and pelvic girdle width, as well as a larger forearm circumference as compared to their adolescent female peers;

➢ From the combination of the two factors (**age & sex**), apart from calf circumference are not significantly affected also dimensions of the waist, hip, thigh and upper arm – relaxed.

➢ The size of the other circumferential dimensions that we have analyzed was influenced separately by **age** and by **sex**, while both these factors influenced relatively more equally both sexes only in the areas of hip and of the thigh.

References

1. **Baciu, A.** Anthropological-medical aspects of feeding behavior of children in modern society. – *Review of Global Medicine and Healthcare Research (RGMHR)*, **2**(1), 2011, 79-99.
2. **Dimitrova, A., I. Pandourska.** Sex-related differences in chest dimensions in 9-10-year-old Bulgarian children. – *Anthrop. Res. and Stud. (ARS)*, **9**, 2019, 35-40**.**
3. **Eiben, O., C. Mascie-Taylor.** Children's growth and socio-economic status in Hungary. – *Econ. Hum. Biol.,* **2** (2), 2004, 295-320.
4. **Gasser, T., A. Sheehy, L. Molinari, R. Largo**. Sex dimorphism in growth. – *Ann. Hum. Biol.,* **27** (2), 2000, 187-197.
5. **Jasicki, B.** The rate of change in body proportions in relation to the motoric function. – *Prace zoologiczne,* CLXXXVII **(15)**, 1969, 7-20.
6. **Kobzova, J., J. Vignerova, P. Blaha, L. Krejcovsky, J. Riedlova.** The 6th nationwide anthropological survey of children and adolescents in the Czech Republic in 2001. – *Cent. Eur. J. Public Health*, **12**(3), 2004, 126-130.
7. **Martin, R., K. Saller.** *Lehrbuch der Anthropologie.* – Gustav Fischer Verlag, Stuttgart, 1957, 1-532.
8. **Mascie-Taylor, C., G. Lasker.** Biosocial correlates of stature in a British national cohort. – *J. Biosoc. Sci.,* **37**(2), 2005, 245-251.
9. **Mc Carthy, H., K. Jarrett, P. Emmeth, I. Rogers.** Trends in waist circumferences in young British children: a comparative study. – *Int. J. Obes.*, **29**(2), 2005, 157-162.
10. **Mitova, Z.** Anthropological characteristics of physical development, body composition and body nutritional status in 9-15-year-old children and adolescents from Sofia city. – *PhD Thesis,* Sofia**,** 2009, 225 p. [In Bulgarian]
11. **Mladenova, S.** Anthropological characteristics of the growth and development of children and adolescents from the Smolyan region in contemporary living conditions. – *Avt. PhD Thesis*, Plovdiv University, 2003, 58 p. [In Bulgarian]
12. **Nacheva, A., L. Yordanova, E. Lazarova.** Body Proportionality during the Growing up Period. – *Acta morphol. anthropol*., **10**, 2005, 141-144.
13. **Nacheva, A., Y. Zhecheva, I. Yankova, Z. Filcheva, Z. Mitova, Y. Yordanov**. *Physical development of children and youths in Bulgaria on the borderline between 20th and 21st century.* – Prof. Marin Drinov Academic Publishing House, Sofia, 2012, 1-419. [In Bulgarian]
14. **Nikolova, M., I. Petrov, J. Cieslik.** A complex assessment of the general physical and sceletonmetric development of the girls aged 7 to 17 years in the area of city of Plovdiv. – *Biology,* Univ. of Plovdiv "P. Hilendarski", **4**(14), 1976, 315-329. [In Bulgarian]
15. **Nikolova, M., I. Petrov.** Sex differences in the growth rate of the characteristics of children aged from 3 to 7 years. – *Biology,* Univ. of Plovdiv "P. Hilendarski", **4**(20), 1982, 375-388. [In Bulgarian]
16. **Papadimitriou, A.** Growth and development of Greek children in the twentieth century.– In: *Secular Growth Changes in Europe* (Eds Bodzsar, E., C. Susanne), Eötvös Univ. Press, Budapest, 1998, 161-175.
17. **Paskaleva, T., B. Tornyova, M. Vizeva , D. Shopov.** Research and analysis of the health status of elderly people. – *ARTTE*, **7**(1), 2019, 73-78.
18. **Paskaleva, T., B. Tornyova, S. Dragusheva, P. Petleshkova**. Modifiable risk factors for premature aging. – *Int. J. Med. Sci. Biom. Res.,* **30** (3), 2019, 426-431.
19. **Paskaleva, T., B. Tornyova, S. Dragusheva, P. Petleshkova.** Survey and analysis of the prophylactic and medical activity of the elderly and the old people. – *Int. J. Med. Sci. Biom. Res.*, **30**(3), 2019, 432-437.
20. **Petrov, I., M. Nikolova, J. Cieslik.** A complex assessment of the general physical and sceletonmetric development of the boys aged 7 to 17 years in the area of city of Plovdiv. – *Biology,* Univ. of Plovdiv "P. Hilendarski", **4**(14), 1976, 255-313. [In Bulgarian]

21. **Petrov, I., M. Nikolova, J. Cieslik.** Growth differences in the overall physical and sceleton-metric development between boys and girls in the area of city of Plovdiv. – *Biology,* Univ. of Plovdiv "P. Hilendarski", **4**(14), 1976, 270-278. [In Bulgarian]
22. **Petrov, I., M. Nikolova.** Gender differences in morphometric signs in children aged from 6 to 16 years. – *Biology,* Univ. of Plovdiv "P. Hilendarski", **6**(28), 1990, 259-265.
23. **Petrov, I., M. Nikolova.** Relationship between puberty,level of baseline height and limbs growth of children aged from 7 to 22 years. – *Biology,* Univ. of Plovdiv "P. Hilendarski", **4**(17), 1979, 263-281. [In Bulgarian]
24. **Prader, A., R. Largo, L. Molinari, C. Issler.** Physical growth of Swiss children from birth to 20 years of age. First Zurich longitudinal study of growth and development. – *Helv. Pediatr. Acta Suppl.*, **52**, 1989, 1-125.
25. **Stoev, R.** Anthropological Characterization of Adolescents – Physical development and sexual maturation in connection with socio-familial conditions. – *PhD Thesis*, Sofia, 2006, 177 p. [In Bulgarian]
26. **Stoev, R.** Somatotype in adolescents from a big city and a smaller town. – *Papers of Anthropol.,* Tartu, Estonia, **XIV**, 2005, 344-352.
27. **Stoev, R., L. Yordanova.** Physical development and social status in university students in 1980s. – *Acta morphol. anthropol*., **21**, 2015, 139-142.
28. **Tanner, J. M.** Growth as a mirror of the condition of society: Secular trends and class distinction. – In: *Human growth. A Multidisciplinary Review* (Ed. Demirjian, A.), Taylor and Francis, London and Philadelphia, 1986, 3-34.
29. **Tanner, J., R. Whitehouse.** Clinical longitudinal standards for height, weight, height velocity, and weight velocity and stages of puberty. – *Arch. Dis. Child*., **51**, 1976, 170-179.
30. **Vignerova, J., P. Blaha, J. Kobzova, L. Krejčovsky, M. Paulova, J. Riedlova.** Growth and development of school children. – *Cent. Eur. J. Publ. Health*, **8**(1), 2000, 21-23.
31. **Yankova, I., Y. Zhecheva.** Growth and proportionality of body and extremities' length during childhood. – *Acta morphol. anthropol.,* **21**, 2015, 149-153.
32. **Yankova-Pandourska, I., R.Stoev, Y. Zhecheva, A. Dimitrova.** Influence of economic and social factors on the body dimensions in newborns. – *Acta morphol. anthropol.,* **26** (1-2), 2019, 121-127.
33. **Živičnjak, M., N. Narančić, L. Szirovicza, D. Franke, J. Hrenović, V. Bišof, Ž. Tomas, T. Škarić-Jurić**. Gender-specific growth patterns of transversal body dimensions in Croatian children and youth (2 to 18 Years of Age). – *Coll. Antropol.,* **32**(2), 2008, 419–431.

Institute of Experimental Morphology, Pathology and Anthropology with Museum
Bulgarian Anatomical Society

Acta morphologica et anthropologica, 26 (3-4)
Sofia ● 2019

Body Composition Characteristics in Bulgarian Rhythmic Gymnasts

Albena Dimitrova, Ivaila Yankova Ivanova-Pandourska*

Institute of Experimental Morphology, Pathology and Anthropology with Museum, Bulgarian Academy of Sciences

* Corresponding author e-mail: albena_84@abv.bg

The aim is to determine the influence of sport activity on the body composition compartments in young rhythmic gymnasts at different age categories. A total of 27 rhythmic gymnasts, who had trained at least for two years and not less than 20 hours weekly, were tested. Athletes were divided into two groups: pre junior (mean age 8.87 ± 0.72 years) and junior (mean age 11.55 ± 0.52 years). The bioelectrical impedance analysis was used to evaluate the body composition. The gymnasts in pre junior` group had significantly lower mean values of height, weight, muscle mass, total body water and fat free mass compared to junior group. A significant positive correlation with strong intensity between muscle mass and height, weight, total body water and fat free mass in both assessed groups was established. The muscle mass of the gymnasts rises with increasing the sport experience but the body fat percentage and other obesity parameters keep relatively constant mean values.

Key words: body composition, rhythmic gymnasts, bioelectrical impedance analysis, young athletes.

Introduction

The development of contemporary sport requires more comprehensive research of the relationship between the body structure and the type and intensity of physical activity.

The morphological characteristic of young athletes is an important indicator for the success and talent identification in each sport. Although the morphological profile in athletes is determined by genetic factors [5], it is influenced by external factors such as proper nutrition, the type and level of sport training, etc. [2, 15, 22]. In many sports the morphological components are not homogeneous. A significant difference is also established in terms of the playing position within the same sport [19].

Specificity and intensity of training in rhythmic gymnasts (RG) along the growth period leads to changes in muscle and skeletal system and determine the specific morphological profile – linear body development, low level of body fat and predominant ectomorph somatotype [7, 16, 18, 21]. In aesthetics sports an increase of body weight, especially body fat can negatively influence sport performance. For this reason body composition profile is a supportive tool in sports, where the body structure may influence

the biomechanics of movement and balance between muscle strength and flexibility [6, 11, 14]. The skin-folds measurements and bioelectrical impedance analysis (BIA), as non-invasive and fast methods are the most commonly used for estimating of body composition [20].

The aim of the study is to determine the influence of sport activity on the body composition compartments in young rhythmic gymnasts (RG) at different age categories.

Materials and Methods

A sample includes 27 rhythmic gymnasts (RG), who have trained at least for two years and not less than 20 hours weekly. All participants in the present study took part at the national championships. Athletes were divided into two experimental groups: pre – junior (mean age 8.87± 0.72 years) and junior (mean age 11.55 ± 0.52 years). All girls and their parents completed an inform consent and voluntarily participated in the study. The study protocol was reviewed and approved by the Ethical Committee of Institute of Experimental Morphology, Pathology and Anthropology with Museum – Bulgarian Academy of Sciences (Protocol № 8/12.11.2018) and was conducted in agreement with the principles stated in the Declaration of Helsinki for human studies [24]. The Martin-Saller's anthropometric method was used for measured the athletes' height. The BIA method (with the use of InBody 170 analyzer) was applied to evaluate the RGs' body composition. Body composition profile included: weight (Wt), muscle mass (MM), total body water (TBW), fat free mass (FFM), fat mass (FM), body mass index (BMI), body fat percentage (PBF), waist-to-hip ratio (WHR) and visceral fat (VF). Statistical analysis was performed by SPSS16 for Windows. T-test was used to identify statistically significant intergroup differences ($p<0.05$). A Pearson's correlation analysis was applied to establish the relationship between body composition compartments.

Results

The study presented the peculiarities of the body composition compartments in young competitive Bulgarian RG. The descriptive analysis of age and basic anthropometric features are presented in **Table 1.**

There were significant differences in the mean values of basic anthropometric features (height and weight) between 8-10 and 11-12 years old Bulgarian RG athletes ($p <0.05$). The gymnasts from junior group are 8.00 cm taller and 4.36 kg heavier than those from pre-junior group. It is due to the growing stage of the athletes.

Table 1. Basic Anthropometric Characteristics

Traits	Pre - junior RG (n=16)	Junior RG (n= 11)	Total (n= 27)	P-value
Age (yr)	8.87 ± 0.72	11.55 ± 0.52	9.96 ± 1.48	0.000*
Height (cm)	138.00 ± 7.46	146.00 ± 3.23	141.00 ± 7.14	0.004*
Weight (kg)	29.20 ± 4.12	33.56 ± 3.13	30.97 ± 4.28	0.006*

Table 2 contains data of body composition characteristics in Bulgarian athletes. Pre-junior group has significantly lower mean values of muscle mass, total body water and fat free mass compared to junior group ($p<0.05$). Fat mass are equal in both investigated groups.

Table 2. Body Composition Parameters in Young Bulgarian Rhythmic Gymnasts

Traits	Pre - junior RG (n=16)	Junior RG (n= 11)	Total (n= 27)	P-value
Muscle mass (kg)	12.81 ± 2.31	15.17 ± 1.24	13.77 ± 2.25	0.005*
Fat mass (kg)	4.15 ± 1.38	4.55 ± 1.77	4.31 ± 1.53	0.520
Fat free mass (kg)	25.04 ± 3.78	29.02 ± 2.07	26.66 ± 3.72	0.004*
Total body water (l)	18.36 ± 2.83	21.28 ±1.50	19.55 ± 2.76	0.004*

No significant intergroup differences were found for fat mass, body fat percentage, visceral fat, waist- to- hip ratio and BMI (p>0.05) **(Table. 3)**.

Table. 3. Obesity Parameters in Young Bulgarian Rhythmic Gymnasts

Traits	Pre - junior RG (n=16)	Junior RG (n= 11)	Total (n =27)	P-value
BMI (kg/cm^2)	15.31± 1.19	15.82 ± 1.13	15.51 ± 1.17	0.273
PBF (%)	14.19 ± 4.11	13.29 ± 4.48	13.82 ± 4.21	0.596
WHR	0.71 ± 0.32	0.73 ± 0.24	0.72 ± 0.03	0.066
Visceral fat	1.31 ± 0.60	1.45 ± 0.52	1.37 ± 0.56	0.531

The correlation coefficients between the body composition compartments in RG athletes are presented in **Table 4** and **Table 5**.

Table 4. Correlation between assessed anthropometric and body composition traits in young junior RG

	Ht	Wt	MM	FM	TBW	FFM	BMI	PBF	WHR	VF
Ht	1	0.857**	0.915**	0.031	0.923**	0.925**	0.188	-0.355	0.230	0.033
Wt		1	0.938**	0.408	0.943**	0.943**	0.664**	0.006	0.570*	0.245
MM			1	0.069	0.999**	0.999**	0.454	-0.336	0.356	-0.040
FM				1	0.080	0.080	0.754**	0.913**	0.726**	0.789**
TBW					1	1.000**	0.451	-0.328	0.362	-0.023
FFM						1	0.449	-0.328	0.357	-0.021
BMI							1	0.550*	0.775**	0.416
PBF								1	0.532*	0.731**
WHR									1	0.641**
VF										1

**Statistically significant differences at p<0.01; * Statistically significant differences at p<0.05; HT- height; Wt- weight; MM- muscle mass; FM- fat mass; TBW- total body water; FFM- fat free mass; BMI- body mass index; PBF- body fat percentage; WHR- waist- to- hip ratio; VF- visceral fat;

Table 5. Correlation between assessed anthropometric and body composition traits in junior RG

	Ht	Wt	MM	FM	TBW	FFM	BMI	PBF	WHR	VF
Ht	1	0.699*	0.810**	0.270	0.822**	0.827**	0.298	0.146	0.045	0.268
Wt		1	0.816**	0.781**	0.835**	0.845**	0.890**	0.671*	0.591	0.575
MM			1	0.279	0.996**	0.996**	0.574	0.122	0.392	0.114
FM				1	0.308	0.325	0.869**	0.985**	0.551	0.798**
TBW					1	1.000**	0.592	0.155	0.426	0.165
FFM						1	0.603*	0.172	0.422	0.186
BMI							1	0.802**	0.765**	0.595
PBF								1	0.513	0.797**
WHR									1	0.358
VF										1

**Statistically significant differences at $p<0.01$; * Statistically significant differences at $p<0.05$; HT- height; Wt- weight; MM- muscle mass; FM- fat mass; TBW- total body water; FFM- fat free mass; BMI- body mass index; PBF- body fat percentage; WHR- waist- to- hip ratio; VF- visceral fat;

A significant positive corrrelation with high intensity between muscle mass and height, weight, TBW and FFM in both assessed groups was established ($p <0.01$).

In the pre-junior RG group, a moderate and negative correlation of body fat percentage with MM, FFM and TBW was observed. Contrary, there was a high and positive correlation of PBF with FM and BMI in the junior RG group.

Discussion

Monitoring of the body composition profile in young competitive RG athletes proves to be basic for the routine practices for good health of athletes and better sport performance [9]. In references of body composition, females who are physically active and have improper nutrition or under-nutrition may lead to very low values of fat mass associated with menstrual disorders (oligomenorrhoea or amenorrhoea) and increase the risk of bone fractures and osteoporosis in adulthood [3, 4, 8, 10].

The results of the present study indicate that rhythmic gymnastic is a sport where the muscle mass of athletes increases with increasing the sport experience but the PBF and the other obesity parameters keep relatively constant mean values.

The mean values of basic anthropometric and body composition characteristics in Bulgarian RG were close to those established by Ariazza et al. [1]. The authors investigated the Chilean RG at the same age and reported data of height, weight and BMI 138.57 cm, 29.85 kg, 15.49 kg/cm^2, respectively. They also determined insignificant differences in the percentage of fat mass and significant difference in the percentage of MM among these age categories [1]. However the Bulgarian gymnasts had lower mean values of body mass, height, BMI and FFM and similar PBF than the Brazilian rhythmic gymnasts [17]. In comparison with Russian rhythmic gymnasts, aged 10 years, Bulgarian athletes are taller, but lighter and have significantly lower values of BMI and FM [23].

Most of the studies emphasized a close correlation between morphological profile (characterized with under-average adipose tissue and development of the skeleton and muscular tissue) and motor ability of young RG athletes [6, 11, 12, 13]. According to our data, there was a significant positive relationship between height, weight, TBW, FFM and muscle mass in athletes aged 8-12 years.

Conclusion

Body composition profile of Bulgarian rhythmic gymnasts is characterized with high level of muscle mass and fat free mass and low level of fat mass, within the expected sport modality.

We concluded that rhythmic gymnastics is a sport where the muscle mass of athletes increases with increment of the age and sport experience, but the PBF and the other obesity parameters keep relatively constant mean values.

Following the changes in morphological characteristics during the early stage of the rhythmic gymnastic training process would be very helpful for coach programs and selecting process as well as the talent identification.

Acknowledgements: This work was supported by the Bulgarian Ministry of Education and Science under the National Research Programme "Young scientists and postdoctoral students" approved by DCM No 577 / 17.08.2018

The authors would like to thank the gymnasts, their parents and coaches for making this study possible.

R e f f e r e n c e s

1. **Arriaza, E., C. Rodriguez, C. Carrasco, C. Mardones, L. Niedmann, A. Lopez-Fuenzalida.** Anthropometric characteristics of elite rhythmic gymnasts. - *Int. J. Morphol., 34*(1), 2016, 17-22.
2. **Beunen, G., R. M. Malina, A. L. Claessens, J. Lefevre, M. Thomis.** Ulnar variance and skeletal maturity of radius and ulnae in female gymnasts. - *Med. and Sci. in Sport and Exercise*, **31**, 1999, 653-657.
3. **Brooks-Gunn, J., M. P. Warren, L. H. Hamilton.** The relationship of eating disorders to amenorrhea in ballet dancers. – *Med. Sci. Sports Exerc.,* **19**, 1987,41–44.
4. **Brownell, K. D., S. N. Steen, J. H. Wilmore.** Weight regulation practices in athletes: analysis of metabolic and health effects. – *Med. Sci. Sports Exerc.,* **19**, 1987, 546-556.
5. **Bouchard, C**. Genomic predictors of trainability. – *Exp. Physiol.,* **97**(3), 2012, 347-352.
6. **Chromiak, J. A., B. Smedley, W. Carpenter, R. Brown, Y. S. Koh, J. G. Lamberth, L.A. Joe, B. R. Abadie, G. Altorfer**. Effect of a 10-week strength training program and recovery drink on body composition, muscular strength and endurance, and anaerobic power and capacity. – *Nutrition,* **20**, 2004, 420-427.
7. **Classens, A. L., J. Lefevre, G. Beunen, R. M. Malina.** The contribution of anthropometric characteristics to performance scores in elite female gymnasts. – *J. Sports Med. Phys. Fitness*, **39**, 1999, 355-360.
8. **DiFiori, J. P.** Menstrual dysfunction in athletes. How to identify and treat patients at risk for skeletal injury. – *Postgrad. Med*., **97**, 1995, 143–156.
9. **Douda, H. T, A. G. Toubekis, A. A. Avloniti, S. P. Tokmakidis.** Physiological and anthropometric determinants of rhythmic gymnastics performance. – *Int. J. Sports Physiol. Perform.,* **3**(1), 2008, 41-54.
10. **Drinkwater, B. L., K. Nilson, C. H. Chesnut, W.J. Bremner, S. Shainholtz, M. B. Southworth**. Bone mineral content of amenorrhoeic and eumenorrhoeic athletes. - *N. Engl. J Med*., **311**,1984, 277-281.
11. **Hanson, E. D., S. R. Srivatsan, S. Agrawal, K. S. Menon, M. J. Delmonico, M. Q. Wang, B. F. Hurley**. Effects of strength training on physical function: influence of power, strength, and body composition. – *J. Strength Cond. Res.,* **23**, 2009, 2627-2637.
12. **Katić, R.** Identification of biomotor structures as a precondition for programming kinesiologic education in children aged seven to nine years. – *Coll. Antropol.,* **27**(1), 2003, 351-360.
13. **Katić, R., A. Pejčić, N. Viskić-Štalec.** The mechanisms of morphological-motor functioning in elementary school female first- to fourth-graders. – *Coll. Antropol.,* **28**(1), 2004, 261-269.
14. **Landers, G. J., B. A. Blanksby, T. R. Ackland, D. Smith**. Morphology and performance of world championship triathletes. – *Ann. Hum. Biol.,* **27**, 2000, 387-400.

15. **Malina, R. M.** Physical growth and biological maturation of young athletes. – *Exerc. Sport. Sci. Rev.*, **22**, 1994, 389-433.
16. **Miletic, D., R. Katic, B. Males.** Some anthropological factors of performance in rhythmic gymnastics novices. – *Coll. Antropol.,* **28**, 2004, 727-737.
17. **Oliveira G. L., P. S. P Gonçalves, T. A. P. Oliveira, J. R. V. Silva, P. R. Fernandes, J. Filho.** Assessment of body composition somatotype and eating disorders in rhythmic gymnasts. – *JEP*, **20**(1), 2017, 125-139.
18. **Purenović-Ivanović, T., R. Popović.** Somatotype of top-level Serbian rhythmic gymnasts. – *Journal of Human Kinetics*, **40**, 2014, 181-187.
19. **Raković, A., V. Savanovic, D. Stanković, R. Pavlović, A. Simeonov, E. Petković**. Analysis of the elite athletes' somatotypes. – *Acta Kinesiologica*, **9** (1), 2015, 47-53.
20. **Roche, A. F., S. B. Heymsfield, T. G. Lohman**. Human body composition. *Human Kinetics, USA*, 1996, 1-366.
21. **Toteva, M**. *Somatotypology in sports*, Sofia, NSA,1992 [in Bulgarian].
22. **Tucker, R., M. Collins**. What makes champions? A review of the relative contribution of genes and training to sporting success. – *Brit. J. Sports Med.*, **46**(8), 2012, 555-561.
23. **Yurchuk-Zuliar, O. A., O. V. Tulyakova, A. A. Kunshin.** Physical and sexual development of 10-year-old girls in rhythmic gymnastics and acrobatics. – *Pedagogics, psychology, medical-biological problems of physical training and sports*, **22**(1), 2018, 56-61.
24. World Medical Association, Declaration of Helsinki – Ethical Principles for Medical Research Involving Human Subjects. – *WMJ*, **54**(4), 2008, 122-125.

Institute of Experimental Morphology, Pathology and Anthropology with Museum
Bulgarian Anatomical Society

Acta morphologica et anthropologica, 26 (3-4)
Sofia ● 2019

Anthropological Characterization of Few Local Populations of Middle North Bulgaria after Archive Materials from 1943-1944

Racho Stoev

Institute of Experimental morphology, pathology and anthropology with museum of BAS, Sofia, Bulgaria, Sofia-1113, Acad. G.Bonchev str. Bl. 25

* Corresponding author e-mail: rastesto@abv.bg

Anthropological data of archive materials from 1943-44, collected by G. Markov, a student of acad. M. Popov in Middle North Bulgaria are processed and analyzed. They include of 284 men – 238 Bulgarians, 23 Turks and 23 so-called Lovchanski Pomaks. The analysis showed significant differences between the three ethnic groups and between the local groups of Bulgarians themselves. Migrations from Southern Bulgaria and from Northwestern Bulgaria, as also in the Middle North Bulgaria itself have been traced. Sharp social urban-rural differences in height have been found. The results of the study are an interesting testimony of centuries of demographic and processes in Middle North Bulgaria.

Key words: ethnic anthropology, Michalski's methods, Middle North Bulgaria, migration history, social differences.

Introduction

National wide ethnoanthropological surveys have been conducted in Bulgaria – of acad. Stefan Vatev around 1899, of acad. Methody Popov at 1938-43, of Aris Poulianos at 1963 and the National Anthropological Program at 1989-1993 [11, 12, 16, 17]. Their results show that the anthropological structure of the present Bulgarian population is very heterogeneous in territorial aspect. Unfortunately, the results of these studies are published only at national and regional level. Only few data are published on local level [11, 16]. The survey of Krum Dronchilov [2] perhaps the best exact and best known outside Bulgaria, presents anthropological data on local level, but does not cover the territory of Middle North Bulgaria. The materials of the extensive local anthropological studies of Peter Boev, Luchia Kavgazova and their collaborators, collected during the 1970s and 1980s are only partly published and also do not cover the territory of Middle North Bulgaria [4, 5, 6]. Resent review and analysis of some incomplete data of Methody Popov study also support the idea that more attention to the investigation of the anthropology of local Bulgarian populations should be paid [14].

Materials and Methods

In the archives of the Institute of Morphology at 1980s by the author a folder of unpublished anthropological materials collected in November 1943-January 1944 have been found. According to oral information these data have been collected by a student of acad. Methody Popov, named Georgi Markov (but not Metody Popov's student and well known cytologist, who in 1959 published the general results of Metody Popov's survey [11].

There were 284 individual anthropological cards in the folder but 285 according the label, one card was probably lost in the period since the investigation until now. They content anthropological data of men only despite the numbering and some information about relatives on the card show that women have been also studied. Probably their data were in other folder which has not survived.

The anthropological cards present data of 284 adult men – 238 Bulgarians, 23 Turks and 23 so-called Lovchanski Pomaks. The terrain study has begun in November in the village Toros (Lukovit county) in November 1943 (Pomaks and local Orthodox Bulgarians), then continued in Pleven in December 1943 (Bulgarians and Turks) and ended in January 1944 in the village Mihaltsi (Pavlikeni county).

The anthropological cards contain data about the birth place of the parents of the investigated persons. Thus they can be distributed after their origin in few local samples **(Fig.1)**.

Only the major anthropological traits are processed and analyzed in this paper. The analysis of the anthropological structure has been made according to the methodic of Michalski [3, 7, 9, 10]. In the methodic are made some minor modifications, which are described in previous article of the author [15].

On the base of the established elementary anthropological structure euclidean distances have been calculated as a measure of anthropological similarity between subsamples.

Results and Discussion

According to their anthropological traits and basically on the pigmentation all subsamples belong to the populations with mixed Southeuropoid and Northeuropoid traits **(Table 1).** Eastern Eurasian traits are rare – mostly the relatively high protrusion of the cheekbones.

Despite their small number the few Bulgarians originating from South Bulgaria significantly differ from the Bulgarians of Northern Bulgaria, especially in their headform. The prevalence of a mesocephalic anthropological populations in South Bulgaria and of brachycephals in North Bulgaria is well established by all major ethnoanthropological studies [11, 12, 15, 16, 17]. On the other hand, the Bulgarians from North Bulgaria also are not a homogeneous group as locally and individually as the standard deviation of cephalic index present. In fact they are as heterogeneous as the population of Switzerland with its four ethnic groups and many isolated cantons [13, 15]

The analysis of the elementary anthropological structure **(Table 2)** presents a very interesting pattern. In South Bulgarians prevails the combination of Nordic (a) and Mediterranean elements (Ibero-Insular – e, and Oriental – k). Thus they belong to the populations of the wide zone of Atlanto-Pontic populations, named after its distribution [1]. In Bulgarians from North Bulgaria, whoever prevail combination of

Nordic, Armenoid (Balvano-Caucasian –h) and Laponoid (l) element. Thus they belong to the populations of Central Europe [1].

The Pomaks from Toros Village present well expressed Atlanto-Pontic combination. Thus there are close to the people from South Bulgaria, not to North Bulgarians **(Tables 3, 4, Figs. 2, 3).** This should not surprise us – the origin of this local group is from Islamized Paulicians, which had migrated from South to North Bulgaria in the second half of the 14th century [18].

It is interesting that the Turks investigated in Pleven (with origin in Pleven, Nikopol, Svishtov and Russe) we find the Centraleuropean combination of elements and there are close to the North Bulgarians **(Tables 3, 4, Fig. 3)**. Whether this is because of the predominantly local origin and intermixing with local Orthodox Bulgarians or because of migrations of Islamized Hungarian population to Danube valley towns in the beginning of 18th century [8] we could not be sure.

Other interesting finding is that the native Bulgarians from the city of Pleven are not similar to the rural population in Pleven county but to the Bulgarians from Teteven county. This could be due to an old migration from the poor in land Teteven county to the city of Pleven. The rural people from Pleven county did not migrate to the county center because Pleven county was affluent in land **(Table 4, Fig.2).**

The population of the village Mihaltsi presents well expressed similarity to the population of Northwest Bulgaria **(Table 4, Fig.2)**. It also could be due to an old migration. Unfortunately we could not find a mention about such a migration or about the origin of the first settlers of the village in the available literature.

May be the reproductive isolation (because of confessional reasons) of Toros Pomaks from their Orthodox neighbors was not complete – they are very different from all North Bulgarian populations but the smallest distance is whoever to the Bulgarians from Toros **(Table. 4**). Or we can suppose that a part of the Paulicians in Toros has not been Islamized but has been converted to Orthodoxy.

There are also well expressed social (urban-rural) differences in the physical development of the men under study. The men from the city of Pleven have a height of 178,2 cm **(Table 1)** one standard deviation above the average height of the whole sample. The shortest are the Turks, the Pomaks (marginalized after the Liberation of Bulgaria social groups) and of the village Mihaltsi – about two standard deviations under Pleven men and one standard deviation below the average of the whole sample.

Conclusion

The processing and analysis of the archive anthropological data of men from Middle North Bulgaria shows significant differences between ethnic groups and between local Bulgarian Subsamples. The mesocephalic inhabitants of Southern Bulgaria differ from the brachycephals of Northern Bulgaria. The mesocephalic Pomaks and the subbrachycephalic Bulgarians from the village of Toros (mixed Bulgarian-Pomak) are also closest to them. Apparently, this is due to a common origin from the Paulicians of Southern Bulgaria who moved to North in 14th century. The city of Pleven differs sharply from its rural surrounding probably because of migration from Teteven county. Also the inhabitants of the village Mihaltsi probably migrated from Northwestern Bulgaria. Sharp social urban-rural differences in height have been found. The results of the study are an interesting testimony of centuries of demographic and ethnographic processes in Middle North Bulgaria.

Acknowledgements: To Lukasz Macuga from Torun for consultations when working on these materials.

References

1. **Cheboksarov, N. N.** The anthropological structure of recent Germans. – *Uchenye Zapiski MGU*, LVIII, 1941, 271-308 [in Russian].
2. **Drontschiloff, Kr.** *Beiträge zur Anthropologie der Bulgaren*. Braunschweig, Friedr. Vieweg @ Sohn, 1914, 1-80.
3. **Henzel, T., I. Michalski**. Principles of human classification after Tadeusz Henzel and Ireneusz Michalski. – *Przegl. Antropol*., **v. XXI,** zeszyt 2, 1955, 537-662 [in Polish].
4. **Kavgazova, L., P. Boev, A. I. Hadjioloff.** Morphological characteristics of highland population in Central Rhodopes. – *Comp. Rend. Acad. Bulg. Sci.,* **37**, 1984, 5, 657-659.
5. **Kavgazova, L., P. Boev.** Anthropological characteristics of Rhodope variant of Dinaric race. – *Comp. Rend. Acad. Bulg. Sci.,* **37**, 1984, 5, 665-667.
6. **Kavgazova, L., Zl. Filcheva, R. Stoev.** Anthropological characteristics of the population in the western part of Smolyan region. – *Acta morphol. anthropol.,* **6**, 1987, 58-64.
7. **Michalski, I.** Anthropological structure of Poland. - *Acta anthropologica universitatis Lodziensis*, **1**, 1949, 1-236 [in Polish].
8. **Mutafchieva, V.** *Othoman socio-economic history*. Sofia, P. Beron Publ. House, 1999, 1-368 [in Bulgarian].
9. **Orczykovska, Z.** An attempt of constructing an anthropological key on the base of classification of Michalski. – *Przegl. Antropol.,* **22**, 1959, 212-229 [in Polish].
10. **Orczykowska, Z.** Anthropological analysis of Tajiks from Pamir. – *Mat. Pr. Antropol.*, **46**, 1959 [in Polish].
11. **Popov, M., G. Markov.** *Anthropology of Bulgarian people*. Sofia, BAS Publ. House, 1959, 1-296 [in Bulgarian]
12. **Poulianos, A. N**. *Anthropological studies on the Balkans (Bulgaria-Greece-Yugoslavia)*. Athens, 1967, 1-157 [in Greek].
13. **Schlaginhaufen, O.** *Anthropologia Helvetica*. Zürich, Art. Inst. Orell Füssli A.-G., 1946, 1-700.
14. **Stoev, R.** Anthropological types in Bulgarian population around 1940 – regional and local level. – *Acta morphol. anthropol*., **23**, 2016, 93-101.
15. **Stoev, R.** Anthropological characteristics of Gagauzes from Kavarna. – *Acta morphol. anthropol*., **26** (1-2), 2019, 79-83.
16. **Vatev, St.** *Anthropology of Bulgarians. Sofia*, 1939, 1-80 [in Bulgarian].
17. **Yordanov, Y., A. Nacheva, S. Tornyova-Randelova, N. Kondova, B. Dimitrova, D. Paskova**
18. **Topalova**. *Anthropology of the population of Bulgaria in the end of 20th century.* Sofia, Academic Publishing House "Marin Drinov", 2006, 1-432 [in Bulgarian].
19. **Yovkov, M.** *Pavlicians and pavlicians settlements in Bulgarian land 15th-18th century.* University Publ. House St. Kliment Ohridski, Sofia, 1991, 1-256 [in Bulgarian].

Table 1. Major anthropological traits and indices in the population under study

Sample	N	Height, cm	Head length	Head breadth	Cephalic index		Face breadth	Face height	Facial indexI	Nasal height	Nasal breadth	Nasal index	Eye color	Hair color	Skin color	Hair form	Nasal profile	Cheekbone protrusion
					mean	SD												
Bulgarians	238	172,6	183,9	155,8	84,8	3,9	141,8	123,0	86,8	58,2	36,3	62,5	6,7	51,1	10,9	2,3	60,2	2,1
South Bulgaria	12	171,1	186,0	150,9	81,2	2,6	138,0	122,3	88,7	56,1	36,7	65,9	7,8	48,3	11,3	2,5	54,6	2,2
North Bulgaria	226	172,6	183,8	156,1	85,0	3,9	142,0	123,0	86,7	58,3	36,2	62,3	6,7	51,3	10,8	2,3	60,5	2,1
Toros village	21	172,3	188,2	154,9	82,4	3,8	142,3	123,9	87,2	58,1	37,2	64,0	7,0	51,0	10,2	2,1	66,4	1,7
Lukovit county	18	173,2	182,4	155,4	85,3	3,8	141,4	122,0	86,4	59,5	36,4	61,3	6,4	44,4	10,0	2,3	67,5	1,8
NorthWest Bulgaria	20	174,6	183,4	158,6	86,5	3,3	141,9	123,1	86,9	57,8	36,5	63,3	7,1	45,0	10,9	2,3	60,0	2,0
Teteven county	10	176,1	180,8	156,0	86,3	2,8	140,5	125,3	89,2	60,9	35,9	59,1	8,1	51,0	9,5	2,0	65,5	1,9
Pleven city	23	178,2	186,6	156,5	83,9	4,1	140,0	124,0	88,6	61,0	36,4	59,9	7,6	51,3	10,9	2,4	60,4	1,6
Pleven county	60	172,5	184,2	156,5	85,1	4,3	142,9	122,8	86,9	57,5	36,2	63,3	5,8	52,1	11,5	2,3	58,8	2,3
NorthEast Bulgaria	30	173,3	184,3	156,3	84,9	3,4	143,4	122,5	85,6	57,8	36,3	63,2	6,4	53,3	11,4	2,1	59,7	2,4
Mihaltsi Village	44	167,7	180,8	155,5	86,1	3,5	141,9	123,4	86,8	57,8	36,0	62,5	7,0	54,5	10,5	2,3	56,9	2,5
Pomaks	23	167,4	184,1	147,9	80,4	3,2	139,5	124,0	88,9	59,6	38,1	64,3	9,2	47,2	11,6	2,1	73,3	1,8
Turks	23	165,0	180,1	151,7	84,3	4,2	137,6	124,4	90,5	58,1	35,7	61,7	7,6	52,6	11,1	2,2	67,4	2,6

Remarks: All measurements except height in mm, all indices – in %; – eye color - after Martin; hair color - after Michalski (10 hell blond, 70 – black); skin color after von Luschan; hair form: 1 – straight hard, 2 – straight soft, 3 wavy and so on; nasal profile after Michalski (10 – very concave, 100 – strongly convex); cheekbone protrusion: 1-3, 3 – strong;

Table 2. Elementary anthropological structure after Michalski

Sample	n	Anthropological elements, %										Eastern complex, %	South complex, %	Formula
		a Nordic	**y** Cromagnoid	**b** Berberic*	**e** Mediterranean *	**k** Oriental*	**h** Armenoid*	**l** Laponoid	**m** Mongolic*	**z** Pacific	**q** Uraloid			
Bulgarians	238	31,4	0,5	0,8	6,5	7,0	26,3	13,9	8,1	3,3	2,2	27,4	56,0	ah(l)
South Bulgaria	12	35,4	-	-	14,6	12,5	6,2	8,3	8,3	8,3	6,2	31,2	48,5	a(ek)
North Bulgaria	226	31,2	0,6	0,9	6,1	6,7	27,3	14,2	8,1	3,3	2,0	27,2	56,4	ah(l)
Toros village	21	32,1	-	-	15,5	10,7	20,2	7,1	3,6	2,4	8,3	21,4	59,1	ah(ek)
Lukovit county	18	40,3	2,8	-	5,6	-	23,6	16,7	4,2	6,9	-	27,8	40,4	ah(l)
NorthWest Bulgaria	20	38,8	-	-	6,2	2,5	23,8	16,2	7,5	2,5	2,5	28,8	44,1	ah(l)
Teteven county	10	42,5	-	-	5,0	7,5	30,0	10,0	5,0	-	-	15,0	50,0	ah(l)
Pleven city	23	42,4	2,2	3,3	4,3	9,8	25,0	9,8	2,2	1,1	-	13,0	48,8	ah
Pleven county	60	22,5	-	1,2	5,4	6,2	30,4	17,1	11,2	5,4	0,4	34,2	65,8	ha(lm)
NorthEast Bulgaria	30	20,8	0,8	-	7,5	9,2	30,8	17,5	8,3	1,7	3,3	30,8	68,7	ha(l)
Mihaltsi Village	44	34,1	-	1,1	2,8	6,8	27,8	12,5	11,4	1,1	2,3	27,3	53,1	ah(lm)
Pomaks	23	44,6	1,1	3,3	16,3	8,7	5,4	8,7	-	3,3	8,7	20,7	42,5	a(e)
Turks	23	27,2	-	-	10,9	5,4	23,9	12,0	6,5	3,3	10,9	32,6	59,7	ah(leq)

Synonims: Berberic = Mediterranoid, Mediterranean = Ibero-insular, Oriental = Eastern Oriental, Armenoidal = Balcano-Caucasian, Mongolic ^ typical Mongoloid

Remarks: Eastern complex = l+m+z+q , Soutern complex = (b+e+k+h)/(a+y+ b+e+k+h), formula – elements over 20% and in brackets element from 10 to 20%.

Table 3. Matrix of Czekanovski, euclidean distances, summarized, %

Sample	Pomaks	South Bulgaria	Turks	North Bulgaria
Pomaks	0			
South Bulgaria	14,7	0		
Turks	27,5	22,6	0	
North Bulgaria	30,2	25,4	11,8	0

Table 4. Matrix of Czekanowski – euclidean distances, all samples, %

Sample	Pomaks	SBg	Toros	Turks	Pleven-county	NEBg	Pleven city	Teteven county	Mihaltsi village	NWBg	Lukovit county
Pomaks	0										
SBulgaria	14,7	0									
Toros village	20,2	16,5	0								
Turks	27,5	22,6	11,3	0							
Pleven-county	38,9	31,7	23,4	16,1	0						
NEBulgaria	38,4	31,9	21,5	14,5	7,0	0					
Pleven –city	24,9	25,7	18,7	21,4	24,5	25,1	0				
Teteven county	29,4	29,2	20,2	21,1	22,8	23,7	7,5	0			
Mihaltsi village	31,5	27,1	19,2	15,3	13,8	15,9	14,0	11,6	0		
NWBulgaria	26,0	24,5	18,5	16,0	18,8	20,6	12,8	11,7	10,0	0	
Lukovit county	26,9	26,5	21,9	19,9	21,5	24,1	14,2	14,3	15,1	7,3	0

Fig. 1. Bulgaria at 1940s - administrative division and territorial distribution of the analyzed in this paper subsamples

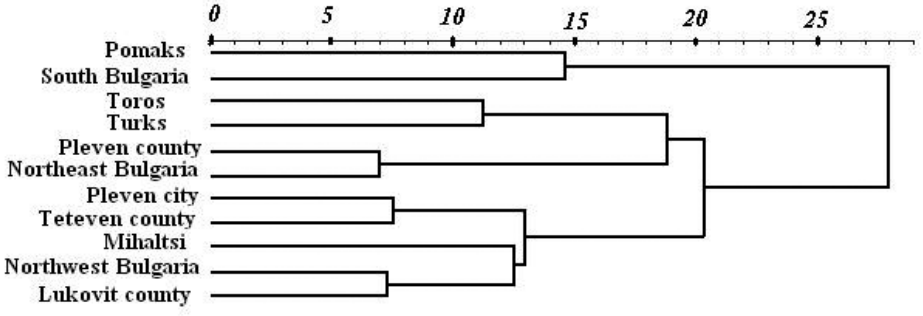

Fig. 2. Cluster analysis of the subsamples under study – euclidean distances, weighted pair group method of analysis (WPGMA)

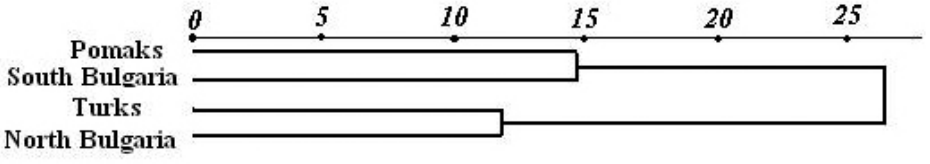

Fig. 3. Cluster analysis of generalized subsamples under study – euclidean distances, weighted pair group method of analysis (WPGMA)

Institute of Experimental Morphology, Pathology and Anthropology with Museum
Bulgarian Anatomical Society

Acta morphologica et anthropologica, 26 (3-4)
Sofia ● 2019

Anthropological Studies of Physical Development of Students at the Faculty of Biology at Sofia University "St. Kliment Ohridski"

*Ivo Vladimirov, Racho Stoev**

Department of Anthropology and Anatomy, Institute of Experimental Morphology, Pathology and Anthropology with Museum, Bulgarian Academy of Sciences, Sofia, Bulgaria

*Corresponding author e-mail: rastesto@abv.bg

The purpose of this study is to characterize anthropometrically physical development of Bulgarian students at the beginning of the XXI century, by comparison with the results of previous studies of students in Sofia. An anthropometric survey of 77 students, 18 to 25 years old, 31 males and 46 females, was conducted in 2016-2017. The results have been compared with data from investigations at 1986 and at 2002. The comparison shows stagnation of the secular changes in height, which should be attributed to the long-term negative impact on the growth and development of the students during the difficult years of their early childhood. Secular weight changes are positive, thus BMI increases sharply as well. This indicates that weight and BMI respond in a shorter time to changes in living conditions than height. Most physical development traits show the similar dynamics as weight and BMI. The observed secular changes are probably due to the large socio-economic changes during the period under review (1986-2017).

Key words: physical development, university students, height, young adults, secular changes.

Introduction

Anthropological studies on various sex and age groups of different parts of the Earth are constantly actual. They are the only sources of metric information for the physical form of human generations. The physical development of the population of each country bears a specificity which is not repeated anywhere in the world, neither because of the different historical development, nor because of the different natural-geographical and socio-economic conditions of life.

The period around and after the age of 20, is a time point when some of the anthropometric characteristics have completed their growth changes, such as height, and others, such as body weight, continue their development. The problems of physical development have been the subject of many researches. Their target are the regularities of natural biological changes, their dynamics, the impact of various economic, social and environmental factors on them. The secular growth changes to higher body length, greater body weight and earlier maturation are related, in addition to the increased

standard of living and improved nutrition and health care [1, 3, 5, 6, 8, 10, 15, 16, 17]. Thus the results of studies on such topics are not only of general biological significance, but also of importance for assessing the health status of the population studied.

In Bulgaria, several national surveys of the physical development of the population were conducted in 1960, 1970-1971, 1980-1982 and 1989-1993 [11, 18, 19, 21]**.** Unfortunately, a nationwide study of physical development has not been conducted since then in Bulgaria. Secular changes in physical development, and especially in the growth of the Bulgarian population, were traced from the end of the 19th century to the end of the 20th century [12, 13]. Due to the lack of nationwide research in recent decades, we have no nationally representative data on the growth and physical development of the adult population born after 1963. The physical development of younger generations can only be evaluated by the results of individual studies of university students or students in the upper classes of high school [13].

The purpose of this study is to characterize anthropometrically physical development of Bulgarian students at the beginning of the XXI century, by comparison with the results of previous studies of students in Sofia.

Materials and Methods

In the period November 2016 - May 2017, an anthropometric survey was conducted at the Faculty of Biology at Sofia University "St. Kliment Ohridski"- Sofia, where young men and girls from all over the country are trained. A total of 77 students (31 males, 46 females), aged 18-25, was investigated.

The anthropometric study was carried out according to the conventional methodology of Martin R. and K. Saller [7, 9, 20]. Standard anthropological instruments ("GPM Anthropologische Instrumente" manufactured by Siber Hegner Masohinen AG – Zurich) was used.

The survey was voluntary, according the principles of Helsinki declaration.

Results and Discussion

The metric data on the anthropological features give a general idea of the anthropometric characteristics of the studied Bulgarian students **(Table 1**). The results can contribute to complement the overall anthropological characteristics of the Bulgarian population, as nationwide physical development studies have been missing for decades.

The comparison of the data from the present study with the corresponding data for the adult Bulgarian population make it possible to discover the specifics of the physical development of the young generation of Bulgaria living in the new century. At the same time, they give an idea of the long-term impact of the socio-economic crisis in our country in the 1990s, when they were born.

A review of all anthropometric features – absolute and relative – indicates a good development of the students. This is in concordance with the results of other studies. According to more detailed and representative studies by foreign authors in contemporary Europe, students are on average about 3 cm higher than the average for young people of the same age group [2, 4].

The results show that most anthropometric features are larger in males. Particularly large intersex differences are observed in indicators that reflect the development of the musculoskeletal system. Subcutaneous adipose tissue is better developed in women. Large are also the sex differences in the thickness of the skin folds on the limbs.

Table 1. Main indicators for the physical development of students.

Anthropological trait	males		females		T st (m-f)	p
	mean	SD	mean	SD		
Weight – kg	80.75	16.45	56.36	8.29	7,63	0,001
Height – cm	178.21	8.44	161.58	6.14	9,42	0,001
BMI – kg/m^2	25.33	4.23	21.62	3.30	4,11	0,001
Sitting height – cm	91.04	4.57	83.93	3.76	7,18	0,001
Height to iliospinale – cm	100.99	5.50	95.83	4.99	4,19	0,001
Chest circuimference at pause – cm	97.46	8.74	80.95	6.12	9,12	0,001
Chest circumference at inspirium – cm	101.89	8.48	83.52	6.16	10,36	0,001
Chest circumference at exspirium – cm	95.25	8.75	79.19	5.98	8,91	0,001
Waist circumference – cm	84.68	11.47	74.52	7.76	4,31	0,001
Hips circumference – cm	102.71	8.93	96.52	7.42	3,19	0,01
Thigh circumference – cm	57.20	7.29	53.69	5.58	2,27	0,05
Calf circumference – cm	38.15	3.49	35.03	2.45	4,31	0,001
Upper arm circumference, relaxed – cm	30.92	3.16	25.69	2.53	7,70	0,001
Upper arm circumference, contracted – cm	33.82	3.24	27.27	2.97	8,99	0,001
Forearm circumference – cm	28.23	2.05	23.32	1.36	11,71	0,001
Biacromial diameter – cm	40.00	2.25	33.37	1.93	13,41	0,001
Chest diameter – transversal – cm	29.12	2.10	24.87	1.68	9,42	0,001
Chest diameter – sagital – cm	21.91	2.37	17.20	1.83	9,35	0,001
Bicristal diameter – cm	23.43	3.10	21.43	2.32	3,06	0,01
Bitrochanterial diameter – cm	33.36	2.55	31.53	1.90	3,41	0,001
Subscapular skinfold – mm	11.03	3.29	11.83	2.82	-1,11	Insign.
Triceps skinfold – mm	8.94	3.59	13.33	3.81	-2,79	0,01
Thoracal skinfold – mm	10.58	4.35	12.39	3.88	-1,87	Insign.
Suprailiac skinfold – mm	13.95	4.90	15.04	4.63	-0,98	Insign.
Thigh skinfold – mm	13.84	3.44	16.21	3.76	-2,86	0,05
Calf skinfold – mm	8.66	3.48	10.67	3.64	-2,44	0,05
Epicondilar diameter of humerus – cm	68.90	9.31	60.98	7.26	3,99	0,001
Epicondilar diameter of femur – mm	100.55	9.26	86.09	5.32	7,86	0,001
Lower limb length – cm	96.41	5.10	92.57	4.66	3,35	0,05
Relative chest circumference, %	54.74	4.74	50.14	4.04	4,43	0,001
Thoracal index, %	75.35	7.16	69.29	7.13	3,65	0,001
Relative sitting height, %	51.12	1.95	51.96	1.70	-1,95	Insign.
Relative biacromial diameter, %	22.49	1.54	20.66	1.12	5,68	0,001
Pelvic index – %	58.82	8.95	64.41	7.70	-2,84	0,01
Relative lower limb length, %	54.11	1.77	57.29	1.80	-7,68	0,001
Relative bicristal diameter, %	13.14	1.55	13.28	1.52	-0,39	Insign.

The predominant tendency for changes in anthropometric indicators for physical development is their decrease in the first half of the comparison period and their increase in the second half **(Tables 2 and 3, Figs. 1, 2, 3)**.

Table 2. Comparison of major physical indicators in Sofia students – males.

	1986			2002			2017			P
Anthropometric trait	N	M	SD	N	M	SD	N	M	SD	
Height – cm	297	175.61	5.78	72	178.78	6.63	31	178.21	8.43	<0.001
Weight – kg	297	75.01	10.4	72	70.4	8.63	31	80.75	16.45	<0.001
Sitting height – cm	297	90.88	3.93	72	93.17	3.76	31	91.04	4.57	<0.001
Lower limb length – cm	297	101.34	4.7	72	99.09	5.18	31	96.41	5.10	<0.001
Chest circumference at pause – cm	296	92.4	6.38	72	87.37	5.79	31	97.46	8.74	<0.001
Waist circumference – cm	297	80.54	7.82	72	77.53	6.11	31	84.68	11.47	<0.001
Hips circumference – cm	296	96.06	5.92	72	91.06	5.54	31	102.71	8.93	<0.001
Thigh circumference – cm	296	55.4	4.37	72	56.05	4.11	31	57.20	7.29	0.983
Calf circumference – cm	297	37.42	2.57	72	35.65	2.49	31	38.15	3.49	<0.001
Upper arm circumference, relaxed – cm	297	29.68	3.05	72	29.73	2.84	31	30.92	3.16	0.094
Forearm circumference – cm	297	27.85	2.04	72	27.11	1.62	31	28.23	2.05	0.007
Biacromial diameter –cm	296	40.01	1.97	72	41.19	2.05	31	40.00	2.25	<0.001
Chest diameter – transversal – cm	296	29.3	1.84	72	29.51	2.00	31	29.12	2.10	0.575
Chest diameter – sagital – cm	296	21.1	1.94	72	20.91	1.71	31	21.91	2.37	0.051
Bicristal diameter – cm	296	28.14	2.01	72	27.23	1.65	31	23.43	3.10	<0.001
Subscapular skinfold – mm	293	12.46	4.74	72	9.66	3.56	31	11.03	3.29	<0.001
Triceps skinfold – mm	293	11.28	4.14	72	9.39	3.48	31	8.94	3.59	<0.001
Thoracal skinfold – mm	293	11.49	5.11	72	7.08	2.87	31	10.58	4.35	<0.001
Suprailiac skinfold – mm	293	11.04	5.91	72	6.99	3.04	31	13.95	4.90	0.00
Thigh skinfold – mm	293	18.28	6.45	72	14.74	6.12	31	13.84	3.44	<0.001
Calf skinfold – mm	292	10.69	5.08	72	10.76	3.77	31	8.66	3.48	0.07
BMI –kg/m^2	297	24.29	2.93	72	22.04	2.56	31	25.33	4.23	<0.001
Relative sitting height, %	297	51.58	3.38	72	52.12	1.31	31	51.12	1.95	0.29
Relative lower limb length, %	297	51.7	1.49	72	55.41	1.67	31	54.11	1.77	<0.001
Relative chest circumference, %	296	52.66	3.72	72	48.92	3.49	31	54.74	4.74	<0.001
Relative biacromial diameter, %	296	22.8	1.10	72	23.06	1.21	31	22.49	1.54	0.06
Relative bicristal diameter, %	296	16.03	1.05	72	15.24	0.91	31	13.14	1.55	<0.001
Thoracal index, %	296	72.09	5.94	72	71.05	6.43	31	75.35	7.16	0.01
Pelvic index -%	296	70.38	4.73	72	66.22	4.43	31	58.82	8.95	<0.001

Table 3. Comparison of major physical indicators in Sofia students – females.

	1986			2002			2017			P
Anthropometric trait	N	M	SD	N	M	SD	N	M	SD	
Height – cm	580	162.55	5.59	70	164.05	5.06	46	161.58	6.14	0.044
Weight – kg	580	59.13	9.03	70	52.39	6.99	46	56.36	8.29	<0.001
Sitting height –cm	580	86.44	3.45	70	87.22	3.12	46	83.93	3.76	<0.001
Lower limb length – cm	579	93.36	4.25	70	89.97	3.91	46	92.57	4.66	<0.001
Chest circumference at pause – cm	578	85.33	6.58	70	73.05	4.45	46	80.95	6.12	<0.001
Waist circumference – cm	579	67.43	6.22	70	65.92	5.18	46	74.52	7.76	<0.001
Hips circumference – cm	580	95.54	7.07	70	87.21	5.43	46	96.52	7.42	<0.001
Thigh circumference - cm	580	55.38	5.20	70	54.13	4.42	46	53.69	5.58	0.023
Calf circumference - cm	579	34.90	2.65	70	33.1	2.65	46	35.03	2.45	<0.001
Upper arm circumference, relaxed – cm	578	24.98	2.85	70	24.72	2.29	46	25.69	2.53	0.167
Forearm circumference – cm	579	23.19	1.82	70	22.73	1.39	46	23.32	1.36	0.095
Biacromial diameter – cm	577	35.77	1.89	70	34.84	1.87	46	33.37	1.93	<0.001
Chest diameter – transversal – cm	576	25.46	1.77	70	24.91	1.56	46	24.87	1.68	0.006
Chest diameter – sagital – cm	577	18.17	1.66	70	17.72	1.48	46	17.20	1.83	<0.001
Bicristal diameter – cm	576	27.25	2.71	70	25.45	1.46	46	21.43	2.32	<0.001
Subscapular skinfold – mm	563	14.63	6.18	70	10.53	3.75	46	11.83	2.82	<0.001
Triceps skinfold – mm	562	15.93	5.46	70	13.62	3.53	46	13.33	3.81	<0.001
Thoracal skinfold – mm	563	13.45	6.19	70	8.79	3.34	46	12.39	3.88	<0.001
Suprailiac skinfold – mm	563	14.94	7.00	70	8.35	2.77	46	15.04	4.63	<0.001
Thigh skinfold – mm	562	25.49	6.14	70	19.29	4.50	46	16.21	3.76	<0.001
Calf skinfold – mm	560	21.61	6.24	70	14.61	3.37	46	10.67	3.64	<0.001
BMI –kg/m^2	580	22.36	3.12	70	19.44	2.21	46	21.62	3.30	<0.001
Relative sitting height, %	580	53.19	1.56	70	53.17	1.26	46	51.96	1.70	<0.001
Relative lower limb length, %	579	57.43	1.41	70	54.83	1.32	46	57.29	1.80	<0.001
Relative chest circumference, %	578	52.53	4.04	70	44.55	2.70	46	50.14	4.04	<0.001
Relative biacromial diameter, %	577	22.02	1.11	70	21.24	1.04	46	20.66	1.12	<0.001
Relative bicristal diameter, %	576	16.77	1.63	70	15.52	0.84	46	13.28	1.52	<0.001
Thoracal index, %	577	71.49	5.87	70	71.32	6.26	46	69.29	7.13	0.058
Pelvic index -%	576	76.19	6.63	70	73.16	4.68	46	64.41	7.70	<0.001

From this trend deviates the height, which increased during the period 1986-2002 and stagnated and decreased during the period 2002-2017. Since most of the growth is formed during the period of birth and early childhood, this change is logical [8]. The growth of students measured in 2017 was definitely influenced by the decline in life conditions in the 1990s, as has been observed in other Eastern European countries [1, 2]. This is followed by a hip circumference (in women), triceps skin folds, a thigh and a thigh for both sexes, the average value of the relative sitting height, while growth is conservative.

Most physical development indicators show the same dynamics as weight and BMI (decrease towards 2002 and increase afterwards). That is because changes in the development of subcutaneous fat tissue and of the osteo-muscular system cause changes in body mass (BMI) and weight.

Data for 1986 and 2002 are taken from a previous article of Stoev, Atanasova-Timeva and Zhecheva [14].

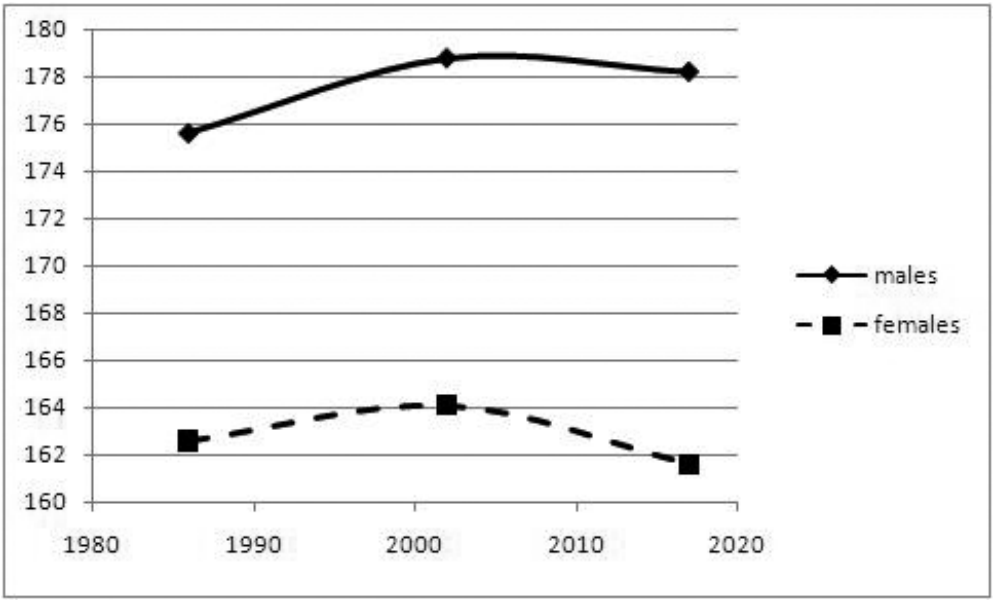

Fig. 1. Body height in students – 1986-2017, cm

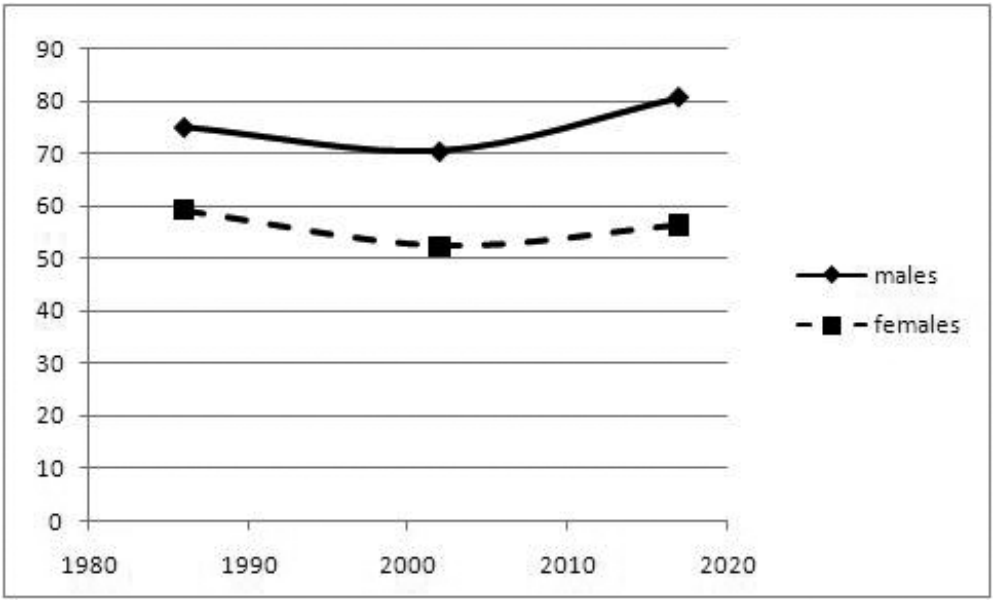

Fig. 2. Body mass in students – 1986-2017, kg

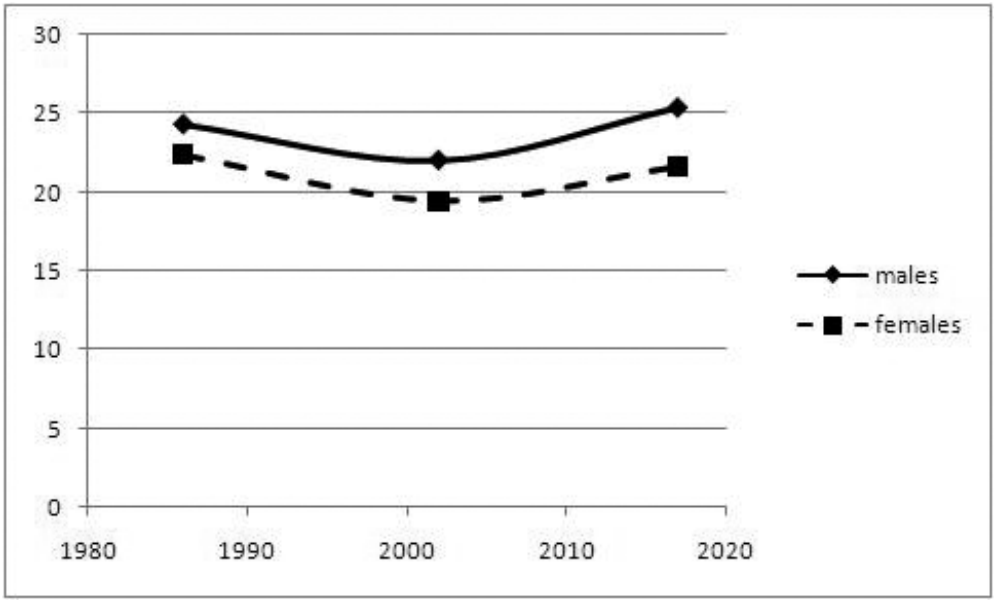

Fig. 3. Body mass index in students – 1986-2017

Conclusions

The comparison with data from previous surveys shows that at the beginning of the 21st century, there was a secular stagnation in height. This should account for the long-term negative impact on their development during the troubled years of their early childhood. In the early 21st century, secondary weight changes were positive. Combined with growth stagnation it causes a sharply BMI increase respectively. This trend is in contrast to the trend observed in students at the late 20th century. This fact indicates, respectively, that weight and BMI respond more quickly to changes in living conditions than height. The observed secondary changes are likely to be due to major socio-economic changes during the period considered (1986-2017).

Sex differences in growth over the comparison period (1986-2017) are increasing.

Acknowledgements: To our teacher professor Tsvetan Minkov [1932-2018].

References

1. **Baten, J.** *A History of the global economy. From 1500 to the Present*. Cambridge, Cambridge Univ. Press, 2016, 1-356.
2. **Grasgruber, P.** Major correlates of male height: A study of 105 countries. – *Econ. Hum. Biol.*, **21**, 2016, 172-195.
3. **Grasgruber, P., J. Cacek, T. Kalina, M. Sebera.** The role of nutrition and genetics as key determinants of the positive height trend. – *Econ. Hum. Biol.,* **15**, 2014, 81-100.
4. **Herpin, N.** Male heights: Their effect on living in a couple and careers. – *Economie et Statistique,* **361** (1), 2003, 71-9 [in French].
5. **Komlos, J.** Nutrition and economic development in eighteenth-century Habsburg monarchy. – In: *Anthropometrie history*. Princeton, Princeton Univ. Press, 1989, 1-344.

6. **Komlos, J.** A history of human height from the 17th to the 21st century. Paper presented on the Vth International Anthropological Congress of Ales Hrdlicka, Prague-Humpolec, 2009.
7. **Martin, R., K. Saller**. *Lehrbuch der anthropologie*. Fischer, Stuttgart, 1957, 1-532.
8. **Mironov, B. N.** Social history of Russia in imperial period (18th - early 20th century). *St. Petersburg, Dmitriy Bulanin,* 1999, **v.2**. 1-566 [in Russian].
9. **Mutafov, S., I. Goranov, D. Sepetliev, S. Tornyova-Randelova, A. Nacheva-Tsatseva.** *Anthropologic-ergonomic characterization of the Bulgarian population*. Sofia, Publishing House of the Bulgarian Academy of Sciences, 1985, 1-156 [in Bulgarian].
10. **Silventoinen, K.** Determinants of variation in adult body height. – *J. Biosoc. Sci.*, **35** (2), 2003, 263-265.
11. **Slanchev, P., B. Yanev, F. Genov, P. Shterev, P. Boev, D. Sepetliev, B. Zahariev.** *Physical development, physical fitness and neuro-psychical reactivity of the population of Bulgaria*. Sofia, National Sports Academy, 1992, 1-336 [in Bulgarian].
12. **Stoev, R., Y. Yordanov.** Secular trend in Bulgaria. – In: *Secular Growth Changes in Europe* (Eds. B. E. Bodzsar, C. Susane), Budapest, Eotvos University Press, 1998, 65-73.
13. **Stoev, R.** Changes in height in adult Bulgarians from the end of 19th to the end of 20th century. – *Acta morphol. anthropol*., **19**, 2012, 261-265.
14. **Stoev, R., N. Atanasova-Timeva, Y. Zhecheva**. Comparative anthropometric characteristics of Bulgarian students (1986-2002). – *Acta morphol. anthropol.,* **16**, 2010, 88-95.
15. **Tanner, J. M.** *A History of the study of human growth.* Cambridge, Cambridge University Press, 1981, 1-499.
16. **Tanner, J. M.** Growth as a mirror for the conditions of society: Secular trends and class distinctions. – In: *Human growth: A Multidisciplinary review* (Ed. A Demirjian), London, Taylor and Francis, 1986, 3-34.
17. **Tanner, J. M.** Growth as a measure of the nutritional and hygienic status of population. – *Horm. Res.,* **38**, 1992, 106-115.
18. **Yanev, B., P. Shterev, P. Boev, R. Semerdjieva, D. Sepetliev**. *Physical development and fitness of the population in Bulgaria from birth until 26 years.* Sofia, Publishing House of the Bulgarian Academy of Sciences, 1965, 1-262 [in Bulgarian].
19. **Yanev, B., P. Shterev, P. Boev, F. Genov, D. Sepetliev, I. Popov, B. Zahariev.** *Physical development, physical fitness and neuro-psychical reactivity of the population*. Sofia, Medicine and Physculture, 1982, 1-352 [in Bulgarian].
20. **Yordanov, Y.** *Manual of anthropology*. Sofia University Publishing House "St. Kliment Ohridski", 1997, 1-208 [in Bulgarian].
21. **Yordanov, Y., A. Nacheva, S. Tornyova-Randelova, N. Kondova, B. Dimitrova, D. Paskova-Topalova.** *Anthropology of the population of Bulgaria in the end of 20th century*. Sofia, Academic publishing house "Marin Drinov", 2006, 1-432 [in Bulgarian].

Institute of Experimental Morphology, Pathology and Anthropology with Museum
Bulgarian Anatomical Society

Acta morphologica et anthropologica, 26 (3-4)
Sofia ● 2019

Monitoring, Comparison and Correlation between the Body Mass Index and Spermatozoa with Normal Motility and Putative Fertility Potential among the Population of Adult Men in Plovdiv Region.

Borislav Mateev[1,2]

[1] *Medical Centre BORA, Plovdiv, Bulgaria*
[2] *Plovdiv Univeristy "Paisii Hilendarski", Faculty of Biology, Department of Developmental Biology, Plovdiv, Bulgaria*

* Corresponding author e-mail: b.mateev@boramedical.com

The aim of this retrospective study was to assess the relationships between body mass index and sperm quality and respectively infertility, among the population of adult men in the region of Plovdiv, comparing sperm concentration to the lower reference value for normal fertility. Samples from 918 male partners in subfertile couples, who visited the clinic between January 2017 and July 2019, were analyzed and compared in the groups according to their body mass index. The results clearly indicated that BMI is a factor influencing sperm parameters in the adult male population in Plovdiv region and participants with overweight and even obesity conditions are more likely to be a risk group for potential infertility.

Key words: body mass index (BMI), overweight, obesity, sperm quality, infertility

Introduction

Infertility is a serious health condition that affects about 10% of all families worldwide [3]. Although assisted reproductive technologies provide an opportunity to address some of the causes of this problem, they are far from being able to provide a solution to each specific case. For this reason, identifying and clarifying each and every risk factors for subfertility is a serious task for clinicians and researchers working in the research field of the problem at the present time.

Overweight and obesity are also a global problem, especially in industrialized countries and societies [25]. The reasons for this are often laid down in childhood development, which of course does not always mean mandatory overweight in adulthood [12, 13, 17].

However, the fact is that overweight and obesity are more common in the Bulgarian population compared to European populations according to WHO statistic data [4, 5, 16]. In the last decade, one out of three adults worldwide is overweight and one out of nine is obese, while the trend of increasing obesity rates is progressing [26].

Researchers have found that significant number of couples in reproductive age are overweight or even obese [18] and in about 40 % of the cases this is due to the so-called male factor [7].

Infertility is defined as a state of inability to achieve the desired / planned pregnancy within one year and to overweight and obesity in men is being associated as a risk and predisposing factor [13, 16, 18].

It is generally accepted that obesity affects the GnRH-FSH/LH pulse, impairs the function of Sertoli and Leydig cells, and influences the release of sex hormones and also sperm maturation [24].

Serum testosterone, sex hormone-binding globulin (SHBG), and inhibin B are reported to decrease with increasing body mass index (BMI), whereas estradiol (E_2) increased with increasing BMI [7, 9]. Moreover, researchers in recent years have found obesity in adult men to be linked to low sperm quality [1, 8, 10], and obese men are 3 times more likely to exhibit a reduction in semen quality than men with normal weight. Overweight and obesity have been associated with an increased prevalence of azoospermia or oligozoospermia [19].

Materials and Methods

The participants, 918 men, were the partners in subfertile couples who submitted semen samples for semen analysis or were attending for therapeutic procedures in Medical Centre Bora in Plovdiv between January 2017 and July 2019. The fertility status of their female partners was not considered. Male participants who had definitive pathological conditions capable of affecting sperm quality were excluded, as well as patients with abnormal morphology and concentration /oligospermia and azoospermia/ (according WHO).

The calculation of body mass index (BMI = kg / m^2), as well as the analysis of the semen sample, were performed by the same specialist, qualified and trained according to WHO criteria and algorithms, in order to avoid methodological and assembly errors in the course of the study.

Samples were described and analyzed in terms of patient age, period of sexual abstinence, medication intake, potential harms, volume and pH of the ejaculate.

Other sperm variables used as outcome variables were as follows: sperm concentration (millions per ml), semen volume (ml), total sperm count, relative number of sperm with rapid motility (Type A motility, %), relative number of sperm with less progressive or linear motility (Type B motility, %), percentage of sperm with sluggish and/or undulating motility (Type C motility, %), total motile sperm count, and relative number of normal sperm as assessed by morphology.

All the sperm samples were kept in a 37°C CO_2 incubator to allow them to liquefy and facilitate routine sperm analysis. Analyses were performed with an Olympus IMT2 inverted microscope at 400x and 1000x magnification and a standard Neubauer counting chamber.

For the statistical analyses was used ***Statview*** **version** ***V software*** and ANOVA test for the comparison of BMI groups and sperm count and motility. In all analyzes, differences with $p < 0.05$ were considered as statistically significant.

Results

Patients were divided into groups by BMI (**Table 1, Fig.1**). Group A – normal weight 18–24,99 kg/m^{-2}, group B – overweight 25–29,99 kg/m^{-2}, group C – obese I class 30-34,99 kg/m^{-2} and group D – obese class II and III ***≥35,0*** kg /m^{-2}

Table 1. Groups by BMI

BMI	*A – 18.5-24.99*	*B – 25-29.99*	*C – 30-34,99*	*D – ≥35,0*
n	266	372	195	85

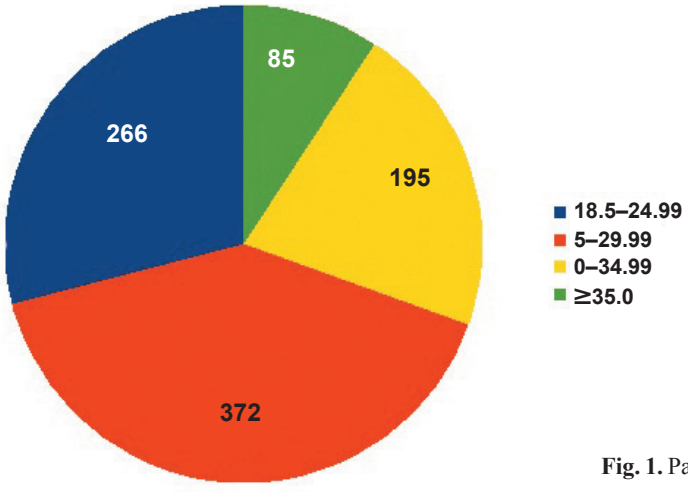

Fig. 1. Patients in the relevant BMI group

As demonstrated in **Table 2** and **Table 3**, we did not find a statistically significant correlation between age and BMI values in the working groups. However, the results indicated significant relationships between BMI and the total sperm count, as well as between BMI and relative amount of type A motility and the relative amount of progressive motility (A + B).

Sperm concentration in the group of overweight and obese men was 20,7± 6.6 mill/ml and 17,5± 5.8 mill /ml, respectively, which was significantly lower than in the subjects with normal BMI where the mean value of total sperm count was 27,7± 5,7 mill/ml.

If we take into account the WHO 2010 criteria, which postulate that men with normal fertility are having no less than $7{,}2\times10^6$ [28] normally motile spermatozoa and after processing and analyzing the obtained results, we observed the following: in group A – with normal weight and BMI values, the ratio fertile to infertile men is 69.56% to

Table 2. Mean age in the relevant BMI groups

BMI group	*A 18.5–24.99*	*B 25–29.99*	*C 30–34,99*	*D ≥35,0*
Age	31,8±2,5	31,2±2,0	32,9±2,9	32,9±1,8
Sperm count x10⁶/ml	27,7± 5,7	20,7± 6.6	17,5± 5.8	

Table 3. Biostatistical data from the applied analyzes

BMI group	*A 18.5–24.99*	*B 25–29.99*	*C 30–34,99*	*D ≥35,0*
Volume	3,1±1,2	2,9±1,1	3,5±1,1	
pH	7,5±0,1	7,5±0,2	7,6±0,1	
Sperm count x10⁶/ ml	27,7± 5,7	20,7± 6.6*	17,5± 5.8*	
Motility in % A+B	37,7± 8,7	39,7± 6.4	35,5± 8.8	
Motility in % C	10,9± 3,1	9,3± 3,8	9,1± 3,6	
Morphology %	7,9± 4,8	7,8± 4,7	7,6± 4,6	

* Significant difference between A and B – C/D; p <0.05 (p-value as differences between BMI groups for one way ANOVA-test)

30.43% – or in general, in the group two out of three men have normal fertility potential. Similar is the ratio in group B – overweight: 70.21% fertile versus 29.78% subfertile – again two out of three men with normal fertile parameters. Significant deviation was observed in the groups of men with obesity I, II, and III degree. The ratio of fertile to infertile men is almost 1:1 (54.54% to 45.45%) as shown in **Fig. 2**.

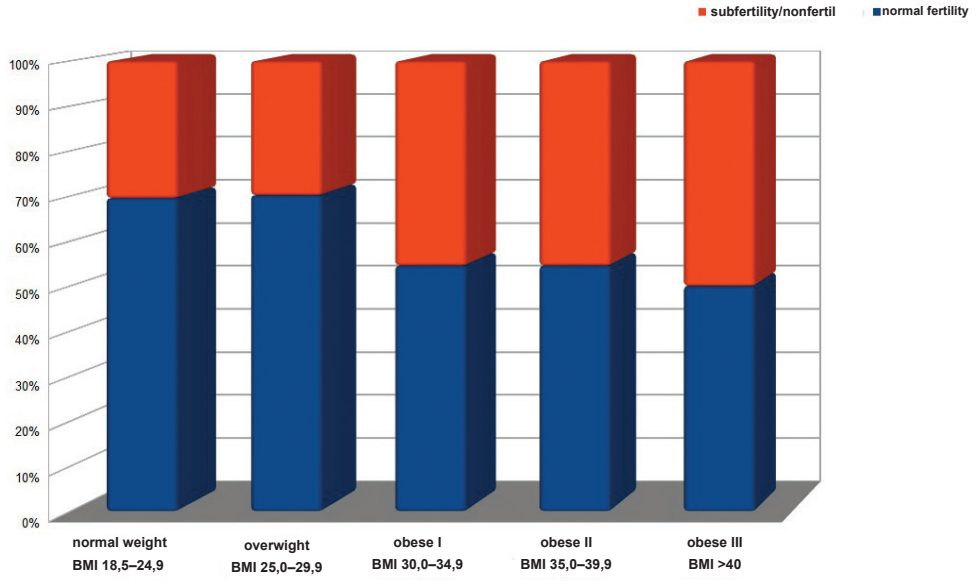

Fig. 2. The ratio of fertile to infertile men

Discussion

The results of this study demonstrate that there were changes in the number and proportions of patients in groups, as well as fertility criteria (total sperm count and number of normally motile sperm cells), which absolutely links to the conclusion, that there is a correlation between the increased BMI values and the reduction of total sperm count. As the body mass index increases, the likelihood of subfertility in a man due to and resulting in a low number of normally motile sperm, increases as well.

Following this sense, our results and their analyses confirm the results published in 2014 by the study of Belloc et al. in France from over 10 600 patients who also demonstrate in their interpretation a clear link between overweight and obesity and spermatogenesis (volume, concentration, motility) [2].

Obesity condition affects negatively the reproductive potential of men, reducing sperm parameters, but also through the physiological and biochemical effects on germ cells in the testes and subsequently the maturation and functionality of sperm [24].

In contrast, there are other studies that show no significant correlation between BMI and semen parameters [5, 6, 20]. A meta-analysis from MacDonald *et al.* found no evidence of a relationship between BMI and sperm concentration or total sperm count, but there was a negative relationship between testosterone, SHBG, and free testosterone with an increased BMI [10].

However, there are some study limits in these reports such as the small number of obese male subjects and the study populations consisting of multinationals. Therefore, our retrospective study was designed and concepted to explore eventual relationship between BMI and sperm parameters in the male population in Plovdiv region, comparing sperm concentration with the lower reference value for normal fertility – sufficient enough to achieve pregnancy, according to the World Health Organization 2010 criteria (WHO 2010).

Conclusion

The current findings and the summary results of our study indicate a prerequisite to confirm, that Body mass index (BMI) is a factor influencing sperm parameters in the adult male population in the Plovdiv region, as overweight and obese individuals fall into the risk group for potential infertility.

References

1. **Aggerholm, A. S., A. M. Thulstrup, G. Toft, C. H. Ramlau-Hansen, J. P. Bonde**. Is overweight a risk factor for reduced semen quality and altered serum sex hormone profile? – *Fertil. Steril*., **90**, 2008, 619-626.
2. **Belloc, S., M. Cohen-Bacrie, E. Amar, V. Izard, M. Benkhalifa, A. Dalléac, J**. **de Mouzon.** High body mass index has a deleterious effect on semen parameters except morphology: results from a large cohort study. – *Fertil. Steril.,* **102**, 2014, 1268-1273.
3. **Boivin, J., L. Bunting, J. A. Collins, K. G. Nygren**. International estimates of infertility prevalence and treatment-seeking: potential need and demand for infertility medical care. – *Hum. Reprod. (Oxford, England)*, **22**, 2007, 1506-1512.
4. **Boukov, S., M. Nikolova, D. Boyadzhiev.** Basic somatometric indices in three generations of children from Plovdiv. – *Journal of Anthropology*, **3**, 2000, 41-49.
5. **Duits, F. H., M. van Wely, F. van der Veen, J. Gianotten.** Healthy overweight male partners of subfertile couples should not worry about their semen quality. – *Fertil. Steril.,* **94**, 2010, 1356-1359.
6. **Eskandar, M., M. Al-Asmari, S. Babu Chaduvula, M. Al-Shahrani, M. Al-Sunaidi, M. Almushait, O. Donia, S. Al-Fifi**. Impact of male obesity on semen quality and serum sex hormones. – *Advances in Urology,* 2012, ID407601.

7. **Güney, A. I., D. Javadova, D. Kırac, K. Ulucan, G. Koc, D. Ergec, H. Tavukcu, T. Tarcan**. Detection of Y chromosome microdeletions and mitochondrial DNA mutations in male infertility patients. - Genetics and molecular research: *GMR*, **11**, 2012,1039-1048.
8. **Jensen, T. K., A-M. Andersson, N. Jørgensen, A-G. Andersen, E. Carlsen, J. H. Petersen, N. E. Skakkebaek**. Body mass index in relation to semen quality and reproductive hormones among 1,558 Danish men. – *Fertil. Steril.,* **82**, 2004, 863-870.
9. **Koloszár, S., I. Fejes, Z. Závaczki, J. Daru, J. Szöllosi, A. Pál**. Effect of body weight on sperm concentration in normozoospermic males. – *Arch. Androl.,* **51**, 2005, 299-304.
10. **MacDonald, A. A., G. P. Herbison, M. Showell, C. M. Farquhar.** The impact of body mass index on semen parameters and reproductive hormones in human males: a systematic review with meta-analysis. – *Hum. Reprod. Update,* **16**, 2010 , 293-311.
11. **Martini, A. C., A. Tissera, D. Estofán, R. I. Molina, A. Mangeaud, M. F. de Cuneo, R. D. Ruiz**. Overweight and seminal quality: a study of 794 patients. – Fertil. Steril, **94**, 2010, 1739-1743.
12. **Mladenova, S., M. Nikolova**. Components of body mass and their relations during the growth period of the boys.– *Proceedings from Balkan Scientific Conference of Biology*, 2005, 138-150.
13. **Mladenova, S., M. Nikolova, D. Boyadzhiev.** Body Mass Index, Some Circumference Indices and their Ratios for Monitoring of Physical Development and Nutritional Status of Children and Adolescents. – *Acta Morphol. Anthropol.,* **10**, 2005, 226-229.
14. **Nguyen, R. H. N., A. J. Wilcox, R. Skjaerven, D. D. Baird**. Men's body mass index and infertility. – *Hum. Reprod*. (Oxford, England), **22**, 2007, 2488-2493.
15. **Nikolova, M., S. Mladenova.** Anthropometric indicators for assessment of body composition. – *Acta Morphol. Anthropol.,* **10**, 2005 218-225.
16. **Nikolova, M., S. Sivkov, V. Akabaliev, S. Mladenova**. Body composition of children and adolescents in Plovdiv. – Plovdiv University Press, *Proceedings from Balkan Scientific Conference of Biology*, 2005, 150-159.
17. **Nikolova, M., S. l. Tineshev.** Comparison of the Body Mass Index to other Methods of Body Fat Assessment in Bulgarian Children and Adolescent. – *Biotechnology & Biotechnological Equipment*, **24**, 2010, 329-337.
18. **Pasquali, R., L. Patton, A. Gambineri**. Obesity and infertility. – *Current Opinion in Endocrinology, Diabetes, and Obesity*, **14**, 2007, 482-487.
19. **Ramlau-Hansen, C. H., A. M. Thulstrup, E. A. Nohr, J. P. Bonde, T. I. A. Sørensen, J. Olsen.** Subfecundity in overweight and obese couples. – *Hum. Reprod. (Oxford, England),* **22**, 2007, 1634-1637.
20. **Relwani, R., D. Berger, N. Santoro, C. Hickmon, M. Nihsen, A. Zapantis, M. Werner, A. J. Polotsky, S. Jindal**. Semen parameters are unrelated to BMI but vary with SSRI use and prior urological surgery. – *Reprod. Sci.,* **18**, 2011, 391-397.
21. **Sallmén, M., D. P. Sandler, J. A. Hoppin, A. Blair, D. D. Baird**. Reduced fertility among overweight and obese men. – *Epidemiology*, **17**, 2006, 520-523.
22. **Sermondade, N., C. Faure, L. Fezeu, A. G. Shayeb, J. P. Bonde, T. K. Jensen, M. Van Wely, J. Cao, A. C. Martini, M. Eskandar, J. E. Chavarro, S. Koloszar, J. M. Twigt, C. H. Ramlau-Hansen, E. Borges, F. Lotti, R. P M Steegers-Theunissen, B. Zorn, A. J. Polotsky, S. La Vignera, B. Eskenazi, K. Tremellen, E. V. Magnusdottir, I. Fejes, S. Hercberg, R. Lévy, S. Czernichow**. BMI in relation to sperm count: an updated systematic review and collaborative meta-analysis. – *Hum. Reprod. Update,* **19**, 2013, 221-231.
23. **Sharma, R., K. R. Biedenharn, J. M. Fedor, A. Agarwal**. Lifestyle factors and reproductive health: taking control of your fertility. – *Reprod. Biol. Endocrinol.,* **11**, 2013, 66
24. **Shukla, K. K., S. Chambial, S. Dwivedi, S. Misra, P. Sharma**. Recent scenario of obesity and male fertility. – *Andrology,* **2**, 2014, 809-818.
25. **Stefan, N., H-U. Häring, F. B. Hu, M. B. Schulze**. Metabolically healthy obesity: epidemiology, mechanisms, and clinical implications. – *Lancet Diabetes Endocrinol*., **1**, 2013, 152-162.
26. **Stevens, G. A., G. M. Singh, Y. Lu, G. Danaei, J. K. Lin, M. M. Finucane, A. N. Bahalim, R. K. McIntire, H. R. Gutierrez, M. Cowan, C. J. Paciorek, F. Farzadfar, L. Riley, M. Ezzati**, National, regional, and global trends in adult overweight and obesity prevalences. – *Popul. Health Metr.*, **10**, 2012, 22.
27. **Vermeulen, A**. Environment, human reproduction, menopause, and andropause. – *Environ. Health Perspect.,* **101**, 1993, 91-100.
28. **World Health Organization**, WHO laboratory manual for the examination and processing of human semen. 5th ed. 2010. Available at: https://www.who.int/reproductivehealth/publications/infertility/9789241547789/en/

Institute of Experimental Morphology, Pathology and Anthropology with Museum
Bulgarian Anatomical Society

Acta morphologica et anthropologica, 26 (3-4)
Sofia ● 2019

Cone Beam Computed Tomographic Study of Mucosal Thickness of Maxillary Sinus Floor

Elena Bozhikova[1], Nikolay Uzunov[2], Tanya Kitova[1]*

[1] *Department of Anatomy, histology and embryology, Faculty of Medicine, Medical University, 4000 Plovdiv, Bulgaria*
[2] *Department of Maxillofacial surgery, Faculty of Dentistry, Medical University, bul. V. Aprilov 15A, 4000 Plovdiv, Bulgaria*

* Corresponding author e-mail: elibozhikova@gmail.com

The purpose of the present study was to determine the mucosal thickness of the maxillary sinus floor. The study included the 3D-cone beam computed tomograms of 53 patients (32 women and 21 men; aged 18-72 years, mean 46,3±13,4). The mucosal thickness was measured on cross-sectional images in its thickest part above the apexes of the molars and premolars, or in the absence of such– above the corresponding position of future dental implants.The average thickness measured was 2,24±3,11 mm, with mucosal thickening in 92,5% of all patients and above 56,3% of all teeth. A significant association was found between the thickness and pathological processes (p=0,002). Highest percentage of changes occurred in the age over 26 years and there is significant association between the thickness and patient's age (p<0,001). Pathology related to the lateral maxillary teeth and maxillary sinus is one of the main factors for mucosal thickening. The preoperative evaluation of the sinus mucosa is essential for the correct planning and prevention of complications in dental implant treatment and maxillary sinus elevation surgery.

Key words: mucosa, maxillary sinus floor, 3D- cone beam computed tomography, maxillary sinus floor elevation

Introduction

During the past two decades dental implants (DI) proved to be a reliable treatment modality in the prosthetic rehabilitation of partially or totally edentulous patients. A restriction for their use in the posterior maxilla is the insufficient residual bone height for implant placement. The reasons for this are due to the continuing alveolar bone resorption which begins immediately after tooth loss, the proximity of the maxillary sinus floor (MSF) and the progression of sinus pneumatization. To provide enough volume of bone for adequate prosthetic support in such cases the sinus floor is grafted with a bone graft or substitute inserted between the elevated maxillary sinus floor membrane (MSFM) and the cranial surface of the inferior sinus wall. A major prerequisite for successful MSF elevation is the healthy sinus with strong MSFM. Sinus pathology of

different origin can complicate or irreversibly compromise the result of the operation. Pathological involvement of the maxillary sinus is often presented as thickening of the mucous membrane. That is why membrane dimensions are used to indicate the presence or absence of disease in the sinus itself or in the vicinity neighboring the implant site.

The thickness of the MSFM, known also as Schneiderian membrane, is variable [4, 5, 10]. Masurements exceeding 2 mm are considered pathology. Factors causing MSFM thickening include, but are not restricted to, infection, allergy, trauma, oncologic conditions, and smoking [3]. It is accepted that the MSFM lying above teeth with periodontal and endodontic lesions shows higher thickness. The situation is well presented above the molars in case of thin bone plate between the dental roots and maxillary sinus floor or in cases having periapical lesions [3,4]. The possibility of inflamatory sinus pathology or a periodontal lesion next to implant and/or graft site to cause supuration or implant failure, thus jeopardasing the treatment and making further surgeries impossible, is high. This turns the preoperative assessment of the condition of the sinus mucosa into a keystone for the planning and prevention of complications in sinus floor elevation surgery. The presence of the pathology aforementioned may shift the treatment plan to such treatment modalities like "All-on-Four", the use of short, zygomatic or pterygomaxillary implants or, something more, can abundon implant treatment at all.

The aim of the present study is to evaluate the thickness of maxillary sinus floor membrane in patients in need of maxillary sinus elevation surgery in conjunction with DI placement and its application in preoperative patient assessment and planning. We also assessed the relationship between periapical pathology and the incidence of mucosal thickening.

Materials and Methods

Patients: Inclusion criteria for the patients consisted of: 1) At least one sided partially or totally edentulous distal maxilla; 2) Need of dental implant treatment; 3) Teeth with and without periapical pathology; 4) Preoperative bilateral 3D-cone beam computed tomography (3D-CBCT) of the maxilla; 5) Clearly visualised maxillary sinus floor. Patients with signs of congenital anomalies, acute sinusitis, and oncologic involvement, as well as patients with history of heavy inflamatory sinus pathology, trauma, preliminary surgery of the distal maxilla and/or the maxillary sinus, were excluded from the study.

Radiological investigations: The 3-DCBCT of all patients was performed with Kodak Carestream 9000 3D machine (Carestream Health, Inc, Rochester, NY) with fixed isotropic field of 0,76 × 0,76 x 0,76 μm (isotropic voxel), image size 17 × 11 cm, maximum exposure of 14 sec. The resulting images were processed with Kodak Carestream Simple Browser Software.

Regions of interest: The regions of interest were defined as the position of the MSF and alveolar ridge of the distal maxilla subjected to DI placement (**Fig 1**). These included edentulous, partially edentulous or dentate alveolar ridges extending from the first premolar to the third molar planned for replacement of failing or already missing teeth with DI. For evaluation of relationship between pathology and the incidence of mucosal thickening were also included teeth without periapical pathology. Teeth with apical root proximity to the nasal cavity instead of the maxillry sinus were excluded from the study (**Fig. 2a and 2b**).

Measurements: The Kodak Carestream Simple Browser Software was used for for evaluation of sinus anatomy and implant planning. The thickest part of the MSFM was measured in millimeters on cross-sectional images with the built-in precise measuring

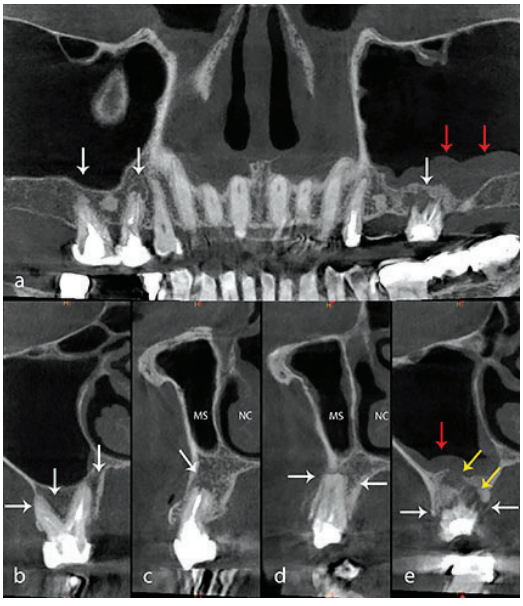

Fig. 1. Region of interest subjected to DI placement- teeth with different types of pathological processes: **a)** Panoramic view of teeth planned for replacement with DI; **b)** Tooth with dehiscence, furcation involvement and periapical lesion; **c)** Tooth with periapical lesion; **d)** Tooth expanded periodontal cleft; **e)** Tooth with periodontitis and alveolar resorption (marked with yellow arrows; with red arrow is marked pathological thickening of sinus mucosa).\

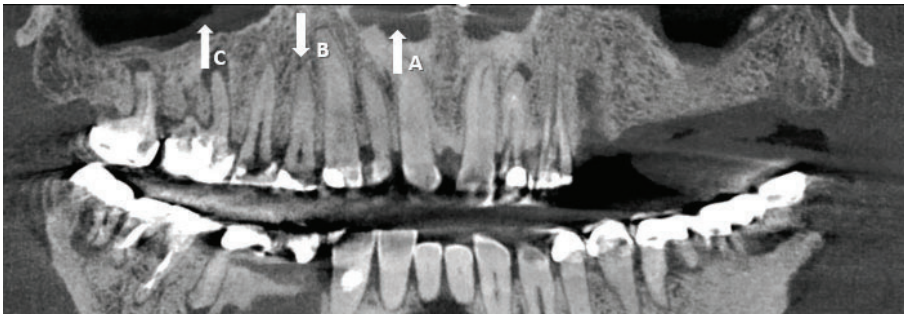

a)

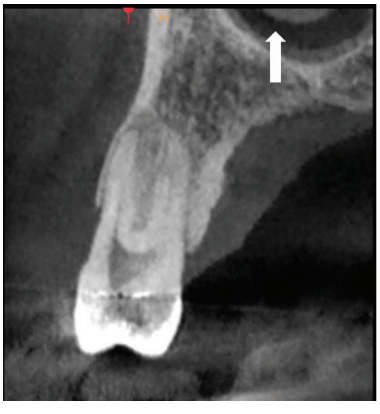

b)

Fig. 2. Relations between dental roots and the floor of the nasal cavity – "missing" data. **a)** Panoramic view – with arrows are marked the nasal cavity (A), a tooth, related to nasal cavity (B), maxillary sinus (C); **b)** Cross-sectional view of the same tooth – with arrow is marked the nasal cavity.

tool in a plane perpendicular to the tangent to the MSF above the root apeces (**Fig. 3a**) and/or corresponding to the planned positions of future DI. Implant positions were planned with the built-in implant library with 4,0 mm in diameter implant projections and positioning the implant shoulders to keep 1,5 mm distance from the necks of the adjacent teeth or 3,0 mm between the shoulders of neighboring implants.

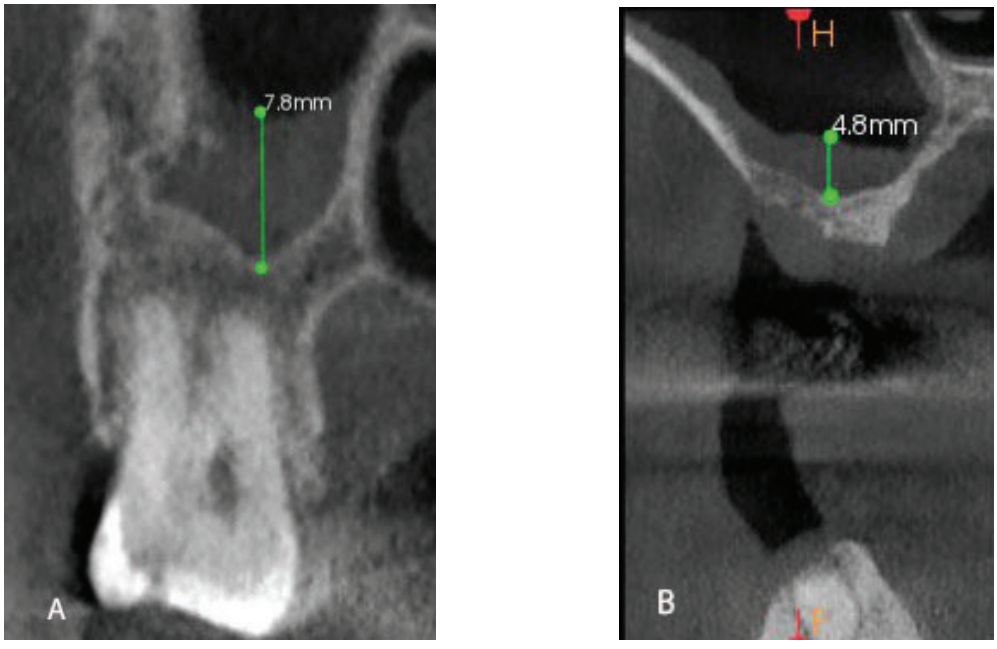

a) Dentate site b) Edentulous site

Fig. 3. Measurements of the thickness of sinus mucosa

Statistics: The data was processed with IBM SPSS Statistics for Windows, Version 19 (IBM CORP, Armonk, NY). For non-parametric data the Mann-Whitney test was used to determine differences in mucosal thickening between sexes and the Chi-square test to evaluate the association of mucosal thickening with age and the presence or absence of MSF pathology. p-value was calculated defined using Fisher'Exact test and statistical significance was set at the $p<0,05$ level. Categorical variables are presented by **n** and **%** values.

Results

The 3D-cone beam computed tomograms of 53 patients (32 women and 21 men; aged 18-72 years, mean 46,3±13,4) nessesitating sinus floor elevation and dental implant treatment were included in the study. The patients were divided into 5 age groups: group 1– under 18 years; group 2 – between 19 and 25 years; group 3 – between 26 and 40 years; group 4 – between 41 and 60 years; group 5 – over 60 years (**Fig. 4**). A total of 424 implant sites and maxillary premolars and molars subjected to replacement with DI were observed.

In reference to pathology the patients were divided in two groups – with and without periapical pathological changes.

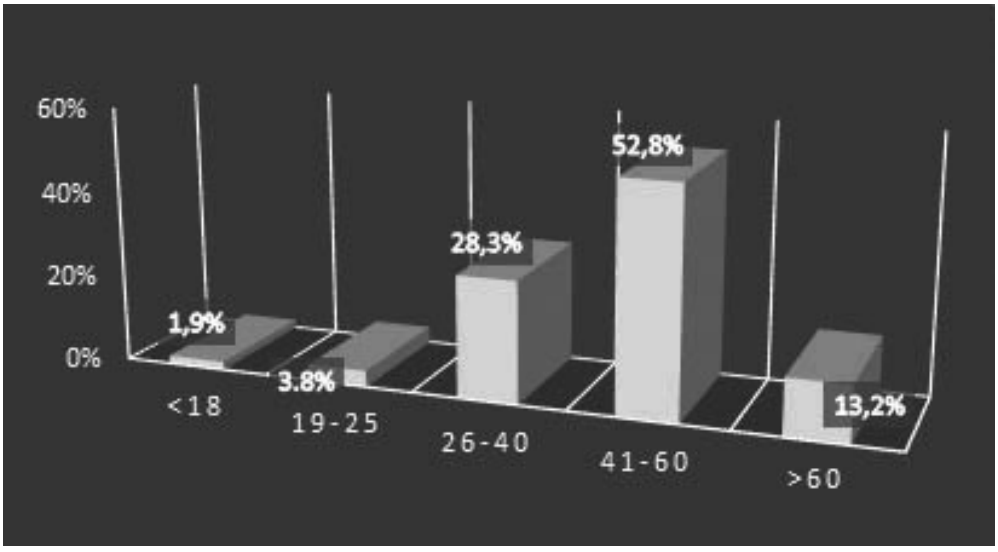

Fig. 4. Distribution of patients in age group

Patients were also divided in two groups according to incidence of mucosal thickening – with and without mucosal thickening.

The Schneiderian membrane thickness ranged between 0 and 15,90 mm, average 2,24±3,11 mm. Mucosal thickening was found in 92,5% of all patients and above 56,3% of all teeth (**Table 1**). The mucosal thickness was divided into 5 groups according to the classification of Goller-Bulut et al. [4]:

Table 1. Frequency of the mucosal thickness

		Frequency	**Percent %**	**Valid Percent %**
Thickness	**yes**	215	50,7%	56,3%
	no	167	39,4%	43,7%
	Total	382	90,1%	100,0%
Missing		42	9,9%	
Total		424	100,0%	

Class 1. 0 mm
Class 2. 0-2 mm
Class 3. 2-4 mm
Class 4. 4-10 mm
Class 5. More than 10 mm (**Fig. 5**)

Fifty nine precent of all cases were distributed in Group 1 and Group 2 with mucosal thickening up to 2 mm. In these pateints the MSFM was classified as normal (**Fig. 6**).

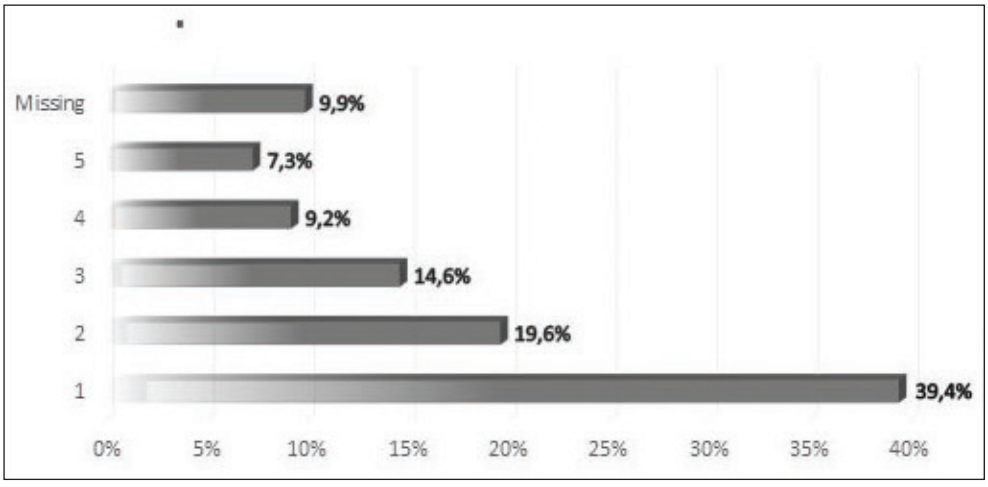

Fig. 5. Distribution of the mucosal thickness due to classes.

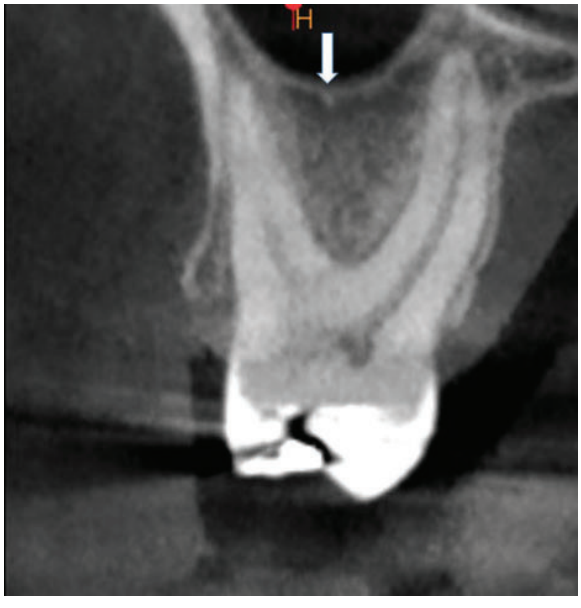

Fig. 6. Normal mucosa (marked with an arrow)

In 31,6% of the sites thickening was accompanied by periodontal lesions (**Table 2**), and in 69,40% of all cases having pathology the pathological changes presented with mucosal thickening (**Fig. 7**).

There was a significant association between the thickness and periodontal pathology, p=0,002 (**Table 3**).

The incidence of mucosal thickening increased significantly in the age over 26 years with highest percentage of frequency over 60 years (66,7%) (**Fig. 8**).

The association between the mucosal thickness and age is statistically significant, p<0,001 (**Table 4**).

Table 2. Relationship between the mucosal thickening and pathology

		Pathology	
		no	**yes**
Thickness	**yes**	68,4%	31,6%
	no	82,0%	18,0%
Total		74,3%	25,7%

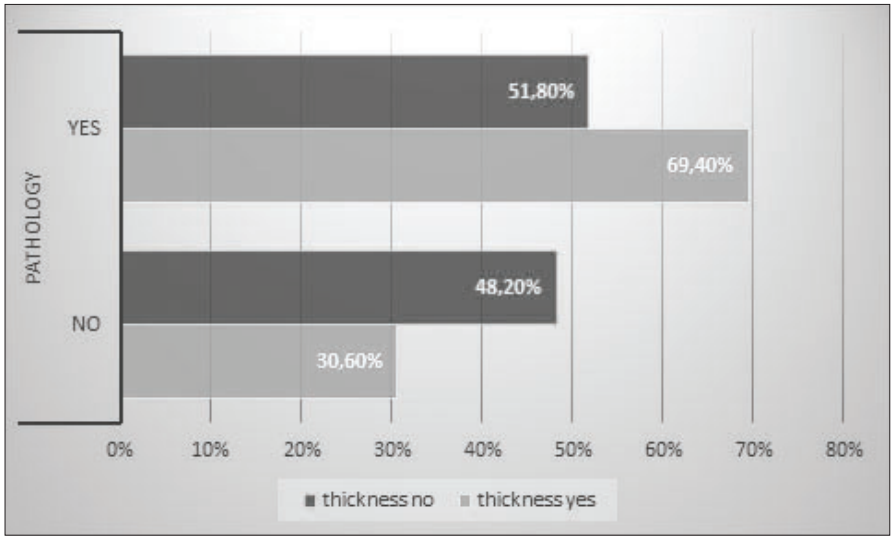

Fig. 7. Mucosal thickening in case of periapical pathology

Table 3. Association between the mucosal thickening and pathology

		Thickness
Pathology	**p value**	p=0,002
	N of Valid Cases	382

There is statistically significant difference between males and females (p=0,008). Thickness of the sinus mucosa is higher in males. The calculated average in males is 2,95±3,66 mm and in females – 1,81±2,64 mm (**Table 5**). But there is no statistically significant association between gender and incidence of mucosal thickening (p=0,07) (**Table 6**).

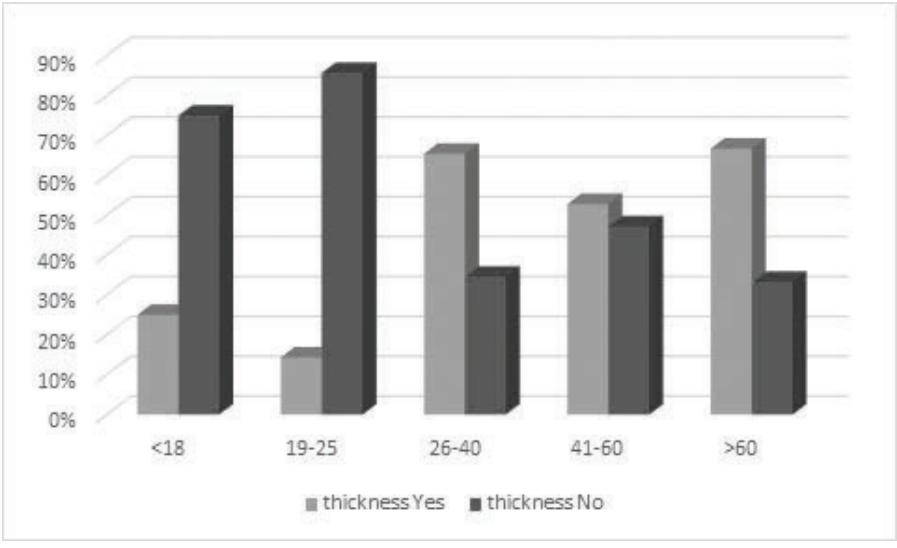

Fig. 8. Relationship between the mucosal thickness and age

Table 4. Association between the mucosal thickness and age

		Thickness
Age	**p value**	p<0,001
	N of Valid Cases	382

Table 5. Mucosal thickness according to the gender

Gender	N	Mean	SD	SEM	Median	IQR	Min	Max	p
M	143	2,95	3,66	0,31	1,60	3,90	0,00	12,40	p=0,008
F	239	1,81	2,64	0,17	1,10	2,60	0,00	15,90	

Table 6. Association between gender and incidence of mucosal thickening

			Gender		Assossiation
			M	**F**	**p**
Thickening of sinus mucosa	**no**	N	54	114	p=0,07
		%	32,1%	67,9%	
	yes	N	89	125	
		%	41,6%	58,4%	

Discussion

The Schneiderian membrane's thickening is with high percentage of occurrence. The proximity of the MS floor to the roots of the superior molars and premolars determines the influence of the periapical pathological processes on the sinus mucosa. The thickening of the mucous membrane predisposes to a greater incidence of its perforations in the MS floor elevation surgery [13].

The normal mucosa is about 1 mm thick and over than 2 mm [5] is considered pathological. Lu Y et al. [6] found that, for sinusitis, the thickness of the sinus membrane is greater than 2 mm. Therefore it is considered to be an indicator of presence of sinusitis and is assumed as a pathological condition. In the present study, mucosal thickening was found in more than the half of all measured positions. This frequency is significantly higher than the results reported by other studies [2, 4, 9] but is similar to the percentage found by Shanbhag S et al. [11] and Nurbakhsh B et al. [7].The measured average mucosal thickness is similar to the established thickness in previous studies [4, 5, 9].

Janner et al. [5] found that there is a correlation between sinus membrane thickening and the presence of sinus or periapical pathology. The results of the present study proved the significant relations between the mucosal thickness and the periapical pathological processes. Therefore the pathology appears as a main factor for thickening of Schneiderian membrane. These results are supported by other authors [1, 3, 4, 8, 10].

The frequency of the mucosal thickening increases with progressing of the age and there is significant association between these two indices. We found highest percentage of changes in the age group over 60 years and in the age over 25 years it increases considerably. These results are also confirmed by the study of Lu Yet al. [6] and Goller-Bulut et al. [4]. These researches determined highest percentage (51,2%) of mucosal thickening at the age of 41-60 years. The results are similar to those in our research (52,8%) for the same age group.

In their studies, Sheikhi et al. [12] and Goller-Bulut et al [4] proved that periapical pathological processes as well as greater incidence of mucosal thickening are more common in males. The results in our study confirm that the thickness of the sinus mucosa is higher in males, but there is no statistically significant association between the gender and incidence of mucosal thickening.

Conclusion

Within the limitation of this study it was show that the mucosal thickening of the MS's floor is a condition with high percentage of occurrence. The present study confirmed that there is significant correlation between thickness of the sinus mucosa and age. Periodontal pathology proved to be critical factor for thickening of the Schneiderian membrane. The preoperative evaluation of the mucosal thickness is essential for the correct planning in dental implant treatment and maxillary sinus elevation surgery.

R e f f e r e n c e s

1. **Bornstein, M., J. Wasmer, P. Sendi, S. F. Janner, D. Buser, T. von Arx.** Characteristics and dimensions of the Schneiderian membrane and apical bone in maxillary molars referred for apical surgery: a comparative radiographic analysis using limited cone beam computed tomography. – *J. Endod.,* **38**(1), 2012, 51-57.

2. **Carmeli, G., Z. Artzi, A. Kozlovsky, Y. Segev, R. Landsberg.** Antral computerized tomography pre-operative evaluation: relationship between mucosal thickening and maxillary sinus function. – *Clin. Oral Implants Res.*, **22**(1), 2011, 78-82.
3. **Dagassan-Berndt, D. C., N. U. Zitzmann, J. T. Lambrecht, R. Weiger, C. Walter.** Is the Schneiderian membrane thickness affected by periodontal disease? A cone beam computed tomography-based extended case series. – *J. Int. Acad. Periodontol.*, **15**(3),2013, 75-82.
4. **Goller-Bulut,D., A. Sekerci, E. Köse, Y. Sisman.**Cone beam computed tomographic analysis of maxillary premolars and molars to detect the relationship between periapical and marginal bone loss and mucosal thickness of maxillary sinus. – *Med. Oral Patol. Oral Cir. Bucal.*, **20(5)**, 2015, 572-579.
5. **Janner, S. F., M. D. Caversaccio, P. Dubach, P. Sendi, D. Buser, M. M. Bornstein.** Characteristics and dimensions of the Schneiderian membrane: A radiographic analysis using cone beam computed tomography in patients referred for dental implant surgery in the posterior maxilla. – *Clin. Oral Implants Res.*, **22**(12), 2011, 1446-1453.
6. **Lu, Y., Z. Liu, L. Zhang, X. Zhou, Q. Zheng, X. Duan, G. Zheng, H. Wang, D. Huang.** Associations between maxillary sinus mucosal thickening and apical periodontitis using cone-beam computed tomography scanning: a retrospective study. – *J. Endod.*, **38**, 2012, 1069-1074.
7. **Nurbakhsh, B., S. Friedman, G. V. Kulkarni, B. Basrani, E. Lam.** Resolution of maxillary sinus mucositis after endodontic treatment of maxillary teeth with apical periodontitis: a cone-beam computed tomography pilot study. – *J. Endod.*, **37**(11), 2011, 1504-1511.
8. **Phothikhun, S., S. Suphanantachat, V. Chuenchompoonut, K. Nisapakultorn.** Cone-beam computed tomographic evidence of the association between periodontal bone loss and mucosal thickening of the maxillary sinus. – *J. Periodontol.*, **83**, 2012, 557-564.
9. **Schneider, A. C., U. Brägger, P. Sendi, M. D. Caversaccio, D. Buser, M. M. Bornstein.** Characteristics and dimensions of the sinus membrane in patients referred for single-implant treatment in the posterior maxilla: A cone beam computed tomographic analysis. – *Int. J. Oral Maxillofac. Implants*, **28**(2), 2013, 587-596.
10. **Shahbazian, M., D. Xue, Y. Hu, J. Cleynenbreuge, R. Jacobs.** Spiral computed tomograpfy based maxillary sinus imaging in relation to tooth loss, implant placement and potential grafting procedure. – *J. Oral Maxillofac. Res.*, **1**, 2010, 1-7.
11. **Shanbhag, S., P. Karnik, P. Shirke, V. Shanbhag.** Cone-beam computed tomographic analysis of sinus membrane thickness, ostium patency, and residual ridge heights in the posterior maxilla: implications for sinus floor elevation. – *Clin. Oral Implants Res.*, **26**(6), 2014, 755-760.
12. **Sheikhi, M., N. J. Pozve, L. Khorrami.** Using cone beam computed tomography to detect the relationship between the periodontal bone loss and mucosal thickening of the maxillary sinus. – *Dent. Res. J. (Isfahan).*, **11**(4), 2014, 495-501.
13. **Wen, S. C., Y. H. Lin, Y. C. Yang, H. L. Wang.**The influence of sinus membrane thickness upon membrane perforation during transcrestal sinus lift procedure. – *Clin. Oral Implants Res.*, **26**(10), 2014, 1158-1164.

Institute of Experimental Morphology, Pathology and Anthropology with Museum
Bulgarian Anatomical Society

Acta morphologica et anthropologica, 26 (3-4)
Sofia ● 2019

Anatomical Variation of Corona Mortis

Konstantin Gospodinov, Ivan Maslarski

Department of Anatomy, Histology, Pathology and Forensic Medicine,
Medical Faculty, Sofia University "St. Kl. Ohridski", Sofia, Bulgaria

* Corresponding author e-mail: maslarsky@gmail.com

Corona mortis is the name of arterial or venous anastomosis between the external iliac (more commonly the inferior epigastric) and the obturator vessels. This structure, located on the posterior surface of the superior pubic ramus, is at risk during surgical approaches to the pelvis and acetabulum. The corona mortis ominous name, meaning "crown of death", reflects its significance in pelvic trauma, particularly pubic symphysis and superior pubic ramus fractures.The case reported was described after a routine dissection during anatomy class with students from the Department of Anatomy, Histology and Pathology at the Medical Faculty of the University of Sofia. The cadaver was a 82-year old woman and was fixed with the formaldehyde method. We encountered a variant obturator artery that originated from the external iliac artery. Each vascular variant in this area is important for description in order to confirm the classification of variations in order to prevent future errors in surgery.

Key words: corona mortis, pelvic fractures, inguinal hernioplasty, venous anastomosis

Introduction

The obturator artery, usually a branch of the internal iliac artery, is a relatively small blood vessel, which passes through the obturator foramen and blood supplies the adductor group of thigh muscles. If the obturator artery originates from the inferior epigastric artery, which typically arise from the external iliac artery, it is called corona mortis (CM). CM is also the name of arterial or venous anastomosis between the external iliac (more commonly the inferior epigastric) and the obturator vessels [1]. CM runs along the posterior aspect of the superior pubic ramus in the retropubic space (of Retzius) at a variable distance from the pubic symphysis (range 40-96 mm) [2]. The laceration of CM, meaning "crown of death", can cause a life-threatening bleeding in trauma cases or in scheduled operations [3, 5, 6, 7, 9, 10].

Materials and Methods

In the past eight years 30 embalmed human bodies were assessed, that included 18 males and 12 females. During dissections of the cadavers in routine anatomy exercises

the pelvic vessels were carefully dissected in searching of anastomoses between the obturator and external iliac vessels.

Results

The case described here was found after a routine dissection during the anatomy class with students from the Department of Anatomy, Histology and Pathology at the Medical Faculty of the University of Sofia. The cadaver was a 82-year old woman and was fixed with the formaldehyde method. During our dissection we encountered a variant obturator artery that originated from the external iliac artery (Fig. 1). Averagely, the division occurred approximately at around 9.8 cm from the beginning of the external iliac artery. The diameter of the last mentioned vessel has been measured at 5.5 mm and the aberrant obturator artery's diameter at 3.6 mm.

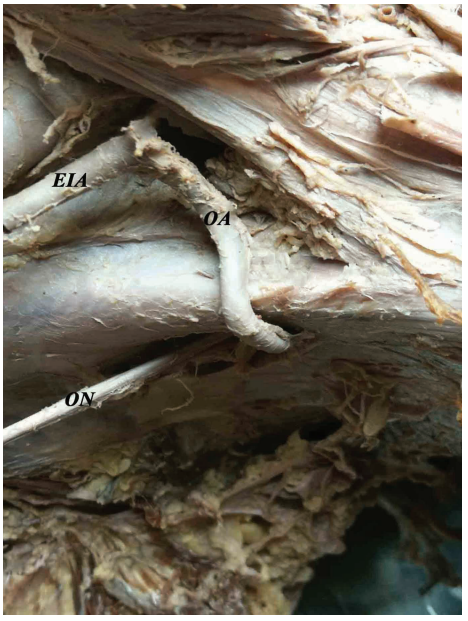

Fig. 1. Anatomical variation of corona mortis. EIA – external iliac artery; OA – obturator artery; ON – obturator nerve

Discussion

Although classic anatomical texts only describe arterial corona mortis, more recent studies described the presence of venous connections. Several terms have been linked to corona mortis, such as accessory obturator artery, accessory obturator vein, aberrant obturator artery and anomalous origin of obturator artery [9]. The term corona mortis is used exclusively to describe large anomalous connections, while small calibre anastomoses are believed to be anormal pattern [4]. The average reported diameter according to one series, which looked at both cadaveric, and patients specimen was of 2.6 mm (range 1.6 – 3.5 mm) [10]. Tornetta et al. [10] found vascular channels consistent with a corona mortis in 84%

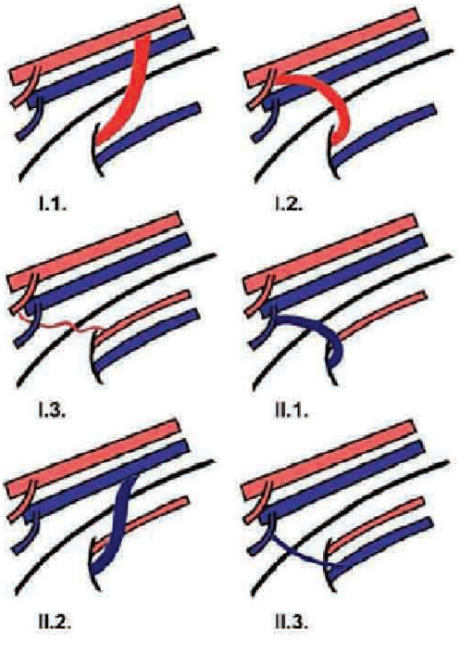

Fig. 2. Anatomic classification of corona mortis (after Rusu et al. 2010). I.1. Obturator artery originating from the external iliac artery; I.2. Obturator artery emerging from the inferior epigastric artery; I.3. Anastomosis of the obturator artery and inferior epigastric artery; II.1. Obturator vein going into the external iliac vein; II.2. Obturator vein fuse into the inferior epigastric vein; II.3. Venous anastomosis of the obturator vein and inferior epigastric vein.

of 50 fresh cadaveric hemipelvises [10]. In a cadaveric study, the arterial connection between the internal and external iliac systems was found in 0% of 54 hemipelves, in another to be 34% of 55 hemipelves and in an angiographic study to be 28.5% out of 98 hemipelves. Rusu et al. [8] classified corona mortis based on pattern and type of vessels involves. In their classification, there were three types of corona mortis: Type I-arterial; Type II-venous and Type III-a combined arteriovenous vascular network (Fig. 2). CM can be also located using computer tomography – a three-dimensional model of corona mortis can be constructed using contrasted enhanced CT scanning. This would be helpful in order to study the location and morphological patterns of the anastomosis and avoid further complications during surgical interventions.

During pelvic operation, corona mortis is accused to be a source of major bleeding in case of a surgical error. For instance, totally extraperitoneal inguinal hernioplasty can be associated with vascular complications especially during the fixation of the mesh [3, 5, 6, 7]. This structure is also at risk during surgical approaches to the pelvis and acetabulum [9, 10]. In addition, traumatic pelvic fractures are associated with a substantial mortality rate, with reported mortality rates up to 50%. In case of pelvic fracture, massive extraperitoneal hemorrhage may arise due to the presence of CM. So, endovascular specialists managing pelvic injury by coil embolization should keep CM in mind as a potential source of prolonged and dangerous hemorrhage [11]. In urinary surgery, when dealing with bladder suspension (stress incontinence), the use of tension-free vaginal tape (TVT-Secur method), may lead to severe bleeding in case of rupture of CM. Finally, the blood variations in the pelvic region are helpful in exercises for medical students during pelvic and lower limb dissections.

References

1. Atles, M., E. Kinaci, E. Kose. Corona mortis: in vivo anatomical knowledge and the risk of injury in totally extraperitoneal inguinal hernia repair. – *Hernia*, **20**, 2016, 659-65.

2. Berberoglu, M., A. Uz, M. M. Ozmen, M. C. Bozkurt, C. Erkuran, S. Taner, A. Tekin, I. Tekdemir. Corona mortis: an anatomic study in seven cadavers and an endoscopic study in 28 patients. – *Surg. Endosc.,* **15**, 2001, 72-75.

3. Dermanis, S., A. Lewis, A. Mansoor, M. Bircher. Corona mortis: an anatomical study with clinical implications in approaches to the pelvis and acetabulum. – *Clin. Anat.,* **20**, 2007, 433-439.

4. Gray, H. The blood-vascular system. *In: Anatomy, descriptive and surgical*. 15th Ed., Pennsylvania, Courage Books, 1901, 564-565.

5. Jensen, K., K. Spengel, L. Mica. Surgical relevance of corona mortis and clinical outcome in pelvic trauma. – *Austin J. Anat.,* **2**, 2015, 1029-1033.

6. Karakurt, L., I. Karaca, E. Yilmaz, O. Burma, E. Serin. Corona mortis: incidence and location. – *Arch. Orthop. Trauma Surg*., **2**, 2002, 163-164.

7. Piersol, G. A. *Human anatomy*. 9th Ed., Philadelphia, Lippincott, 1930, 813–814.

8. Rusu, M. C., R. Cergan, A. G. Motoc, R. Folescu, E. Pop. Anatomical considerations on the corona mortis. – *Surg. Radiol. Anat.,* **32**(5), 2010, 17-24.

9. Sanna, B., B. M. Henry, J. Vikse, B. Skinningsrud. The prevalence and morphology of the corona mortis (Crown of death): A meta-analysis with implications in abdominal wall and pelvic surgery. – *Injury*, **49**, 2018, 302-308.

10. Tornetta, P, N. Hochwald, R. Levine. Corona mortis. Incidence and location. – *Clin. Orthop. Relat. Res.,* **4**, 1996, 97-101.

11. Tosounidis, T., P.V. Giannoudis. Pelvic fractures presenting with haemodynamic instability: treatment options and outcomes. – *Clin. Orthop. Relat. Res.,* **329**, 1996, 97-101.

Institute of Experimental Morphology, Pathology and Anthropology with Museum
Bulgarian Anatomical Society

Acta morphologica et anthropologica, 26 (3-4)
Sofia ● 2019

Review Articles

Expression of Specific Mitochondrial Proteins in Germ Cells during Spermatogenesis

I. Ilieva, I. Sainova

Institute of Experimental Morphology, Pathology and Anthropology with Museum, BAS, Sofia, Bulgaria

* Corresponding author e-mail: iilieva@abv.bg

The current review is focused on the identity and function of some specific mitochondrial proteins/enzymes, their localization, gene expression, properties and activity, as well as their significance in the normal development of different germ cell populations during spermatogenesis and thus, sperm quality and fertility. Some of these molecules could be used as valuable markers for the diagnosis/prognosis of male infertility. Characterization of the potential of the mitochondrial proteins could open infinite possibilities for future research in the field of andrological clinical practice, but it may also be successfully applied for assisted reproduction procedures.

Key words: mitochondrial membrane proteins, mitochondrial genome/mtDNA, spermatogenesis, spermatozoa.

Introduction

Among the most widespread hypotheses is that the distant ancestors of mitochondria are bacteria from the α-proteobacterial lineage [23]. However, the events leading to endosymbiosis between bacteria (prokaryotes) and eukaryotes, and the subsequent evolution of mitochondria as integrated cellular organelles is not still clearly recognized [18]. The mitochondrion possesses its own independent genome (mtDNA) that shows substantial similarity to bacterial genomes. Its internal compartment, protein-rich liquid matrix, is bounded by the highly structured inner membrane, which in turn is bounded by the intermembrane space and the outer membrane. The inner mitochondrial membrane (IMM) possesses many cristae or invaginations, which increases the surface area available for energy production. The IMM is the site of ATP-production via oxidative

phosphorylation (OXPHOS), but it also controls the transport of ions and metabolites via transporters, as well as the oxidative status of the cell [50]. The mitochondrial membrane potential (MMP) presents the proton gradient formed by the flow of electrons along the electron transport chain (ETC), which is then used by the enzyme ATP-synthase for ATP synthesis. Decreased membrane potential (or depolarization) indicates mitochondrial damage and inability to meet energy demands of the cells, whereas hyperpolarization can lead to increased reactive oxygen species (ROS) production and cell damage [83].

The outer mitochondrial membrane (OMM) possesses non-specific protein pores, called porins, which are necessary for the passage of ions and other metabolites less than 10 kDa into the mitochondria (for example, those from VDACs family) [50]. The import of mitochondrial proteins synthesized in the cytoplasm and their homing to the appropriate compartments, membranes and correct membrane spaces/topologies involve multiple pathways and macromolecular mechanisms. Most proteins then pass through the translocase of the OMM to the intermembrane space, where divergent pathways sort them to the outer membrane, inner membrane and matrix, or trap them in the intermembrane space. Mitochondrial proteins (transcribed by the mtDNA) vary depending on both tissues and species. In humans, 615 distinct types of proteins have been identified from cardiac mitochondria [74], whereas in rats have been reported 940 proteins [86]. The mitochondrial proteome has been proposed as dynamically regulated [87]. In yeasts approximately 1000 proteins are available in these organelles, from which eight major constituents are coded and synthesized in the matrix. Roughly 25% of the mitochondrial proteins participate in the mitochondrial genome maintenance and/or expression at the inner surface of the IMM, providing 7 membrane proteins whose synthesis nucleates the assembly of three respiratory complexes.

Several mitochondria proteins are known to be synthesized in the germ cells during their morphological and functional development. These transit proteins, such as heat shock proteins (Hsp) hsp 60 and hsp 70, Lon protease, sulphydryl oxidase (SOx) and cytochrome c_t, serve as germ cell markers in different stages of spermatogenesis.

1. Heat shock proteins (HSPs). The physiological data indicate that their production is essential for cell survival and recovery from heat shock or other stress factors [54]. In the testis, these proteins (cytoplasm/ct-hsp90 and 70, mitochondria/mt-hsp60 and 70, nucleus/nuc-hsp70, etc.) are important for the heat protection of the germ cells at temperature above 35°C by binding unfolded or partially folded proteins to prevent their aggregation or irreversible thermal denaturation. The long-term rise in temperature above 35°C could lead to inevitable male infertility [63].

Mt-hsp60. Most of the hsp are also expressed by normal (non-stressed) cells, where they usually function as molecular chaperones. Mt-hsp60 is essential for the correct folding of the native structures of imported mitochondrial proteins followed by a stepwise process of ATP-dependent release. According to studies on human testicular biopsies, mt-hsp60 is located in the spermatogonia, early primary spermatocytes, Sertoli and Leydig cells in normal unaffected tubules [46]. The expression of this protein also correlates positively with the mitochondria type and activity, and it is increased in orthodox, but decreased in condensed and intermediate organelles [81]. The elevated mt-hsp60 levels in stages with proliferating spermatogonia suggest the existence of highly active mitochondrial protein import and assembly machinery, which is necessary for general new mitochondria for the daughter cells. Apparently, production of mt-hsp60 is required primarily during the initial steps of spermatogenesis, when most of the cell divisions occur, while its expression during the differentiation of spermatids and spermatozoa is not necessary. In general, the number of mt-hsp60 positive spermatogonia decreases with the loss of spermatogenic function, as with maturation arrest of spermatogenesis at the level of primary spermatocytes [81].

Hsp70-family. Numerous studies have been conducted to clarify the expression of hsp70 and its isoforms during different stages of the spermatogenesis, as well as during the proliferation, differentiation and maturation of germ cells [16, 35, 88]. Two specific forms are found in rodent testes: hsp70-2 (spermatocyte-specific) and HSC70t (testis-specific) proteins, expressed during spermatogenesis [16]. In the mouse testes, hsp70-2 is first detectable in pachytene spermatocytes and post-meiotic round spermatids (from day 17th postnatally), but in rat testes it is found in late pachytene spernatocytes, diakinesis and in steps 1-7 of spermiogenesis (day 22 postnatally) [35]. These data prove the active function of this chaperone during the differentiation of spermatocytes into spermatids [16]. According to other experiments, hsp70-2 participates in synaptonemal complex (SC) desynapsis, as a component of SC lateral elements [16], and it also interacts with the cyclin B-dependent CDC2 kinase, an enzyme with a key role in triggering the G2/M-phase transition during mitotic and meiotic cell cycle (in pachytene spermatocytes) [88]. Disruption of this formation could prevent G2-M-phases transition during meiosis and to cause increased apoptosis levels [16]. The chaperon protein mt-hsp70 from hsp70-family also plays an essential role during the import of mitochondrial matrix proteins. It is involved in a variety of different processes, as protein folding, disassembly of oligomeric protein complexes, delivery of proteins to proteases and translocation of polypeptides across the intracellular membranes.

In immunofluorescence experiments with application of monoclonal antibody to mt-hsp70, localization in the mitochondria of all germ cells up to pachytene spermatocytes has been shown [46]. Mt-hsp70, an element from the inner import complex, has been found to bind to the precursor sequence after the translocation of the N-terminal segment to avoid premature folding [29]. Most of the proteins (after cleavage of the pre-sequence by metalloproteinase) imported into the mitochondrial matrix are refolded directly by mt-hsp70 in co-operation with DnaJ (hsp40, Mdj-1) and GrpE (mt-hsp23) [29]. Besides the translocation of proteins across the mitochondrial inner membrane, mt-hsp70 also mediates the folding of these precursor molecules in the matrix. This fact correlates with the existence of two different populations of mt-hsp70: one bound to the inner membrane and the other one - soluble in the matrix [29]. Additionally, this protein supports the assembly of proteins, synthesized in the mitochondria to supra-molecular complexes. Another important function is that misfolded or denatured proteins exclusively bind to it and are then degraded by mitochondrial ATP-dependent protease (LON protease, PIM-1 protease) [80]. This is an indication that mt-hsp70 and Lon protease expression probably overlap in early primary spermatocytes [80].

2. Lon protease. Lon protease is a proteolytic ATP-dependent mitochondrial matrix enzyme involved in catabolic activity of the cells [70]. The appearance of this protein has been established in the orthodox mitochondria of leptotene spermatocytes, but it has also been determined as a specific marker for the intermediate type of the organelles (which are transit to condensed form), and have been found in zygotene and early pachytene spermatocytes [46]. The enzyme Lon protease has been connected with the protection of the mtDNA integrity, but also with degraded malfolded proteins in the mitochondrial matrix [46].

3. Cytochrome *c* (Cyc) and Cytochrome C oxidase (COX). Mitochondrial genome (mtDNA) encoded 13 polypeptides (subunits) that are included in the complexes of the ETC (except complex II), whereas the remainder of the subunits (totally 67) are encoded by the nucleus [72]. Mitochondrial polypeptides formed seven subunits of NADH CoQ reductase (complex I), cytochrome b (complex III); subunits I, II, and III of cytochrome C oxidase (complex IV), as well as subunits VI and VIII of the H+ ATPase [3]. Specific enzyme isoforms, such as cytochrome c_t and subunit VIb-2 of the cytochrome *c* oxidase

(COX), have also been found in the testicular mitochondria [27, 30], which underlines namely the increased mitochondrial activity in the germ cells. Cytochrome c (Cyc) has been determined as the only component of the mitochondrial respiratory chain known to express a testes-specific isoform in mammals. It is located in the intermembrane space of mitochondria.

Testicular cytochrome c_t isoform (T-Cyc) starts its expression in zygotene spermatocytes slowly taking the place of the somatic cytochrome c_s [27]. Cells in transition states during the sperm maturation have been found to express both Cyc isoforms [27]. Despite the equal function, indicated for both isoforms, cytochrome c_t isoform has shown higher pro-apoptotic activity and ability to catalyze the reduction of H_2O_2 three-fold faster than its counterpart in somatic cells. These findings strongly imply that T-Cyc can protect sperm from the damages caused by H_2O_2 [40]. The dramatically stronger apoptotic activity of T-Cyc might be important for the suicide activity of male germ cells, which has been considered as a physiological mechanism, necessary to regulate the number of sperm produced and to eliminate those with damaged DNA. Besides in primary spermatocytes, cytochrome c_t isoform has also been found in cell types, comprising the later stages of spermatogenesis, unlike the interstitial cells, Sertoli cells and spermatogonia, which have been established to contain the somatic form of cytochrome c_s [27, 40]. The appearance and action of T-Cyc during the stages of spermatogenesis correlates with the condensed and intermediate mitochondrial configuration, but also with the activated metabolism of germ cells.

Cytochrome C oxidase (COX) or Complex IV, has been characterized as the terminal enzyme in the electron transport chain located in the inner membrane of mitochondria. Its main function is connected with generation of ATP, required for the cellular living processes [26]. Complex IV consists of thirteen subunits, the genes for three of which (I, II and III) are localized within the mitochondrial genome, whilst the rest are located in nuclear chromosomes [71]. In the biochemical processes, COX receives electrons from each of the four cytochrome c molecules and transfers them to an oxygen molecule, converting molecular oxygen into two molecules of water, and in addition transporting four protons through the membrane (thus helping to establish proton electrochemical potential), used by the enzyme *ATP synthase* for ATP synthesize [21]. Importantly, COX has been shown to be the rate-limiting enzyme in the mitochondrial ETC [79], thus controlling respiration rate and the membrane potential [30].

Subunit Vib-2 of the COX is a testicular isoform of COX subunit Vib-2 (nuclear genome-encoded mitochondrial polypeptide). Similarly to cytochrome c, it is solely located in the intermembrane space [30]. Sampson and Alleyne (2001) have suggested a direct interaction between Cyc and COX subunits II, IV and VIb [60]. Later, Hüttemann et al. (2003) have reported that COX subunit VIb-2 (and/or VIb-1), analogically to *cytochrome c_t*, displays a testes-specific isoform in human, bull, rat and mouse, but unlike the rodent testes, where a lack of subunit VIb-1 has been established, both isoforms (VIb -2 and VIb-1) have been found to be transcribed in human testes. *In situ* hybridizations of testes sections has revealed VIb-2 transcripts in all testicular cell types (in human, rat and mouse), but within the seminiferous tubules, VIb-1 has shown stronger signals in the periphery than in the lumen. The authors have proposed any interaction between the isoforms of Cyc and VIb sub-unit in the context of sperm-specific energy requirements [30].

Messages for a specific stage-dependent change in the expression of another COX component – COXII (subunit II) during the spermatogenic cycle in testes from rat, have also been obtained [64]. According to this study, pachytene spermatocytes in seminiferous tubules at stage VII have shown the highest level of expression of mitochondrial COXII mRNA, which probably reflected the higher energy requirements of this cells entered the final stages of their meiosis [64].

4. Sulphydryl oxidase (*SOx*). Sulphydryl oxidase (*SOx*) is an enzyme that catalysis the oxidation of sulphydryl components (as glutathione, cysteine and thioglycerol), utilizing molecular oxygen as an electron acceptor, and newly formed disulphide bonds are thought to result in conformational changes of membrane proteins [67, 77]. This enzyme has first been established in mitochondria of condensed type in pachytene spermatocytes at stage I in the seminiferous epithelium of rat and hamster testes [36]. Compared to both rodent species (where SOx appears in a stage-dependent manner, presented mainly in pachytene spermatocytes and early spermatids), SOx distribution in the human testis is less dependent of the stage and not confined to certain germ cell types [8]. These authors investigated SOx in the seminiferous epithelium of human biopsy material in order to evaluate the possible value of this mitochondrial marker in the diagnosis of male infertility. In biopsies of oligozoospermic men (with hypospermatogenesis), the observed significant increase of SOx-labeled spermatogonia was associated with a significant decrease of sperm concentration in the ejaculate [8]. The assessed significant difference in the presence of SOx in human seminiferous epithelium has been established predominantly in A_{dark} spermatogonia (regarded as stem cell population) [52], whereas in A_{pale} spermatogonia only in stage V of spermatogenesis are significantly positive [6]. In the mature human testis moderate SOx amounts have been found in Leydig cells, whereas no SOx has been reported for the Sertoli cells and peritubular cells. In the mitochondria in leptotene (stages IV and V) and zygotene (stage VI) primary spermatocytes only moderate SOx amounts have been found, which are highest in pachytene spermatocytes of stages I-IV, but they decrease in stage V and are low during diakinesis and in secondary spermatocytes. The midpieces of the human spermatozoa are free of SOx-positive mitochondria, whereas in residual bodies small amounts of SOx are visible [6].

5. Other proteins, associated with mitochondrial function and sperm quality. Many mammalian genes expressing testis- or sperm-specific isoforms, have been identified [69]. Some of the examples are mitochondrial transcription factor A (Tfam) [37], lactate dehydrogenase (LDH-X), phosphoglycerate kinase 2 (pgk-2) [19] and etc. Genes, coding these proteins, are transcribed post-meiotically, but their expression is regulated at the translational level [10].

***Mitochondrial transcription factor A* (*mtTFA or Tfam*)**, particularly in humans (h-mtTFA), has been characterized as the focal point for regulation of human mtDNA copy number. It is a high mobility group- (HMG-) box protein that is a key activator of mitochondrial transcription [53]. It is likely that h-mtTFA also plays a role in the mtDNA replication since a transcript of a main mitochondrial promoter performs the role as an RNA primer for the initiation of this process [14]. Expression of germ cell-specific Tfam transcript isoforms occurs during spermatogenesis in mice and humans [37]. These Tfam transcript isoforms possess a structure that could prevent protein translation and their expression correlates with the down-regulation of the mitochondrial Tfam protein values. Unlike in mice, where the testis-specific mtTFA transcripts encode protein isoforms that are imported to the nucleus rather than into the mitochondria of spermatocytes and elongating spermatids, in humans the same transcripts predict a nuclear protein isoforms, and Western blot analysis identified only the mitochondrial form of h-mtTFA. Both mtTFA protein and mtDNA have been found to exhibit parallel gradients with high levels in undifferentiated male germ cells and low levels or absence in differentiated male germ cells, but on the other hand**,** testis-specific transcripts exhibit the opposite pattern. Thus probably in both humans and mice, these testis-specific mtTFA transcripts down-regulate mtTFA protein levels in mammalian mitochondria. In round and elongating spermatids this down-regulation coincides with

reduction of mtDNA copy number, which shows that Tfam is probably involved also in the regulation of the mtDNA amount during spermatogenesis [37].

Lactate dehydrogenase-X (LDH-X or C4). Enzyme lactate dehydrogenase catalyzes the interconversion of pyruvate and lactate with concomitant interconversion of NADH and NAD^+. It also converts pyruvate (the final product of glycolysis) to lactate in the absence or in short supply of oxygen, and it performs the reverse reaction during the Cori cycle in the liver. At high concentrations of lactate, the enzyme exhibits feedback inhibition, and the rate of conversion of pyruvate to lactate is decreased. It also catalyzes the dehydrogenation of 2-hydroxybutyrate and α-hydroxyvalerate, but these substrates are much poorer than lactate. In investigation on the catalytic properties and subcellular distribution of lacto-dehydrogenase isozyme-specific for testicles and spermatozoa (LDH X or C4) [9], isozyme X has been found to be located in the cytosol, plasma membrane and in the matrix of a special type of mitochondria, presented in spermatozoa of many mammalian species (including bovine and human) [9], which represents more than 80% of LDH activity in these germ cells [51]. Because of its multiple locations, LDH-C4 is a strong candidate for generation of NADH (by oxidation of lactate into pyruvate) in different sperm compartments. Because of its participation in the energetic metabolism of mature gametes, LDH-C4 has been associated with fertility [9], but also with capacitation in studies with bull and mouse spermatozoa [17]. Moreover, the low activity of LDH-C4 has been associated with partial or total reductions in sperm motility and concentration [11]. Spermatozoa from the bull (and other species) utilize pyruvate and lactate (generated by LDH-C4) as oxidative substrates for mitochondrial respiration and capacitation [51]. The cytosolic isoform of LDH-C4 converts lactate into pyruvate and NADH. The so received pyruvate can then enter into the mitochondria, where it converts into acetyl-CoA by pyruvate dehydrogenase and enters into the Krebs cycle to generate reducing equivalents that would be used in the respiratory chain for ATP-generation. The so produced ATP would be further used for energy purposes and to provide phosphate groups, necessary to support a series of phosphorylation events required during sperm capacitation [51]. The pyruvate not used for energy purposes could be converted into lactate by mitochondrial LDH-C4 and would diffuse to the cytosol to refeed the production of $O2^{\cdot}-$ by oxidase enzymes [51].

According to many studies, the five main types of LDH in mammals are formed by a random combination of two different subunits into tetramers. Each subunit (A and B) is a product of a distinct gene locus [25]. There is substantial evidence that the isoenzyme LDH-X of the male germ cell is also a tetramer, and that it is composed of a third polypeptide type (C), which is also encoded by a separate gene [25]. It is believed that this gene is active only during the primary stage of spermatocytes in the spermatogenic process and is inactive in all other cells of the organism [25], but the presence LDH-X in stem cells of spermatogonia has also been proposed [44]. The finding that LDH-X is indeed an unique protein of the sperm cell may be of considerable practical significance by providing a new approach to contraception in the male. Experimental studies are aimed to determine whether the interference with LDH-X synthesis and/or activity would affect the spermatogenesis or fertilization processes.

Protein kinases. The mitochondrial electron transport chain (ETC) in mammalian spermatozoa has been identified to undergo capacitation dependent tyrosine phosphorylation [34, 68]. The activity of enzyme protein kinase A (PKA) has been proposed as essential for sperm tyrosine phosphorylation, hyperactivation and acrosome reaction [38]. Other kinases implicated in capacitation are protein kinase C (PKC), protein kinase B (PKB/Akt), mitogen activated protein kinase (MAPK), phosphoinositide 3-kinase (PI3K) and extracellular signal regulated kinase (ERK1) [41]. Functional analysis of some of the tyrosine-containing phosphoproteins may predict

similar functions as observed for the proteins in somatic cells. However, the situation is complex for those proteins which are localized in the mitochondria of somatic cells, performing well known functions, but in spermatozoa they are non-canonical in their localization such as for example the enzymes dihydrolipoamide dehydrogenase (DLD), pyruvate dehydrogenase A2 (PDHA2) and glycerol-3-phosphate dehydrogenase 2 (GPD2) [34]. This is a problem in determination of the functional relevance of such proteins. The enzymes of the ETC such as phospholipid hydroperoxide glutathione peroxidase (PHGPx) and voltage-dependent anion channel (VDAC/mitochondrial porins) are localized into the mitochondrion while other enzymes as DLD, GPD2, and PDHA2 (pyruvate dehydrogenase/lipoamide alpha 2) are extra-mitochondrial [68]. Another important aspect is the ascertainment of identical localization of these mitochondrial proteins between human and animal spermatozoa before the establishment of corroboration between findings in both mammalian species [57].

***Phospholipid hydroperoxide glutathione peroxidase* (*PHGPx/GPx4*)** is a unique antioxidant enzyme, able to reduce directly phospholipid hydroperoxide in mammalian cells. This is in contrast with the most antioxidant enzymes, which cannot reduce intracellular phospholipid hydroperoxides directly [32]. Enzyme GPx4 belongs to the family of glutathione peroxidases (GPxs), it also contains selenocysteine at the active site and regulatory domain, which is successively oxidized and then reduced during the catalytic cycles. This selenoenzyme is distinct from cellular glutathione peroxidase (cGPx or GPx1, which has been characterized as "classical") on the basis of molecular weight, amino acid composition and substrate specificity [42]. Among the main structural differences is that PHGPx is a 20–22 kDa monomer protein, whereas the other GPxs are tetramers [78]. Furthermore, PHGPx is the only GPx that use phospholipid hydroperoxides as substrates, it is able to react with hydrogen peroxide and a wide range of lipid hydroperoxides, including with those derived from cholesterol and cholesteryl esters [43]. Kinetic data suggest that cGPx and PHGPx play different roles in hydroperoxide (H_2O_2) metabolism of cells, since in the aqueous phase the reaction of cGPX with peroxides is favored over that with PHGPx [42]. PHGPx, on the other hand, reduces specifically hydroperoxides in membranes [49] and mitochondria that are totally resistant to cGPx [66]. PHGPx has also been proved as able to reduce thymine hydroperoxide [7] and unlike the most GPxs, it can use a wide range of reducing substrates besides glutathione [5]. Similar to cGPx, replacing selenocysteine at the active site of PHGPx with cysteine significantly reduces its catalytic activity. It was also found that L-form of PHGPx (as opposed to its S-form) is mitochondrial PHGPx because it includes a signal peptide for transport to the mitochondria at the N-terminus of the protein, and as well as that the amount of PHGPx is significantly increased in the mitochondria, whileS-form PHGPx was highly expressed in nuclei, endoplasmic reticulum, and cytosol, but not in mitochondria [4].

Human spermatozoa contain high concentrations of polyunsaturated fatty acids (PUFAs), in particular, docosahexaenoic acid with six double bonds of the molecule [33], which makes the sperm vulnerable to peroxidative damage by the oxygen radicals. The ROS generation and sperm lipids peroxidation often have negative effects on the sperm motility [2], they could also cause midpiece abnormalities [58] and sperm-oocyte fusion, each one of which could disturb the fertilization in vertebrates [1]. In the mitochondria of spermatozoa, the main role of PHGPx is connected with the suppression of the effects of ROS that are produced by the mitochondrial respiratory chain [4]. PHGPx is distributed mainly in the midpiece of tails in the human ejaculated spermatozoa (and rat epididymal sperm), but it also presents in the sperm heads [24,31]. In the most somatic cells, hydrogen peroxide (H_2O_2) is reduced primarily by cytosolic glutathione peroxidase (cGPx) [2]. However, the reduction of H_2O_2 by PHGPx is similar

to that by cGPx in normal human spermatozoa. In rat epididymal spermatozoa, PHGPx represents at least 50% of the capsule material that embeds the helix of the sperm mitochondria. Studies have shown that infertile men with insufficient PHGPx expression in spermatozoa (PHGPx-defective gametes, according to WHO criteria) belong to the oligoasthenozoospermia group in which both number and motility of germ cells are significantly below normal and might, and therefore, could lead to serious impairment in fertilization and/or male fertility [31]. When the membrane potential in mitochondria of PHGPx-deficient spermatozoa is decreased compared to that of normal spermatozoa, the ultrastructure of the organelles (assessed by transmission electron microscopy) in the midpiece of PHGPx-defective gametes is extremely variable and abnormal compared to that of normal spermatozoa [31]. Hence, mitochondrial dysfunction could be a direct cause of the spermatozoa functions impairment. Furthermore, PHGPx has been suggested to play a role in the maturation of sperm during their passing through the epididymis by hydroperoxide metabolism and thiol oxidation in processes such as chromatin condensation, in addition to its role as an antioxidant. The oxidation of protamine thiols plays an important role in the sperm maturation. Pfeifer et al. identified a 34 kDa selenoprotein as a sperm-nucleus GPx (snGPx), a new type of PHGPx with a nuclear localization signal that is highly expressed in the nuclei of late spermatids [55]. Both PHGPx and snGPx might play an important role in the stabilization of condensed chromatin and the protection of sperm DNA against oxidation [55]. All of the sperm nuclei in selenium-deficient rats have shown abnormal DNA-condensation. PHGPx is expressed at high levels in rat, mouse and human testes [31, 59], but little is known about its regulation on the molecular level during the process of spermatogenesis. Expression of mitochondrial PHGPx in testes is induced after puberty [59] and an extraordinarily high rate of transcription of the gene for this enzyme, has been detected in the layer, containing late spermatocytes and round spermatids in human and other species [31]. A number of studies with knockout mice have suggested a close link of apoptosis with this regulation [56]. Mutations in genes for proteins from Bcl-2 family such as Bax, Bcl-2, Bcl-xL and Bcl-w lead to the accumulation of pre-meiotic germ cells and disruption of their differentiation [56]. Accelerated levels of apoptosis in germ cells during the formation of rat pachytene spermatocytes and spermatids have been found in experimentally-diminished PHGPx activity (via ethane dimethanesulphonate/EDS) and expression of mRNA for it in rat testis [84]. These results suggest a role of mitochondrial PHGPx as an anti-apoptotic factor in spermatogenesis and also suggest that failed induction of the mitochondrial PHGPx expression (as an anti-apoptotic factor) in late spermatocytes might have a major effect on spermatogenesis.

6. Paracrine mitochondrial maturation factors (PMMFs). The mechanisms that regulate or trigger the various steps of mitochondrial differentiation and metabolism during spermatogenesis are still not studied very well. Here belong different processes and factors as hormonal regulation, essential cell-to-cell interactions and testis-specific enzymes, which are of key importance about the regular testicular functions [20]. Both Sertoli and germ cells secrete various growth factors, which act on a local or paracrine manner [65]**.** Some of the proteins, produced by the Sertoli cells, affect the mitochondrial activity, and are generally determined as paracrine mitochondrial maturation factor (PMMF) [46]. Such a molecule is activin A, which acts on a paracrine fashion on primary spermatocytes.

Activin A. Activin A is the first Sertoli cell product that has been identified to influence differentiation of male meiotic germ cells. It is described as an inducer of the condensed form of mitochondria, contributing to the regulation of the germ cells' differentiation by the Sertoli cells. The mitochondria in spermatogonia change

their morphology as those cells proceed into the prophase of meiosis (primary as spermatocytes). The principal change is the dilatation of the intracristal space to give a vacuolated appearance of a mitochondrion. The role of activin A to control this change has been suggested [46]. This factor has been found to be included in many other functions, including cell proliferation, differentiation, apoptosis [13], metabolism, homeostasis, and immune response. Activin A stimulates both biosynthesis and secretion of pivotal for the spermatogenesis process hormones as follicle-stimulating hormone (FSH) and gonadotropin-releasing hormone, but it also activates the spermatogonia and preleptotene spermatocytes proliferation and regulates the pre-meiotic and meiotic DNA-synthesis as well. On the other hand, a possibility of this protein to inhibit FSH-stimulated conversion of the testosterone to estradiol has been proved. Besides the paracrine effect on spermatogenesis this molecule also has indicated the autocrine mechanism of action on the Sertoli cells. Receptors for activin A have been established besides in these cells, also on the spermatogonia, spermatocytes and spermatids. A cyclic activin secretion has been assessed in the seminiferous tubules – at stage VI, with maximal values at stage VIII of the seminiferous epithelium (in rat). Dibutyryl-cAMP stimulates the secretion of activin A in late stages VII and VIII. As a local mediator of activin A has been characterized interleukin-1alpha (IL-1α), also found to be produced by the Sertoli cells. Another important activator of activin is also the follistatin, which is secreted by the hypophysis, binds to activin and in this way acts as a local buffer.

Follistatin (FS). Follistatin also known as activin-binding protein is an autocrine glycoprotein that in humans is encoded by the *FST* gene [76], consisting of six exon. At least six forms of this protein are known: two basic forms - FS344 and FS317, as well as a few derivatives - FS315, FS300, FS288, etc. [73]. The main function of FS is connected with a complex influence on the activin functions. The finding of this factor in cells, different of spermatids at steps 1-11 (in rodents) suggests that activin A neutralization by follistatin probably accounts for the observed changes in mitochondrial morphology to the intermediated type in post-meiotic germ cells by activin neutralization (in fact, other factors have also been proposed to be involved). In rat testis, follistatin mRNA has been located in many germ cells. Small amounts of follistatin mRNA were found in preleptotene and leptotene primary spermatocytes but declined expression has been noted in the late leptotene and early zygotene stage (stages XI and XII), with slight activation in early pachytene and diplotene stage (stages VIII-XIV). FS levels remain relatively high in spermatids from step 1 to step 10, declined thereafter and from step 16 to step 19 have not been detected. This protein has also been found in Sertoli cells and endothelial cells, but no mRNA has been detected in Leydig cells [46].

Mitochondrial Ferritin (FtMt) is a ferroxidase enzyme (metal-binding protein) which is located within the mitochondria and in humans it is encoded by gene *FTMT*, mapped in chromosome 5q23.1 [39]. FtMt differs from the cytosolic H- (FtH) and L-ferritin chains (FtL) by the presence of a long amino acid N-terminal sequence for mitochondrial import, which is cleaved during the processing. After the protein is taken up by the mitochondria, it can be processed into a mature protein and to assemble functional ferritin shells. Although excess iron is stored primarily in the cytoplasm (by FtH and FtL chains), most of the metabolically active iron in the cells is processed in the mitochondria. Ferritin mitochondrial expression is restricted to specific cells and tissues such as testis and brain. This protein is highly expressed in human testis, particularly in the spermatocytes and Leydig cells [61], and it appears to correlate with the management of ATP burst in a short-time period. As the main function of FtMt in cell types, characterized by high metabolic activity and oxygen consumption (such as spermatocytes, Leydig cells, spermatozoa), is proposed its role in the protection of mitochondria against iron-dependent oxidative damage, not storing iron for the

synthesis of mitochondrial iron enzymes. A high metabolic rate seems to be a common characteristic of the cells positive on FtMt. For example, FtMt-rich Leydig cells in the testis require a high energy levels for the biosynthesis of hormones, and in the seminiferous tubules, the germinal cells with the highest FtMt content have been determined the spermatozoa in the latest phases of maturation in the tail region that lay freely in the lumen. Mitochondria of spermatozoa are highly active in order to meet the requirements for energy-dependent movement, but in few of them, imply very high local FtMt concentration. These cells are exposed to oxygen tension much higher than other internal cells, and thus, FtMt might offer further protection against oxidative damage. The epithelial cells in the epididymis are also rich of FtMt, similarly to all tissues, composed mainly of ciliated cells (which compose bronchus, Fallopian tubes, etc.) that use high energy for motility/transport or absorption/phagocytosis. This specific high-energy requirement is associated with the production of reactive oxygen species (ROS), derived by the Fenton reaction that involves the Fe(II)-catalyzed production of the highly toxic hydroxyl radicals from hydrogen peroxide. The expression of FtMt might be a cellular response to avoid this harmful reaction [61].

7. Proteins that control the mitochondrial fusion and fission. Frequent cycles of fusion and fission adapt the morphology of mitochondria (or of the cellular mitochondrial compartment) to the metabolic needs of the cells, optimizing their bioenergy capacity. The increased fusion activity leads to mitochondrial elongation, whereas the increased fission activity results in mitochondrial fragmentation [12]. The changes in balance between the rates of these two processes directly affect the wide range of mitochondrial length that can be observed in different cell types. The mechanisms of mitochondrial fusion and fission are regulated by proteolysis and post-translational modifications. Many gene products that control them have been identified and they belong to three core groups. These groups of proteins include mitofusins **(**mitochondrial membrane fusion/ MMF family**)**, OPA1 and Drp1. All of these molecules are GTP-hydrolyzing enzymes (GTPases) that belong to the dynamin family. Mitochondrial dynamics (mitochondrial morphology, distribution, fusion and fission) in different cells could be understood by the way in which these proteins regulate and bind to each other [85]. Mitochondrial fusion is particularly important in the respiratory-active cells. In this way, it allows the spreading of metabolites, enzymes and mitochondrial gene products throughout the entire mitochondrial compartment and serves to maintain the function of these organelles, but also to control the accumulation of mtDNA mutations during aging [82].

Mitofusins (Mfn1, Mfn2 and OPA1). Mfn1 and Mfn2 are specific membrane-anchored dynamin family members, which mediate fusion between mitochondrial outer membranes (in mammals) [62, 82]. Both proteins can act either together or separately during the mitochondrial fusion. It is not yet determined whether the two proteins perform the same function in the process or each of them performs separate functions. It is however shown that within the Mfn1–Mfn2 hetero-oligomeric complex, each molecule is functionally distinct [48, 15]. In addition, Mfn2 has been established to associate specifically with Bax and Bak (from Bcl-2 family), resulting in altered Mfn2 activity, indicating that probably the mitofusins possess unique functional characteristics. Cells lacking one or the other protein have reduced mitochondrial fusion possibility and show a mitochondria subpopulation with lacking mtDNA nucleoids. Such mtDNA defects lead to severe cellular injuries as accumulation of respiration-deficient mitochondria in the cells, with decreased cellular respiration respectively and leads to poor cell growth. Indeed, the expression levels of Mfn1 and Mfn2, as well as the mitochondrial morphology, vary according to the cell or tissue type [28]. These features suggest that control on the expression levels of each protein likely represents the most basic form

of regulation to alter mitochondrial dynamics in mammalian tissues. Mitochondrial fusion mediators differ between the outer and inner membranes of the organelle. Opa1 (belonging to dynamin-related protein family) is localized in the intermembrane space and it mediates the fusion between the inner mitochondrial membranes (in mammals) [45]. Fragmented mitochondria are frequently found in resting cells, and mitochondrial fission plays an important role in the removal of damaged organelles by autophagy. Some of the identified proteins that are involved in the mitochondrial fission are associated with mitochondrial diseases [85]. Mitochondrial fission has significant implications in stress response and apoptosis [12, 85].

***Proteins of mitochondrial fission* (*Drp1, Mff*)**. Drp1 controls the final part of the mitochondrial fission, pinching off the membrane stalk between two forming daughter mitochondria. This molecule functions by binding to other mitochondrial fission proteins. Several Drp1-binding proteins have been identified [22]: Mff (called mitochondrial fission factor) binds Drp1 and promotes mitochondrial fission [12]; FIS1 (mitochondrial fission 1 protein) is located on the outer mitochondrial membrane might attract Drp1 to sites of fission [12], but it might require association with another protein, such as MIEF1 (mitochondrial elongation factor 1) to promote mitochondrial division. In contrast, when bound to Drp1, MIEF1 might prevent mitochondrial fission and thus shift the balance towards the fusion of the organelles [12]. Mitochondrial fission occurs at the points of ER-mitochondrial associations that have been related with the formation of Drp1 complexes. On the other hand, the binding of the endoplasmic reticulum (ER) to mitochondria in the ER-mitochondrial association includes a protein complex with the presence of Mfn2. According to recent study, actin polymerization through ER-localized inverted formin 2 (INF2) is required for efficient mitochondrial fission in mammalian cells. This function of the protein has been assessed at the stage before Drp1 perform its function. In this way, the INF2-induced actin filaments may drive initial mitochondrial constriction, which allows Drp1-driven secondary constriction [48]. The activity of the key proteins of mitochondrial dynamics is regulated at multiple levels, including transcription and post-translational modification, and to respond directly to the mitochondria bioenergetic state.

Mitochondrial fission regulator 1 (Mtfr1) is associated with the mitochondrial inner membrane that induces mitochondrial fission [47]. In mice, it is encoded by a nuclear gene located on mouse chromosome 3 A3, containing a short chondrocyte protein with a polyproline region polyproline-rich region (CHPPR) [75]. In mice, the highest expression levels have been observed in pubertal and adult testis, particularly by the haploid spermatids and Leydig cells. In Mtfr1-deficient mice, the lack of this molecule is associated with markedly reduced levels of several proteins involved in the defense against oxidative stress (e.g., an enzyme glutathione peroxidase 3, specifically expressed in the endocrine compartment of the testis), probably due to the protective role of Mtfr1 on the male gonads against oxidative stress, which is important in the regulation of ROS-scavenging genes expression [47].

The activity of the key proteins of all mitochondrial dynamics is regulated at multiple levels, including transcription, post-translational modification and direct response to the bioenergetic state of mitochondria.

Conclusion

We make a review of the existing literature, covering the role of some specific mitochondrial proteins/enzymes from spermatogenesis to mature spermatozoa. Changes in mitochondrial proteins levels (or gene expression) are important to

elucidate mitochondrial function with respect to complex processes of the germ cell differentiation through the separate spermatogenesis stages. Clarification of functional identification and relevance of the proteins, especially in sperm capacitation, is a necessity for better understanding of the relationship between sperm protein tyrosine phosphorylation, hyperactivation, and acrosome reaction, and hence, in elucidating the molecular mechanisms of male infertility. Some of these enzymes could be used as specific biomarkers for the normal development of germ cell populations and for monitoring of sperm fertilization ability. Characterization of the potential of these proteins could open infinite possibilities for future studies in the field of andrological clinical practice, but it could also be applied successfully in the assisted reproduction practice.

References

1. **Aitken, R. J., J. S. Clarkson, S. Fishel**. Generation of reactive oxygen species, lipid peroxidation, and human sperm function. – *Biol. Reprod.,* **41**, 1989, 189–197.
2. **Alvarez, J. G., B. T. Storey.** Role of glutathione peroxidase in protecting mammalian spermatozoa from loss of motility caused by spontaneous lipid peroxidation. – *Gamete Res*., **23**, 1989, 77-90.
3. **Anderson, S., A. T. Bankier, B. G. Barrell, M. H. De Bruijn, A. R. Coulson, J. Drouin, I. C. Eperon, D. P. Nierlich, B. A. Roe, F. Sanger, P. H. Schreier, A. J. Smith, R. Staden, I. G. Young**. Sequence and organization of the human mitochondrial genome. – *Nature,* **290**, 1981, 457-465.
4. **Arai, M., H. Imai, T. Koumura, M. Yoshida, K. Emoto, M. Umeda, N. Chiba, Y. Nakagawa**. Mitochondrial phospholipid hydroperoxide glutathione peroxidase plays a major role in preventing oxidative injury to cells. – *J. Biol. Chem*., **274**, 1999, 4924- 4933.
5. **Aumann, K. D., N. Bedorf, R. Brigelius-Flohe, D. Schomburg, L. Flohe**. Glutathione peroxidase revisited simulation of the catalytic cycle by computer-assisted molecular modelling. – *Biomed. Environ. Sci*. **10**, 1997, 136-155.
6. **Aumüller, G., M. Bergmann, J. Seitz**. Immunohistochemical distribution of sulfhydryl oxidase in the human testis. – *Cell Tissue Res*., **266**, 199, 123-128.
7. **Bao, Y., P. Jemth, B. Mannervik, G. Williamson**. Reduction of thymine hydroperoxide by phospholipid hydroperoxide glutathione peroxidase and glutathione transferases. – *FEBS Lett*., **410**, 1997, 210-212.
8. **Bergmann, M., G. Aumüller, J. Seitz, E. Nieschlag**. Sulfhydryl oxidase immunoreactivity in seminiferous tubules of infertile men. – *Cell Tissue Res*., **267**, 1992, 209-214.
9. **Blanco A.** On the functional significance of LDH X. – *Johns Hopkins Med J.,* **146**(6), 1980, 231-235.
10. **Braun, R. E., R. R. Behringer, J. J. Peschon, R. L. Brinster, R. D. Palmiter**. Genetically haploid spermatids are phenotypically diploid. – *Nature*, **337**, 1989, 373-376.
11. **Burgos, G. N. M., C. Burgos, C. E. Coronel, A. B. de Camusso, T. Pigini T**, **A. Blanco**. Correlation of lactate dehydrogenase isoenzyme C4 activity with the count and motility of human spermatozoa. – *J. Reprod. Fertil.,* **55,** 1979, 107-111.
12. **Chan, D. C**. Mitochondrial fusion and fission in mammals. – *Ann. Rev. Cell Develop. Biol.*, **22**, 2006, 79-99.
13. **Chen, Y. G., Q. Wang, S. L. Lin, C. D. Chang, J. Chuang, J. Chung, S. Y. Ying**. Activin signaling and its role in regulation of cell proliferation, apoptosis, and carcinogenesis. – *Experim. Biol. Med.*, **231**(5), 2006, 534-544.
14. **Clayton, D. A**. Transcription and replication of mitochondrial DNA. - *Human Reprod*., **15**(2), 2000, 11–17.
15. **Detmer, S. A., D. C. Chan**. Complementation between mouse Mfn1 and Mfn2 protects mitochondrial fusion defects caused by CMT2A disease mutations. – *J. Cell Biol.*, **176** (4), 2007, 405-414.
16. **Dix, D. J., J. W. Allen, B. W. Collins**, **P. Poorman-Allen, C. Mori, D. R. Blizard, P. R. Brown, E. H. Goulding, B. D. Strong, E. M. Eddy.** HSP70-2 is required for desynapsis of synaptonemal complexes during meiotic prophase in juvenile and adult mouse spermatocytes. **–** *Development*, **124**, 1997, 4595-4603.

17. **Duan, C., E. Goldberg**. Inhibition of lactate dehydrogenase C4 (LDH-C4) blocks capacitation of mouse sperm *in vitro*. – *Cytogenet. Genome Res*., **103**, 2003, 352-359.
18. **Embley, T. M., W. Martin**. Eukaryotic evolution, changes and challenges. – *Nature*, **440**, 2006, 623-630.
19. **Erickson, L. D., S. A. Rizza, E. R. Bergert, M. C. Charlesworth, D. J. McCormick, R. J. Ryan**. Synthetic alpha-subunit peptides stimulate testosterone production in vitro by rat Leydig cells. – *Endocrinology*, **126**, 1990, 2555-2560.
20. **Erkkila, K., S. Kyttanen, M. Wikstrom, K. Taari, A. P. Hikim, R. S. Swerdloff, L. Dunkel**. Regulation of human male germ cell death by modulators of ATP production. – *Am. J. Physiol. Endocrinol. Metab*., **290**, 2006, 1145-1154.
21. **Ferguson-Miller, S., G. T. Babcock**. Heme/copper terminal oxidases. – *Chem. Rev*., **96**(7), 1996, 2889-2908.
22. **Frezza, C., S. Cipolat, O. M. de Brito, M. Micaroni, G. V. Benznoussenko, T. Rudka, D. Bartoli, R. S. Polishuck, N. N. Danial, B. De Strooper, L. Scorrano**. OPA1 controls apoptotic cristae remodeling independently from mitochondrial fusion. – *Cell,* **126**(1), 2006, 177-189.
23. **Gray, M. W., B. F. Lang, G. Burger**. Mitochondria of protists. – *Ann. Review Genetics,* **38,** 2004, 477-524.
24. **Godeas, C., F. Tramer, F. Micali, A. Roveri, M. Maiorino, C. Nisii, G. Sandri, E. Panfili**. Phospholipid hydroperoxide glutathione peroxidase (PHGPx) in rat testis nuclei is bound to chromatin. Biochem. – *Mol. Med*., **59,** 1996, 118-124.
25. **Goldberg, E**. Immunochemical specificity of lactate dehydrogenase-X. - *National Acad. Sci*., 68 (2), 1971, 349-352.
26. **Herrmann, J. M., M. W. Woellhaf, N. Bonnefoy**. Control of protein synthesis in yeast mitochondria: the concept of translational activators. – *Biochem. Biophys. Acta*, **1833** (2), 2013, 286-294.
27. **Hess, R. A., L. A. Miller, J. D. Kirby**, **E. Margoliash, E. Goldberg.** Immunoelectron microscopic localization of testicular and somatic cytochromes c in the seminiferous epithelium of the rat. – *Biol. Reprod*., **48**, 1993, 1299-1308.
28. **Hoppins, S., J. Horner, C. Song, J. M. McCaffery, J. Nunnari**. Mitochondrial outer and inner membrane fusion requires a modified carrier protein. – *J. Cell Biol*., **184**(4), 2009, 569-581.
29. **Horst, M., W. Oppliger, S. Rospert, H. J. Schönfeld, G. Schatz, A. Azem**. Sequential action of two hsp70 complexes during protein import into mitochondria. – *EMBO J*., **16**(8), 1997, 1842-1849.
30. **Hüttemann, M., S. Jaradat, L. I. Grossman.** Cytochrome c Oxidase of mammals contains a testes-specific isoform of subunit Vib – the counterpart to testes-specific cytochrome c? – *Mol. Reprod. Dev.,* **66**, 2003, 8-16.
31. **Imai, H., K. Suzuki, K. Ishizaka, S. Ichinose, H. Oshima, I. Okayasu, K. Emoto, M. Umeda, Y. Nakagawa**. Failure of the expression of phospholipid hydroperoxide glutathione peroxidase in the spermatozoa of human infertile males. – *Biol. Reprod.,* **64**, 2001, 674-683.
32. **Imai**, **H., Y. Nakagawa**. Biological significance of phospholipid hydroperoxide glutathione peroxidase (PHGPx, GPx4) in mammalian cells. – *Free Radic. Biol. & Med.*, **34(**2), 2003, 145-169.
33. **Kim, J. G., S. Parthasarathy**. Oxidation and the spermatozoa. – *Semin. Reprod. Endocrinol*., **16**, 1998, 235-239.
34. **Kota, V., V. M. Dhople, S. Shivaji**. Tyrosine phosphoproteome of hamster spermatozoa: role of glycerol-3-phosphate dehydrogenase 2 in sperm capacitation. – *Proteomics,* **9**, 2009, 1809-1826.
35. **Krawcyk, L. A., P. Mali, M. Parvinen**. Expression of a testis-specific hsp 70 gene-related RNA in difined stages of rate seminiferous epithelium. – *J. Cell. Biolol*., **107**, 1988, 1317-1323.
36. **Kumari, M., G. Aumüller, M. Bergmann, A. Meinhardt, J. Seitz**. Stage-dependent appearance of sulfhydryl oxidase during spermatogenesis in the testis of rat and hamster. – *Histochem.*, **94**(4), 1990, 365-371.
37. **Larsson, N. G., A. Oldfors, J. D. Garman, G. S. Barsh, D. A. Clayton**. Down-regulation of mitochondrial transcription factor A during spermatogenesis in humans. – *Human Mol. Genet*., **6**, 1997, 185-191.
38. **Lefièvre, L., K. N. Jha, E. de Lamirande, P. E. Visconti, C. Gagnon**. Activation of protein kinase A during human sperm capacitation and acrosome reaction. – *J. Androl*., **23**, 2002, 709-716.
39. **Levi, S., B. Corsi, M. Bosisio, R. Invernizzi, A. Volz, D. Sanford, P. Arosio, J. Drysdale**. A human mitochondrial ferritin encoded by an intronless gene. – *J. Biol. Chem*. **276** (27), 2001, 24437-24440.

40. **Liu, Z., H. Lin, S. Ye, Q-y. Liu, Z. Meng, C-m. Zhang, Y. Xia, E. Margoliash, Z. Rao, X. J. Liu**. Remarkably high activities of testicular cytochrome c in destroying reactive oxygen species and in triggering apoptosis. – *Proc. Natl. Acad. Sci. USA*, **103**, 2006, 8965-8970.
41. **Luconi, M., F. Marra, L. Gandini, E. Filimberti, A. Lenzi, G. Forti, E. Baldi**. Phosphatidylinositol 3-kinase inhibition enhances human sperm motility. – *Human Reprod*. **16**, 2001, 1931-1937.
42. **Maiorino**, **M., F. F. Chu, F. Ursini, K. J. A. Davies, J. H. Doroshow, R. S. Esworth**. Phospholipid hydroperoxide glutathione peroxidase is the 18-kDa selenoprotein expressed in human tumor cell lines. – *J. Biol. Chem*., **266**(12), 1991a, 7728-7732.
43. **Maiorino, M., J. P. Thomas, A. W. Girotti, F. Ursini**. Reactivity of phospholipid hydroperoxide glutathione peroxidase with membrane and lipoprotein lipid hydroperoxides. – *Free Radic. Res. Commun*., **12–13**, 1991, 131-135.
44. **McKee, R.W.**, **E. Longstaff, A. L. Latner**. Lactate dehydrogenase in human testes. – *Clinica Chimica Acta*, **39**(1), 1972, 221-227
45. **Meeusen, S., R. DeVay, J. Block, A. Cassidy-Stone, S. Wayson, J. M. McCaffery, J. Nunnari.** Mitochondrial inner-membrane fusion and crista maintenance requires the dynamin-related GTPase Mgm1. – *Cell,* **127**, 2006, 383-395.
46. **Meinhardt, A., B. Wilhelm, J. Seitz**. Expression of mitochondrial marker proteins during spermatogenesis. – *Human Reprod. Update*, **5**, 1999, 108-119.
47. **Monticone, M., L. Tonachini, S. Tavella, P. Degan, R. Biticchi, F. Palombi, R. Puglisi, C. Boitani, R. Cancedda, P. Castagnola**. Impaired expression of genes coding for reactive oxygen species scavenging enzymes in testes of Mtfr1/Chppr-deficient mice. – *Reproduction*, **134**, 2007, 483-492.
48. **Naotada I., E. Yuka, M. Katsuyoshi**. Mitofusin 1 and 2 play distinct roles in mitochondrial fusion reactions via GTPase activity. – *J. Cell Sci*. **117** (Pt 26), 2004, 6535-6546.
49. **Nomura, K., H. Imai, T. Koumura, Y. Nakagawa**. Involvement of mitochondrial phospholipid hydroperoxide glutathione peroxidase as an antiapoptotic factor. – *Biol. Signals Recept.*, **10**, 2001, 81-92.
50. **Nicholls, D.G., S. J. Ferguson**. *Bioenergetics* (Ed. D. Nicholls), 4th edition, San Diego, Academic Press, , 2013, 288.
51. **O'Flaherty, C.** Redox regulation of mammalian sperm capacitation. – *Asian J. Androl*., **17,** 2015, 583-590.
52. **Paniagua, R., J. Codesal, M. Nistal**, **M. C. Rodrigues, L. Santamaria**. Quantification of cell types throughout the cycle of the human seminiferous epithelium and their DNA content. A new approach to the spermatogonial stem cell in man. – *Anat. Embryol*., **176**, 1987, 225-230.
53. **Parisi, M. A., D. A. Clayton**. Similarity of human mitochondrial transcription factor 1 to high mobility group proteins. – *Science*, **252**, 1991, 965-969.
54. **Parsell, D.A., S. Lindquis**. The function of heat shock proteins in stress tolerance: reactivation of damaged proteins. – *Annu. Rev. Genet*., **27**, 1993, 437-496.
55. **Pfeifer, H., M. Conrad, D. Roethlein, A. Kyriakopoulos, M. Brielmeier, G.W. Bornkamm, D. Behne**. Identification of a specific sperm nuclei selenoenzyme necessary for protamine thiol cross-linking during sperm maturation. – *FASEB J.,* **15**, 2001, 1236-1238.
56. **Print, C. G., K. L. Loveland, L. Gibson, T. Meehan, A. Stylianou, N. Wreford, D. de Kretser, D. Metcalf, F. Kontgen, J. M. Adams, S. Cory**. Apoptosis regulator bcl-w is essential for spermatogenesis but appears otherwise redundant. – *Proc. Natl. Acad. Sci. USA*, **95,** 1998, 12424-12431.
57. **Rajender, S., P. Rahul, A. A. Mahdi**. Mitochondria, spermatogenesis and male infertility. – *Mitochondrion*, **10**, 2010, 419-428.
58. **Rao, B., J. C. Soufir, M. Martin, G. David**. Lipid peroxidation in human spermatozoa as related to midpiece abnormalities and motility. – *Gamete Res*., **24**, 1989, 127-134.
59. **Roveri, A., A. Casasco, M. Maiorino, P. Dalan, A. Calligaro, F. Ursini**. Phospholipid hydroperoxide glutathione peroxidase of rat testis. Gonadotropin dependence and immunocytochemical identification. – *J. Biol. Chem*., **267**, 1992, 6142-6146.
60. **Sampson, V., T. Alleyne**. Cytochrome c/cytochrome c oxidase interaction. Direct structural evidence for conformational changes during enzyme turnover. – *Eur. J. Biochem*., **268**(24), 2001, 6534-6544.
61. **Santambrogio, P., G. Biasiotto, F. Sanvito, S. Olivieri, P. Arosio, S. Levi.** Mitochondrial ferritin expression in adult mouse tissues. – *J. Histochem. & Cytochem*., **55**(11), 2007, 1129-1137.

62. **Santel, A., M. T. Fuller**. Control of mitochondrial morphology by a human mitofusin. – *J. Cell Sci*., **114,** 2001, 867-874.
63. **Sarge, K. D., K. E. Cullen**. Regulation of hsp expression during rodent spermatogenesis. – *Cell. Mol. Life Sci.,* **53**, 1997, 191-197.
64. **Saunders, P. T., M. R. Millar, A. P. West, R. M. Sharpe**. Mitochondrial cytochrome C oxidase II messenger ribonucleic acid is expressed in pachytene spermatocytes at high levels and in a stage-dependent manner during spermatogenesis in the rat. – *Biol. Reprod*., **48**, 1993, 57-67.
65. **Schlatt, S., A. Meinhardt, E. Nieschlag.** Paracrine regulation of cellular interactions in the testis: factors in search of a function. – *Eur. J. Endocrinol*., **137**, 1997, 107-117.
66. **Schneider, M., H. Förster, A. Boersma, A. Seiler, H. Wehnes, F. Sinowatz, C. Neumüller, M. J. Deutsch, A. Walch, M.H. de Angelis, W. Wurst, F. Ursini, A. Roveri, M. Maleszewski, M. Maiorino, M. Conrad**. Mitochondrial glutathione peroxidase 4 disruption causes male infertility. – *FASEB J*., **23**(9), 2009, 3233-3242.
67. **Seitz, J., J. Moëbius, M. Bergmann, A. Meinhardt**. Mitochondrial differentiation during meiosis of male germ cells. – *Int. J. Androl*., **18**, 1995, 7-11.
68. **Shivaji, S., V. Kota, A. B. Siva**. The role of mitochondrial proteins in sperm capacitation. – *J. Reprod. Immunol*., **83**, 2009, 14-18.
69. **Siva, A. B., D. B. Kameshwari, V. Singh, K. Pavani, C.S. Sundaram, N. Rangaraj, M. Deendayal, S. Shivaji**. Proteomics-based study on asthenozoospermia: differential expression of proteasome alpha complex. – *Mol. Hum. Reprod*., **16**, 2010, 452-462.
70. **Sonezaki, S., K. Okita, T. Oba**, **Y. Ishii, A. Kondo, Y. Kato**. Protein substrates and heat shock reduce the DNA-binding ability of *Escherichia coli* Lon protease. – *Appl. Microbiol. Biotechnol*., **44**, 1995, 484-488.
71. **Soto, I. C., F. Fontanesi, J. Liu, A. Barrientos**. Biogenesis and assembly of eukaryotic cytochrome c oxidase catalytic core. – *Biochim. Biophys. Acta*, **1817** (6), 2012, 883-897.
72. **St. John, J. C., D. Sakkas, C. L. Barratt**. A role for mitochondrial DNA and sperm survival. – *J. Androl*., **21**, 2000, 189-199.
73. **Sugino, K., N. Kurosawa, T. Nakamura**, **K. Takio, S. Shimasaki, N. Ling, K. Titani, H. Sugino**. Molecular heterogeneity of follistatin, an activing-binding protein. – *J. Biol. Chem*., **268**, 1993, 15579-15587.
74. **Taylor, S .W., E. Fahy, B. Zhang, G. M. Glenn, D. E. Warnock, S. Wiley, A. N. Murphy, S. P. Gaucher, R. A. Capaldi, B. W. Gibson, S. S. Ghosh**. Characterization of the human heart mitochondrial proteome. – *Nature Biotechnol*., **21**(3), 2003, 281-286.
75. **Tonachini, L., M. Monticone, C. Puri, C. Tacchetti, P. Pinton, R. Rizzuto, R. Cancedda, S. Tavella, P. Castagnola**. Chondrocyte protein with a polyproline region (CHPPR) is a novel mitochondrial protein and promotes mitochondrial fission. – *J. Cell. Physiol.,* **201**, 2004, 470-482.
76. **Tortoriello, D. V., Y. Sidis, D. A. Holtzman, W. E. Holmes, A. L. Schneyer**. Human follistatin-related protein: a structural homologue of follistatin with nuclear localization. – *Endocrinol.*, **142** (8), 2001, 3426-3434.
77. **Tury, A., G. Mairet-Coello, A. Esnard-Fève, B. Benayoun, P. Y. Risold, B. Griffond**. Cell-specific localization of the sulphydryl oxidase QSOX in rat peripheral tissues. - *Cell Tissue Res.*, **323**(1), 2006, 91-103.
78. **Ursini, F., M. Maiorino, C. Gregolin**. The selenoenzyme phospholipid hydroperoxide glutahtione peroxidase. – *Biochim. Biophys. Acta*, **839**, 1985, 62-70.
79. **Villani, G., G. Attardi.** In vivo control of respiration by cytochrome c oxidase in human cells. – *Free Radic. Biol. Med*., **29**, 2000, 202-210.
80. **Wagner, I., H. Arlt, L. van Dyck**, **T. Langer, W. Neupert.** Molecular chaperone cooperate with P1M1 protease in the degradation of misfolded proteins in mitochondria. – *EMBO J*., **1**, 1994, 5135-5145.
81. **Werner, A., A**. **Meinhardt, J. Seitz, M. Bergmann.** Distribution of heat shock protein 60 immunoreactivity in testes of infertile men. - *Cell Tissue Res*., **288**, 1997, 539-544.
82. **Westermann, B**. Bioenergetic role of mitochondrial fusion and fission. – *Biochim. Biophys. Acta*, **1817,** 2012, 1833–1838.
83. **Wolken, G. G., E. A. Arriaga.** Simultaneous measurement of individual mitochondrial membrane potential and electrophoretic mobility by capillary electrophoresis. - *Anal Chem*., **86**(9), 2014, 4217-1426.

84. **Woolveridge, I., M. de Boer-Brouwer, M. F. Taylor, K. J. Teerds, F. C. Wu, I. D. Morris**. Apoptosis in the rat spermatogenic epithelium following androgen withdrawal: changes in apoptosis-related genes. – *Biol. Reprod.,* **60**, 1999, 461-470.
85. **Youle, R. J., A. M. van der Bliek**. Mitochondrial Fission, Fusion, and Stress. – *Sci*., **337**(6098), 2012, 1062-1066.
86. **Zhang, J., X. Li, M. Mueller, Y. Wang, C. Zong, N. Deng, T. M. Vondriska, D.A. Liem, J. I. Yang, P. Korge, H. Honda, J. N. Weiss, R. Apweiler, P. Ping**. Systematic characterization of the murine mitochondrial proteome using functionally validated cardiac mitochondria. – Proteomics, **8**(8), 2008, 1564-1575
87. **Zhang, J., D. A. Liem, M. Mueller, Y. Wang, C. Zong, N. Deng, T. M. Vondriska, P. Korge, O. Drews, W. R. Maclellan, H. Honda, J. N. Weiss, R. Apweiler, P. Ping**. Altered proteome biology of cardiac mitochondria under stress conditions. – J.Proteome Research., **7**(6), 2008, 2204-2214.
88. **Zhu, D., D. J. Dix, E. M. Eddy.** HSP70-2 is required for CDC2 kinase activity in meiosis I of mouse spermatocytes**.** – *Development*, **124**, 1997, 3007-3014.

Institute of Experimental Morphology, Pathology and Anthropology with Museum
Bulgarian Anatomical Society

Acta morphologica et anthropologica, 26 (3-4)
Sofia ● 2019

Carnivores and Ixodid Ticks as Important Factors in the Emergence, Circulation and Distribution of Dangerous Infections

Delka Salkova[1], Mariana Panayotova-Pencheva[1], Vassilena Dakova[1], Zuzana Hurnikova[2], Martina Miterpakova[2], Bronislava Víchová[2], Viktória Čabanová[2]*

[1] *Institute of Experimental Morphology, Pathology and Anthropology with Museum, Bulgarian Academy of Sciences, Sofia, Bulgaria*
[2] *Institute of Parasitology, Slovak Academy of Sciences, Košice, Slovakia*

* Corresponding author e-mail: dsalkova@abv.bg

Climate changes in the recent years led to a sharp rise in the tick population and an increase in the number of animals and people with tick-borne infections. The domestic and wild carnivores, especially the dogs, have a huge role for the distribution of ticks in certain areas. It is necessary to carry out a complex fight against the ticks and diseases transmitted by them, which includes systematic control of the tick population in a given area, as well as in-depth studies on their contamination with particular pathogens, especially those causing zoonoses. This work presents a short review on the recent research on the role of carnivores and ticks in the emergence, circulation and distribution of some dangerous viral, bacterial and parasitic infections.

Key words: carnivores, ixodid ticks, vector-borne diseases

Currently, multiple anthropogenic stressors - including climate change, habitat loss and fragmentation, urbanization, agricultural expansion and intensification, together with other changes in the use of water and land resources - are directly or indirectly impacting all species on earth. Such processes have also significant impacts on host-parasite interactions and infectious disease risks.

Due to the global changes (climate, economic and social) in the last decades, emergence of new serious infectious diseases of different etiology as well as spreading of already known diseases can be seen. Carnivores and ticks (Arachnida: Ixodidae) are involved in the emergence and circulation of some viral, bacterial and parasitic infections, including such with zoonotic character. In most of the cases, they appear to be the leading biotic factors in the distribution of these infections.

The aim of the present work is to perform a short overview on the studies conducted in this area in the recent years.

Prevalence data for tick-borne pathogens have been used to assess the risk for human health by Christova et al. [3]. The presence and identity of *Borrelia burgdorferi* sensu lato, *Ehrlichia*, *Anaplasma*, and *Rickettsia* species in Bulgarian *Ixodes ricinus* ticks and in non-*Ixodes* ticks from Turkey and Albania have been determined by polymerase chain reaction (PCR) and reverse line blot hybridization. In the adult Bulgarian ticks, the prevalence of *Borrelia burgdorferi* sensu lato infection has been approximately 40%, while *Borrelia afzelii* has been the predominant species, representing more than half of all *Borrelia*-positive ticks. *Ehrlichia* and *Anaplasma* species have been detected in 35% of the adult *Ixodes ricinus* ticks and in 10% of the nymphs. Sequence analysis of PCR products reacting with the *Anaplasma phagocytophila* probe has revealed a 16S rRNA gene identical to that of the *Anaplasma phagocytophila* prototype strain. *Ehrlichia* and *Anaplasma* species have been found in approximately 7% of the non-*Ixodes* ticks. Sequence analysis of some of these samples has revealed the presence of *Anaplasma ovis*, *Ehrlichia canis*, and species closely resembling *Ehrlichia chaffeensis*. About half of all adult ticks examined and approximately 20% of all nymphs have been infected with *Rickettsia* species. In *Ixodes ricinus* ticks, *Rickettsia helvetica* and *Rickettsia* species designated as IRS3 have been found in high prevalence. *Rickettsia conorii* has been found in virtually all non-*Ixodes* tick species from Albania and Turkey. The results of this study have shown that many tick-borne diseases are most probably endemic in the Balkan area. Furthermore, the results have suggested that there is a considerable chance for simultaneous transmission of tick-borne pathogens to human beings.

The occurrence of hard tick species (Acari: Ixodidae) infesting domestic dogs in Hungary has been studied by Földvári and Farkas [4]. Forty veterinary clinics from a wide geographical area have been asked to collect hard ticks from dogs and to complete a questionnaire. In total, 25 veterinary clinics submitted 900 ticks from 310 dogs. Intensity of infestation has ranged from one to 78 per dog. The most preferred sites of tick attachment in decreasing order have been head, neck and legs. The majority of ticks (91.7%) have been adults, which have been identified to species level, the others have been nymphs. Six species have been found: *Dermacentor reticulatus* (48.9%), *Ixodes ricinus* (43.2%), *Ixodes canisuga* (5.6%), *Haemaphysalis concinna* (2%) and there has been one specimen of both *Dermacentor marginatus* and *Ixodes hexagonus*. Single species infestation with *I. ricinus* or *D. reticulatus* has been found on 145 (46.8%) and 120 animals (38.7%), respectively. Mixed infestation caused by these two species has been detected on 24 dogs (7.7%). *I. canisuga* and *H. concinna* have been found on seven and five dogs, respectively. *D. reticulatus* and *I. ricinus* have been collected almost throughout the year, except for a single month. The activity peaks have been in spring and in autumn for both species. Based on clinical signs, canine babesiosis has been diagnosed by the veterinarians in 66 (21.3%) tick infested dogs. These dogs have been more frequently infested with *D. reticulatus* than the others.

A broad-range 16S rRNA gene PCR assay followed by partial sequencing of the 16S rRNA gene has been used for the detection of members of the family *Anaplasmataceae* in ticks in North Africa [12]. A total of 418 questing *Ixodes ricinus* ticks collected in Tunisia and Morocco, as well as 188 *Rhipicephalus* ticks from dogs and 52 *Hyalomma* ticks from bovines in Tunisia, have been included in this study. Of 324 adult *I. ricinus* ticks, 16.3% have been positive for *Ehrlichia* spp., whereas only 3.4% and 2.8% of nymphs and larvae, respectively, have been positive. A large heterogeneity has been observed in the nucleotide sequences. Partial sequences identical to that of the agent of human granulocytic ehrlichiosis (HGE) have been detected in *I. ricinus* and *Hyalomma detritum*, whereas partial sequences identical to that of *Anaplasma platys* have been detected in *Rhipicephalus sanguineus*. However, variants of *Anaplasma*, provisionally designated *Anaplasma*-like, have been predominant in the *I. ricinus* tick population in

Maghreb. Otherwise, two variants of the genus *Ehrlichia* have been detected in *I. ricinus* and *H. detritum*. Surprisingly, a variant of *Wolbachia pipientis* has been evidenced from *I. ricinus* in Morocco. These results have emphasized the potential risk of tick bites for human and animal populations in North Africa.

From 2000 to 2004, ticks have been collected by dragging a blanket in four habitat areas in the Netherlands: dunes, heather, forest, and a city park [14]. Tick densities have been calculated, and infection with *Borrelia burgdorferi* and *Anaplasma* and *Ehrlichia* species has been investigated by reverse line blot analysis. The lowest tick density has been observed in the heather area (1 to 8/100 m^2). In the oak forest and city park, the tick densities have ranged from 26 to 45/100 m^2. The highest tick density has been found in the dune area (139 to 551/100 m^2). The infection rates varied significantly for the four study areas and years, ranging from 0.8 to 11. 5% for *Borrelia* spp. and 1 to 16% for *Ehrlichia* or *Anaplasma* (*Ehrlichia/Anaplasma*) spp. *Borrelia* infection rates have been highest in the dunes, followed by the forest, city park, and heather area. In contrast, *Ehrlichia/Anaplasma* has been found most often in the forest and less often in the city park. The following *Borrelia* species have been found: *Borrelia* sensu lato strains not identified to the species level (2.5%), *B. afzelii* (2.5%), *B. valaisiana* (0.9%), *B. burgdorferi* sensu stricto (0.13%), and *B. garinii* (0.13%). *Borrelia lusitaniae*, *Ehrlichia chaffeensis*, and the human granylocytic anaplasmosis agent have not been detected. About 1.6% of the ticks have been infected with both *Borrelia* and *Ehrlichia/Anaplasma*, which has been higher than the frequency predicted from the individual infection rates, suggesting hosts with multiple infections or a possible selective advantage of coinfection.

A population of 731 naturally exposed pet dogs examined at a private practice in Baxter, Minnesota, an area endemic for Lyme disease and anaplasmosis, has been tested by serological and molecular methods for evidence of exposure to or infection with selected vector-borne pathogens [8]. Serum samples have been tested by enzyme-linked immunosorbent assay (ELISA) for *Aanaplasma phagocytophilum*, *Borrelia burgdorferi*, and *Ehrlichia canis* antibodies and for *Dirofilaria immitis* antigen. Blood samples from 273 dogs have been also analyzed by polymerase chain reaction (PCR) for *Anaplasma* and *Ehrlichia* species DNA. Based on the owner history and the attending veterinarian‘s physical examination findings, dogs exhibiting illness compatible with anaplasmosis or borreliosis have been considered clinical cases, and their results have been compared to the healthy dog population. Antibodies to only *A. phagocytophilum* have been detected in 217 (29%) dogs; to only *B. burgdorferi*, in 80 (11%) dogs; and seroreactivity to both organisms, in 188 (25%) dogs. Of 89 suspected cases of canine anaplasmosis or borreliosis, *A. phagocytophilum* or *B. burgdorferi* antibodies have been detected in 22 dogs (25%) and 8 dogs (9%) respectively, whereas antibodies to both organisms have been found in 38 dogs (43%). *Ehrlichia canis* antibodies and *D. immitis* antigen have been each detected in 11 (1.5%) dogs. *Anaplasma phagocytophilum* DNA has been amplified from 7 of 222 (3%) healthy dogs and 19 of 51 (37%) clinical cases. Seroreactivity to both *A. phagocytophilum* and *B. burgdorferi* has been detected more frequently in suspected cases of anaplasmosis and/or borreliosis than seroreactivity to either organism alone. Based on PCR testing, *A. phagocytophilum* DNA has been more prevalent in suspected cases of anaplasmosis or borreliosis than in healthy dogs from the same region.

Sobrino et al. [13] have studied the ixodid tick fauna of wild carnivores in Peninsular Spain and the environmental factors driving the risk of wild carnivores to be parasitized by ixodid ticks. They have hypothesized that the adaptation of tick species to differing climatic conditions may be reflected in a similar parasitization risk of wild carnivores by ticks between bioclimatic regions in the study area. To test this, the authors have surveyed ixodid ticks in wild carnivores in oceanic, continental-Mediterranean, and

thermo-Mediterranean bioclimatic regions of Peninsular Spain. They have analyzed the influence of environmental factors on the risk of wild carnivores to be parasitized by ticks by performing logistic regression models. Models have been separately performed for exophilic and endophilic ticks under the expected differing influence of environmental conditions on their life cycle. Differences in the composition of the tick community parasitizing wild carnivores from different bioclimatic regions have been found. Modelling results partially have confirmed the null hypothesis because bioclimatic region has not been a relevant factor influencing the risk of wild carnivores to be parasitized by exophilic ticks. Bioclimatic region has been however a factor driving the risk of wild carnivores to be parasitized by endophilic ticks. The authors consider that Spanish wild carnivores are hosts to a relevant number of tick species, some of them being potential vectors of pathogens causing serious animal and human diseases.

In all, 1146 serum samples have been tested in Romania by SNAP® 4Dx® (IDEXX Laboratories, Inc., Westbrook, ME) for *Anaplasma phagocytophilum, Borrelia burgdorferi,* and *Ehrlichia canis* antibodies, and for *Dirofilaria immitis* antigen [9]. The correlation between positive cases and their geographic distribution, as well as potential risk factors (age, sex, breed, type of dog, habitat, and prophylactic treatments) have been evaluated. Overall, 129 dogs (11.3%) have been serologically-positive to one or more of the tested pathogens. The seroprevalence for the four infectious agents has been: *A. phagocytophilum* 5.5% (63/1146), *D. immitis* 3.3% (38/1146), *E. canis* 2.1% (24/1146), and *B. burgdorferi* 0.5% (6/1146). Co-infection with *E. canis* and *A. phagocytophilum* has been registered in 2 dogs (0.2%). According to the authors the geographical distribution of the seropositive cases suggests clustered foci in southern regions and in the western part of the country for *D. immitis*, and in the southeastern region (Constanţa County) for *E. canis*. *A. phagocytophilum* and *B. burgdorferi* have showed a homogenous distribution, with a tendency for Lyme-positive samples to concentrate in central Romania. Associated risk factor with infection has been the type of dog (stray dogs have been at risk being positive for *D. immitis,* shelter dogs for *E. canis*, and hunting dogs for *B. burgdorferi*). The prevalence of *D. immitis* has been significantly higher in males and in dogs older than 2 years.

A South African strain of *Ehrlichia canis* has been isolated and used to infect a laboratory-bred Beagle dog [5]. *Rhipicephalus sanguineus* nymphs, fed on this dog, moulted to adult ticks with infection rates of *E. canis* between 12% and 19% have been used in a series of *in vivo* and *in vitro* experiments. Five groups of 6 dogs have been challenged with the infected *R. sanguineus* ticks, which have been removed 24 h, 12 h, 6 h or 3 h after the ticks had been released onto the dogs. The animals have been monitored for fever and thrombocytopenia and have been considered infected if they became serologically positive for *E. canis* antibodies as well as PCR positive for *E. canis* DNA. Seven dogs have been infected with *E. canis* in the following groups: Group 1 (24 h tick challenge) 1 out of 6; Group 2 (12 h) 1 of 6; Group 3 (6 h) 2 of 6; Group 4 (6 h) 2 of 6 and Group 5 (3 h) 1 out of 6. Six of those 7 infected dogs have developed fever and a significant thrombocytopenia. One dog has not shown any symptoms, but has been found PCR positive on several occasions. Five additional dogs have been PCR positive on one test sample only but have not been considered infected because they have not developed any specific *E. canis* antibodies. *In vitro*, *R. sanguineus* ticks have attached and fed on bovine blood through silicone membranes with attachment rates up to 72.5% after 24 h increasing to 84.2% at 72 h. The ticks have transmitted *E. canis* as soon as 8 h post application as demonstrated by *E. canis* DNA found in the nutritive blood medium. The authors have concluded that transmission of *E. canis* by *R. sanguineus* ticks starts within a few hours after attachment, which is earlier than previously thought. These findings underpin the need for acaricides to

provide either a repellent, an anti-attachment and/or a rapid killing effect against ticks in order to decrease the risk of transmission of *E. canis*.

To monitor the emergence of thermophilic, Mediterranean ixodid tick species and tick-borne pathogens in Southern Hungary, 348 ticks have been collected from shepherd dogs, red foxes and golden jackals during the summer of 2011 [6]. Golden jackals have shared tick species with both the dog and the red fox in the region. *Dermacentor* nymphs have been collected exclusively from dogs, and the sequence identification of these ticks has indicated that dogs are preferred hosts of both *D. reticulatus* and *D. marginatus* nymphs, unlike previously reported. Subadults of three ixodid species have been selected for reverse line blot hybridisation (RLB) analysis to screen their vector potential for 40 pathogens/groups. Results have been negative for *Anaplasma*, *Babesia* and *Theileria* spp. Investigation of *D. marginatus* nymphs has revealed the presence of *Ehrlichia canis*, *Rickettsia massiliae* and *Borrelia afzelii* for the first time in this tick species. *Ehrlichia canis* has been also newly detected in *Ixodes canisuga* larvae from red foxes. The authors have concluded: in absence of transovarial transmission in ticks this implies that Eurasian red foxes may play a reservoir role in the epidemiology of canine ehrlichiosis.

Blood samples and ticks have been collected from 100 shepherd dogs, 12 hunting dogs and 14 stray dogs in southern Hungary, in order to screen them for the presence of *Hepatozoon* spp. by PCR [7]. Out of 126 blood samples, 33 have been positive (26%). Significantly more shepherd dogs (31%) have been infected, than hunting (8%) and stray dogs (7%). Three genotypes of *Hepatozoon canis* have been identified by sequencing, differing from each other in up to six nucleotides in the amplified portion of their 18S rRNA gene. In *Dermacentor marginatus* larvae/nymphs and *Dermacentor reticulatus* nymphs, *H. canis* has been present only if they had been collected from PCR-positive dogs, and the genotypes have been identical in the ticks and their hosts. However, two *Haemaphysalis concinna* nymphs removed from a PCR-negative dog have been found positive for *H. canis*, and the genotype detected in specimens of this tick species differed from that in the blood of their respective hosts. These results have indicated that canine hepatozoonosis may be highly prevalent in regions where *Rhipicephalus sanguineus* is considered to be non-endemic. Canine hepatozoonosis has been significantly more prevalent west of the Danube river (where higher densities of red fox and golden jackal populations occur), suggesting a role of wild carnivores in its epidemiology.

In order to detect *Ehrlichia* spp. in cats from the central-western region of Brazil, blood and serum samples have been collected from a regional population of 212 individuals originated from the cities of Cuiabá and Várzea Grande [1]. These animals have been tested by the Immunofluorescence Assay (IFA) and the Polymerase Chain Reaction (PCR) designed to amplify a 409 bp fragment of the *dsb* gene. The results obtained have shown that 88 (41.5%) of the cats have been seropositive by IFA and 20 (9.4%) of the cats have been positive by PCR.

The seroprevalence of important canine vector-borne diseases (CVBDs) in 167 dogs from Central-Southern Bulgaria (Stara Zagora), with special emphasis on hitherto uninvestigated babesiosis and angiostrongylosis, on poorly investigated Lyme borreliosis and canine granulocytic anaplasmosis, and on the potentially zoonotic dirofilariosis and leishmaniosis has been determined by Pantchev et al. [11]. Relatively high prevalence rates have been documented for anti-*Babesia canis* antibodies, *Dirofilaria immitis* antigen (16.2 %; 27/167 each), anti-*Ehrlichia canis* (21 %; 35/167) and anti-*Anaplasma phagocytophilum* antibodies (30.5 – 46.1 %; 51 – 77/167), while *Borrelia burgdorferi* seroprevalence has been low (2.4 %; 4/167). All samples have been negative for *Leishmania infantum* antibodies and *Angiostrongylus*

vasorum antigen and antibodies. In total, 64.7 % (108/167) of the samples indicated infection or exposure to at least one agent and a high proportion of dual infections (39.8 %; 43/108) has been demonstrated. Multiple infections with up to four different organisms have been also detected. The authors underline the importance of CVBDs and especially of co-infections which could influence the clinical outcome in dogs.

Çetinkaya et al. [2] have studied the presence of *Anaplasma* spp., and *Ehrlichia* spp. in dogs and ticks in the Thrace region of Turkey. A total of 400 blood samples and 912 ticks have been collected from dogs living in shelters that are located in four cities (Istanbul, Edirne, Tekirdag and Kirklareli) of the Thrace Region. Blood and buffy coat smears have been prepared for microscopic examination. Hematologic and serologic analyses have been performed using cell counter and commercial Snap3Dx test kit, respectively. Eight hundred fifty of collected ticks have been classified as *Rhipicephalus* sanguineus, 33 as *Rhipicephalus turanicus* and 29 as *Ixodes ricinus*. After DNA extraction from blood samples and pooled ticks (127 tick pools, in total), nested PCR has been performed to detect the DNA of *Anaplasma* spp., and *Ehrlichia* spp. The seroprevalence of Ehrlichia *canis* has been 27.25% (109) by Snap3Dx test and the total molecular positivity has been 11.75% (47) in dog blood samples and 21.25% (27) in tick pools by nested PCR. The frequencies of the infected blood samples with *E. canis*, *Anaplasma phagocytophilum* and *Anaplasma platys* have been detected as 6%, 4% and 6%, respectively. *E. canis* and *A. platys* have been detected in *R. sanguineus* pools with a ratio of 15.75% and 0.7%, respectively. In addition, *A. platys* has been also detected in *R. turanicus* pools (0.7%). *A. phagocytophilum* has been found only in *I. ricinus* pools (3.93%). Morulae of three species have been detected in buffy coat and blood smears. While anemia has been observed in dogs infected with *E. canis* and co-infected (with one or more species), thrombocytopenia has been observed only in co-infected dogs. Based on the results of the tests used in this study, the authors have recommended the combined use of serologic, molecular, cytologic, hematologic analyses and physical examination of tick exposure for an accurate diagnosis of ehrlichiosis and anaplasmosis.

Nader et al. [10] have performed a study intended to detect the prevalence of tick-borne bacteria and parasites occurring at the Black Sea in Bulgaria and evaluate the zoonotic potential of the tick-borne pathogens transmitted by ticks in this area. In total, cDNA from 1541 ticks (*Dermacentor* spp., *Haemaphysalis* spp., *Hyalomma* spp., *Ixodes* spp. and *Rhipicephalus* spp.) collected in Bulgaria by flagging method or from hosts has been tested in pools of ten individuals each for *Anaplasma phagocytophilum*, *Babesia* spp., *Borrelia burgdorferi* (s.l.), *Rickettsia* spp. and "Candidatus Neoehrlichia mikurensis" via conventional and quantitative real-time PCR. Subsequently, samples from positive pools have been tested individually and a randomized selection of positive PCR samples has been purified, sequenced, and analyzed. Altogether, 23.2% of ticks have been infected with at least one of the tested pathogens. The highest infection levels have been noted in nymphs (32.3%) and females (27.5%). Very high prevalence has been detected for *Rickettsia* spp. (48.3%), followed by *A. phagocytophilum* (6.2%), *Borrelia burgdorferi* (s.l.) (1.7%), *Babesia* spp. (0.4%) and "Ca. Neoehrlichia mikurensis" (0.1%). Co-infections have been found in 2.5% of the tested ticks (mainly *Ixodes* spp.). Sequencing has revealed the presence of *Rickettsia monacensis*, *R. helvetica*, and *R. aeschlimannii*, *Babesia microti* and *B. caballi*, and *Theileria buffeli* and *Borrelia afzelli*. This study has shown very high prevalence of zoonotic *Rickettsia* spp. in ticks from Bulgaria and moderate to low prevalence for all other pathogens tested. The authors underline the risk that the tick bites from this area could lead to *Rickettsia* infection in humans and mammals.

As a conclusion to the current literature review, the following can be said:

In the recent years carnivores and ixodid ticks most often have been studied as factors in the development of the ehrlichiosis, anaplasmosis and borreliosis. Fewer studies in this connection have been conducted to babesiosis, dirofilariosis, and ricketsiosis. Single ones have about leishmaniasis, *Hepatozoon* sp. and "Candidatus Neoehrlichia mikurensis".

The studies carried out have mainly aimed at determining the species composition of ticks that have been spread and affected carnivores in different geographic areas, as well as the pathogens identified in them. For this purpose both standard immunological methods of investigation and newer molecular-biological methods are used.

Conclusions

Here are some conclusions from different research:

● The combined use of serologic, molecular, cytologic, hematologic analyses and physical examination of tick exposure for an accurate diagnosis of vector-borne diseases is recommended.

● The percentige of the ticks, infected with both *Borrelia* and *Ehrlichia/Anaplasma*, which has been higher than the frequency predicted from the individual infection rates, suggesting hosts with multiple infections or a possible selective advantage of coinfection.

● Multiple infections with up to four different organisms have been also detected in other study. Its authors underline the importance of Canine vector-borne diseases and especially of co-infections which could influence the clinical outcome in dogs.

● Wild carnivores are hosts to a relevant number of tick species, some of them being potential vectors of pathogens causing serious animal and human diseases.

● Eurasian red foxes may play a reservoir role in the epidemiology of canine ehrlichiosis.

● Red fox and golden jackal may have an important role in epidemiology of Canine hepatozoonosis.

● Associated risk factor with the vector-borne diseases is the type of dog (stray dogs have been at risk being positive for *Dirofilaria immitis,* shelter dogs for *Ehrlichia canis*, and hunting dogs for *Borrelia burgdorferi*).

● Cats have been positive for *Ehrlichia* spp.

● Many tick-borne diseases are most probably endemic in the Balkan area.

● The prevalence of zoonotic *Rickettsia* spp. in ticks from Bulgaria established in one of the studies has been very high. The risk that the tick bites from this area could lead to *Rickettsia* infection in humans and mammals has been underlined.

● Based on clinical signs, canine babesiosis has been diagnosed by the veterinarians in dogs, more frequently infested with *Dermacentor reticulatus* than other tick species.

● Human granulocytic ehrlichiosis have been detected in *Ixodes ricinus* and *Hyalomma detritum*.

● Transmission of *E. canis* by *Rhipicephalus sanguineus* ticks starts within a few hours after attachment, which is earlier than previously thought.

Acknowledgements: This work is connected with the bilateral project between the Institute of Experimental Morphology, Pathology and Anthropology with Museum – Bulgarian Academy of Sciences and the Institute of Parasitology, Slovak Academy of Sciences: "Parasites in domestic and wild carnivores from Slovakia and Bulgaria in the era of global changes" (2018-2020).

The work is supported by the Bulgarian Ministry of Education and Science under the National Program for Research "Young Scientist and Postdoctoral Students" approved by DCM 577/17.08.2018.

References

1. **Braga, Í. A., L. G. F. dos Santos, D. G. de Souza Ramos, A. L. T. Melo, G. L. da Cruz Mestre, D. M. de Aguiar.** Detection of *Ehrlichia canis* in domestic cats in the central-western region of Brazil. – *Braz. J. Microbiol.*, **45**(2), 2014, 641-645.
2. **Çetinkaya, H., E. Matur, İ. Akyazi, E. E.Ekiz, L. Aydin, M. Toparlak**. Serological and molecular investigation of *Ehrlichia* spp. and *Anaplasma* spp. in ticks and blood of dogs, in the Thrace Region of Turkey. – *Ticks and Tick-borne Diseases*, **7**(5), 2016, 706-714.
3. **Christova, I., J. Van De Pol, S. Yazar, E. Velo, L. Schouls.** Identification of *Borrelia burgdorferi* sensu lato, *Anaplasma* and *Ehrlichia* Species, and Spotted Fever Group Rickettsiae in Ticks from Southeastern Europe. – *Eur. J. Clin. Microbiol. Infect. Dis*., **22**(9), 2003, 535-542.
4. **Földvári, G., R. Farkas.** Ixodid tick species attaching to dogs in Hungary. – *Vet. Parasitol.,* **129** (1–2), 2005, 125-131.
5. **Fourie, J. J., D. Stanneck, H. G.Luus, F. Beugnet, M. Wijnveld, F. Jongejan.** Transmission of *Ehrlichia canis* by *Rhipicephalus sanguineus* ticks feeding on dogs and on artificial membranes. – *Vet. Parasitol.,* **197** (3–4), 2013, 595-603.
6. **Hornok, S., J. Fuente, G. Horváth, I. Fernández de Mera, M. Wijnveld, B. Tánczos, R. Farkas, F. Jongejan.** Molecular evidence of *Ehrlichia canis* and *Rickettsia massiliae* in ixodid ticks of carnivores from South Hungary. – *Acta Veterinaria Hungarica*, **61**(1), 2013a, 42-50.
7. **Hornok, S., B. Tánczos, I. G. Fernández de Mera, J. la Fuente, R. Hofmann-Lehmann, R. Farkas.** High prevalence of *Hepatozoon*-infection among shepherd dogs in a region considered to be free of *Rhipicephalus sanguineus. – Vet. Parasitol.,* **196**(1–2**)**, 2013b, 189-193.
8. **Melissa, J. B., R. Chandrashekar, M. D. Eberts, K. E. Cyr, P. P. V.P. Diniz, C. Mainville, B. C. Hegarty, J. M. Crawford, E. B. Breitschwerdt.** Serological and Molecular Prevalence of *Borrelia burgdorferi*, *Anaplasma phagocytophilum*, and *Ehrlichia* Species in Dogs from Minnesota. – *Vector-Borne and Zoonotic Diseases*, **8**(4), 2008, 455.
9. **Mircean, V., M. O. Dumitrache, A. Györke, N. Pantchev, R. Jodies, A. D. Mihalca, V. Cozma.** Seroprevalence and geographic distribution of Dirofilaria immitis and tick-borne infections (Anaplasma phagocytophilum, Borrelia burgdorferi sensu lato, and Ehrlichia canis) in dogs from Romania. – *Vector-Borne and Zoonotic Diseases*, **12**(7), 2012, 595-604.
10. **Nader, J., N. Król, M. Pfeffer, V. Ohlendorf, M. Marklewitz, C. Drosten, S. Junglen, A. Obiegala**. The diversity of tick-borne bacteria and parasites in ticks collected from the Strandja Nature Park in south-eastern Bulgaria. – *Parasites & Vectors*, **11**, 2018, 165.
11. **Pantchev, N., M. Schnyder, M. G. Vrhovec, R. Schaper, I. Tsachev.** Current Surveys of the Seroprevalence of *Borrelia burgdorferi*, *Ehrlichia canis*, *Anaplasma phagocytophilum*, *Leishmania infantum*, *Babesia canis*, *Angiostrongylus vasorum* and *Dirofilaria immitis* in Dogs in Bulgaria. – *Parasitol. Res.,* **114**(1), 2015, 117.
12. **Sarih, M., Y. M'Ghirbi, A. Bouattour, L. Gern, G. Baranton, D. Postic.** Detection and Identification of *Ehrlichia* spp. in Ticks Collected in Tunisia and Morocco. – *J. Clin. Microbiol.,* **43**(3), 2005, *1127–1132.*
13. **Sobrino, R., J. Millán, Á. Oleaga, C. Gortázar, J. la Fuente, F. Ruiz-Fons.** Ecological preferences of exophilic and endophilic ticks (Acari: Ixodidae) parasitizing wild carnivores in the Iberian Peninsula. – *Vet. Parasitol.*, **184**(2-4), 2012, 248-257.
14. **Wielinga, P. R., C. Gaasenbeek, M. Fonville, A. de Boer, A. de Vries, W. Dimmers, G. A. Op Jagers, L. M. Schouls, F. Borgsteede, J. W. B. van der Giessen.** Longitudinal Analysis of Tick Densities and *Borrelia*, *Anaplasma*, and *Ehrlichia* Infections of *Ixodes ricinus* Ticks in Different Habitat Areas in The Netherlands. – *Appl. Environ. Microbiol.*, **72**(12), 2006, 7594-7601.

Guidelines for Authors

Acta morphologica et anthropologica is an open access peer review journal and publishes original articles, short communications, reviews, letters to the Editors. The aim of the journal is to provide a forum for cytological, histological, anatomical and anthropological research community in life sciences, including cell biology, immunobiology, pathology, neurobiology, environmental and toxicological research, reproductive biology, pharmacology, physical development and medical anthropology, paleoanthropology, anatomy, paleoanatomy, etc.

Acta morphologica et anthropologica is published twice a year as one volume with 4 issues. For the first two issues (1-2) the deadline for manuscript submission is March 15th and for the next two issues (3-4), the deadline is September 15th. Electronic version for issues 1-2 is uploaded on the website till June 30th and for issues 3-4 – till December 30th.

Contact details and submission

Manuscripts should be in English with total length not exceeding 10 standard pages, line-spacing 1.5, justified with 2.5 cm margins. The authors are advised to use Times New Roman, 12 pt throughout the text. Pages should be numbered at the bottom right corner of the page. Manuscript submission is electronic only. The manuscripts should be sent to: **ygluhcheva@hotmail.com.**

All correspondence, including notification for Editor's decision, requests for revision, is sent by e-mail.

Article structure

The article should be arranged under the following headings: Introduction, Material and Methods, Results, Discussion, Conclusion, Acknowledgements and References.

Title page – includes:

- **Title** – concise and informative;
- **Author(s)' names and affiliations** – indicate the given name(s) and family name(s) of all authors. Present the authors' affiliation addresses below the names. Indicate all affiliations with a lower-case superscript after the author's name and in front of the appropriate address. Provide the full postal address information for each affiliation, including the country name.
- **Corresponding author** – clearly indicate who will handle the correspondence for refereeing, publication and post-publication. An e-mail should be provided.
- **Abstract** – state briefly the aim of the work, the principal results and major conclusions and should not exceed 150 words. References and uncommon, or non-standard abbreviations should be avoided.
- **Key words** – provide up to 5 key words. Avoid general, plural and multiple concepts. The key words will be used for indexing purposes.

Introduction – state the objectives of the work and provide an adequate background, avoiding a detailed literature survey or summary of the results.

Material and Methods – provide sufficient detail to allow the work to be reproduced. Methods already published should be indicated as a reference: only relevant modifications should be described.

Results – results should be clear and concise.

Discussion – should explore the significance of the results in the work, not repeat them. A combined *Results and Discussion* section is often appropriate. Avoid extensive citation and discussion of published literature.

Conclusions – the main conclusions of the study should be presented in a short section.

Acknowledgements – list here those individuals who provided help during the research and the funding sources.

Units – please use the International System of Units (SI).

Math formulae – please submit math equations as editable text, not as images.

Electronic artwork – number the tables and illustrations according to their sequence in the text. Provide captions for them on a separate page at the end of the manuscript. The proper place of each figure in the text should be indicated in the left margin of the corresponding page. **All illustrations (photos, graphs and diagrams)** should be referred to as "figures" and given in abbreviation "Fig.", and numbered in Arabic numerals in order of its mentioning in the manuscript. They should be provided in grayscale as JPEG or TIFF format, minimum 300 dpi. The illustrations should be submitted as separate files.

References –they should be listed in alphabetical order, indicated in the text by giving the corresponding numbers in parentheses. The „References" should be typed on a separate sheet. The names of authors should be arranged alphabetically according to family names. In the reference list titles of works, published in languages other than English, should be translated, original language must be indicated at the end of reference (e.g., [in Bulgarian]). Articles should include the name(s) of author(s), followed by the full title of the article or book cited, the standard abbreviation of the journal (according to British Union Catalogue), the volume number, the year of publication and the pages cited, for books - the city of publication and publisher. In case of more than one author, the initials of the second, third, etc. authors precede their family names.

For articles: **Davidoff, M. S., R. Middendorff, G. Enikolopov, D. Riethmacher, A. F. Holstein, D. Muller**. Progenitor cells of the testosterone-producing Leydig cells revealed. – *J. Cell Biol.,* **167**, 2004, 935-944.

Book article or chapter: **Rodriguez, C. M., J. L. Kirby, B. T. Hinton. The development of the epididymis.** - In: *The Epididymis - from molecules to clinical practice* (Eds. B. Robaire, B. T. Hinton), New York, Kluwer Academic Plenum Publisher, 2002, 251-269.

Electronic books: **Gray, H.** *Anatomy of the human body* (Ed. W.H.Lewis), 20th edition, NY, 2000. Available at http://www.Bartleby.com.

PhD thesis: **Padberg, G**. Facioscapulohumeral diseases. *PhD thesis*, Leiden University, 1982, 130 p.

Website: National survey schoolchildren report. National Centre of Public Health and Analyses, 2014. Available at http://ncphp.government.bg/files

Page charges

Manuscript publication is free of charges.

Ethics in publishing

Before sending the manuscript the authors must make sure that it meets the Ethical guidelines for journal publication of Acta morphologica et anthropologica.

Human and animal rights

If the work involves the use of human subjects, the authors should ensure that work has been carried out in accordance with *The Code of Ethics of the World Medical Association* (Declaration of Helsinski). The authors should include a statement in the manuscript that informed consent was obtained for experimentation with human subjects. The privacy rights of human subjects must always be observed.
All animal experiments should comply with the *ARRIVE guidelines* and should be carried out in accordance with the U.K. Animals (Scientific procedures) Act, 1986 and the associated guidelines *EU Directive 2010/63/EU* for animal experiments, or the National Institutes of Health guide for the care and use of Laboratory animals (NIH Publications No. 8023, revised 1978) and the authors should clearly indicate in the manuscript that such guidelines have been followed.

Submission declaration

Submission of the manuscript implies that the work described has not been published previously, is not considered under publication elsewhere, that its publication is approved by all authors, and that if accepted, it will not be published elsewhere in the same form, in English or in any other language, including electronically, without the informed consent of the copyright-holder.

Contributors

The statement that all authors approve the final article should be included in the disclosure.

Copyright

Upon acceptance of an article, the authors will be asked to complete a "Journal Publishing Agreement". An e-mail will be sent to the corresponding author with the Journal Publishing Agreement Form or a link to the online version of this agreement.

Peer review

This journal operates a single blind review process. All contributions will be initially assessed by the Editor for suitability for the journal. All suitable papers are then sent to two independent expert reviewers to assess the scientific quality of the paper. The Editor is responsible for the final decision regarding acceptance or rejection of articles.

After acceptance

Proof correction

The corresponding author will receive proofs by e-mail in PDF format and will be requested to return it with any corrections within a week.

Offprints

The journal provides free access to all papers in each volume that can be downloaded from the following website: http://www.iempam.bas.bg/journals/acta.html